Photodynamic High-Level Disinfection for Medical Surfaces

Michael J. Pascoe

Cardiff School of Pharmacy & Pharmaceutical Sciences

Cardiff University

A thesis submitted for the degree of:

Doctor of Philosophy

2019

CONTENTS

Dedication

To my grandparents, Jack and Enid Cardew.

Acknowledgements

The completion of this thesis could not have been achieved without the support and guidance of many individuals, who I would like to thank.

Firstly, I would like to offer my sincerest gratitude to Professor Jean-Yves Maillard, who has been a wonderful and patient mentor throughout my studies. I couldn't have asked for a better supervisor and consider myself lucky to have shared the experience with you. I am truly grateful for your continued support from start to finish.

I would also like to thank Dr Daniel Slocombe and Professor Adrian Porch of the School of Engineering for their guidance in understanding the engineering and physics elements of the project. Your insights were invaluable to the development of this work and I appreciate your understanding as I got to grips with an unfamiliar discipline.

To my sponsors at Laboratoires Anios, particularly Gaétan Rauwel, Jacques Criquelion and Jean-Noël Bertho. Thank you for financially supporting this project and for providing ongoing technical expertise and essential materials for developing this technology. I look forward to our future collaborations.

For their technical assistance in determining the mechanism of action of the formulation developed in this project, I would like to thank Dr Thomas Davies, Dr Andrea Folli and Dr Mike Beeton.

I would also like to express my gratitude to the following:

To Andrew Robertson and Rebecca Wesgate, who helped me to develop my technical skills, and the support of all my other lab mates (Melissa, Hélène, Lauren, Grzegorz, Joana, Issy, Kate, Matt, Leo & Maru) who were always there to offer a helping hand and understanding ear when needed.

To my wonderful friends and colleagues in the School of Pharmacy, particularly Justine, Dean, Rhys the Pharmabees team and CITER. Thank you for our many stimulating conversations and the opportunities to participate with community engagement projects.

To the continued support of Dr Sarah Maddocks, whose tutelage in my early research continues to inspire and shape my academic work.

Last, but certainly not least, to my dearest friends and family who stood with me throughout this undertaking and always offered much needed distractions. Your love and support won't be forgotten.

Thesis Summary

This project sought to evaluate photosensitisers as feasible alternatives to traditional biocide products for disinfecting medical surfaces. Photosensitisers produce damaging reactive oxygen species in the presence of light and may be safer than traditional disinfectants. However, their biocidal efficacy has yet to be determined using standardised methods and so comparisons with current technology are not possible.

After establishing the photosensitiser toluidine blue O (TBO) as a lead compound, a biocide formulation was developed which exhibited broad spectrum bactericidal activity against a range of bacterial species. In the following chapter, the effect of photosensitiser-treatment on target cells was established and was observed to target the bacterial cytoplasmic membrane and nucleic acids. Upon testing against a broad spectrum of challenge organisms, the formulation was highly biocidal against yeasts, non-enveloped viruses and fast-growing mycobacteria and moderately effective against bacterial biofilms. However, its biocidal activity was found lacking against *Aspergillus* conidia, slow-growing mycobacteria and bacterial endospores. Further investigation determined that pigments, permeability barriers and DNA protection mechanisms confer resistance to photosensitisation.

Evaluation of the scalability of photosensitiser-based disinfection determined that photosensitisers boast an exceptional ecotoxicological profile and can be produced at a price comparable to other disinfectants. Whilst photosensitisers are yet to be registered as an active substance in the European Union, they fulfil the general requirements of registration and do not contradict any exclusion criteria. Incorporating photosensitiser-based disinfection technology into complex devices such as an automated endoscope reprocessors is feasible, though would require complex design considerations which may discourage its use.

Overall, these data demonstrate that photosensitiser-based biocide formulations are insufficiently effective for high-level disinfection of medical surfaces. However, their low production costs and ecotoxicological properties may make them suitable for alternative applications. The technology can be readily scaled-up the disinfection of commercial food preparation surfaces and so further investigations into alternative uses are recommended.

Annex 1: List of Figures and Tables

Chapter 1

Chapter 2

Chapter 3

Chapter 4

Chapter 5

Chapter 6

Chapter 7

Annex 2: Referenced Standards

Standard	Full Title	Reference
E2197	ASTM E2197-17$^{\varepsilon 1}$: Standard quantitative disk carrier test method for determining bactericidal, virucidal, fungicidal, mycobactericidal, and sporicidal activities of chemicals.	ASTM International (2017)
EN 13624	BS EN 13624:2013: Quantitative suspension test for the evaluation of fungicidal or yeasticidal activity in the medical area.	British Standards Institute (2013a)
EN 13697	BS EN 13697:2015: Quantitative non-porous surface test for the evaluation of bactericidal and/or fungicidal activity of chemical disinfectants used in food, industrial, domestic and institutional areas.	British Standards Institute (2015a).
EN 13727	BS EN 13727:2012+A2:2015: Quantitative suspension test for the evaluation of bactericidal activity in the medical area.	British Standards Institute (2012).
EN 14348	BS EN 14348:2005: Quantitative suspension test for the evaluation of mycobactericidal activity of chemical disinfectants in the medical area including instrument disinfectants.	British Standards Institute (2005)
EN 14561	BS EN 14561:2006: Quantitative carrier test for the evaluation of bactericidal activity for instruments used in the medical area.	British Standards Institute (2006)
EN 16615	BS EN 16615:2015. Quantitative test method for the evaluation of bactericidal and yeasticidal activity on non-porous surfaces with mechanical action employing wipes in the medical area (4-field test).	British Standards Institute (2015b)
ISO 15883	ISO 15883-4:2018: Washer-disinfectors - Part 4: Requirements and tests for washer-disinfectors employing chemical disinfection for thermolabile endoscopes	British Standards Institute (2018)

Annex 3: List of Suppliers

Supplier name	Location
Amersham Biosciences	Amersham, UK
BASF	Ludwigshafen, Germany
Bemis	Swansea, UK
Berthold	Harpenden, UK
Ceti	Chalgrove, UK
Clariant	Muttenz, Switzerland
E&O Laboratories	Bonnybridge; UK
Electrovision	St. Helens, UK
Fisher Scientific	Loughborough, UK
GraphPad Software	San Diego (CA), USA
Greiner Bio-One International	Kremsmünster, Austria
Memmert	Schwabach, Germany
Merck	Kenilworth (NJ), USA
Mettler Toledo	Columbus (OH), USA
Mycoplasma experience	Surrey, UK
nanoComposix	San Diego (CA), USA
Ocean Optics	Oxford, UK
Oxoid	Basingstoke, UK
Promega UK	Southampton, UK
Quorum Technologies	Laughton, UK
Sartorious	Stonehouse, UK
Sigma Aldrich	Gillingham, UK
Syngene	Cambridge, UK
Tecan	Männedorf, Switzerland
Tescan	Brno, Czech Republic
Thermo Fisher Scientific	Newport, UK
Thorlabs	Newton (NJ), USA

Annex 4: List of abbreviations

AER: Automated endoscope reprocessor

ASTM: American Society for Testing and Materials

ATCC: American Type Culture Collection

BPR: Biocidal products regulation

BSA: Bovine serum albumin

BSI: British Standards Institute

CFU: Colony forming unit

ECHA: European Chemicals Agency

EN: European Standard

EU: European Union

FEA: Finite element analysis

GTA: Glutaraldehyde

HLD: High-level disinfection

ISO: International Organization for Standardization

LED: Light-emitting diode

MGDA: Methylglycine diacetic acid

NCTC: National Collection of Type Cultures

OECD: Organisation for Economic Co-operation and Development

OPA: o-phthaldehyde

PAA: Peracetic acid

TBO: Toluidine blue O

TSA: Tryptone soya agar

TSB: Tryptone soya broth

TSC: Tryptone sodium chloride

UV: Ultraviolet

Chapter 1.

Introduction and Project Aims

1.1 Contamination and disinfection of medical surfaces

Controlling the spread of pathogenic microorganisms is a central tenet of infection prevention and control. In healthcare environments, surfaces and devices come into contact with numerous sources of contamination, including hands, bodily fluids and air. Contamination of these surfaces with pathogenic microorganisms can transform an object into a reservoir from which infections disease can be transferred between persons. Decontamination of medical surfaces thus plays a vital role in patientcare.

Cleaning is defined as the removal of organic soil, such as proteins and blood and can be considered the first step in surface decontamination. Cleaning is often achieved using warm water, detergents and digestive enzymes which solubilise and break down the constituent molecules and aid their removal (Beilenhoff et al., 2018). To control the spread of microorganisms, the surface must then be disinfected or sterilised. Sterilisation is the complete elimination of viable organisms from a surface whilst disinfection is a reduction in the viability of organisms to a level which renders the surface microbiologically safe. The extent to which a medical device must be disinfected can be determined using the Spaulding's classification system. This system, which is detailed in table 1.1, stratifies medical devices based on an assessment of the infection risks they pose to patients during use (World Health Organisation, 2016).

Table 1.1: Spaulding's classification system. Adapted from World Health Organisation (2016).

Classification	Contact area	Example instrument	Control measure
Non-critical	Intact skin	Stethoscope, blood pressure cuff	Disinfection with mid-level disinfectant wipes
Semi-critical	Mucous membranes	Duodenal endoscope, respiratory tubing	Disinfection with high-level disinfectants
Critical	Sterile body sites	Surgical tools, prostheses, implants	Sterilisation by autoclaving

Flexible duodenoscopes are medical devices which are used to facilitate diagnostic and surgical procedures affecting the gastrointestinal tract. Under the Spaulding's system, duodenal endoscopes can be classified as semi-critical instruments as they come into contact with intact patient mucous membranes (ASGE Quality Assurance in Endoscopy Committee et al., 2011). As they are heat-sensitive and cannot be simply autoclaved, they must be sanitised through high-level disinfection using chemical biocides (BSG Endoscopy Committee Working Party, 1998).

1.2 Automated endoscope reprocessors

Automated endoscope reprocessors (AERs), also termed washer-disinfectors, are devices which automate high-level disinfection (HLD) of endoscopes. They consist of a large basin into which devices are loaded, a tank and filtration system which dispenses rinse water throughout the reprocessing cycle and several channels, which flush the internal channels with disinfectant (British Standards Institute, 2018). AER usage is recommended by several gastroenterology societies due to the distinct benefits they offer to reprocessing units (ASGE Technology Committee et al., 2016; Working Party of the British Society of Gastroenterology Endoscopy Committee, 2017). AERs standardise the disinfection process and ensure adherence to described disinfection protocols by reducing the possibility of operator error. Their use also reduces exposure of reprocessing technicians to infectious agents and hazardous disinfectants. Some AER models are capable of automating the cleaning and leak test stages of endoscope reprocessing (ASGE Technology Committee et al., 2016) and so it is foreseeable that AERs might automate the entire reprocessing cycle in the future.

During the reprocessing cycle, the AER components are exposed to soil and microbial contaminants. Since AERs are responsible for disinfecting semi-critical devices, they must undergo periodic high-level disinfection to prevent contamination of endoscopes during reprocessing. Disinfection is especially important for preventing the formation of biofilms, which can colonise the AER and cause repeated contamination of endoscopes and pseudo outbreaks (Gubler et al., 1992; Kressel & Kidd, 2001; Roberts et al, 2013). Guidelines state that AERs must undergo a self-disinfection cycle at least once per day to disinfect the basin, channels and filtration system (British Standards Institute, 2018). However, as biofilms can form throughout the day, it would be desirable to incorporate a self-disinfection step following each endoscope reprocessing cycle.

1.3 High-level disinfectants

High-level disinfectants are chemical biocides which are able to reduce the viability of all classes of microorganisms to reasonably safe levels. This includes mycobacteria, small non-enveloped viruses and bacterial endospores, which are particularly resistant to disinfection (McDonnell & Burke, 2011). As they are active at ambient temperature, these disinfectants are well suited for decontaminating heat-sensitive surfaces and instruments (Centers for Disease Prevention and Control, 2008). High-level disinfectants can be broadly classified by their chemistry and the mechanisms by which they inactivate microorganisms.

1.3.1 Alkylating agents

Alkylating agents are the most commonly utilised group of high-level disinfectants. These agents are available at a low wholesale cost, are shelf stable over extended periods and exhibit broad spectrum microbicidal activity. Exposure to these agents results in nucleophilic reactions with the amino, sulfhydryl and imidazole groups of macromolecules such as proteins, leading to their alkylation (Okuda et al., 1991; Modenez et al., 2018). This in turn causes covalent cross-links to form between target residues, inhibiting macromolecule function and causing cell death (McDonnell & Russell, 1999). Glutaraldehyde (GTA) and o-phthaldehyde (OPA) are the most widely used alkylating agents and both exhibit greater bactericidal activity at alkaline pH. This is due to deprotonation of target groups which renders them more susceptible to addition reactions. GTA and OPA-based formulations are typically activated prior to use by adding buffers which increase the pH (Migneault et al., 2004). Whilst OPA alkylates less effectively than GTA, it exhibits superior microbicidal activity due to its lipophilicity, which improves its interactions with microbial surfaces (Simons et al., 2000). Alkylating agents have long been noted to retain biocidal activity in the presence of organic loads (Gélinas & Goulet, 1983; Al-Adham et al., 2013), making them appropriate for applications where heavy soiling is anticipated.

1.3.2 Oxidising agents

Oxidising agents inactivate microorganisms by oxidatively damaging a range of intracellular targets, including the cytoplasmic membrane, nucleic acids and enzymes (Denyer & Stewart, 1998; Finnegan et al., 2011). Peroxygen compounds such as hydrogen peroxide and peracetic acid (PAA) are the principle oxidising agents utilised for the disinfection of endoscopic surfaces. These agents are rapidly sporicidal, particularly when co-formulated (Leggett et al., 2016a). This synergy between agents is due to weakening of the proteinaceous spore coat by peroxide, which facilitates greater penetration of PAA into the spore core (Leggett et al., 2016a). Numerous formulations containing this combination are available commercially. Oxidising agents can achieve the same level of microbial inactivation more rapidly than alkylating agents, which can improve throughput of high-level disinfection processes (BSG Endoscopy Committee Working Party, 1998). PAA and hydrogen peroxide also offer ecological advantages over alkylating agents by decomposing into inert by-products such as acetic acid, water and oxygen (Al-Adham et al., 2013).

As an oxidising agent, chlorine dioxide (ClO_2) also exhibits excellent sporicidal activity and has been investigated as an alternative to peracetic acid for endoscope disinfection (Henoun Loukili et al., 2017). Likewise, vaporised hydrogen peroxide (vHP) isunder investigation as an alternative high-level disinfectant due to proposed differences in mechanism of action compared to its liquid-phase counterpart (Linley et al., 2012). This suggests that oxidising agents as a

broad group are highly suitable for high-level disinfection applications. It should be noted that the biocidal effectiveness of oxidising agents can be reduced in the presence of organic soil (Gélinas & Goulet, 1983), though this can be partly overcome through formulation with synergistic additives (Chowdhury et al., 2019).

1.4 Weaknesses of current HLD technologies

Endoscopy units in the UK report that they are currently operating at peak capacity. With the recent expansion of bowel cancer screening programmes and the Single Cancer Pathway in Wales, pressure on endoscopy units is due to reach unprecedented levels. Improving decontamination regimens offers opportunities to improve throughput, streamline costs, and protect the health of patients and workers. The following section outlines the drawbacks of current HLD technologies and identifies areas which could be improved by alternative methods.

1.4.1 Time constraints

The effective decontamination of surfaces using alkylating agents requires long contact times. For example, HLD using 2% GTA requires contact times between 20-30 minutes to achieve satisfactory reductions in microbial viability (Rutala & Weber, 2004). Other studies have indicated that satisfactory reductions in the viability of some organisms were only observed after 60 minutes of exposure to peroxide (Martin et al., 2008). Long turnaround times lowers the throughput and raises the expense of endoscopic procedures whilst also necessitating that AERs self-disinfect only once daily. Whilst there is a desire to reduce reprocessing cycle times in endoscopy, poor execution in the past has led to disinfectant-induced injuries (Kim & Baek, 2012). This indicates there is an unmet need which could be fulfilled by more rapid disinfection methodologies, which can allow AERs to be disinfected more regularly and improve machine hygiene.

1.4.2 Chemical hazards and material incompatibility

Due to their non-selective mechanisms of action, high-level disinfectants pose hazards to the health to end-users. Occupational exposure of cleaning technicians to widely used biocides has been linked to conditions such as asthma (Cristofari-Marquand et al., 2007) and contact dermatitis (Shaffer and Belsito, 2000). Whilst the correct use of personal protective equipment (PPE) may reduce the risk of harm to the user, compliance is poor and spillages occur with alarming frequency (Henn et al., 2015). Furthermore, standard issue PPE can be insufficient in protecting workers from corrosive disinfectants and so specialised protective equipment must be provided (Sylvain & Gibbins, 2009). The concerns of staff health and wellbeing was identified as a central motivator for seeking alternative biocides at endoscope reprocessing units in British Columbia (Rideout et al., 2005).

Some materials and finishes utilised in medical device designs present compatibility issues with certain disinfectants. For example, cosmetic changes, blistering and even functional damage have been observed after using peracetic acid and chlorine dioxide-based disinfectants for reprocessing Olympus endoscopes (Olympus KeyMed, 2012).

1.4.3 Biocide resistance

Several microbial strains have been isolated which exhibit increased resistance to high-level disinfectants. *Mycobacterium* species are particularly noteworthy in their resistance to high-level disinfectants; several strains have been isolated from automated endoscope reprocessors (AERs) which exhibit resistance to alkylating agents such as glutaraldehyde (Griffiths et al., 1997; Fisher et al., 2012; De Groot et al., 2014). A range of Gram-positive bacteria have been isolated from the connectors, drain and rinse water of automated endoscope reprocessors disinfected with ClO_2 (Martin et al., 2008).

Biofilms also contribute extensively to disinfection resistance. These communities can rapidly form on endoscope and AER surfaces and are very difficult to remove with enzymatic detergents (Vickery et al., 2004). Extracellular polymeric substance (EPS) secreted by these biofilms may create a diffusion barrier through which biocides permeate poorly and may become inactivated in this process. This is particularly problematic for peroxide-based biocides, which can be rapidly inactivated by catalases produced by *Staphylococcus aureus* and *Pseudomonas aeruginosa* (Stewart et al., 2000). A pseudo-outbreak of *Mycobacterium abscessus* has been previously linked to the formation of biofilms within AERs, which enabled them to resist disinfection with glutaraldehyde (Kressell & Kidd, 2001).

Alkylating agents such as GTA and OPA can chemically fix biofilms to surfaces which can cause them to build-up over many reprocessing cycles and occlude endoscopes and AERs channels; this can protect microorganisms from the HLD process and facilitates survival post-processing (Alfa & Howie, 2009). A systematic review has concluded that PAA, an oxidising agent, is also capable of fixing biofilms, dried blood and tissue to medical surfaces, which raises concerns on the long-term suitability of these agents (Kampf et al., 2014).

Whilst endoscopy units in many economically developed countries have phased out the use of alkylating agents, ISO 15883 states that the biocide or parameters used for AER self-disinfection cycles must be different to those which is used for endoscope disinfection to avoid promoting resistance to a single agent (British Standards Institution, 2018). Exploring novel alternatives offers an opportunity to expand the toolkit of biocides available to reprocessing units and fill the gap left by alkylating agents.

1.4.4 Production and supply concerns

Synthesis of hydrogen peroxide via the anthraquinone process is energy intensive and is only economically feasible when synthesis is performed on a large scale; production tends to be centralised in large facilities and is less environmentally friendly than the decomposition products might lead one to believe (Compos-Martin et al., 2006). Disruptions to the running of centralised facilities can therefore have large effects on the supply of these compounds. This is compounded by the limited shelf-stability of peroxygen compounds, which decompose during long-term storage (Denny & Marsik, 2004). In the wake of Hurricane Harvey, damage to hydrogen peroxide production plants led to warnings of prolonged disruption to the supply of peracetic acid to the American poultry industry (Laube, 2017).

The transport of peroxygen compounds, particularly in concentrated forms, raises unique safety concerns. For example, reactions between hydrogen peroxide and organic compounds can produce explosive by-products (Schreck et al., 2004), which has contributed to disasters such as the 1989 Helena train wreck in Montana, which resulted in several million dollars of damage and led to a partial evacuation of the city (National Transportation Safety Board, 1989). Non-explosive alternatives to peroxygen compounds would mitigate this risk.

1.5 Photosensitisers

1.5.1 Introduction to photosensitisers

Photosensitisers are a diverse class of compounds which are characterised by the ability to produce reactive oxygen species (ROS), such as singlet oxygen and radicals, under conditions of light excitation. Photosensitisers have been applied to several technological challenges, including producing self-disinfecting surfaces (Craig et al., 2015), dental disinfection (Konopka & Goslinski, 2007) and cancer therapy (Kinsella et al., 2001).

Organic photosensitisers consist of a central aromatic *chromophore* and peripheral *auxochrome* groups (Fig. 1.1). Whilst the photosensitiser class is defined by the chromophore, specific properties such as lipophilicity and excitation wavelength are strongly determined by the auxochromes. The auxochromes are vital to the functioning of a photosensitiser as chromophores are colourless in their own right; the colouration of photosensitisers is a result of the contribution of auxochrome electrons to the delocalised π-system of the aromatic region. (Wainwright, 2009). There are many different classes of photosensitiser which are grouped according to chromophore structure and further differentiated by the auxochromes present. Methylene blue and toluidine blue O, for example, are both centred around a phenothiazine chromophore whilst erythrosin B is classed as a fluorescein dye.

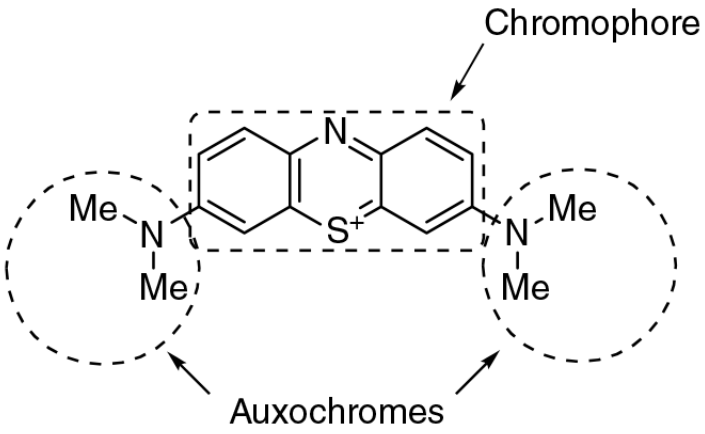

Figure 1.1: Chemical structure of methylene blue, a phenothiazine-class photosensitiser. Note the abundance of π orbitals in the central chromophore which contribute to a delocalised electron system. Reprinted with permissions from Wainwright (2009). Copyright 2009 John Wiley & Sons, Ltd

1.5.2 Mechanism of ROS production

ROS production by photosensitisers is a light-dependent process. Absorption of light at the photosensitiser excitation wavelength results in excitation of ground state electrons to a more energetic valence state. Returning to ground state requires dissipation of this energy, either radiatively by fluorescence or non-radiatively by vibrational relaxation or chemical reaction (Atkins & Friedman, 2011). In photosensitisers, the excited electron may also transition to a triplet quantum state via the process of intersystem crossing. In this state, the spin momentum of the exited electron is independent from that of the ground state electron to which the spin was previously paired (Marian, 2012).

In a triplet state, the photosensitiser produces ROS through two mechanisms (fig. 1.2). Electron transfer through a type-I photosensitisation mechanism results in the production of radical species whilst energy transfer through type-II photosensitisation produces singlet oxygen. Unlike radical species, singlet oxygen is non-paramagnetic and does not contain unpaired electrons. Singlet oxygen is instead produced from molecular oxygen, which naturally exists in a triplet state; the process of energy transfer inverts its spin to produce singlet oxygen (Wainwright, 2009), which is highly reactive and can oxidise a range of cellular macromolecules (DeRosa & Crutchley, 2002).

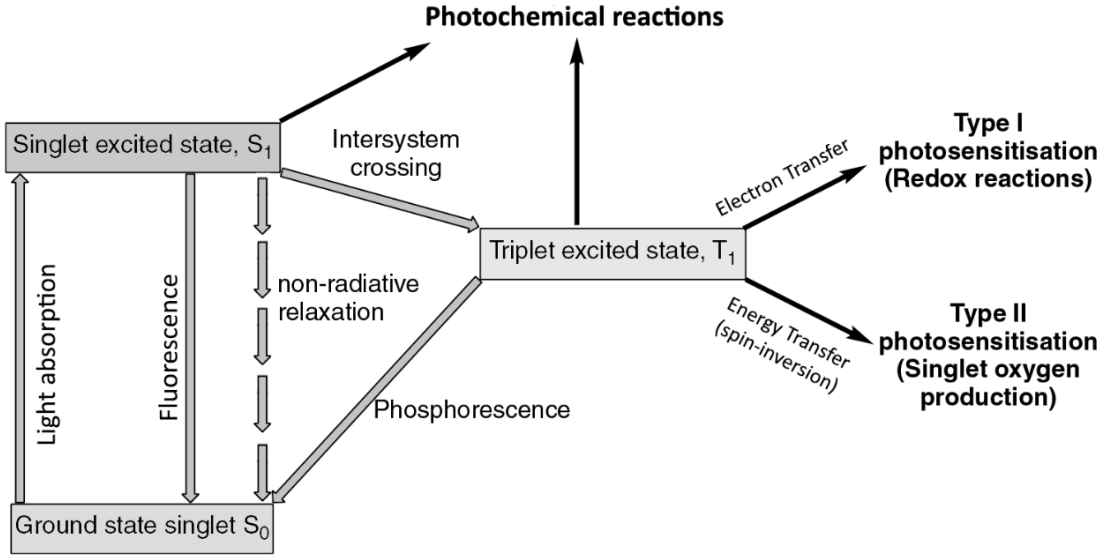

Figure 1.2: Mechanisms of ROS production by organic photosensitisers. Reprinted with permissions from Wainwright (2009). Copyright 2009 John Wiley & Sons, Ltd

1.6 Advantages of photosensitisers

1.6.1 Oxidising agent

Oxidising high-level disinfectants such as peroxygen compounds are utilised as high-level disinfectants due to their rapid broad-spectrum antimicrobial activity (BSG Endoscopy Committee Working Party, 1998). Due to the production of singlet oxygen, which is a potent oxidising species, photosensitisers may also possess broad spectrum antimicrobial activity.

1.6.2 Low use-concentration and cost

Rather than directly attacking microbes, photosensitisers catalyse the formation of singlet oxygen, which is the active biocidal species. Since each molecule of a photosensitiser is capable of producing 10^3-10^5 molecules of singlet oxygen before it degrades (Pen Luengas et al., 2014), photosensitisers may be used at concentrations below that of other biocides. Peracetic acid is often used at a concentration of 0.2% w/v (Centers for Disease Control and Prevention, 2008a), which is equivalent to 26 mM. By contrast, the photosensitiser toluidine blue O is widely reported to be bactericidal at micromolar concentrations (Tang et al., 2007; Kashef et al., 2012; Tseng et al., 2017). Photosensitisers are therefore usable at substantially more dilute concentrations than other disinfectants which may offer substantial cost savings in the production of a commercial product.

1.6.3 Non-hazardous

Photosensitisers are relatively inert under biological conditions and produce biocidal species only following light excitation. Chemicals with photosensitising properties are already used widely in applications such as food colouring, as anthelmintic drugs, and targeted cancer therapy (Pan et al., 2005; Agostinis et al., 2011; Varga et al., 2017). The established safety profile of these photosensitisers indicate that their utilisation may reduce the risks of disinfectant-induced injuries and occupational exposure illnesses in healthcare workers. Photosensitisers have been proposed as a safe and environmentally friendly alternative for the disinfection of foodstuffs as toxic by-products are not produced (Luksiene & Brovko, 2013).

1.7 Limitations of current knowledge

Standardised tests such as EN 13727 set threshold requirements for the biocidal efficacy of disinfectants and facilitate like-for-like comparisons between products. Currently, there is a deficit in published studies which detail the biocidal activity of photosensitiser-based formulations under standardised test conditions. It is therefore not possible to determine whether photosensitiser-based formulations are suitably effective for the disinfection of medical surfaces, nor is it possible to readily draw comparisons to other biocides. The boundaries of current knowledge have been limited by the large diversity of photosensitisers available, which

has resulted in few in depth studies on a specific agent. As of the 30th September 2019, neither photosensitisers nor singlet oxygen have been approved for use as biocidal products within the European Union (European Chemicals Agency, 2019). A detailed study which assess a single optimised formulation would provide useful information on the strengths and limitations of photosensitiser technology.

1.8 Study aims

This study seeks to investigate the suitability of photosensitiser chemicals as alternative biocides for the disinfection of medical surfaces. This will be achieved by developing a formulation which exhibits optimal biocidal activity against vegetative bacteria. By elucidating its mechanism of action and determining its efficacy against all the major classes of microorganisms which contaminate medical surfaces, it will be possible to determine whether photosensitisers are suitable for high-level disinfection processes. Using an automated endoscope reprocessor as a case study device and through evaluating its ecotoxicological profile and cost of production, the real-world scalability of photosensitiser technology will be considered.

Chapter 2.

General Materials and Methods

2.1 Materials

2.1.1 Chemicals & storage conditions

Unless noted to the contrary, all chemicals used in this study were sourced from Sigma Aldrich. Stock solutions of chemicals were stored in the refrigerator at 4ºC except for surfactants, liquid media, buffers and diluent; these were stored at room temperature in the dark.

2.1.2 Preparation of formulations

Toluidine blue O (TBO) was the primary photosensitiser used during the development of formulations used in this study. TBO stocks were prepared by dissolving in sterile deionised water and refrigerating in the dark at 4ºC to prevent photodegradation. Other major formulation components include MGDA (BASF), various surfactants and pH modifying agents. These are discussed in more detail in section 3.2. Formulations were prepared on the day of use from refrigerated stock solutions and allowed to equilibrate to test temperature (20ºC) for 30 minutes in the dark prior to use.

In Chapter 3, the composition of the formulation varied significantly during optimisation and is detailed throughout the chapter. The optimised formulation used during Chapters 4, 5 and 6 (Formulation TCM+S) consisted of: 40 µM TBO, 10 mM MGDA, 15 mM sodium $NaHCO_3$, 10 mM Na_2CO_3, 0.01% Plurafac LF 901 (BASF) and 0.01% Praepagen TQ (BASF); pH was adjusted to 10.2.

2.1.3 Media

Liquid cultures of organisms were prepared using tryptone sodium broth (TSB) (Oxoid). Unless otherwise stated, tryptone sodium agar (TSA) was used for recovery of organisms and for maintenance of fridge stocks. TSA plates were obtained pre-poured from E&O Laboratories. TSB was stored at room temperature in the dark whilst TSA plates were stored at 4ºC until use.

2.1.4 Microbial diluents

Diluents were used for the preparation of microbial suspensions, serial dilutions, and to wash cells. The major diluents used throughout this study are included in table 2.1.

Table 2.1: Buffers and diluents used in this study.

Buffer / Diluent	Composition
Tryptone sodium chloride (TSC)	1 g/L tryptone; 8.5 g/L sodium chloride; pH 7.4
Phosphate buffered saline (PBS), prepared from tablets (Sigma Aldrich)	137 mM NaCl; 2.7 mM KCl; 10 mM phosphate; pH 7.4
Sodium cacodylate buffer	0.1 M sodium cacodylate; pH 7.4

2.1.5 pH adjustment

Adjustments to pH were achieved by adding 1M hydrochloric acid or 1M sodium hydroxide dropwise to solutions whilst being continuously mixed by magnetic stirrer. Changes in pH were continuously monitored using a FE20 FiveEasy benchtop pH meter (Mettler Toledo) until the desired pH was reached.

2.1.6 Sterilisation of materials

Media, diluents and plasticware were sterilised by autoclaving for 15 minutes at 121ºC / 100 kPa (British Pharmacoepia Commission, 2008). Due to their sensitivity to heat, bovine serum albumin (Fisher Scientific) and components of the formulation (MGDA, pH modifying agents, surfactants) were sterilised by filtration through Minisart 0.2-micron membrane filters (Sartorious).

2.1.7 Light source

Due to their low production cost, ease of use and low heat emission, light emitting diodes (LEDs) were chosen as the photosensitiser excitation source. An Eagle L330F/FW LED floodlight was used for photodisinfection experiments (Electrovision, 2019). This light source had options for light output at three different wavelengths, including 420 nm (blue), 525 nm (green) and 630 nm (red). The red-light option was used alone during the experiments detailed here.

To standardise the distance between the light source and surfaces, the lamp was placed over a light box made from expanded polystyrene. The area directly beneath the red LEDs was outlined with a permanent marker so that test inocula would be placed in standardised positions to minimise variability.

2.1.8 Validation of emission wavelength

The emission wavelength of the red LEDs in the light source was validated by measuring the emission spectrum using a Maya2000 Pro spectrometer (Ocean Optics) in tandem with OceanView v1.5.2 software (Ocean Optics). The LED lamp exhibited a monochromatic peak at 630 nm.

2.1.9 Measurement radiant flux

The intensity of electromagnetic energy emitted by a light source or received by a surface is defined by the term radiant flux, which can be expressed in watts (W) or Joules per second (Fitt & Thornley, 2002). Likewise, irradiance is a measurement of radiant flux over time and is measured in W/minute. Radiant flux received by samples at differing distances from the source was measured using a S121C standard photodiode power sensor (Thorlabs) with its accompanying software (PM100 Optical Power Meter Utility version 5.4; Thorlabs). Radiant flux was measured at distances of 55 and 75 mm from the LED source, which was equivalent to the distances used in the experiments described in this work. As in 2.1.8, light measurements were performed in a dark room. The results of this test are described in table 2.2.

Table 2.2: Light source radiant flux and irradiance.

Test Format	Distance from LED (mm)	Radiant flux (mW/cm^2)	Irradiance (mW/min)	Energy (J/second)
Suspension tests in cuvettes	75	3	180	0.18
Surface carrier tests and suspension tests in 35 mm tissue culture dishes	55	5	300	0.30

2.1.10 Test organisms

The basins of automated endoscope reprocessors can become contaminated by a diverse range of microorganisms during normal use. The formulations developed throughout this study were tested against a number of microbial species and strains, as described in table 2.3.

Table 2.3: List of microorganisms used in this study.

Type	Species	Strain
Gram-positive bacteria	*Staphylococcus aureus*	NCTC 10788
	Enterococcus hirae	NCTC 13383
	Deinococcus radiodurans	ATCC 13939
Gram-negative bacteria	*Escherichia coli*	ATCC 10798
	E. coli (MS2 host)	ATCC 15597
	Pseudomonas aeruginosa	NCTC 13359
Mycobacteria	*Mycobacterium smegmatis*	NCTC 8159
	M. avium	NCTC 15769
	M. terrae	NCTC 15755
Bacterial endospores	*Bacillus subtilis PS 533*	Isogenic derivatives of Strain 168
	B. subtilis PS3394	
	B. subtilis PS578	
Fungi	*Candida albicans*	ATCC 10231
	C. auris	DSM 21092
	Aspergillus brasiliensis	NCTC 16404
Non-enveloped viruses (phage)	MS2 Bacteriophage	ATCC 15597-B1

NCTC: National Collection of Type Cultures

ATCC: American Type Culture Collection

DSM: Leibniz Institute DSMZ - German Collection of Microorganisms and Cell Cultures

2.1.11 Storage and maintenance of organism stocks

Long-term glycerol stocks were prepared immediately upon receipt of organisms. Overnight cultures of organism were prepared by resuspending the freeze-dried pellet in 1 mL TSB. 500 µL aliquots of these suspensions were then transferred to 10 mL of TSB and incubated at 37ºC overnight (18-hours). To eliminate any risk of contamination during washing and resuspending, 500 µL aliquots of the overnight culture were mixed with equal volumes of 80% sterile glycerol in general long-term storage cryovials (Nalgene; Thermo Fisher Scientific) and stored at -80ºC. Streak plates were prepared with the remaining culture to validate that colonies exhibited a single morphology and the stocks were pure.

Shorter-term stocks were prepared by isolating a single colony on an inoculation loop and suspending in a vial of Protect beads (Thermo Fisher Scientific). Vials were then vortexed to coat the beads and the supernatant removed; vials were then stored at -20ºC. Working stocks of bacterial species were maintained on TSA plates which were sealed with Parafilm M (Bemis) and stored at 4ºC for 6-8 weeks before replacing with fresh stocks from protect beads.

2.1.12 Spectral measurements

Changes in the spectral characteristics of formulations were measured by loading 100 µL aliquots of sample into wells of transparent flat-bottom 96-microwell plates (Thermo Fisher Scientific). Absorbance spectra were then analysed in an Infinite M200 plate reader (Tecan) across a 350-950 nm waveband with a resolution of 2 nm.

2.2 Biocidal efficacy testing

2.2.1 Biological replicates

Unless otherwise noted, three biological replicates were used for each of the experiments described in this study. These were obtained from three independently cultured groups of organisms which were treated separately.

2.2.2 Bacterial culture conditions

The culture conditions described in this section refer specifically to the culturing of *S. aureus*, *E. coli*, *P. aeruginosa* and *E. hirae*. These organisms were used during the optimisation of the formulation (Chapter 3) and in determining the effect of treatment on target cells (Chapter 4). In Chapter 5, the optimised formulation was tested against an extended panel of challenge organisms which have more complex culture requirements; these are detailed in the respective chapter.

To prepare liquid overnight cultures, a single colony was taken from a working culture plates (2.1.11) using an inoculation loop. This was suspended in 10 mL sterile TSB and incubated aerobically overnight (18 hours) at 37ºC in an ICH110 stationary incubator (Memmert).

Working test suspensions were prepared by centrifuging overnight cultures at 3500 G for 10 minutes at 20ºC. The supernatant was then discarded, and the pellet washed in TSC and centrifuged again. The resulting pellet was resuspended in 10 mL TSC. 2 g of 3 mm sterile borosilicate glass beads (Sigma Aldrich) were then added to each suspension and vortexed for a minute to separate microbial aggregates. Using an Ultrospec 3100 pro UV/Vis spectrophotometer (Amersham Biosciences), additional TSC was added to each suspension to adjust A_{630} to 0.75 ± 0.05. This rendered a concentration of 1.5-5 x 10^8 colony forming units/mL (CFU/mL), when suspensions were quantified by the Miles & Misra method.

2.2.3 Quantification of microorganisms by Miles and Misra method

Viable counts of bacteria, in CFU/mL, were determined by the Miles and Misra recovery method (Miles et al., 1938). A 10-fold dilution series was prepared by adding a 100 µL aliquot of sample to 900 µL neutraliser (10^{-1} dilution), vortexing and repeating down a series of 900 µL aliquots of TSC. Three 20 µL aliquots of each dilution were then dropped onto labelled sectors of TSA plates. After allowing spots to dry onto the agar, plates were inverted and incubated overnight.

Colonies were counted for each drop and the average count per sector was recorded. To calculate total viability of bacteria in CFU/mL the average colony number was multiplied by the dilution factor and 50 (20 µL drops are $^{1}/_{50}$ of 1 mL). As 20 µL aliquots were used and the smallest dilution factor counted was 10^{1}, the lower limit of detection of this quantification method was 500 CFU/mL; bacterial counts lower than this value were recorded as <500. Changes in bacterial viability were rendered as $\log_{10}$-reductions using the equation Log_{10} (A/B), where A represents the viability of the untreated control group and B the viability of tested groups.

2.2.4 Quantification of microorganisms by spread plating method

In some experiments, surviving microorganisms were quantified using the spread plating method, as described in the EN 13697 standard. After preparing a 10-fold serial dilution series, microbial suspensions were added to agar plates. The suspension was then spread over the surface of the plate using disposable L-shaped spreaders; after drying for 30 minutes, plates were inverted and placed in the incubator. The type of agar and volume of suspension used for spread plating varied depending on the test organism; further information is provided in the respective methodologies of these experiments.

2.2.5 Biocide neutralisation

For accurate measurement of the biocidal activity of disinfectants, it is essential to quench any residual biocidal activity following contact so that efficacy is not overestimated. This involves diluting samples 1:10 in neutraliser at the end of the contact time; this both dilutes and chemically quenches the disinfectant product to a level which is non-biocidal. In the case of photosensitisers, removal of the light source also contributes to neutralisation. In this study formulations were quenched using a universal neutraliser, prepared in accordance to EN 13727 (table 2.4). Neutraliser was prepared in deionised water, was sterilised by autoclaving and was stored for up to four weeks at 4°C. For some experiments, double strength neutraliser was required; this contained double the concentration of each component.

Table 2.4: Contents of universal neutraliser (British Standards Institute, 2015a).

Component	Concentration (g/L)
Polysorbate 80	30
Saponin	30
Sodium Thiosulphate	3
L-α-lethicin	3
L-histidine	1

2.2.6 Validation of neutraliser efficacy and toxicity

Technical guidelines published by the British Standards Institution (2015a) state that neutralisers must be validated to ensure they are both effective at quenching biocidal activity and non-toxic to microbial cells. The neutraliser was validated against vegetative cells of *S. aureus* and *E. coli* only. Out of the organisms tested in this study, these species are considered to be most susceptible to damage according to McDonnell & Burke's hierarchy of microbial resistance to disinfectants (McDonnell & Burke, 2007). The absence of toxicity to these organisms would indicate it is unlikely to be toxic to more robust microorganisms such as mycobacteria and bacterial endospores, fungi and non-enveloped viruses.

To determine the toxicity of the neutraliser, 100 µL of test suspensions of *S. aureus* and *E. coli* (1.5-5 x 10^8 CFU/mL) were suspended in 900 µL universal neutraliser and incubated for 60 minutes. For comparison to an untreated control, test suspensions were also added to an equivalent volume of TSC. Following incubation suspensions were serially diluted and survival was quantified using the Miles and Misra method (2.2.3). As indicated by EN 13727, the neutraliser was validated as non-toxic as there was less than a 25% reduction in viability after treatment with the neutraliser, compared with the untreated control group.

In order to validate its ability to quench the residual biocidal activity of the formulation, neutraliser efficacy tests were performed using the optimised formulation described in 2.1.2. 100 µL of 0.3 g/L bovine serum albumin was added to 800 µL of the formulation and vortexed. 100 µL of this mixture was then transferred to 800 µL of universal neutraliser and incubated for 5 minutes. 100 µL of test suspensions of *S. aureus* and *E. coli* were then added to each tube and incubated for 30 minutes. Bacterial survival was quantified using the Miles and Misra method (2.2.3) and compared to an untreated control.

2.2.7 Test temperature

The objective of this project is to deliver a low-cost and environmentally friendly alternative to traditional disinfectants for automated endoscope reprocessors. Consequently, the formulation should be active at low temperatures so as to not require heating. Therefore, with the exception of the experiment described in section 3.2.10, all efficacy tests were performed in a temperature-controlled laboratory at 20°C.

2.2.8 Suspension tests

Phase 1 determination of the biocidal efficacy of disinfectant products utilises suspension tests. For disinfectants used in medical areas, this is described by the EN 13727 standard (British Standards Institute, 2012).

2.2.7.1 Reaction vessel

As photodisinfection is a light-dependent process, it was anticipated that the dimensions of the test suspension may have an effect on biocidal activity due to optical effects. During optimisation of the formulation (Chapter 3), 2 mL polystyrene cuvettes were used as the reaction vessel as this standardised test suspension dimensions as 10 mm^3. In later experiments (Chapters 4 and 5) suspensions were treated by transferring the 960 µL of test suspension to 35mm-diameter sterile tissue culture dishes (Greiner Bio-One International); this facilitated treatment of films of test suspension with a thickness of 1 mm.

Cuvettes containers were disinfected prior to use by placing under a UV lamp for 30 minutes; this method of disinfection was validated by flushing with 1 mL of TSB, transferring to a sterile 7 mL bijou tube (Fisher Scientific) and incubating overnight to check for the absence of growth.

2.2.7.2 Interfering substance

Contamination of surfaces by microorganisms usually occurs alongside the deposition of dirt and grime. To account for the effect of this soiling on biocidal activity, interfering substances were added to the efficacy tests described in this thesis. Interfering substances were prepared in TSC as a 10X stock for suspension tests and 2X stock for surface carrier tests.

As in accordance with EN 13727, clean conditions were simulated by the addition of 0.3 g/L bovine serum albumin fraction V (BSA; Fisher Scientific) to the reaction mixture. Dirty conditions followed the EN 14248 standard and were simulated by the addition of 3 g/L BSA and 3 mL/L sheep erythrocytes. Sheep erythrocytes were prepared by centrifuging whole defibrinated sheep blood (Thermo Fisher Scientific) at 800 G for 10 minutes, washing with TSC and centrifuging again. This was repeated until the supernatant was clear (approximately 3 times).

2.2.7.3 Test procedure

In suspension tests, the formulation was tested at 80% of its in-use concentration; this is typical for ready-to-use products tested using the EN 13727 standard due to the addition of interfering substances and test suspensions of microorganisms.

800 µL aliquots of formulation were added to sterile microcentrifuge tubes. Immediately prior to illumination, 100 µL of interfering substance and 100 µL of bacterial suspension (1.5-5 x 10^8 CFU/mL) was added. After mixing by vortex, the contents were transferred to the reaction vessel and placed under the LED lamp for illumination. After treating for the appropriate contact time, the LED was turned off and the sample diluted 1:10 in neutraliser. Samples were incubated for 5 minutes to allow neutralisation to occur and survival was quantified by the Miles & Misra method (2.2.3).

2.3 Statistical analyses

To facilitate statistical comparison between treatment groups, three biological replicates were used during most experiments outlined in this thesis. The distribution of values around the mean value was calculated by standard deviation (SD); all error bars on the graphs presented throughout this thesis describe SD.

Production of graphs and statistical analyses were performed using Prism 8.1.0 (GraphPad Software). To facilitate testing of multiple means, one-way and two-way analysis of variance (ANOVA) were used to determine whether there were any statistically significant differences in the data. One-way ANOVA was used when comparing interventions with a single time point whereas two-way ANOVA was used when we wanted to compare paired data across time-points (e.g. compare paired values at 0.5 min, 1 min and 5 min). The cut-off value used to denote statistical significance (α) was <0.05.

Several post-hoc tests were used in this study to facilitate multiple comparisons between means including Tukey's, Dunnett' and Šidák's. These methods were chosen over conducting multiple T-tests as they make adjustments to compensate for the alpha inflation which occurs when making multiple comparisons; this makes them better at minimising type-I errors (i.e. false-positive findings) (McHugh, 2011). Tests were chosen based on the type of comparisons to be made and are specified in figure legends. Examples of the use of each of these post-hoc tests are included in table 2.5.

Table 2.5: Multiple comparison tests for statitistical analyses.

Post-Hoc Test	Comparison
Tukey	Comparison of all pairwise combinations after one-way ANOVA
Dunnett	Comparison of all tested means to control column after one-way ANOVA
Šidák	Comparison of all pairwise combinations at each time point after two-way ANOVA

Chapter 3.

Formulation Development

3.1 Introduction

3.1.1 The design of disinfectant formulations

Contrary to being simple solutions of antimicrobial compounds, many disinfectant products are co-formulated withof carefully selected ingredients. The pairing of active compounds and excipients can improve microbicidal activity and confer additional properties to the product. Solvents, chelators, surfactants, pH-modifying and buffering agents can all have profound effects on the biocidal activity of disinfectants whilst thickeners, stabilisers and organoleptic compounds (colours and fragrances) can be added to improve product usability, shelf-life and marketability (Maillard, 2013).

The design of a biocide formulation is an evolutionary process informed by the product requirements. High-level disinfectants should demonstrate efficacy versus vegetative bacterial cells, fungi, viruses, mycobacteria and bacterial endospores (Rutala & Weber, 2011). To fulfil the aims of this project, a photosensitiser-based formulation should possess a rapid broad spectrum of microbicidal activity, afavourable ecotoxicological profile and low wholesale costs. For products designed for the disinfection of automated endoscope reprocessors (AERs), particular attention should be paid to demonstrating activity against *P. aeruginosa* as this organism is a common source of machine contamination and gives rise to pseudo-outbreaks (Robertson et al., 2015).

3.1.2 Standardised testing

Under the EU Biocides Regulation 528/2012 (EU BPR), biocidal products must be assessed using standardised tests to substantiate label claims of efficacy against microorganisms (European Parliament & Council of the European Union, 2012). These standards establish minimum efficacy requirements for microbicidal activity and set a level playing field for all products. By standardising assessment, end-users are better able to compare products objectively. Selecting which testing standard to use is dependent on the end-application and informed by the EN 14885 standard (British Standards Institute, 2018). For products designed for use in medical areas, basic bactericidal efficacy can be evaluated using suspension tests described in the EN 13727 standard (British Standards Institute, 2012) and can be followed up with more rigorous testing such as is described in EN 13697 (British Standards Institute, 2015a).

3.1.3 Photosensitiser properties

3.1.3.1 Ionic charge

As discussed in Chapter 1, photosensitisers consist of a central aromatic chromophore with functional side chains termed auxochromes. Auxochromes are vital to the functioning of a photosensitiser as they determine many of its properties, including ionic charge. PS can be cationic, anionic or non-ionic, depending on the auxochromes present. Analogous to quaternary ammonium compounds, cationic PS contain basic functional groups such as amines which deprotonate to yield positively charged residues upon ionisation. Conversely, anionic photosensitisers are rich in acidic groups and ionise to yield negatively charged molecules. Cationic PS have been observed to self-promote their own uptake into microorganisms due to the negative charge of the microbial cell surface (George et al., 2009) and are noted to be more potent antimicrobials compared to anionic and uncharged photosensitisers (Hamblin & Hasan, 2004; Tegos et al., 2009).

3.1.3.2 Quantum yield

Photosensitisers exhibit considerable variation in the efficiency at which they generate singlet oxygen ($^1O_2$). This property is measured by its quantum yield (Φ), which is defined as the number of molecules of $^1O_2$ produced per photon absorbed. Since the absorbance of one photon can only ever yield a single molecule of singlet oxygen as a product, the absolute value of Φ lies between 0 and 1. Φ is affected by photosensitiser structure and environmental factors such as the solvent (Durmuş, 2011). Due to the difficulties of measuring absolute yields of $^1O_2$, Φ are often reported as a value relative to that of known photosensitisers such as methylene blue; by comparing their ability to decompose fluorescent singlet oxygen probes such as diphenylisobenzofuran (DPBF), these authors are able to ascertain a relative singlet oxygen yield (Phoenix et al., 2003; Kotska et al., 2006). For example, Phoenix et al. (2003) used methylene blue as a standard and reported its value at 1.0; all other photosensitisers were compared to this value and reported as “relative quantum yield”.

3.1.3.3 Lipophilicity

Lipophilicity denotes how well a compound partitions into non-polar phases such as organic solvents and lipid membranes. The lipophilicity of a compound is measured by its octanol/water partition coefficient (P). A positive P indicates that the substance will preferentially partition into non-polar phases whilst a negative P value indicates that the compound better dissolves in polar solvents such as water (i.e. hydrophilic).

The lipophilicity of biocides determines the ways they interact with target sites, such as lipid-rich cell membranes (Byers & Sarver, 2009). Despite being a poorer cross-linking agent than glutaraldehyde, ortho-phthalaldehyde (OPA) exhibits greater mycobactericidal activity due to the presence of an aromatic group which substantially increases its lipophilicity (Simons et al., 2000). Likewise, when comparing the biocidal activity of aromatic alcohols, 5-phenyl-1-pentanol exhibits superior antimicrobial activity than 2-phenylethanol; this is due to a longer alkyl chain between the alcohol and phenyl groups in the former, which increases its lipophilicity (Fraud et al., 2003). Greater alkyl chain length in quaternary ammonium compounds has also been correlated with improvements in antibacterial activity (Li et al., 2012).

In photosensitisers derived from the same chromophore, variations in lipophilicity are determined by the auxochromes. Auxochromes with long alkyl chains but lacking polar functional groups such as carboxylic acids and amines increase the lipophilicity of a photosensitiser. In a study using lethicin-based micelles, Bacellar et al. (2014) observed that the lipophilic photosensitisers dimethyl methylene blue and DO15 were superior at liberating liposome-encapsulated fluorophores than TBO and methylene blue, which are hydrophilic. It is unclear whether these findings would translate into greater biocidal activity against microorganisms, which contain diffusion channels and charged/hydrophilic regions which may also be targets of photosensitisation.

3.1.4 Selection of toluidine blue O as the lead photosensitiser

The phenothiazine toluidine blue O (TBO) was selected as the lead compound for formulation development in this thesis due to its cationic charge, solubility in water and a comparable quantum yield to other phenothiazines (Bacellar et al., 2014). TBO has been reported as effective against a broad spectrum of organisms including bacteria, yeasts and mycobacteria (Feese et al., 2009; Pupo et al., 2011; Tseng et al., 2018). TBO has an established safety record and several products containing this agent are licensed for use *in vivo* for cancer diagnostics (Lejoy et al., 2016) and endodontic disinfection of root canals (Bonsor et al., 2006). TBO has also been investigated for use in photodynamic therapy of diabetic foot ulcers (Tardivo et al., 2017). This favourable toxicological profile means that accidental exposure to this agent is unlikely to cause harmful side effects. TBO is a metachromatic dye and has two major absorbance peaks at 630 and 590 nm which correspond to monomers and dimers respectively (Usacheva et al., 2002). The molecular structure of toluidine blue O is illustrated in figure 3.1, overleaf.

3.1.5 New methylene blue as a lipophilic alternative

New methylene blue (NMB) is a phenothiazine derivative characterised by longer alkyl chains on the auxochrome groups. The increase in chain length confers greater hydrophobicity on the molecule and this is reflected by octanol/water (O/W) partition coefficient of +1.20 P; this is contrasted to -0.21 P for TBO (Phoenix et al., 2003). As Gram-negative organisms are surrounded by a hydrophobic outer membrane, it was hypothesised that new methylene blue may better interact with the bacterial surface and possess greater bactericidal activity than TBO. The relative singlet oxygen quantum yield of new methylene blue has also been reported as approximately 1.5 times greater than TBO (Phoenix et al., 2003). When combined with potentially improved membrane interactions, this greater quantum yield may substantially improve activity. Figure 3.1 contrasts the differences in the molecular structure of TBO and NMB which give rise to their differing lipophilicities.

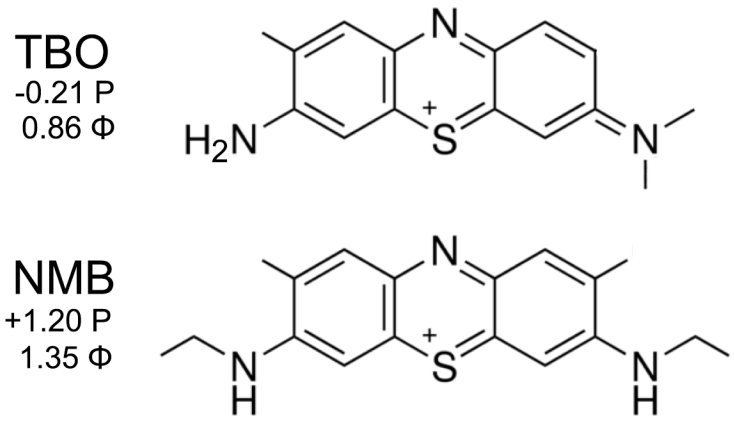

Figure 3.1: Molecular structures of toluidine blue O (TBO) and new methylene blue (NMB). Note the presence of several additional alkyl chains throughout the structure of NBM, which confer a substantially greater degree of lipophilicity. P denotes lipophilicity whilst Φ denotes singlet oxygen quantum yield relative to methylene blue. Supporting data obtained from Phoenix et al. (2018).

3.1.6 Biocide concentration and adsorption isotherms

It has long been established that microbial inactivation is dependent of both biocide concentration and time (Cowles, 1940). The relationship between the dilution of a biocide and rate of disinfection is described by its concentration exponent (η) which is defined as the difference in time required to achieve the same level of microbial inactivation using two different concentrations of a biocide (Maillard, 2013). As a general rule, increasing the concentration of a biocide means that shorter contact times are required to achieve the same level of microbial inactivation. This is due to a greater availability of active species which can inflict injury on the target organisms. This relationship means that disinfection cycles can be accelerated rather simply by increasing the concentration of a biocide.

With the advent of modern analytical methods, more sophisticated models of biocide uptake have been developed. Adsorption isotherms describe the relationship between biocide concentration and uptake. The shape of the isotherm can provide insight into the method by which an antimicrobial interacts with target cells. As a basic dye, TBO uptake can be modelled with a Langmuir (i.e. L-shaped) adsorption isotherm (Denyer & Maillard, 2002), as illustrated in figure 3.2. Whilst adsorption onto the cell surface is directly proportional to biocide concentration in the initial stages, adsorption begins to taper off and halt once target sites become fully saturated. After this point, the addition of more TBO will not lead to any further adsorption onto target sites.

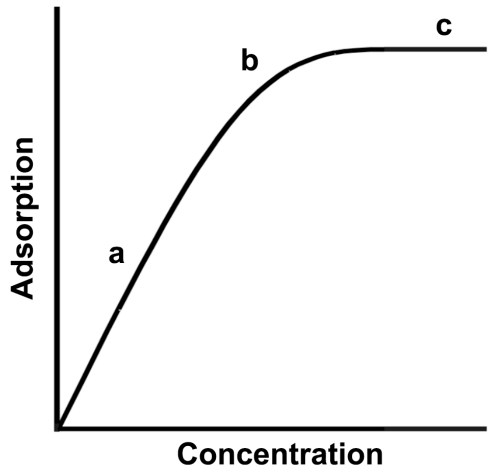

Figure 3.2: Langmuir adsorption isotherm of cationic dyes such as TBO. During the initial phase, adsorption is directly proportional to dye concentration (a). As more target sites become occupied, the rate of adsorption begins to slow (b). In the final phase, all target sites become occupied and so no further adsorption can occur (c).

In the case of photosensitiser dyes, the relationship between concentration and biocidal efficacy may be more complex due to its light-dependent mechanism of action. As the production of singlet oxygen is facilitated by excitation of the photosensitiser, light transmission through the formulation may play an important role in determining biocidal activity. It is hypothesised that, as the concentration of TBO increases, the biocidal activity of the formulation will increase. However, after reaching an optimal point, further addition of TBO may impair biocidal activity by inhibiting light transmission through the formulation.

3.1.7 Formulation pH

The acidity or alkalinity of a system is proportional to the concentration of proton (H^+) concentration and is expressed as pH. The pH of biocides can have a strong impact on its microbicidal activity due to a two-fold effect of modifying the biocide itself and microbial target sites (Maillard, 2013). Modification of microbial target sites can consist of protonation or deprotonation and affects their charge. For example, deprotonation at alkaline pH exposes negatively charged target sites (e.g. NH^-), which are susceptible to attack by cationic biocides and copper ions (Sharan et al., 2010). The effect of pH on the biocide itself occurs by affecting the degree of dissociation. Many biocides consist of an acid and conjugate base in equilibrium. Modifying the pH can therefore unbalance this equilibrium in a way which liberates the active form of the biocide, thus enhancing its microbicidal activity.

Biocides which exhibit greater activity at alkaline pH include glutaraldehyde (Fraise, 2013) and quaternary ammonium compounds (Lindstedt et al., 1990). The addition of a base to these biocides sometimes precedes use; glutaraldehyde-based products are typically stored under acidic conditions to promote product stability and are activated prior to use through the addition of sodium bicarbonate (Fraise, 2013). In the case of cationic dyes, Chen et al. (2009) reported higher efficacy of methylene blue at pH 9.0 compared to pH 5.0. A follow up study indicated that this increase in activity is also due to increased triplet lifetime and singlet oxygen quantum yield in the ionised state (Chen et al., 2011).

Using the Henderson-Hasselbalch equation, the pH of a given solution can be determined using its concentration and the $\log_{10}$ of its acid dissociation constant (pK_a). A lower pK_a value denotes a greater readiness to dissociate at lower pH. Some biocides can have multiple dissociation constants due to the presence of multiple ionisable moieties. TBO has two pK_a values at 2.6 and 11.6, which correspond to the two nitrogenous auxochrome groups flanking the chromophore (Sabnis, 2010). The amide auxochrome dissociates at low pH and yields a positively charged residue. Conversely, the amine auxochrome dissociates at high pH and yields a negatively charged residue.

Buffering agents stabilise the pH of a solution and resist changes in pH. They consist of an acid-conjugate base pair which exist in equilibrium and can both donate or accept protons, depending on the direction of pH change. Many buffering agents are available. They are chosen based on their effective buffering range and compatibility with other formulation components. Popular biological buffering agents include citrate, phosphate, carbonate and borate buffers, though many more exist.

3.1.8 Disinfection temperature

Much like the concentration of an active ingredient, temperature can have a profound impact on disinfection rates. This is due to increased reaction kinetics which increases the speed at which a disinfectant can cause damage to target microorganisms. The relationship between a disinfectant's use temperature and its microbicidal activity can be expressed by its temperature coefficient (Q_{10}), which is calculated from the fold-change in biocidal activity observed upon a 10ºC shift in temperature (Rogers, 2014).

3.1.9 Chelating agents

Chelating agents (chelators) are utilised widely for cleaning and disinfection. They contain multiple groups of unpaired electrons which facilitates the formation of high-affinity coordination complexes with metal ions. Metal ions, which can be prolific in hard water, can impair the cleaning performance of anionic surfactants by forming insoluble precipitates. Chelators can counteract this effect and soften hard water by coordinating excess cations. Divalent cations (Fe^{2+}, Cu^{2+}, Mn^{2+}) also catalyse the Fenton reaction, which can rapidly decompose biocides such as hydrogen peroxide and sodium hypochlorite. At sufficiently high ratios of ligand to metal (e.g. 10:1), chelators can stabilise these agents (Engelmann et al., 2003; Hutcheson et al., 2004).

Metals are also important cofactors in degradative enzymes and maintain biological membranes. Chelating agents can also be used to extend the spectrum of activity of biocides against bacterial species. The outer membrane (OM) of Gram-negative organisms is a barrier to the penetration of antimicrobials; hydrophilic biocides are poorly soluble through this membrane and must instead transverse porin channels to enter the periplasmic space (Denyer 1990; Denyer & Maillard, 2002). Even upon reaching the periplasm, the presence of degradative enzymes, biological quenching molecules and efflux pumps can actively prevent antimicrobial agents from reaching intracellular targets and promote their export from the cell (Zhou et al., 2015).

The outer membrane of Gram-negative bacteria consists of negatively-charged lipopolysaccharide (LPS) molecules, which are stabilised by divalent cations such as Ca^{2+}

and Mg^{2+} (see fig. 3.3). These cations form hexahedral complexes between phosphate and carboxylate groups within the lipid A core of LPS and promote outer membrane cohesion and stability (Wu et al., 2013). Loss of calcium cations causes membranes to destabilise and reanngage to more thermodynamically stable configurations (Clifton et al., 2015) and so chelators such as EDTA can be used to potentiate the activity of antimicrobials against Gram-negative species such as *Pseudomonas aeruginosa* (Walker et al., 2002; Lambert et al., 2004; Umerska et al., 2018). Chelators have also been shown to improve the activity of antimicrobials against bacterial biofilms (Cavaliere et al., 2014; Liu et al., 2017). Calcium plays an important role in the production of extracellular polymeric substance (EPS) by biofilm organisms (Ozerdem Akpolat et al., 2003) and its chelation can aid in the dispersal of biofilms (Banin et al., 2006).

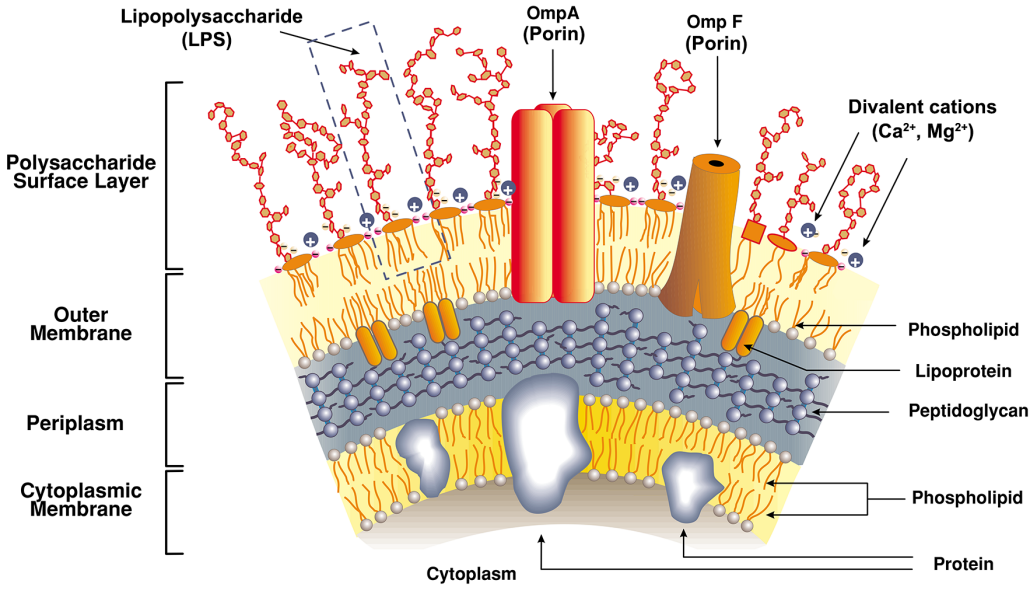

Figure 3.3: Architecture of the outer membrane of Gram-negative bacteria. The external face of the outer membrane contains a high density of negatively charged lipopolysaccharide (LPS). Stability of the outer membrane is maintained by the presence of positively charged divalent cations such as Ca^{2+} and Mg^{2+}. Access to the periplasm and cytoplasmic membrane by hydrophilic solutes is achieved via diffusion through porins (e.g. OmpA/F) or by disruption of the outer membrane. Adapted from Alexander & Rietschel (2001). Reproduced with permissions. © SAGE.

Ethylenediamine tetraacetic acid (EDTA) has been reported to improve the activity of photosensitisers against Gram-negative species (Bertoloni et al., 1990; Usacheva et al.,

2006) and *Staphylococcus biofilms* (Sharma et al., 2008). Addition of excess calcium quenches this effect, indicating that chelation of calcium is responsible for improved biocidal activity (Usacheva et al., 2006). Interestingly, George et al. (2009) reported a reduction in methylene blue uptake in the Gram-negative *Actinobacillus actinomycetemcomitans* when the photosensitiser was co-applied with EDTA, though did not perform any measurements on changes in its biocidal activity. Whilst EDTA may reduce the overall uptake of methylene blue, permeablisation of the outer-membrane could ensure that a larger amount was able to reach intracellular targets (i.e. the *quality* of photosensitiser uptake was greater, even though the overall *quantity* decreased).

Whilst EDTA is an effective chelator, it is poorly biodegradable and can accumulate in the environment; a new generation of chelating agents have therefore been developed to reduce the ecological impact of these widely utilised compounds (Pinto et al., 2014). Methylglycine diacetic acid (MGDA) is a promising alternative to EDTA and passes the OECD requirements for "ready biodegradability" (OECD, 1992; BASF, 2007). MGDA can also operate over a broader pH range and has a greater affinity for calcium ions than EDTA (BASF, 2007). The addition of MGDA to TBO-based formulations is anticipated to improve their biocidal activity against Gram-negative organisms such as *P. aeruginosa* without compromising its environmental profile.

3.1.10 Surfactants

3.1.10.1 Properties of surfactants

Surface active agents (surfactants) are amphiphilic compounds which contain hydrophilic "head" and hydrophobic "tail" regions. Surfactants facilitate the formation of interfaces between otherwise immiscible compounds and allow lipid-based matter to be solubilised by aqueous solutions, and vice versa (Kronberg et al., 2014). When added to bulk aqueous solutions, surfactants first coat the interfaces as a monolayer; this conformation is the most thermodynamically stable as it minimises contact between their hydrophobic tails and a polar aqueous phase (Maibaum et al., 2004). At the "critical micellar concentration" (CMC) all interfaces become saturated and the addition of further surfactant to the bulk-phase results in the formation of micelles. These structures are thermodynamically favoured as hydrophilic heads may interact with the aqueous phase whilst hydrophobic tails are contained away from the polar phase (Maibaum et al., 2004). It is by this process that non-polar substances such as oil can be solubilised by aqueous cleaning products.

Surfactants can increase the wettability of surface disinfection and cleaning products. Wetting reduces the surface tension of a solution so that it spreads across a surface as a thin film, rather than forming beads and droplets. The propensity for a solution to spread across a hard surface is determined by two major factors: the critical surface tension (γ_c) of the surface and the surface tension (γ) of the solution. A solution's γ must be lower than a surface's γ_c in order to wet (Kronberg et al., 2014). γ can be reduced through the addition of surfactants; this process is rapid until the CMC is reached, after which further addition yields only modest decreases in γ (Kronberg et al., 2014). Increasing wettability will be necessary in the development process of photosensitiser-based formulations as these formulations are water-based whilst the surfaces of an automated endoscope reprocessor are constructed from polyvinyl chloride (PVC). For water, γ is 72 and for PVC γ_c is 39 (Kronberg et al., 2014).; therefore, surfactant-free formulations will not spread across PVC surfaces.

Surfactants can be broadly categorised as non-ionic, anionic or cationic based on the ionic charge of the head region. So far, no studies have attempted to determine the effect of surfactants on the biocidal activity of photosensitisers. Therefore, we aim to investigate this area of formulation to determine how these different classes of surfactant may affect biocidal activity against surface-dried bacteria.

3.1.10.2 Non-ionic surfactants

Non-ionic surfactants (NIS) have an uncharged head group and are compatible with a broad spectrum of ionic compounds, including anionic and cationic surfactants. They do not form complexes with dissolved cations and so their surfactant performance largely tolerates differences in water harness (St. Laurent et al., 2007). Non-ionic surfactants can likely be added to photosensitiser-based formulations to improve wettability without compromising biocidal activity. Due to reduced surface tension, the formulation may spread over the surface as a thinner film which may improve light transmission and biocidal activity.

3.1.10.3 Anionic surfactants

Anionic surfactants (AIS) are characterised by a negatively-charged head group. AIS are popular cleaning agents and account for up to 70% of worldwide surfactant consumption (Kronberg et al., 2014). Compared to other surfactant types, they are simple to synthesise and inexpensive to produce in large quantities. They also have a high propensity to form foams which can be useful for applications such as soil removal (Kronberg et al., 2014). A major drawback of AIS is their tendency to form insoluble precipitates with hard water cations, which can inhibit their cleaning performance (Noïk et al., 1987; Rodriguez & Scamehorn, 2001).

Anionic surfactants are known to interact with cationic photosensitisers and alter their spectral properties. The addition of sub-micellar concentrations of sodium dodecyl sulphate (SDS) to photosensitiser solutions leads to an initial decolourisation whereby the absorbance peak decreases substantially; addition of larger amounts of SDS leads to a reversal of this phenomenon and eventually causes the absorbance peak to hyper colourise and exhibit a greater absorbance intensity than surfactant-free solutions (Jebaramya et al., 2009; Edbey et al., 2015). Photosensitiser colouration is dependent on the donation of auxochrome electrons to the conjugated π system of the chromophore (Wainwright, 2009). Decolourisation at premicellar concentrations of SDS may occur due to the formation of aggregates between anionic SDS monomers and cationic photosensitisers, which disrupts the electron delocalisation responsible for colouration. Further addition of SDS leads to the formation of SDS micelles; these may disrupt dye-dimers and so micelle-incorporated photosensitisers would exist only in a monomeric form (Jebaramya et al., 2009).

3.1.10.4 Cationic surfactants

Cationic surfactants are popular antimicrobial agents employed in a wide variety of consumer and medical products as biocides and as preservatives. The most common examples include quaternary ammonium compounds (QACs) and esterquats. The head group of cationic surfactants interacts strongly with the negatively charged bacterial cell surface which facilitates initial sorption to the bacterial membrane. The hydrophobic tails then partition into the lipid portion of the cytoplasmic membrane and disrupts intermolecular forces between adjacent phospholipids; this leads to destabilisation and permeablisation of the membrane, loss of intracellular contents (e.g. K^+ and ATP) and depletion of the membrane potential (Luppens et al., 2001; Ioannou et al., 2007).

Popular examples of QACs utilised for disinfection and preservation include benzalkonium chloride (BZC), didecyl methyl ammonium chloride (DiDAC) and cetrimonium bromide (CTAB). Whilst Gram-positive bacteria tend to be most susceptible to the antimicrobial effects of these agents, biocidal efficacy of QACs has also been demonstrated against Gram-negative bacteria, fungi and enveloped viruses (Gerba, 2015). Mycobacteria, non-enveloped viruses and bacterial endospores are significantly more resistant to the biocidal effects of QACs (Best et al., 1990; Russel, 1990). Consequently, they are not recommended for disinfection of semi-critical devices and surfaces likely to be contaminated with these organisms (Yoo, 2018).

As membrane active agents, QACs can potentiate the action of other antimicrobial agents. For example, copper and benzalkonium chloride exhibit synergy when used in combination against vegetative cells and biofilms of *P. aeruginosa* (Harrison et al., 2008). Gorman & Scott (1979) reported considerable potentiation in the biocidal activity of glutaraldehyde against *Bacillus subtilis* endospores through the addition of cetrimide, which is a mixture of several QAC compounds. This effect appeared to be unique to formulations containing cetrimide and was independent of the pH; similar formulations containing a non-ionic surfactant (Solan E) exhibited considerably lower sporicidal activity despite the pH being almost equivalent (Gorman & Scott, 1979). As of yet, there have been no investigations into potential biocidal synergy between cationic surfactants and photosensitisers. It is reasonable to suggest that co-formulation of TBO with cationic surfactants may increase its biocidal activity, particularly against Gram-positive organisms.

Despite their widespread use, QACs are resistant to biodegradation. They are toxic to many organisms used in wastewater treatment and can form complexes with anionic surfactants; these complexes are insoluble and can accumulate in anoxic environments such as the bottom of water-treatment ponds where they are unable to be degraded (Zhang et al., 2015). In contrast, esterquats are a newer generation of cationic surfactant characterised by an ester linkage which is easily cleaved under aerobic and anoxic conditions (Garcia et al., 2000). Esterquats are considerably less environmentally persistent than QACs and are an attractive alternative for applications in which cationic surfactants are required (Mishra & Tyagi, 2007). Esterquats may also potentiate the biocidal activity of photosensitiser-based formulations.

3.1.10 Metal nanoparticles

Nanoparticles (NPs) are commonly defined as particles with at least one aspect measuring between 1-100 nm (Jeevanandam et al., 2018). The past decade has seen intensive growth in research interest in utilising nanomaterials for medical diagnostics, therapeutic agents and as drug delivery vehicles (Wilkinson et al., 2011; Dreaden et al., 2012; Singh et al., 2018). The small dimensions of nanoparticles confer incredibly high relative surface areas as well as distinct properties which differ from that of the bulk material. Some nanoparticles can exert antimicrobial effects directly whilst others enhance the activity of antibiotics and biocides (dos Santos et al., 2012; Alkawareek et al., 2019). NPs derived from titanium oxide and silver can be used as photosensitisers (Kubaka et al., 2014; Akram et al., 2016).

3.1.10.1 Optical properties of nanometals

Metal NPs exhibit unique optical properties which can be used to modulate the biocidal activity of photosensitisers. As a conductive material, metal NPs contain a delocalised field of conductive band electrons. In those derived from noble metals (i.e. silver, gold and platinum), electrons at the surface of the NP collectively resonate at the same frequencies as visible light. This oscillation is referred to as the surface plasmon and facilitates strong interactions between nanoparticles and light. Resonance at specific frequencies causes certain wavelengths of light energy to be absorbed by the nanoparticle whilst others are transmitted, resulting in bright colouration (Kristensen et al., 2016). The resonance frequency of surface plasmons is determined by factors including the material, size and shape and so nanoparticles can be engineered for specific optical applications (Eustis & El-Sayed, 2006).

Interactions between incident light and surface plasmons allow nanoparticles to strongly affect light-dependent processes such as fluorescence. In this process light fields around a nanoparticle can be enhanced by many orders of magnitude and coupling between nanoparticle surface plasmons interactions and fluorophores can enhance photoactivation and improve quantum yields (Jeong et al., 2018). This process underlies the theory of metal-enhanced fluorescence (MEF), which is utilised in biosensors to facilitate tremendous gains in signal amplification and assay sensitivity (Jeong et al., 2018).

3.1.10.2 Nanometals for the enhancement of photosensitisers

Photosensitisers and fluorophores share the same activation mechanism of light capture and electron excitation. In an attempt to improve their biocidal activity, several research groups have investigated the use of plasmonic nanoparticles to enhance the activation of photosensitisers in a manner similar to MEF. By combining silver nanoparticles with the anionic photosensitiser rose bengal, Zhang et al. (2007) reported a three-fold increase in singlet oxygen yields. Likewise, Hu et al. (2014) observed significant improvements in singlet oxygen yield after combining a range of photosensitisers with silver-silica nanoparticles. A spectral overlap between nanoparticle surface plasmons and photosensitisers appears to play an important role in determining the singlet oxygen quantum yield. Hu et al. (2009) observed the strongest enhancement when there were substantial overlaps between the two and that the weakest enhancement was observed with rose bengal, whose excitation peak varied substantially from that of the surface plasmons.

Interestingly, some authors have observed decreased singlet oxygen yields of photosensitiser-nanoparticle combinations, despite also reporting enhanced biocidal activity (Narband et al., 2008; Misba et al., 2016). In both cases, the authors theorised that the nanoparticles may have both enhanced activation and induced a shift toward type-I photosensitisation, which yields hydroxyl and superoxide radicals rather than singlet oxygen (Narband et al., 2008; Misba et al., 2016). A follow up study by Narband et al. (2009) confirmed that supplementation of photosensitisers with gold nanoparticles facilitated greater light capture. Whilst Misba et al. (2016) detected the production of radical species via fluorescence microscopy, their methodology was qualitative and only confirmed that radicals were present. It therefore remains unclear whether a shift toward type-I photosensitisation was responsible for the enhancement of biocidal activity.

3.1.10.3 Nanoparticles as optical quenchers

In contrast to enhancing photoexcitation, nanoparticles may also quench photoexcited species in close proximity. This contradictory property is due to a charge transfer mechanism in which the energy from excited electrons is transferred to the electrophilic nanoparticle; this effect becomes dominant when the distance between nanoparticle and fluorophore/photosensitiser is less than 5 nm (Eustis & El-Sayed, 2006). In contrast, the greatest enhancement occurs in the "near-field" of the nanoparticle, approximately 10 nm from the surface (Eustis & El-Sayed, 2006). In photosensitisers, Kotiaho et al. (2010) reported a substantial decrease in the excitation lifetime of a phthalocyanine after conjugation to gold nanoparticles via short 5 nm linkers. To ensure enhancement occurs rather than quenching, "spacers" can be used to maintain a correct degree of separation (Jeong et al., 2018).

The addition of metal nanoparticles to TBO-based formulations may provide significant enhancements to biocidal activit.y Given the observations of Hu et al. (2009), this enhancement may be greatest using nanoparticles whose surface plasmons share a significant spectral overlap with TBO. Triangle shaped silver nanoparticles (nanoplates) exhibit significant absorbance in this range and so these will be tested.

3.2 Chapter aims and objectives

The aim of this chapter is to develop a TBO-based photosensitiser formulation to maximise its biocidal activity against vegetative bacteria. The formulations will be optimised through optimising the concentration of constituents and by co-formulating with prospective excipients, as identified in section 3.1. Biocidal activity will be ascertained by testing against suspensions of *Staphylococcus aureus*, *Enterococcus hirae*, *Escherichia coli* and *Pseudomonas aeruginosa,* and against surface-dried *S. aureus* and *E. coli*. The following disinfection parameters and excipients will be investigated: photosensitiser concentration, photosensitiser-type, formulation pH, use-temperature, contact time, pH buffering agents, chelating agents, metal nanoparticles and surfactants. This optimisation process will yield a formulation which will be investigated further in the following chapters.

3.3 Methods

For ease of following the development of the formulation, the flow chart in figure 3.4 outlines the various optimisation steps taken throughout the optimisation process. It also contains the names and constituents of key formulation iterations referenced in this chapter.

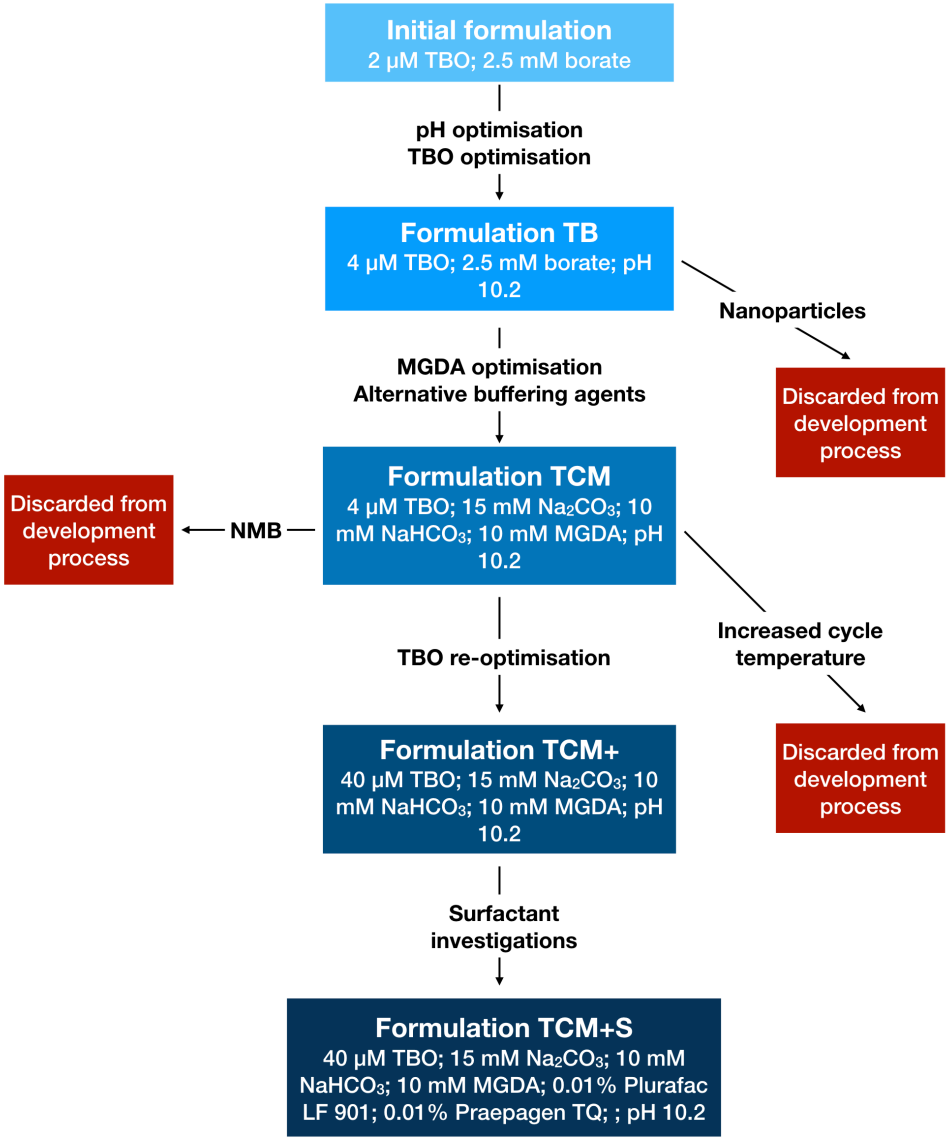

Figure 3.4: Summary of the formulation development process. Note that nanoparticles, new methylene blue (NMB) and increased cycle temperatures were development dead-ends whereas the central column outlines successful progress.

3.3.1 Formulations and contact times

As the purpose of this chapter was to optimise and refine the formulation through the addition of excipients and by varying cycle parameters, many different iterations of the initial formulation were tested. To begin optimisation, a concentration of 2 μM TBO was selected arbitrarily as a starting point for development of the formulation. This was dissolved in a solution of 2.5 mM sodium tetraborate since silver nanoparticles investigated in later experiments were also provided in this buffer. Formulations used are detailed at each stage of the process and the major iterations are described in table 3.1. In some experiments, very short contact times (10-30 seconds) were used so that $\log_{10}$ reductions did not exceed the lower limit of detection. This ensured that multiple formulations did not all reduce viability beyond this limit and make comparisons impossible. The contact times used are detailed in the respective methods and results sections.

Table 3.1: Evolution of the phototensitiser formulation throughout development.

Abbreviated name	Components
TB	TBO (4 μM), sodium tetraborate (2.5 mM); pH 10.2
TCM	TBO (4 μM), sodium bicarbonate (15 mM), sodium carbonate (10 mM); MGDA (10 mM); pH 10.2
TCM+	TBO (40 μM), sodium bicarbonate (15 mM), sodium carbonate (10 mM), MGDA (10 mM); pH 10.2
TCM+S	TBO (40 μM), sodium bicarbonate (15 mM). sodium carbonate (10 mM), MGDA (10 mM), Plurafac LF 901 (0.01%), Praepagen TQ (0.01%); pH 10.2

Key: T =TBO; B = Borate buffer; C = Carbonate buffer; M = MGDA; + Increased TBO concentration; S = Surfactants

3.3.2 Effect of pH on biocidal activity

The effect of pH on TBO-based disinfection was initially investigated by preparing formulations containing 2 μM TBO and 2.5 mM sodium tetraborate as an alkaline buffering agent. Formulations were adjusted to pH 7.2, 8.2, 9.2 10.2 and 11.2 and tested against suspensions of *S. aureus* NCTC 10788, in accordance with section 2.2. To ensure it was possible to draw comparisons between treatment groups, a 10 second contact time was used.

3.3.3 Effect of TBO concentration on biocidal activity

To determine the optimal concentration of TBO for maximum biocidal activity, TBO was added to the formulation at concentrations ranging from 2 to 20 µM. These formulations were made up using sodium tetraborate buffer and were adjusted to pH 10.2. They were tested against suspensions of *S. aureus* NTCC 10788 using a contact time of 30 seconds.

3.3.4 Effect of silver nanoparticles on biocidal activity of Formulation TB

Two types of plasmonic silver nanoparticle (AgNPs) were used in this study. They were described as "nanoplates" as their geometry was similar to flattened triangles. Nanoplates were obtained from NanoComposix and were provided at a concentration of 20 µg/mL in 5 mM sodium tetraborate buffer (pH 9.2). Nanoplates were selected so that their surface plasmon resonance (SPR) peaks overlapped with the absorbance peak of TBO. Table 3.2 includes additional information on the properties of these nanoparticles.

To determine the effect of these nanoparticles on the biocidal activity of TBO, each type was added to Formulation TB at a concentration of either 0.5 or 5 µg/mL. The resulting formulations were tested against *S. aureus* NCTC 10788 in accordance with section 2.2 and compared with a nanoparticle-free control.

Table 3.2: Properties of plasmonic silver nanoparticle used in this study

Name	Diameter of largest aspect (nm)	Advertised SPR peak (nm)	Actual SPR peak (nm)
550-nm AgNPs	31	550	562
650-nm AgNPs	53	650	692

SPR - surface plasmon resonance; data obtained from provided product specification sheets.

3.3.5 Effect of silver nanoparticles on relative singlet oxygen yield of Formulation TB

The effect of silver nanoparticles on the production of singlet oxygen ($^1O_2$) was determined by measuring the decomposition of 1,3-diphenylisobenzofuran (DPBF) (Kostka et al., 2006). DPBF exhibits strong light absorbance at 417 nm but reacts with $^1O_2$ to yield a colourless product. Therefore, singlet oxygen production can be quantified by measuring a decrease in absorbance at this wavelength (Schwerin et al., 2010). DPBF was dissolved in 100% ethanol to a concentration of 200 µM. Formulation TB and variants containing two concentrations of 650-nm AgNPs were prepared as described in section 3.3.4. Each formulation was mixed with the DPBF stock to yield a 50:50 mixture and added to polystyrene cuvettes.

To provide baseline measurements, A_{417} for each sample was measured at 0 minutes. To reduce the rate of decomposition, cuvettes were placed 30 cm from the light source. Each sample was illuminated for a total of 5 minutes, with A_{417} recorded at 1-minute intervals. DPBF decomposition was then calculated using: $\ln(A_0/A_t)$, where A_0 and A_t denote the A_{417} at 0 minutes and at the various time points respectively (Kostka et al., 2006).

3.3.5 Determination of broader bactericidal activity of Formulation TB

To ascertain whether the TBO-Borate formulation (4 µM TBO, 2.5 mM sodium tetraborate; pH 10.2) was effective against organisms other than *S. aureus*, additional suspension tests were performed using a broader range of bacterial species. The species tested include *Enterococcus hirae* (NCTC 13383), *Escherichia coli* (ATCC 10798) and *Pseudomonas aeruginosa* (NCTC 13359). Suspension tests were performed in accordance with Chapter 2, section 2.2 against bacterial inocula of 1.5-5 x 10^8 CFU/mL using contact times of 0.5, 1 and 5 minutes.

3.3.6 Effect of chelator on biocidal activity of Formulation TB

3.3.6.1 Effect of chelator on biocidal activity against *P. aeruginosa*

Preliminary suspension tests indicated that the formulation containing 4 µM TBO, 2.5 mM sodium tetraborate (pH 10.2) exhibited poor activity against *Pseudomonas aeruginosa* (refer to section 3.4.4). To determine whether the addition of chelators to the formulation would improve activity versus this species, 5 mM MGDA was added to Formulation TB, containing 4 µM TBO and borate buffer (pH 10.2). This was tested against suspensions of *P. aeruginosa* for 0.5, 1 and 5 minutes and compared to a formulation lacking MGDA. 5 mM was added as a starting point as this was reported by George et al. (2009) to improve uptake of methylene blue by Gram-positive and Gram-negative bacteria.

3.3.6.2 Optimisation of MGDA concentration

In a later experiment, the optimal concentration of chelator to be added to the formulation was determined by adding MGDA to Formulation TB at concentrations of 1, 10, 25, 50 and 100 mM. The formulation used for this experiment was based on 4 µM TBO and carbonate buffer (pH 10.2), due to the results of experiment 3.3.7. The formulations were tested against suspensions of both *P. aeruginosa* and *S. aureus*, using a 15 second contact time.

3.3.7 Effect of alternative pH buffering agents on biocidal activity

To determine whether there was a suitable alternative to sodium tetraborate for buffering the pH of the formulation, two additional buffering agents were selected. Each was selected based on their capacity to buffer solutions at pH 10.2. The type of buffer and concentration of constituents are included in table 3.3. Formulations containing 4 μM TBO and the respective buffering agent were prepared, adjusted to pH 10.2. Each was tested against suspensions of *S. aureus* for 30 seconds.

Table 3.3: pH buffering agents.

Buffer-Type	Chemical Name	Final Concentration (mM)
Borate	Sodium Tetraborate	2.5
CAPS	N-cyclohexyl-3-aminopropanesulfonic acid	10
Carbonate-Bicarbonate [a]	Sodium Bicarbonate	15
	Sodium Carbonate	10

[a] Delorey & King (1945)

3.3.8 Efficacy of alternative photosensitiser (new methylene blue) against *E. coli*

In order to determine whether new methylene blue (NMB) was a suitable alternative photosensitiser, a formulation was prepared by substituting 4 μM TBO for 4 μM NMB. Similar to Formulation TCM, NMB was co-formulated with 10 mM MGDA and carbonate buffer (pH 10.2). NMB stock solution was prepared by dissolving the photosensitiser in sterile deionised water over a 2-hour period on a magnetic stirrer; this was necessary due to the poorer solubility in water compared to TBO. The formulation was tested against suspensions of *E. coli* ATCC 10798 in accordance with section 2.2 and its biocidal activity was compared to that of Formulation TCM. The photosensitiser shares the same λ_{max} as TBO (630 nm) and so the same light source was able to be used for this experiment.

3.3.9 Determination of biocidal activity against surface-dried bacteria

As the aim of this project is to develop a technology which is appropriate for surface disinfection, later stages of optimisation were performed against surface-dried bacteria. This procedure is described by the EN 13697 standard (British Standards Institute, 2015a) and was carried out as follows:

3.3.9.1 Surface carriers

Polyvinyl chloride (PVC) coupons measuring 10 mm in diameter were used as carriers during these experiments. PVC carriers were cut to size from a sample of internal surface of a prototype Serie 5 AER provided by Laboratoires Anios (Lille, France). Care was taken not to scratch the glossier side of the coupons as this side was used during efficacy tests and corresponded to the internal surface of an AER.

3.3.9.2 Preparation of surfaces

Coupons were cleaned by soaking in 1% polysorbate-20 for 60 minutes and vortexing periodically to remove debris from the surface. They were then rinsed in deionised water, wiped with a paper towel and rinsed again. After disinfecting by soaking in 70% ethanol for a further 30 minutes, coupons were removed from ethanol with sterile forceps and allowed to dry in a laminar flow hood (British Standards Institute, 2015a). As an additional disinfection measure, PVC coupons were irradiated with UV on both sides to ensure sterility. Using sterile forceps, coupons were transferred into individual sterile petri dishes prior to use.

3.3.9.3 Preparation of inoculum

Bacterial inocula were prepared as described in section 2.2.2.2 and adjusted to 1.5-5 x 10^8 CFU/mL. To simulate clean soiling conditions, 0.3 g/L BSA was added as an interfering substance. 50 µL of inoculum was added to the centre of each coupon and allowed to dry in a laminar flow hood for approximately 60 minutes. Samples were tested immediately once the droplets were visibly dried onto the surface. In the case of *E. coli*, substantial losses in viability were observed as a result of the drying process. Consequently, sterile glycerol was added to the inoculum at a concentration of 2 g/L prior to drying, as described in the EN 16615 standard (British Standards Institute, 2015b).

3.3.9.4 Test procedure

100 µL of formulation was added gently to the centre of each coupon to ensure the inocula were not disturbed but completely covered. Samples were placed immediately beneath the light source (section 2.1.7) and illuminated for 0.5, 1, 2.5 and 5 minutes. Following illumination, coupons were immediately transferred to Duran bottles containing 10 mL of universal neutraliser (section 2.2.5.1) and 5 g of sterile glass beads. Samples were vortexed for 1 minute to re-suspend inoculum and left for a further 5 minutes to ensure neutralisation. A water-treated control was also transferred to neutraliser for comparison.

3.3.9.5 Recovery and quantification of survival

Neutralised samples were serially diluted in a 10-fold series in TSC. 1 mL aliquots of each dilution were spread across two TSA plates using sterile plastic spreaders (section 2.2.4). Plates were incubated overnight at 37°C and colonies were counted to determine survivability. Only plates with 14 and 330 colonies were counted as this is the range which is considered countable by the EN 13697 standard; this yields a lower limit of detection of 140 CFU/mL if colonies are counted on the lowest dilution plate of 10^{-1} (British Standards Institute, 2015a). CFU/mL was calculated using the following equation and $\log_{10}$ reductions were then calculated using $\log_{10}(A/B)$, where A represents the viability of the control group and B the viability of tested groups. Total colony counts were multiplied by 10 to account for being resuspended in 10 mL neutraliser.

$$\text{CFU / mL} = \frac{\text{Total colony count } \times 10}{2 \times \text{Dilution Factor}}$$

3.3.10 Effect of cycle temperature and degassing on biocidal activity against surface-dried bacteria

To determine whether increasing the cycle temperature could improve the efficacy of Formulation TCM, the light box and LED were moved into a stationary incubator (ICH110; Memmert). The temperature was set to 30, 40 or 50°C and allowed to equilibrate. Formulations were placed in the incubator and left for a further 30 minutes to allow them to equilibrate to temperature. after which they were used to treat *S. aureus* for 1 minute, in accordance with the section 3.3.9. To ensure it was maintained at the correct temperature, the test was performed in the incubator.

As we observed the formation of bubbles on the side of the container when the formulation was held at 50°C, we were interested in determining whether loss of dissolved gasses would have a negative impact on the formulations' biocidal activity. Therefore, dissolved gasses were displaced by sparging with nitrogen gas. A 4 mL aliquot of Formulation TCM was

added to a 7 mL bijou tube and two holes were made in the lid using a syringe needle. The needle was then placed in one hole so that the tip was submerged in the formulation. A cylinder of nitrogen gas (BOC) was attached to the needle via rubber tubing and nitrogen gas was bubbled gently through the formulation for 30 minutes at a rate of 50 mL/minute. The resulting formulation was then equilibrated to 20°C and used against surface-dried *S. aureus*.

3.3.11 Optimisation of TBO concentration for biocidal activity against surface-dried bacteria

To determine the optimal concentration of TBO for disinfection of PVC surfaces, several variants of Formulation TCM were prepared so that the TBO concentration ranged from 4 to 80 μM. Each formulation was tested against surface-dried *S. aureus* NCTC 10788 in accordance with section 3.3.9 using a contact time of 1 minute to determine the optimal concentration for biocidal activity.

3.3.12 Effect of Surfactants on Surface Disinfection Efficacy

Surfactants were hypothesised to affect the efficacy of the formulation, particularly against surface-dried bacteria. Therefore, a range of different surfactant types were added to Formulation TCM+ (40 μM TBO and 10 mM MDGA in carbonate buffer; pH 10.2). Surfactants were added at concentrations of 0.01 and 0.1%. The surfactants selected for these experiments are included below in table 3.4.

Table 3.4: Surfactants added to Formulation TCM+.

Class	Sub-class	Surfactant
Non-ionic	Ethoxylated sorbitan ester	Polysorbate-80 [a]
	Alkoxylated fatty alcohol	Plurafac LF 901 [b]
		Plurafac LF 120 [b]
		Genapol EP [b]
Cationic	Quaternary ammonium compounds	Benzalkonium chloride a
		DiDAC [a]
		Praepagen HY [c]
	Triethanolamine-based esterquat	Praepagen TQ [c]
Anionic	Organosulfate	Sodium dodecyl sulfate [a]

[a] Obtained from Sigma Aldrich

[b] Obtained from BASF

[c] Obtained from Clariant

3.3.13 Determination of TBO adsorption

The extent of TBO adsorption to microbial cells was determined using an in-house procedure developed by drawing inspiration from George et al. (2009). Suspensions of *Staphylococcus aureus* NCTC 10788 were prepared as previously described (section 2.2.2) and adjusted to A_{630} 2.0. Several variations of Formulation TCM+ were prepared by adding the following surfactants at a concentration of either 0.01 and 0.10%: Plurafac LF 901 (non-ionic), Praepagen TQ (cationic) and sodium dodecyl sulfate (anionic). 900 µL aliquots of each formulation were placed in 1.5 mL microcentrifuge tubes and 100 µL of *S. aureus* suspension was added to each. After vortexing, tubes were incubated at 20°C for 5 minutes and then centrifuged at 5000 G for 10 minutes. 180 µL aliquots of the resulting supernatant was transferred to wells of a transparent 96-well microtiter plate. 20 µL of 1% SDS was then added to each well and mixed by pipetting; this step was necessary to improve the signal produced by remaining TBO molecules by trapping monomers in an excess of SDS micelles thus counteracting the hypochromic effects of low concentrations of SDS. Absorbance at 630 nm was then read using an Infinite M200 plate reader (Tecan). Figure 3.5 illustrates the format of the assay and differences in supernatant colouration with and without the addition of surfactants.

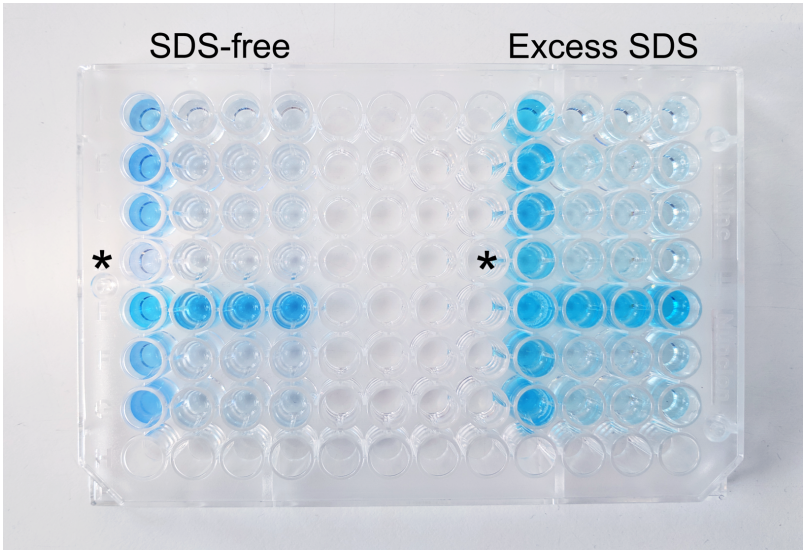

Figure 3.5: Format of the TBO adsorption assay. Note the wide variation in supernatant colouration in the supernatants in unadjusted samples (left). The hyperchromic samples (*) contained 0.01% SDS, which interfered with the assay in the unadjusted sample by making it appear as though more TBO had adsorbed to cells. Subsequent addition of excess SDS to the samples (right) neutralised the hypochromic effect and so facilitated more accurate TBO quantification.

3.4 Results

3.4.1 Optimal pH

Of the tested pH levels, optimal biocidal activity of 2 μM TBO against suspensions of *S. aureus* NCTC 10788 was observed at pH 10.2 (fig. 3.6). There were no statistically significant differences in activity between groups treated with formulations at pH 7.2, 8.2 and 9.2 ($P > 0.05$; ANOVA, Tukey). Increasing to pH 10.2 led to a significant increase in activity compared to pH 7.2 ($P < 0.0001$; ANOVA, Tukey) and 9.2 ($P < 0.001$; ANOVA, Tukey). Further increasing the pH from 10.2 to 11.2 led to a significant decrease in activity ($P < 0.05$; ANOVA, Tukey).

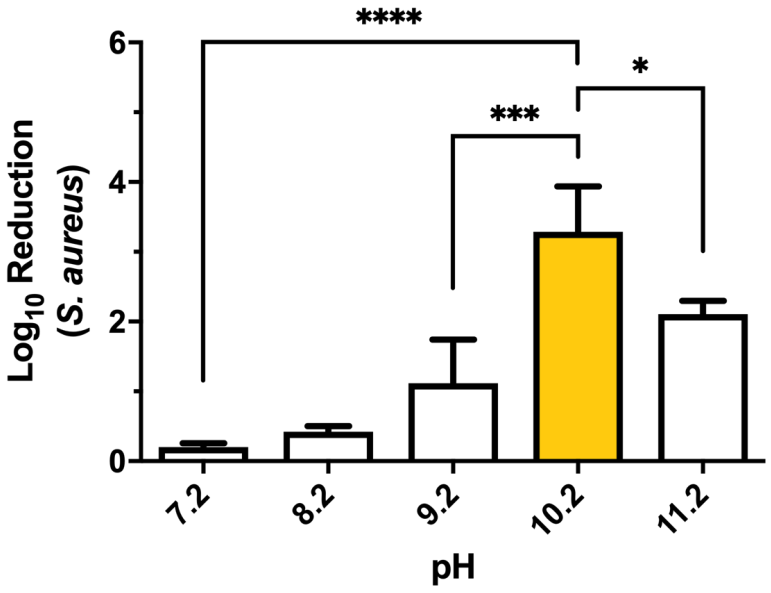

Figure 3.6: Optimal pH of 2 μM TBO against *S. aureus* suspensions. 10 second contact time. Of the tested pH levels, optimal activity was observed at pH 10.2 (yellow column). * $P < 0.05$; *** $P < 0.001$; **** $P < 0.0001$.

3.4.2 Optimal TBO Concentration for suspensions

Of the tested concentrations, optimal biocidal efficacy against suspensions of *S. aureus* NCTC 10788 was observed at a TBO concentration of 4 μM (fig. 3.7). We observed an initial increase in biocidal activity upon increasing the concentration from 2 μM to 4 μM ($P < 0.05$; ANOVA, Tukey). This was followed by a subsequent decrease after increasing from 4 to 10 μM ($P < 0.0001$; ANOVA, Tukey) and from 10 to 20 μM ($P < 0.05$; ANOVA, Tukey).

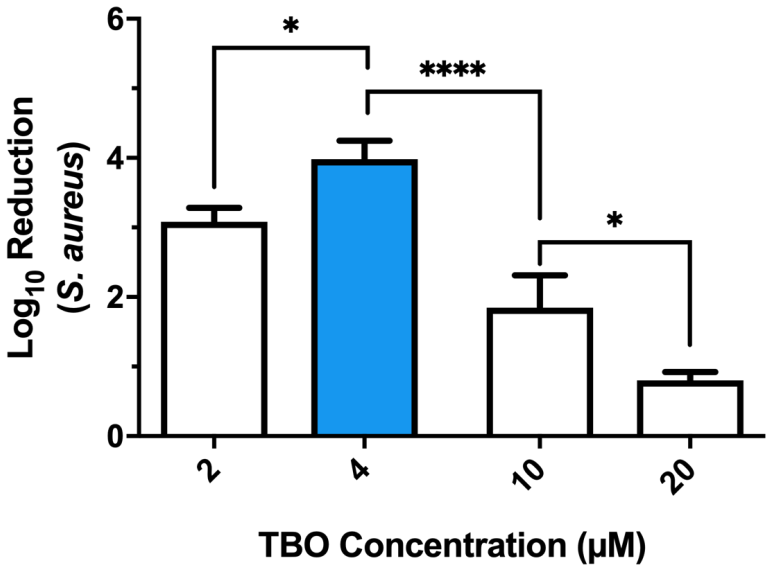

Figure 3.7: Optimal concentration of TBO for biocidal activity against *S. aureus* suspensions. 30 second contact time. Of the tested concentrations, optimal activity was observed at 4 μM (blue column). * $P < 0.05$; **** $P < 0.0001$.

3.4.3 Silver nanoparticles

The addition of silver nanoparticles to 2 μM TBO (pH 9.2) did not improve its biocidal activity against suspensions of *S. aureus* NCTC 10788 (fig. 3.8). Compared to the nanoparticle-free control, the addition of 0.5 μg/mL 550 nm-resonant and 650 nm-resonant silver nanoparticles (AgNPs) did not lead to a statistically significant change in biocidal activity ($P < 0.05$; ANOVA, Tukey). However, there was a significant decrease in activity upon the addition of 5.0 μg/mL 550 nm-resonant ($P < 0.001$; ANOVA, Tukey) and 650 nm-resonant AgNPs ($P < 0.0001$; ANOVA, Tukey).

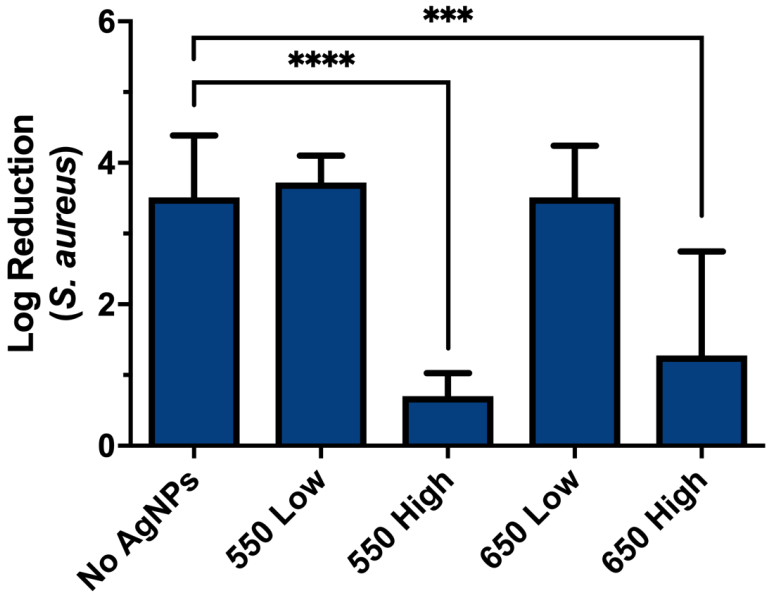

Figure 3.8: The effect of various types of silver nanoparticles (AgNPs) on the biocidal activity of TBO against suspensions of *S. aureus*. 15 second contact time. 550 denotes 550 nm-resonant AgNPs whilst 650 denotes 650 nm-resonant AgNPs. "Low" corresponds to a nanoparticle concentration of 0.5 μg/mL whereas "High" corresponds to a concentration of 5.0 μg/mL. *** $P < 0.001$; **** $P < 0.0001$.

The addition of 5.0 µg/mL 650 nm-resonant silver nanoparticles (AgNPs) to Formulation TB led to a considerably decrease in DPBF decomposition compared to the nanoparticle-free control at each time point ($P < 0.05$; ANOVA, Dunnett) (fig. 3.9). This indicated that there was a marked decrease in singlet oxygen yield. After 5 minutes, there was almost a 4-fold difference in DPBF decomposition compared to Formulation TB ($P < 0.05$; ANOVA Dunnett). In contrast, the addition of 0.5 µg/mL 650 nm-resonant AgNPs did not lead to a change in DPBF decomposition compared to the control ($P > 0.05$; ANOVA, Dunnett). This indicated that there was no change in singlet oxygen yield.

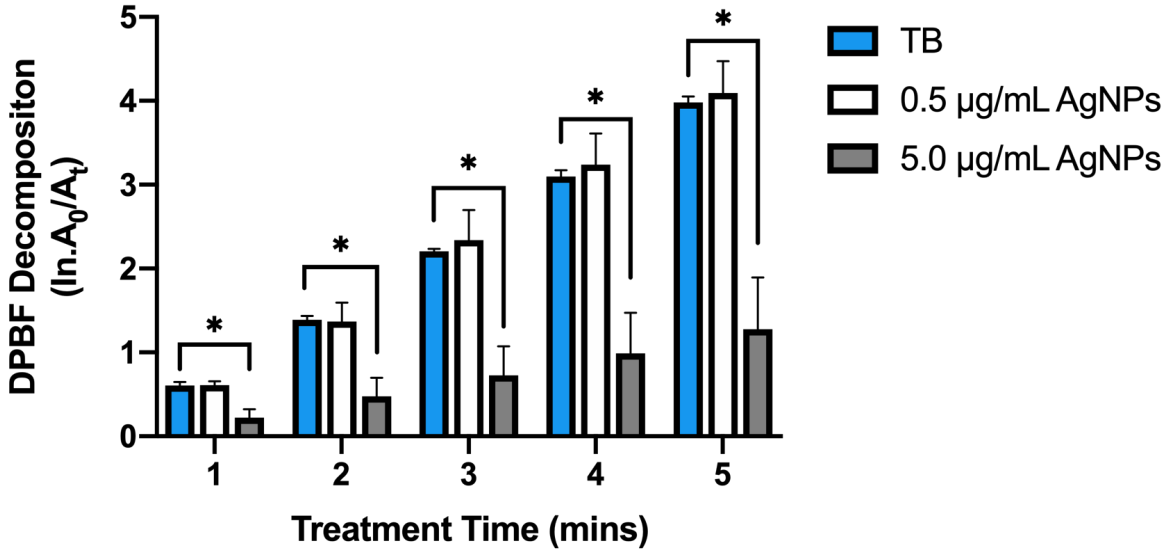

Figure 3.9: Changes in decomposition of DPBF by Formulation TB following addition of silver nanoparticles (AgNPs). Bars corresponding to the nanoparticle-free control (TB) are blue. White bars denote Formulation TB with 0.5 µg/mL AgNPs added whilst grey indicates Formulation TB with 5.0 µg/mL AgNPs.

3.4.4 Bactericidal activity of Formulation TB

Formulation TB exhibited rapid bactericidal activity versus suspensions of *Staphylococcus aureus* NCTC 10788, *Enterococcus hirae* NCTC 13383 and *Escherichia coli* ATCC 10798 and performed equally well against these species at 0.5 and 1 minute ($P > 0.05$; ANOVA, Tukey) (fig. 3.10). Within 1 minute of treatment, >5 $\log_{10}$ reductions in viability were observed in all three species. In contrast, the formulation performed very poorly against *Pseudomonas aeruginosa* NCTC 13359. At 1 minute, we observed only a 0.6 $\log_{10}$ reduction and at 5 minutes, only 2.6 $\log_{10}$ reduction in viability. This was well below the 5 $\log_{10}$ threshold required to claim bactericidal efficacy (British Standards Institute, 2012). The differences in biocidal activity against *P. aeruginosa* was significant at all three time points when compared to the other species tested ($P < 0.0001$; ANOVA, Tukey).

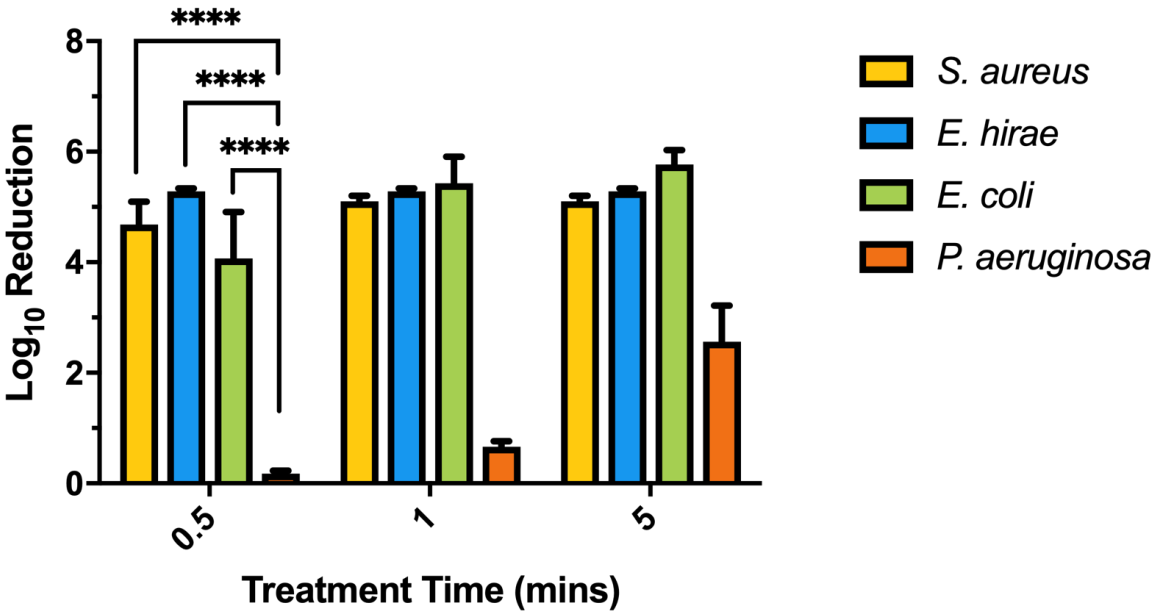

Figure 3.10: Bactericidal activity of Formulation TB (4 µM TBO, 2.5 mM sodium tetraborate, pH 10.2) against suspensions of *S. aureus*, *E. hirae*, E. coli and *P. aeruginosa*. Note the marked difference in activity between *P. aeruginosa* and the other species testing. For graphing simplicity, only the 0.5-minute treatment time has been annotated with the results of statistical analysis. **** $P < 0.0001$.

3.4.5 Effect of MGDA on the biocidal efficacy against *P. aeruginosa*

The addition of 5 mM MGDA to Formulation TB led to a considerable increase in its biocidal activity against *P. aeruginosa* NCTC 13359 (fig. 3.11). When no MGDA was added, we observed 0.18 $\log_{10}$ (0.5 min) 0.66 $\log_{10}$ (1 min) and 2.57 $\log_{10}$ (5 min) reductions in *P. aeruginosa* viability. Upon the addition of 5 mM MGDA to the formulation, this increased to 2.18 $\log_{10}$ (0.5 min), 3.41 $\log_{10}$ (1 min) and 5.05 $\log_{10}$ (5 min). This represents a 100 to 1000-times improvement in biocidal activity. The differences in biocidal activity were statistically significant at each time point (P <0.0001; ANOVA, Šidák).

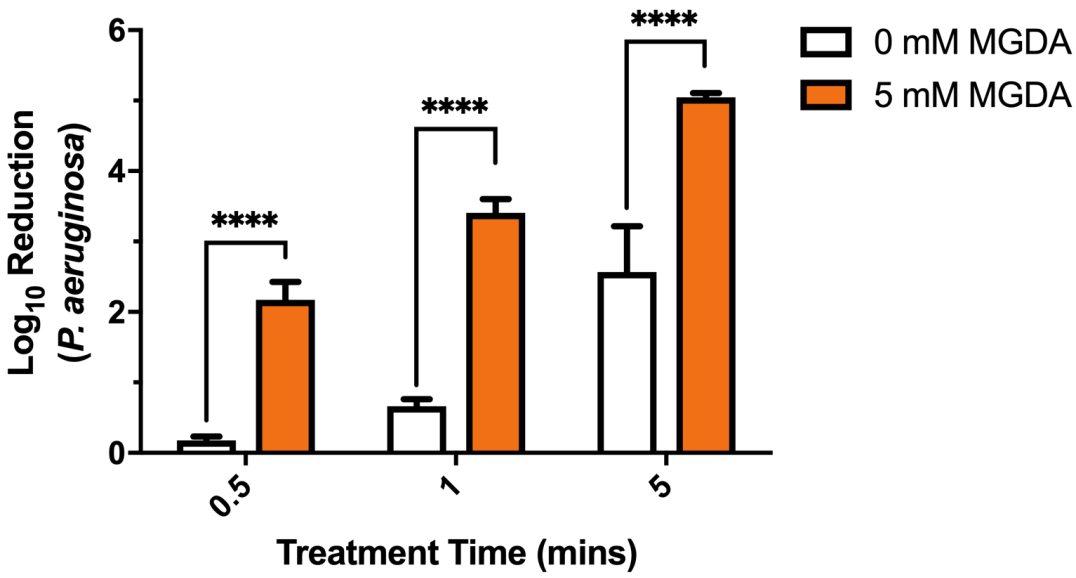

Figure 3.11: Changes in the biocidal activity of Tormulation TB (4 µM TBO, 2.5 mM sodium tetraborate, pH 10.2) against *P. aeruginosa* following addition of 5mM MGDA. **** P <0.0001.

3.4.7 Optimal concentration of MGDA

Of the concentrations tested, optimal biocidal activity against *P. aeruginosa* NCTC 13359 was observed when 10 mM MGDA was added to Formulation TB (fig. 3.12). Upon the addition of 1 mM MGDA, there was a large increase in biocidal activity compared to 0 mM ($P < 0.0001$; ANOVA, Tukey). This was followed by a further increase when it was increased from 1 to 10 mM ($P < 0.001$; ANOVA, Tukey). Further increasing the concentration from 10 to 25 mM led to a slight decrease in biocidal activity ($P < 0.05$; ANOVA Tukey) which then stabilised and did not change as MGDA concentration was further increased to 50 and 100 mM ($P > 0.05$; ANOVA, Tukey).

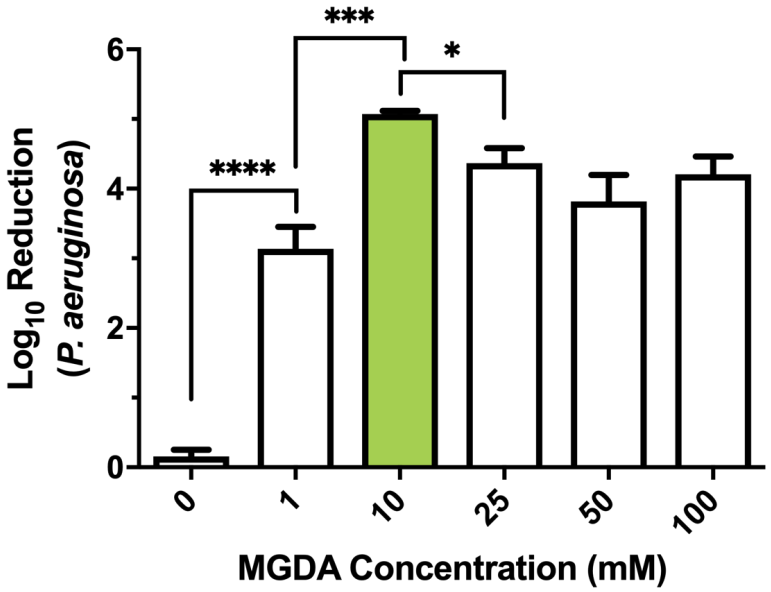

Figure 3.12: The effect of MGDA concentration on biocidal activity of Formulation TB against *P. aeruginosa*. Optimal biocidal activity was observed at a concentration of 10 mM MGDA (green column). * $P < 0.05$; *** $P < 0.001$; **** $P < 0.0001$.

Of the tested concentrations, optimal activity of Formulation TB against *S. aureus* was observed at 0, 1 and 10 mM MGDA (fig. 3.13). There were no differences in activity when MGDA was added at these concentrations ($P > 0.05$; ANOVA, Tukey). However, further increasing the concentration of MGDA from 10 to 25 mM led to a decrease in biocidal activity ($P < 0.01$; ANOVA, Tukey), as did increasing it from 25 mM to 50 mM ($P < 0.001$; ANOVA, Tukey). Further increases from 50 to 100 mM did not result in a statistically significant decrease in activity from 50 mM ($P > 0.05$; ANOVA, Tukey).

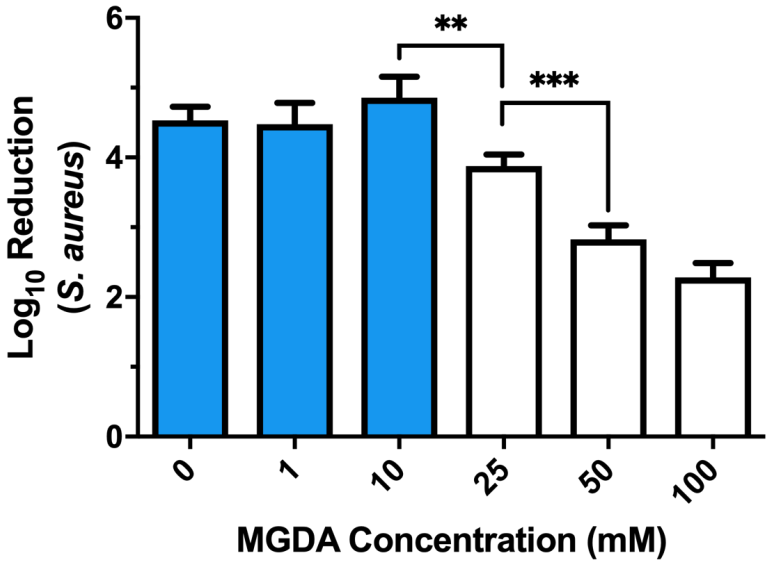

Figure 3.13: The effect of MGDA concentration on biocidal activity of Formulation TB against *S. aureus*. Optimal biocidal activity was observed at MGDA concentrations of 0, 1 and 10 mM (blue columns). ** $P < 0.01$; *** $P < 0.001$.

3.4.8 Effect of alternative pH buffering agents

To determine whether sodium borate buffer could be substituted with other pH buffering agents, alternative versions of Formulation TB (i.e. 4 µM TBO + buffering agent; pH 10.2) were prepared which contained CAPS or carbonate-bicarbonate (carbonate) buffer. Substitution of borate with CAPS or carbonate buffer had no effect on the formulation's biocidal activity against *S. aureus* (P >0.05; ANOVA) (fig. 3.14). This demonstrated that sodium tetraborate could be substituted with either of the alternative buffering agents.

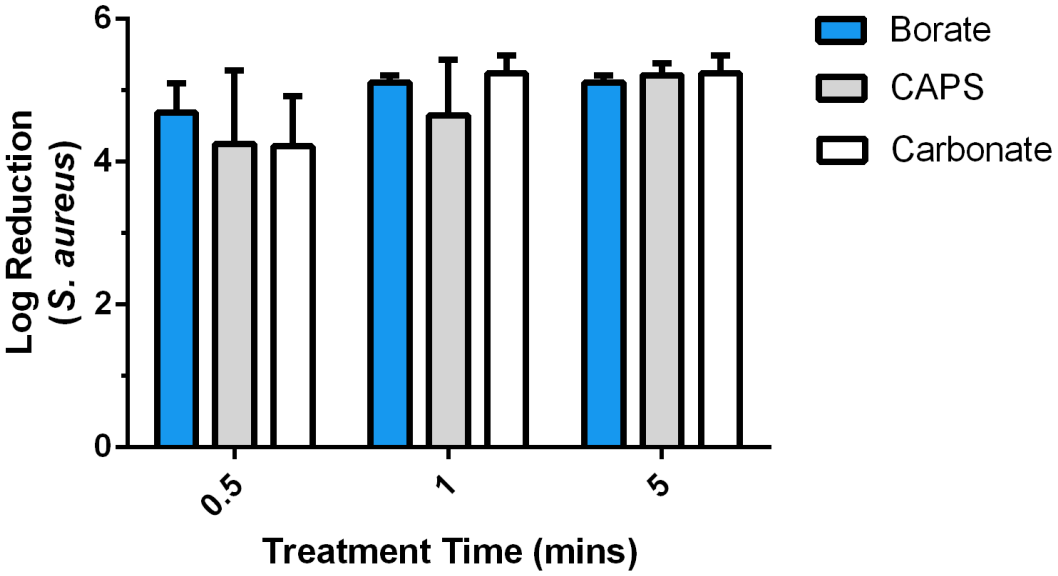

Figure 3.14: The effect of different pH buffering agents on the biocidal activity of 4 µM TBO at pH 10.2. Note that there were no differences in activity. Borate = 2.5 mM sodium tetraborate; CAPS = 10 mM N-cyclohexyl-3-aminopropanesulfonic acid; Carbonate = 15 mM $NaHCO_3$, 10 mM Na_2CO_3.

3.4.9 Bactericidal activity of new methylene blue against *E. coli*

Substitution of TBO with new methylene blue (NMB) in Formulation TCM led to a marked decrease in biocidal activity against suspensions of *E. coli* ATCC 10798 (fig. 3.15). At each of the time points tested (0.5, 1 and 5 minutes), there was an extremely significant decrease in activity (P <0.0001; ANOVA; Šidák). At 1 minute, the NMB-based formulation was able to only effect a 0.87 $\log_{10}$ reductions in *E. coli* viability; this compared to a 4.77 $\log_{10}$ reduction in those treated with the TBO-based formulation. At 5 minutes, the viability of NMB-treated *E. coli* decreased by only 1.64 $\log_{10}$, compared to 5.9 $\log_{10}$ in those treated with the TBO-based formulation. After 5-minutes, the NMB-based formulation had completely decolourised whilst the TBO formulation still retained a blue coloration.

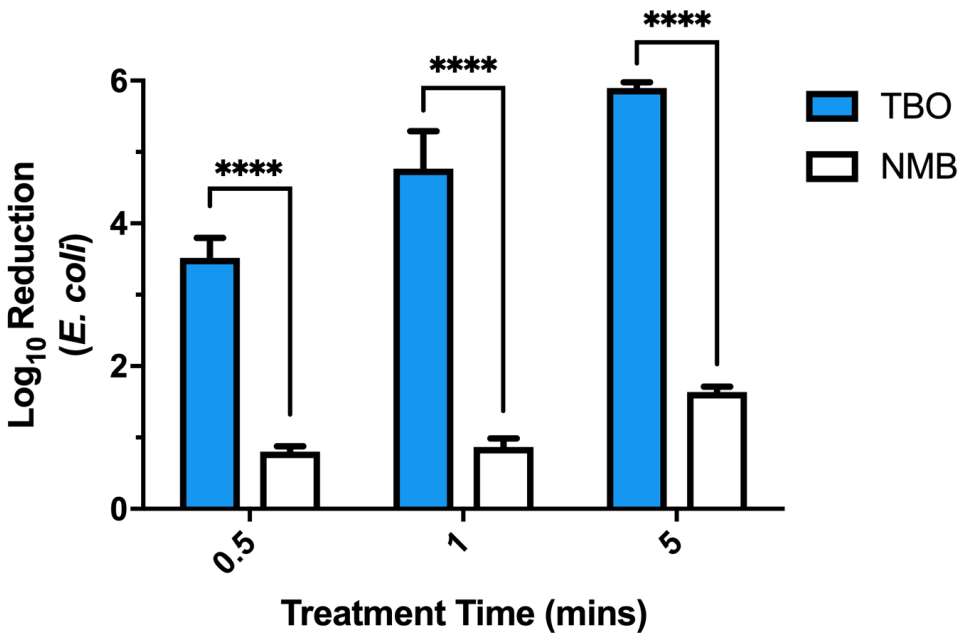

Figure 3.15: Comparative biocidal activity of toluidine blue O (blue) and new methylene blue (white) against *E. coli*, when added to 10 mM MGDA and carbonate buffer (pH 10.2). **** P <0.0001

3.4.10 Bactericidal activity of Formulation TCM

Formulation TCM (4 μM TBO, 15 mM sodium bicarbonate, 10 mM sodium carbonate, 10 mM MGDA, pH 10.2) performed well against suspensions of all four bacterial species tested (fig. 3.16). Within 0.5 minutes, viability of both Gram-positive species (*S. aureus* and *E. hirae*) was reduced by >5 $\log_{10}$. In 1 minute, the viability of both Gram-negative species (*E. coli* and *P. aeruginosa*) was also reduced by greater than 5 $\log_{10}$.

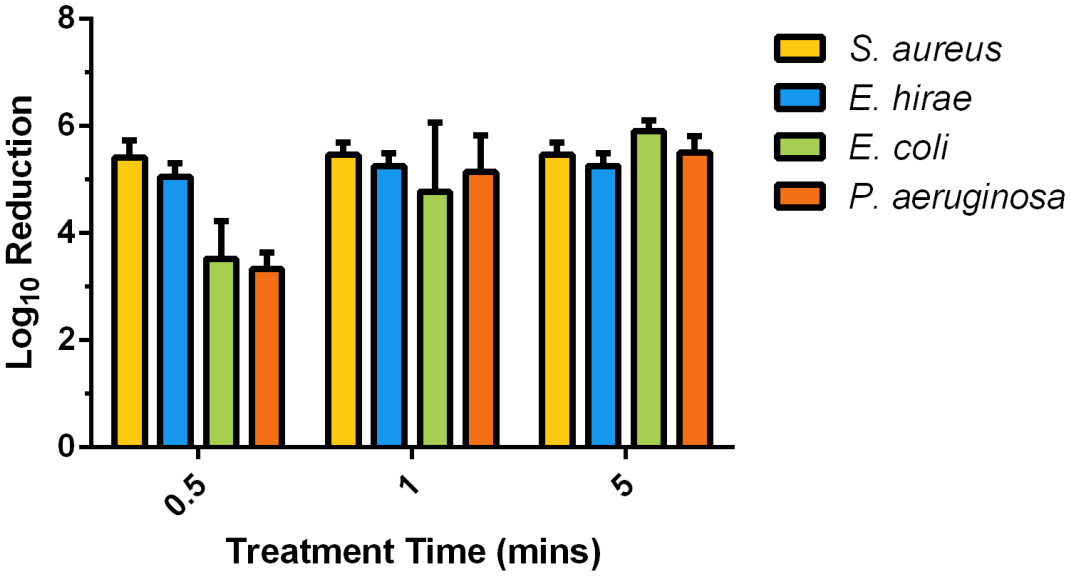

Figure 3.16: Bactericidal activity of Formulation TCM against suspensions of *S. aureus*, *E. hirae*, *E. coli* and *P. aeruginosa*.

3.4.11 Bactericidal activity of Formulation TCM against surface-dried *S. aureus*

Formulation TCM was insufficiently bactericidal against *S. aureus* NCTC 10788 dried on surface carriers. 0.72, 1.08 and 2.68 $\log_{10}$ reductions in viability following 0.5, 1 and 5 minutes of treatment respectively (table 3.5). This was markedly below the >4 $\log_{10}$ reduction required by the EN 13697 standard.

Table 3.5: Bactericidal activity of Formulation TCM against surface-dried *S. aureus.* EN 13697 test conditions.

Species	Contact time (mins)	$\log_{10}$ CFU reduction	SD	Pass/Fail*
S. aureus	0.5	0.72	0.21	Fail
	1	1.08	0.07	Fail
	5	2.68	0.20	Fail

*Pass threshold = 4 $\log_{10}$ reduction; SD = standard deviation.

3.4.12 Effect of cycle temperature and degassing

As illustrated in figure 3.17, increased cycle temperature negatively correlated with the biocidal activity of Formulation TCM against surface-dried *S. aureus* NCTC 10788. compared to the 20ºC control, increasing the temperature to 40 and 50ºC led to a small decrease in biocidal activity (P <0.05; ANOVA, Dunnett). There was no difference in activity between 20 and 30ºC (P >0.05; ANOVA, Dunnett). Degassing the formulation led to a large decrease in activity compared to 20ºC (P <0.001; ANOVA, Dunnett) and biocidal activity was almost entirely lost.

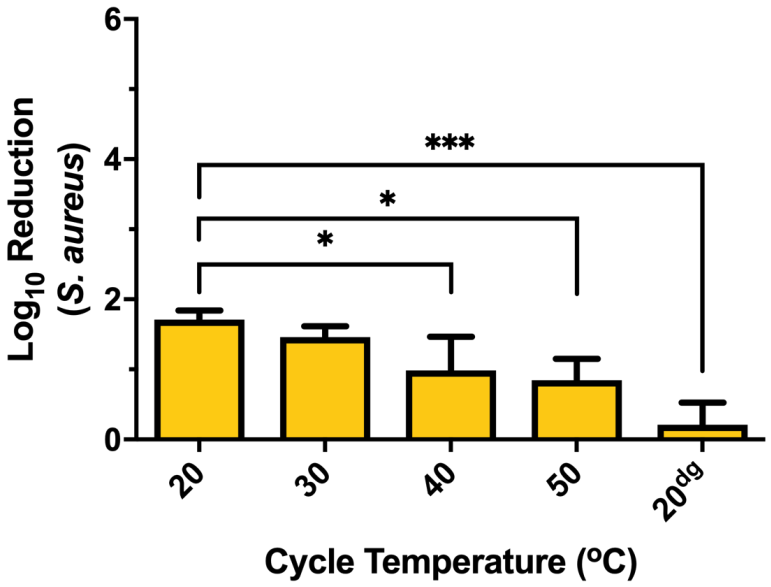

Figure 3.17: The effect of temperature on the biocidal activity of Formulation TCM against surface-dried *S. aureus*. 5-minute contact time. Degassing the formulation (20dg) led to almost complete loss of activity. * P <.005; **** P <0.0001.

3.4.13 Optimal concentration of TBO against surface-dried *S. aureus*

Of the tested concentrations, optimal biocidal activity was observed against surface-dried *S. aureus* NCTC 10788 when TBO was added to the formulation at 20 and 40 µM (fig. 3.18). Increasing the concentration from 4 to 10 µM did not lead to an increase in activity (P 0.45; ANOVA, Tukey). However, increasing the concentration to 20 µM led to a marked increase in activity compared to 4 µM (P <0.0001; ANOVA, Tukey) and 10 µM (P <0.01). Whilst there was not a statistically significant difference between 20 and 40 µM (P 0.087; ANOVA, Tukey), the P value was close to the significance threshold of 0.05. Further increasing the concentration to 80 µM led to diminished biocidal activity compared to 40 µM (P <0.05; ANOVA, Tukey) but not compared to 20 µM (P >0.05; ANOVA, Tukey). At 40 µM, there was a 3.6 log_{10} reduction in *S. aureus* viability after 1 minute of treatment, which was much higher than the 1.3 log_{10} reduction observed when using 4 µM TBO (P <0.0001; ANOVA, Tukey).

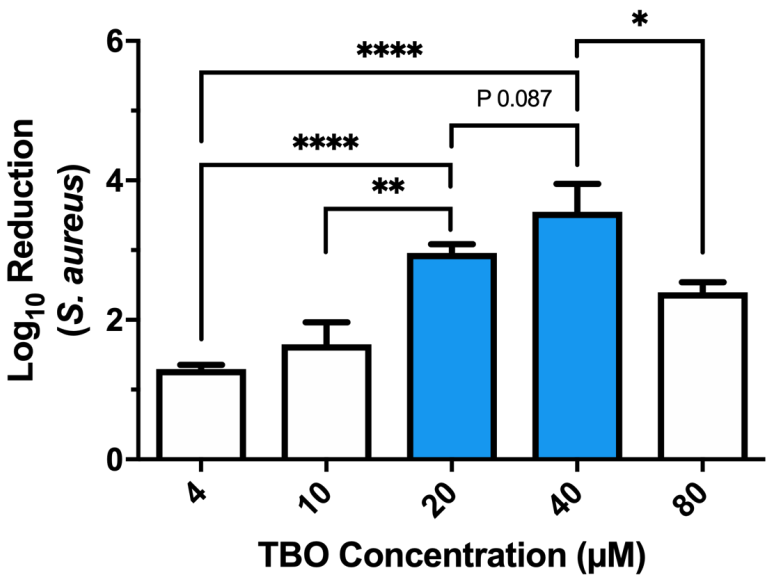

Figure 3.18: The effect of TBO concentration on the biocidal activity of Formulation TCM against surface-dried *S. aureus* on PVC coupons. 1-mintue contact time. Optimal activity was observed at 20 and 40 µM (blue columns). * P <0.05; ** P <0.01; **** P <0.0001

3.4.14 Non-ionic surfactants

As illustrated in figure 3.19, there were no differences in the biocidal activity of Formulation TCM+ (40 μM TBO, 10 mM MGDA, 15 mM sodium hydrogen carbonate, 10 mM sodium carbonate; pH 10.2) against surface-dried *S. aureus* NCTC 10788 when various non-ionic surfactants were added at a concentration of 0.01% (P >0.05; ANOVA). There were also no differences in the biocidal activity of Formulation TCM+ against surface-dried *E. coli* ATCC 10798 when various non-ionic surfactants were added at a concentration of 0.01% (P >0.05; ANOVA) (fig. 3.20).

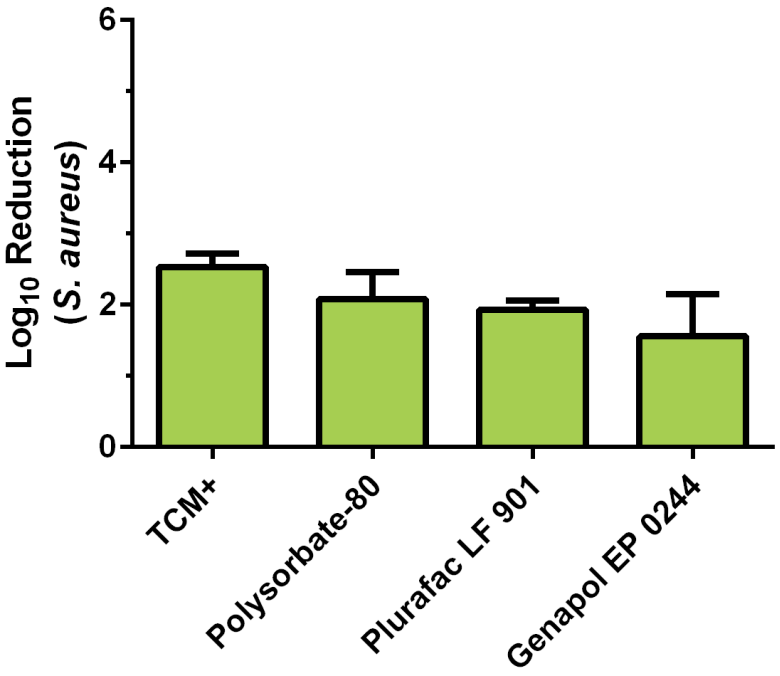

Fig. 3.19: Effect of non-ionic surfactants on biocidal activity of Formulation TCM+ against surface-dried *S. aureus.* 0.5-minute contact time.

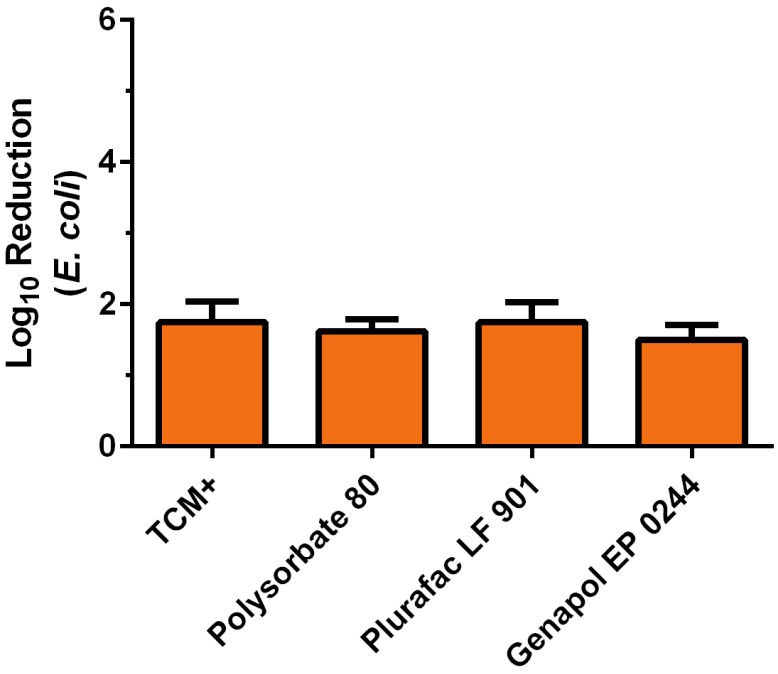

Fig. 3.20: Effect of non-ionic surfactants on biocidal activity of Formulation TCM+ against surface-dried *E. coli.* 1-minute contact time.

3.4.15 Cationic surfactants

All four cationic surfactants increased the biocidal activity of Formulation TCM+ against surface-dried *S. aureus* NCTC 10788 when added at a concentration of 0.01% (fig. 3.21). This included benzalkonium chloride ($P < 0.01$; ANOVA, Dunnett), didecyl dimethyl ammonium chloride ($P < 0.001$; ANOVA, Dunnett), Praepagen TQ ($P < 0.01$; ANOVA, Dunnett) and Praepagen HY ($P < 0.01$ ANOVA, Dunnett). Compared to the surfactant-free control, the dark biocidal activity of the formulation increased upon addition of benzalkonium chloride ($P < 0.001$; ANOVA, Dunnett) and didecyl dimethyl ammonium chloride ($P < 0.001$; ANOVA, Dunnett). Formulations containing Praepagen TQ and Praepagen HY did not exhibit any differences in dark biocidal activity ($P > 0.05$; ANOVA, Dunnett). This indicated that they lacked intrinsic biocidal properties at this concentration.

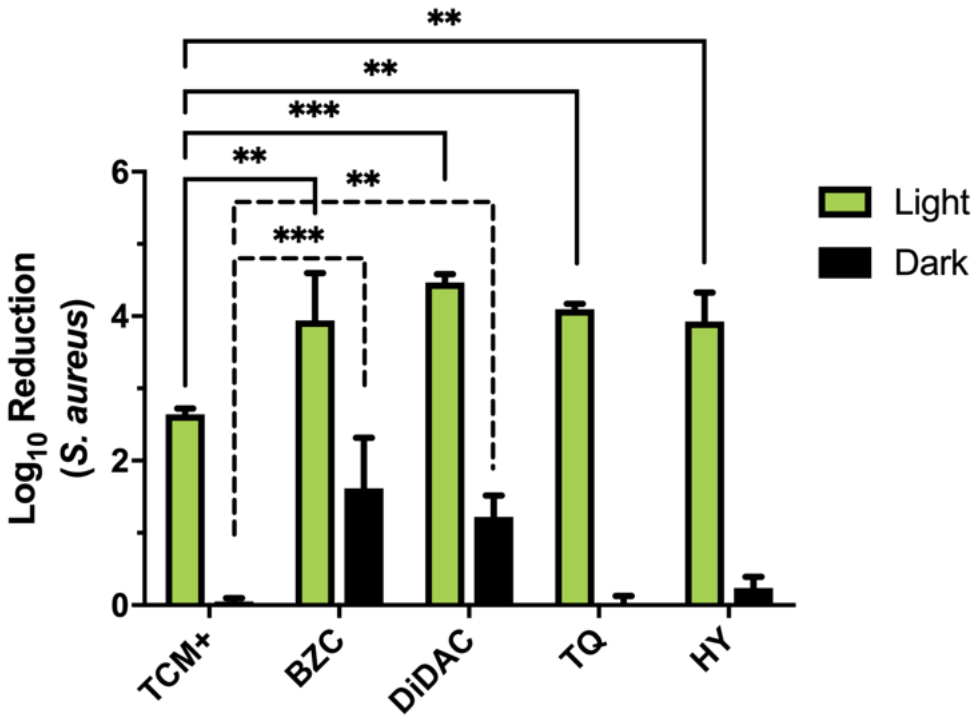

Figure 3.21: Effect of cationic surfactants on the biocidal activity of Formulation TCM+ against surface-dried *S. aureus* when combined with light or used in the dark. 1-minute contact time. TCM+ = surfactant-free control; BZC = benzalkonium chloride; DiDAC = didecyl dimethyl ammonium chloride; TQ = Praepagen TQ; HY = Praepagen HY. Solid lines illustrate statistical comparison between light-treated groups whereas dashed lines illustrate treated in the dark. ** $P < 0.01$; *** $P < 0.001$.

There were no changes in the light biocidal activity against surface-dried *E. coli* ATCC 10798 when cationic surfactants were added to Formulation TCM+ at a concentration of 0.01% (P >0.05; ANOVA) (fig. 3.22). However, when compared to the surfactant-free control, we observed a slight increase in biocidal activity in the dark upon the addition of benzalkonium chloride (P <0.01; ANOVA, Dunnett) and Praepagen HY (P <0.05; ANOVA, Dunnett).

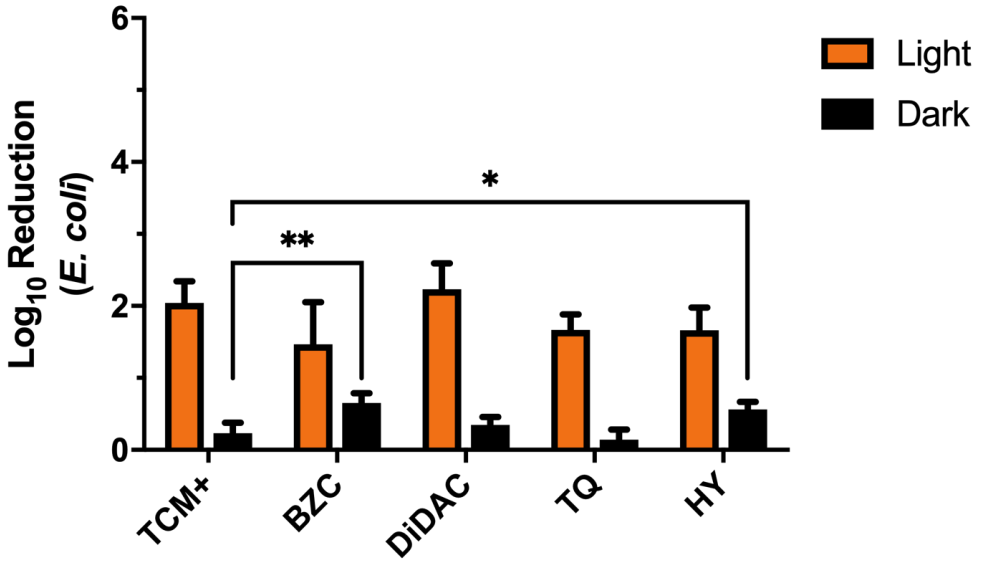

Figure 3.22: Effect of cationic surfactants on the biocidal activity of Formulation TCM+ against surface-dried *E. coli* when combined with light or used in the dark. 1-minute contact time. TCM+ = surfactant-free control; BZC = benzalkonium chloride; DiDAC = didecyl dimethyl ammonium chloride; TQ = Praepagen TQ; HY = Praepagen HY. * P <0.05; ** P <0.01.

3.4.16 Anionic surfactants

Figure 3.23 illustrates the absorbance spectra of Formulation TCM+, with and without the addition of SDS at two concentrations. Initially, the spectrum of Formulation TCM+ had two peaks at 590 and 630 nm, corresponding to TBO dimers and monomers respectively. The peak at 590 nm was slightly more dominant and the peak at 630 nm had an intensity of 0.31 units. Upon the addition of 0.01% of SDS to Formulation TCM+, we observed a visual change in its hue, changing from deep blue to a muted purple-grey tone. The spectrum demonstrated a flattening of the curve and the absorbance at 630 nm decreased to 0.16. Conversely, the addition of 0.10% SDS led to a return of colour, which was brighter than the SDS-free formulation. Analysis of the spectrum indicated that the absorbance at 630 nm absorbance peak rose to 0.56, which was substantially higher the initial absorbance. The shape of the peak also exhibited a redshift and the 630 nm peak, corresponding to TBO monomers, became dominant.

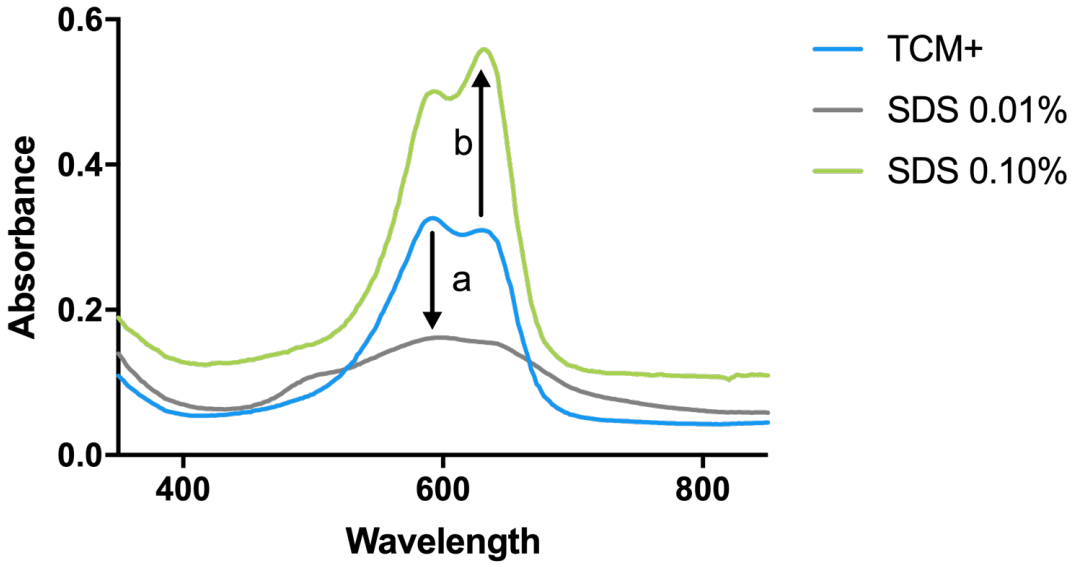

Figure 3.23: The effect of SDS on the spectral characteristics of Formulation TCM+. The addition of 0.01% SDS resulted in a marked decrease in the absorbance peak (a) whilst the addition of 0.10% SDS caused the peak intensity to increase and redshift (b).

The addition of 0.01% and 0.1% sodium dodecyl sulphate (SDS) to the formulation did not lead to a statistically significant change in photodynamic activity against *S. aureus* when co-administered with light (P >0.05; ANOVA) (fig. 3.24). However, when treated in the dark, however, we observed a statistically significant increase in dark biocidal activity in *S. aureus* exposed to TCM supplemented with 0.1% SDS (P <0.0001; ANOVA, Dunnett). There was no change in dark biocidal activity when supplemented with 0.01% SDS (P >0.05 ANOVA, Dunnett).

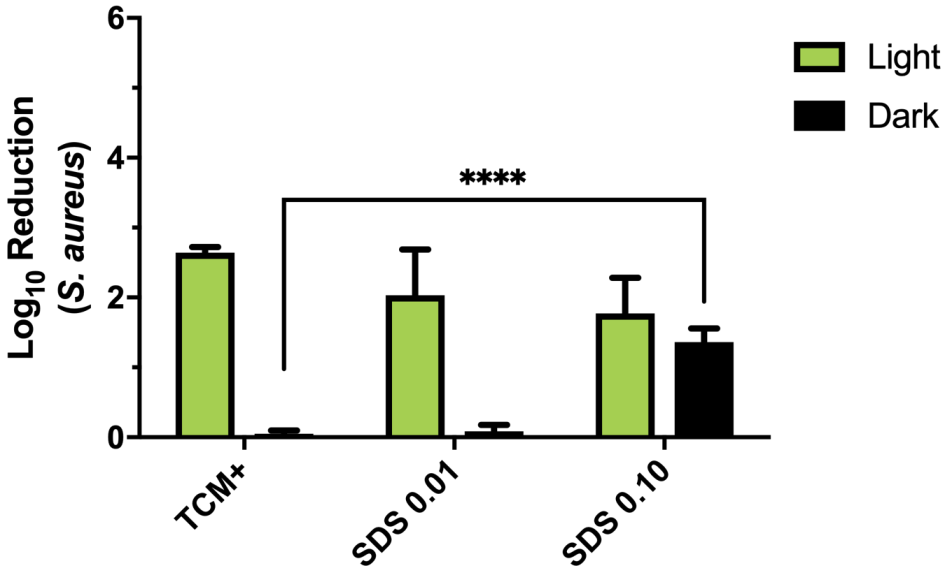

Figure 3.24: The effect of sodum dodecyl sulphate (SDS) on the light and dark biocidal activity of Formulation TCM+ against surface-dried *S. aureus*. 1-minute contact time. **** P <0.0001.

The addition of 0.01% SDS to Formulation TCM+ did not lead to a statistically significant change in activity against *E. coli* either in the light or in the dark (fig.3.25). There was, however, a decrease in photodynamic activity when 0.1% SDS was added to the formulation.

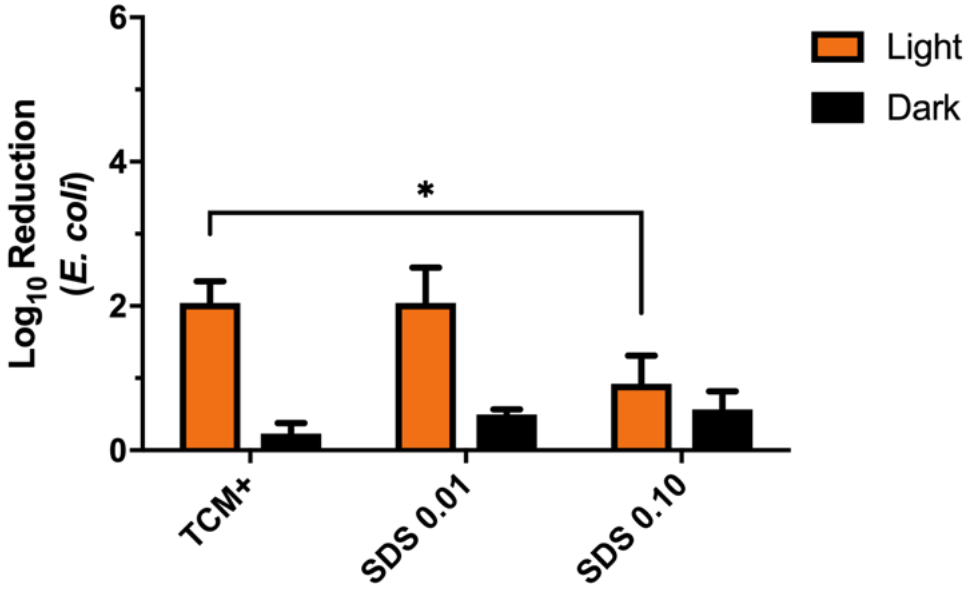

Figure 3.25: The effect of sodum dodecyl sulphate (SDS) on the light and dark biocidal activity of Formulation TCM+ against surface-dried *E. coli*. 1-minute contact time. Biocidal activity with co-application of light is denoted by orange columns. Biocidal activity of the formulations in the dark is represented by black columns. * P <0.05.

3.4.17 Effect of surfactants on TBO binding

The addition of Plurafac LF 901 and Praepagen TQ to Formulation TCM+ did not affect the binding of TBO to *S. aureus* NCTC 10788 at concentrations of 0.01 and 0.10% (P >0.05; ANOVA, Dunnett) (fig. 3.26). Likewise, there were no differences in TBO binding upon addition of 0.01% SDS (P >0.05); ANOVA, Dunnett). In the case of these formulations, TBO binding ranged from 90-96%. However, the addition of 0.10% SDS led to a considerable decrease in TBO binding as only 6% bound to *S. aureus* cells (P <0.0001; ANOVA, Dunnett).

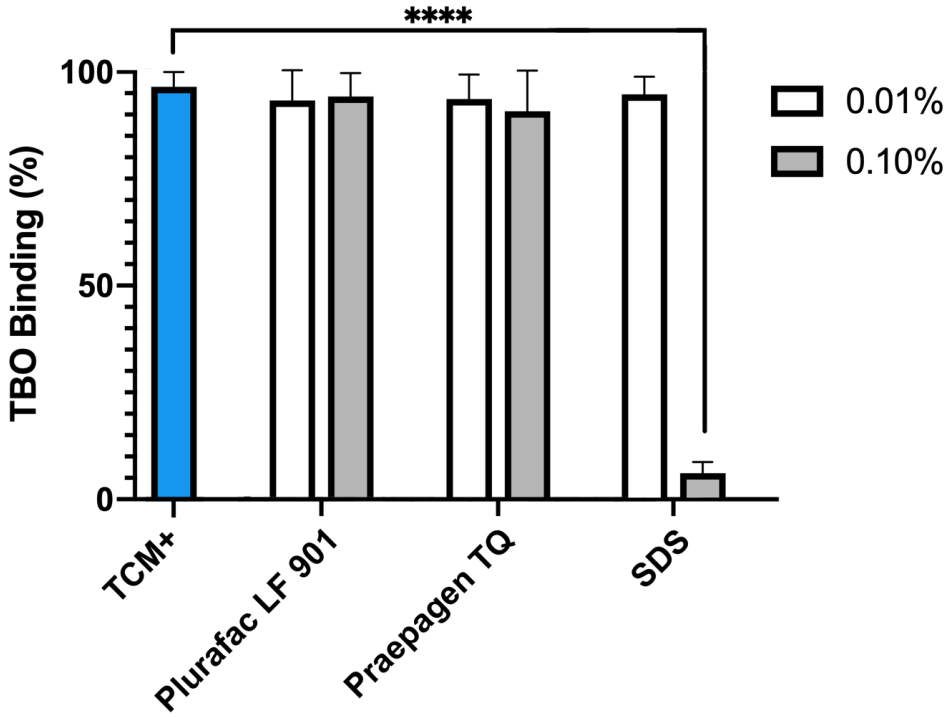

Figure 3.26: The effect of different surfactants on TBO adsorption to *S. aureus* cells. Plurafac LF 901 and Praepagen TQ are non-ionic and cationic surfactants respectively whilst sodium dodecyl sulfate (SDS) is an anionic surfactant. Formulation TCM+ (blue) was used as the control column for statistical comparison. **** P <0.0001.

3.4.18 Biocidal activity of Formulation TCM+S against surface-dried bacteria

Formulation TCM+S exhibited biocidal activity against surface-dried *S. aureus* NCTC 10788 and *E. coli* ATCC 10798 (table 3.6). After a treatment time of 1 minute, we observed a 4.1 $\log_{10}$ reduction in the viability of *S. aureus* viability and 2.0 $\log_{10}$ in *E. coli*. *E. coli* viability was reduced by 4.2 $\log_{10}$ after 2.5 minutes. At 5 minutes, we reached the limit of detection and observed ≥4.5 $\log_{10}$ reductions in the viability of both organisms. This meets the EN 13697 threshold of demonstrating >4 $\log_{10}$ reduction in viability to make claims of bactericidal efficacy against these species (British Standards Institute, 2015a).

Table 3.6: Bactericidal activity of Formulation TCM+S against surface-dried bacteria. EN 13697 test conditions.

Species	Contact time (mins)	$\log_{10}$ CFU reduction	SD	Pass/Fail*
S. aureus	1	4.1	0.07	Pass
	5	≥4.5	0.03	Pass
E. coli	1	2.0	0.30	Fail
	2.5	4.2	0.17	Pass
	5	≥4.5	0.04	Pass

*Pass threshold = 4 $\log_{10}$ reduction; SD = standard deviation

3.5 Discussion

3.5.1 pH is a strong determinant of biocidal activity

During the initial stages of optimisation, we attempted to determine the optimal pH of TBO-based formulations for bactericidal activity against suspensions of *S. aureus*. Other cationic compounds such as quaternary ammonium compounds exhibit increased bactericidal activity at alkaline pH (Lindstedt et al., 1990) and so it was anticipated that TBO-based formulations would benefit in a similar manner. We observed a strong correlation between increased pH and biocidal activity of TBO. Bactericidal activity against *S. aureus* increased concomitantly with increased pH and peak activity was observed at a tested pH of 10.2; this was followed by a subsequent decrease in biocidal activity after further increasing the pH to 11.2 (fig. 3.6). Our observations corroborate those of Kömerik & Wilson (2002), who noted that TBO was more bactericidal against Gram-negative organisms at alkaline pH.

It was curious to observe that the biocidal activity of TBO decreased when the pH was increased from 10.2 to 11.2. TBO is zwitterionic and has two ionisable groups with pKa values of 2.6 and 11.6 (Sabnis, 2010). It is likely that increasing pH to 11.2 may have resulted in deprotonation of the second ionisable group, yielding a negatively charged moiety within the TBO molecule and neutralising its cationic charge. This would impair its ability to interact with negatively-charged bacterial target sites.

Buffering agents are used in many biocidal products to control the pH of the biocide solution. Whilst sodium tetraborate (borate) was initially utilised, it was later determined that borate is an excluded substance from EU Ecolabel requirements (European Commission, 2014) due to its potentially deleterious effects on reproductive health (Weir & Fisher, 1972; Durmuş & Büyükgüzel, 2008). Therefore, alternative buffering agents were sought to be used in place of borate. As the buffering agents themselves were not anticipated to directly affect bactericidal activity, it was anticipated that alternatives could be used without impacting efficacy. Our observations indicated that the choice of buffering agent had little impact on the biocidal activity of TBO-based formulations (fig. 3.14) and that the formulation can tolerate changes to cheaper and less hazardous alternatives. For the developmental purposes of this thesis, carbonate-bicarbonate was selected for use as a buffering system as it its components are relatively non-hazardous and of low cost.

3.5.2 Optimum photosensitiser concentration is dependent on application

The concentration of TBO used in the formulation played a clear role in its biocidal activity against *S. aureus*. Of the concentrations tested, , optimal biocidal activity was observed at a TBO concentration of 4 μM (fig. 3.7) during early optimisation using EN 13727-based suspension tests. Further increasing the concentration from this point led to significantly diminished bactericidal activity. This was in line with our original hypothesis as it was anticipated that excess TBO would cause optical quenching of the photosensitiser by restricting light transmission through the bulk phase of the suspension. The data presented here demonstrates that quenching became problematic at TBO concentrations upwards of 10 μM when using the light source used in these experiments. Whilst it would be reasonable to suggest that a more powerful light source could counteract this effect, time limitations prevented investigations of this aspect.

The optimal concentration of TBO used in formulations was dependent on the format of test used to assess biocidal efficacy. In suspension tests based on the EN 13727 standard, we determined that the optimal concentration of TBO was 4 μM from the concentrations tested (fig. 3.7). However, this concentration was somewhat ineffective against surface-dried bacteria as only 2.7 $\log_{10}$ reductions in *S. aureus* viability were observed after a 5-minute contact time (table 3.5). As previously mentioned, optical quenching of excitatory light was hypothesised to cause diminished returns in biocidal activity when performing suspension tests in a cuvette. However, in EN 13697-based surface carrier tests, the use of a much smaller volume of formulation (100 μL) resulted in it covering the surface as a thin film. It was hypothesised that this would reduce the optical quenching effect and so TBO concentration could be increased to improve bactericidal activity. After performing a re-run of the TBO optimisation experiment using the EN 13697 surface carrier method, peak bactericidal activity was observed at a tested TBO concentration of 40 μM (fig. 3.18). This was ten-times higher than the optimal concentration determined using suspension tests.

3.5.3 *P. aeruginosa* intrinsically resists TBO photosensitisation

In further testing against a broader spectrum of bacteria, we determined that *P. aeruginosa* was considerably more resistant to Formulation TB than other species. Treatment of *P. aeruginosa* suspensions with Formulation TB for 1 minute resulted in only a 0.6 log reduction in the viability. This contrasted with >5 $\log_{10}$ reductions in viability of the other three bacterial species which were tested (fig. 3.11). It was interesting to observe such a stark contrast in activity between *E. coli* and *P. aeruginosa*. Being Gram-negative, both species possess an outer membrane which was anticipated to provide a measure of protection against TBO. *P. aeruginosa* is well established to be intrinsically resistant to many chemical

agents and it is one of the most common contaminants of products such as cosmetics and even hand sanitisers (Sutton & Jimenez, 2012). The major mechanism of resistance to antimicrobials by *Pseudomonas* is the impermeability of its outer membrane. Compared to *E. coli*, another Gram-negative species, the outer membrane of *P. aeruginosa* is up to 100 times less permeable to hydrophilic molecules (Yoshimura & Nikaido, 1982).

In contrast to other Enterobacteriaceae, which contain general diffusion porins for a large range of compounds (e.g. OmpC in *E. coli*), the outer membrane of *P. aeruginosa* contains numerous types of substrate-specific porins (Chevalier et al., 2017). This protects pseudomonads from the action of antimicrobials by restricting their access to the periplasm and inner membrane. These differences in the outer membrane physiology of *E. coli* and *P. aeruginosa* likely underlie the differences observed in the biocidal activity of Formulation TB against these species. In addition to being highly impermeable, the outer membrane of *P. aeruginosa* is also rich in efflux pumps. These transporter channels are able to export periplasmic contents out of the cell and confer an additional layer of resistance to antimicrobials. The role of efflux in protecting against photosensitisation is unclear. Whilst Tegos et al. (2008) observed an increase in *P. aeruginosa* susceptibility to TBO photosensitisation after application of an efflux pump inhibitor, other authors reported that mutants which overexpressed multi-drug efflux pumps were no more resistant to disinfection (Tseng et al., 2009).

3.5.4 Chelators potentiate TBO-photosensitisation against *P. aeruginosa*

To further optimise the formulation against *P. aeruginosa*, the chelator methylglycinediacetic acid (MGDA) was added to Formulation TB. Chelators are well documented to improve the activity of antimicrobials against Gram-negative species due to disruption and permeablisation of the outer membrane due to calcium coordination (Lambert et al., 2004). Consequently, MGDA was hypothesised to improve the biocidal activity of the formulation against *P. aeruginosa*. MGDA was selected over the more commonly used EDTA due to its superior ecological profile (Pinto et al., 2014). Marked improvements in bactericidal activity against *P. aeruginosa* was observed following the addition of 5 mM MGDA to Formulation TB and biocidal activity increased by two to three orders of magnitude compared to the MGDA-free control (fig. 3.11). This clearly demonstrated that MGDA was suitable for potentiating the activity of TBO against *P. aeruginosa*. We anticipate that is likely to be the case with other photosensitiser-chelator combinations. These data also support the hypothesis that the outer membrane of *P. aeruginosa* is primarily responsible for its intrinsic resistance to TBO photosensitisation.

The next stage in the development of the formulation was determination of the optimum concentration of MGDA necessary for antibacterial activity against suspensions of *P. aeruginosa* and *S. aureus*. MGDA was added to Formulation TCM at concentrations ranging from 1-100 mM. The addition of MGDA at all tested concentrations led to substantial increases in biocidal activity against *P. aeruginosa* (fig. 3.12) Of the concentrations tested, peak activity was observed at 10 mM; increasing the concentration to 25 mM and beyond resulted in a decrease in biocidal activity. In the case of *S. aureus*, there was not a statistically significant difference in activity when 1 and 10 mM MGDA were added to the formulation, compared to the MGDA-free control. However, increasing the concentration to 25 mM and beyond resulted in increasingly diminished biocidal activity (fig. 3.13).

Examination of the structure of MGDA may hold clues as to why an excess inhibits TBO photosensitisation. MGDA is synthesised as a trisodium salt and dissociates in solution into a tri-anionic form containing three negatively charged residues (fig. 3.27). In the presence of an excess of MGDA, cationic TBO may interact with these negative sites rather than those in bacterial intracellular targets. This would reduce the amount of TBO which binds to bacteria and thus interfere with its biocidal activity.

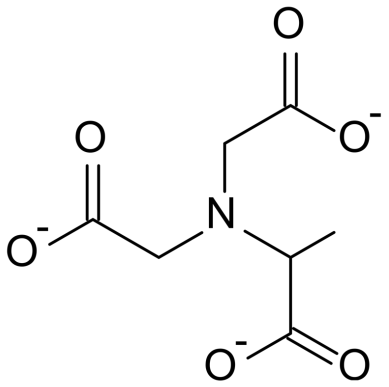

Figure 3.27: Ionised structure of MGDA. As a trisodium salt, MGDA dissociates into a tri-anionic molecule which could outcompete intracellular targets for TBO adsorption.

These observations demonstrate that MGDA should be added to the formulation at a concentration of 10 mM to ensure optimal biocidal activity against *P. aeruginosa* without compromising efficacy against *S. aureus*. The resulting Formulation TCM (4 μM TBO, carbonate buffer, 10 mM MGDA; pH 10.2), exhibited excellent bactericidal activity against both species, as well as *Enterococcus hirae* and *Escherichia coli*. Formulation TCM was rapidly bactericidal against all four species and was able to achieve >5 $\log_{10}$ reductions in all four species in 1 minute (fig. 3.16).

When compared to the works of other researchers, Formulation TCM performed exceedingly well. When using a commercial formulation containing 50 μM methylene blue, de Oliviera et al. (2014) reported only 0.5 to 1.5 $\log_{10}$ reductions in the viability of several bacterial species after 3 mins. After accounting for differences in the light source fluence, the amount of light delivered by these authors (9 J) was similar to a 1-minute exposure using the experimental set up described in this thesis (10.8 J). However, we were able to achieve >5 $\log_{10}$ reductions using Formulation TCM. This indicates that the formulations developed throughout this chapter offer superior biocidal activity than currently available products.

Despite the rapid bactericidal activity of TCM against bacterial suspensions, it performed surprisingly poorly against surface-dried *S. aureus*. A contact time of 5 minutes was insufficient at decreasing *S. aureus* viability to the >4 $\log_{10}$ requirement of the EN 13697 (table 3.5). Fortunately, re-optimisation of the TBO concentration yielded significant improvements in the formulation (fig. 3.18), as previously discussed. Consequently, the formulation was adapted to account for these observations; the resulting iteration was dubbed Formulation TCM+.

3.5.5. Surfactants enhance photosensitiser-based surface disinfection

Non-ionic surfactants (NIS) were added to Formulation TCM+ to improve its wetting properties. This would improve the ability of the formulation to spread over PVC surfaces, such as those of automated endoscope reprocessors, and would be an important property for future product development. Several NIS were selected for addition to the formulation at a concentration of 0.01%. This included 2 fatty alcohol alkoxylates (Plurafac LF 901 and Genapol EP 0244) and polysorbate 80. When tested against surface-associated bacteria, no statistically significant differences in efficacy were observed upon the addition of any of the three NIS either against *S. aureus* (fig. 3.19) or *E. coli* (fig. 3.20). However, surfactant-supplemented formulations coated the PVC coupons surface much better than without surfactant. These observations indicate that NIS are compatible with TBO-based formulations and can be added to the formulation to improve wettability.

Cationic surfactants are widely used antimicrobial agents which are known to disrupt bacterial membranes. It was hypothesised that cationic surfactants would increase biocidal activity against surface-associated *E. coli* and *S. aureus.* In these experiments, we tested three quaternary ammonium compounds (QACs) and one esterquat, which is an ecologically friendly alternative to QACs (Garcia et al., 2000; Mishra & Tyagi, 2007). The addition of each cationic surfactant to Formulation TCM+ led to an increase in its biocidal activity against surface-dried *S. aureus* (fig. 3.21). Benzalkonium chloride, didecyl dimethyl ammonium chloride (DiDAC), Praepagen TQ and Praepagen HY were all able to

substantially improve the biocidal activity of Formulation TCM+. In the cases of DiDAC and Praepagen TQ, >4 log_{10} reductions in *S. aureus* viability were achieved within 1 minute, compared to only 2.6 log_{10} in the surfactant free control; this exceeds the threshold required by the EN 13697 standard. To our knowledge, this is the first time that cationic surfactants have been co-formulated with photosensitisers to successfully potentiate their activity.

As illustrated by figure 3.21, formulations supplemented with DiDAC and BZC both exhibited increased dark biocidal activity compared to Formulation TCM+. As these QACs are widely used biocides, this result was somewhat expected. Consequently, the observed increase in light biocidal activity after adding these compounds may be a simple additive effect. In contrast, formulations containing Praepagen TQ and Praepagen HY exhibited no difference in dark biocidal activity compared to Formulation TCM+. However, they were both able to substantially increase the light biocidal activity. There strongly supports the hypothesis of synergism between cationic surfactants and TBO. We hypothesise that these gentler surfactants transiently interact with the cell surface to enhance TBO adsorption without exerting biocidal effects on their own.

Interestingly, cationic surfactants were unable to improve the light biocidal activity of Formulation TCM+ against *E. coli* at a concentration of 0.01% (fig3.22). However, Gram-negative organisms are less susceptible to quaternary ammonium compounds compared to their Gram-positive counterparts (Wickham, 2017). Given more time to develop the formulation, a higher concentration of cationic surfactant may also yield improvements in TBO photosensitisation against Gram-negative species.

It was hypothesised that the addition of anionic surfactants to Formulation TCM+ would inhibit its biocidal activity. At 0.01% SDS, the formulation decolourised markedly whilst 0.10% SDS led to a marked increase in the formulation's absorbance peak (fig 3.23). Decolourisation was anticipated to reduce biocidal activity by reducing the ability of TBO to absorb excitatory light required for production of $^1O_2$. Whilst the addition of 0.1% SDS reversed the decolourisation effect, it was posited that the TBO would become trapped within negatively charged micelles and be prevented from interacting with bacterial target sites.

Interestingly, the addition of 0.01% SDS to Formulation TCM+ did not lead to a decrease in biocidal activity against *S. aureus* (fig 3.24) or *E. coli* (fig. 3.25). This unexpected result contradicted our hypothesis and may hint that the ionic interactions between SDS and TBO (which underlie the process of decolourisation) are of lower affinity than the interaction of TBO and microbial target sites. In this proposed model, TBO-SDS aggregates dissociate in

the presence of microbial cells so that TBO preferentially binds to target sites instead. These results indicate that, despite appearing decolourised, TBO formulations can tolerate the presence of trace anionic surfactant residues which may remain on surfaces after previous cleaning steps.

In contrast to these observations, the addition of 0.10% SDS to Formulation TCM+ led to a marked decrease in the activity against *E. coli* (fig. 3.25). Previous authors have posited that the rebound hypercolourisation of cationic photosensitisers in the presence of high concentrations of SDS is due to trapping of photosensitisers within anionic micelles (Jebaramya et al., 2009; Edbey et al., 2015). Investigations of TBO adsorption in the presence of various surfactants at different concentrations demonstrated that 0.10% SDS almost completely inhibited TBO adsorption to *S. aureus* (fig.3.26). In contrast, 0.01% SDS did not affect TBO adsorption, nor did the non-ionic or cationic surfactants at either concentration. These results strongly support the hypothesis that the interactions between sub-micellar SDS-TBO aggregates are of lower affinity than TBO and microbial target sites.

Curiously, we did not observe a statistically significant decrease in the biocidal activity of Formulation TCM+ against *S. aureus* after adding 0.10% SDS (fig. 3.24). However, there was a concurrent increase in dark toxicity at this concentration which may have masked any decrease in photosensitisation efficacy. The results of the TBO binding assay support this view.

3.5.6 Plasmonic silver nanoparticles inhibit photosensitisation

Metal nanoparticles (NPs) possess unique optical properties and have been previously described to enhance the inactivation of microorganisms by photosensitisers (Narband et al., 2008; Narband et al., 2009; Misba et al., 2016). We hypothesised that the addition of plasmonic silver NPs to Formulation TB would improve its biocidal activity against *S. aureus* by increasing the singlet oxygen quantum yield. Two types of silver NP were selected which shared overlapping spectra with TBO, which has been suggested to be an important factor in plasmonic enhancement (Hu et al., 2014). The addition of both types of silver nanoparticle to Formulation TB at a concentration of 5.0 μg/mL decreased biocidal activity against *S. aureus* (fig. 3.8) In contrast, the addition of 0.5 μg/mL NPs had no effect on biocidal activity. These results contradict the hypothesis and indicate that these types of nanoparticle are unsuitable for enhancing TBO photosensitisation.

Further investigations into the ability of each formulation to decompose DPBF indicated that the addition of 5.0 μg/mL NPs led to a marked decrease in singlet oxygen yields (fig. 3.9). Interestingly, this supports the spectroscopic data of Narband et al. (2008), who observed a

decrease in singlet oxygen production when combining TBO with gold nanoparticles. It is curious, however, that we observed the opposite effect in relation to its impact on the biocidal activity of our formulation. They and other authors proposed that the presence of metal nanoparticles partly enhanced photosensitisation by inducing a shift toward type-I photosensitisation; this favours the production of radical species rather than singlet oxygen which they predicted may inflict greater damage on target cells (Narband et al., 2008; Misba et al., 2016).

Narband et al. (2008) reportedly used a polychromatic argon discharge lamp as the excitation source in their experiments. As they did not use an optical filter or monochromator to isolate the 630 nm (red-orange) light band, it is plausible that their light source was also able to excite the gold nanoparticles directly which may have had secondary photothermal effects on the target cells. Alternatively, the gold nanoparticles used by these authors were considerably smaller than the silver nanoplates used in this study; they may have had effects on the bacterial membrane which potentiated photosensitisation by improving adsorption of TBO, rather than by enhancing photoexcitation.

We propose that the observed quenching of singlet oxygen by silver nanoplates was directly related to the spectral overlap between the nanoparticles and TBO. As nanoparticle dispersions are strongly coloured, it is reasonable to suggest that they may have inhibited the transmission of light through the suspensions. This process would be similar to that which occurs when the concentration of TBO becomes too high (fig. 3.7). Given the expense of silver nanoplates and growing concerns on the ecotoxicological impacts of nanomaterials (De Jong and Borm, 2008; Scientific Committee on Emerging and Newly Identified Health Risks, 2014), it may never have been feasible to eventually incorporate them into an affordable and eco-friendly disinfectant product. As such, these findings were not unwelcomed as they supported the removal of nanoparticles from the formulation development process.

3.5.7 Lipophilic photosensitisers are less effective against *E. coli*

New methylene blue (NMB) is a phenothiazine derivative which exhibits greater lipophilicity and singlet oxygen quantum yields compared to TBO (Phoenix et al., 2008). It was hypothesised that substituting TBO for the more lipophilic NMB could improve biocidal activity against Gram-negative species such as *E. coli* by facilitating interactions with lipids components of the outer and cytoplasmic membranes. Consequently, we produced a formulation based on Formulation TCM in which TBO was completely substituted with NMB. The resulting formulation was tested against suspensions of *E. coli*.

Substituting TBO with NMB led to significantly poorer biocidal activity against suspensions of *E. coli* (fig. 3.15). Whilst decolourisation of the NMB-based formulation was observed following illumination (indicating complete oxidation of the photosensitiser), a markedly higher rate of bacterial survival was observed. These observations refute the original hypothesis and demonstrate that lipophilic photosensitisers exhibit poorer biocidal activity against *E. coli* when compared to hydrophilic analogues. This may indicate that membrane lipids are not the major target of microbial inactivation during photosensitisation or that the photosensitiser must enter the cytoplasm of target cells via hydrophilic porins to achieve microbicidal effects. The photosensitiser may also interact with hydrophilic regions such as in proteins. Proteins are rich in negatively charged carboxylate residues which likely facilitate interactions with cationic phenothiazines such as TBO and therefore may be important targets of photosensitisation. This will be discussed in more detail in Chapter 4.

Bacellar et al. (2014) reported greater damage of lethicin-based liposomes when using lipophilic phenothiazine derivatives. As these simple liposomes did not contain negatively charged proteins, it stands to reason that lipophilic photosensitisers would interact better with them due to being able to partition into the lipid bilayer. However, this is a poor model for the interactions between photosensitisers and bacteria, which contain a multitude of negatively charged moieties. In addition, porins are likely to facilitate diffusion of photosensitisers across the outer membrane of Gram-negative bacteria and so diffusion through the lipid bilayer itself may play a fairly minor role in the photosensitisation process.

3.5.8 Increased cycle temperatures inhibit photosensitisation

In order to improve the activity of Formulation TCM against surface-associated bacteria, we attempted to increase the cycle temperature. Higher temperatures are known to facilitate faster reaction kinetics and so it was hypothesised that increasing the cycle temperature would improve the activity of the formulation. Contrary to the hypothesis, increased cycle temperatures were associated with a distinct decrease in biocidal activity. At 40ºC and 50ºC, statistically significant decreases in biocidal activity were observed compared to at 20ºC. Upon increasing the temperature to 50ºC, 1-minute biocidal activity against *S. aureus* decreased to 0.5 $\log_{10}$; this compared to a 1.7 $\log_{10}$ decrease in those treated at 20ºC. At 30ºC, statistically significant differences in activity were not observed, indicating that the formulation tolerates a small rise in temperature. However, these observations indicate that the formulations storage conditions should be considered, particularly in endoscopy units with high ambient temperatures.

In the formulations held at 40 and 50ºC, bubbles were observed to form on the sides of the container, which indicated gasses such as dissolved oxygen (DO) were lost from the solution. The loss of DO from the formulation was hypothesised to underlie the observed decrease in biocidal activity. As the production of singlet oxygen during photosensitisation requires energy transfer to ground state oxygen, decreased DO would impair activity by reducing singlet oxygen yield. Degassed formulations of the formulation exhibited extremely poor activity against *S. aureus*, even when used at 20ºC (fig. 3.17). Whilst this supported the hypothesis, it would also be useful to measure the DO content of formulations held at different temperatures and replicate this in in a formulation used at 20ºC to facilitate more direct comparisons.

3.6 Chapter conclusions

The results presented throughout this chapter represent a significant step forward in the development of a TBO-based formulation for use as a disinfectant product. Numerous factors, including pH, active component concentration and the effect of various excipients, were investigated and the resulting data was used to guide the evolution of the formulation. As part of this development phase, the resulting formulations exhibited a broad spectrum of bactericidal activity (fig. 3.16) and was also effective against surface-dried bacteria (table 3.6).

The results contained in this chapter demonstrate that considerable improvements in the biocidal activity of photosensitiser-based formulations can be achieved through careful selection of excipients and by modifying their concentration. In the case of TBO, modifying the pH, photosensitiser concentration and adding chelators and surfactants can all yield improvements in its bactericidal efficacy. Conversely, we observed impeded biocidal activity when using increased cycle temperatures and upon the addition of plasmonic silver nanoparticles. The lipophilic photosensitiser new methylene blue was also considerably less bactericidal compared to TBO.

Throughout this process, we demonstrated biocidal activity against suspensions of several vegetative bacterial species, including *P. aeruginosa*, and also against surface-dried *S. aureus* and *E. coli*. These results indicate that the formulation passes the first phase of development and that more rigorous testing is warranted. The final optimised formulation which was used as the basis for the rest of this thesis was termed TCM+S and comprised the following: TBO (40 μM); Na_2CO_3 (15 mM); $NaHCO_3$ (10 mM), MGDA (10 mM); Plurafac LF 901 (0.01%); Praepagen TQ (0.01%); pH 10.2.

Chapter 4.

Mechanism of Action and Effect on Target Cells

4.1 Introduction

4.1.1 Intracellular targets of biocides

Understanding the effect of an antimicrobial treatment on target cells is useful for formulation development. By understanding the mechanisms which underlie cell inactivation, potential weaknesses can be identified so that future development can focus on overcoming specific obstacles. An important process in identifying the mechanism of action is to determine which parts of a target cell are affected by the treatment. In contrast to antibiotics, which mimic endogenous molecules and inhibit specific vital enzymes, biocides are characterised by their ability to target non-specific cell components such as the cytoplasmic membrane or DNA. Examples of some of the major intracellular targets targeted by known biocides are described in table 4.1.

Table 4.1: Target sites and mechanism of action of commonly used biocides

Target site	Example biocide	Mechanism of action	Reference
Cytoplasmic membrane	QACs & surfactants	Disruption of intramolecular bonds between membrane phospholipids	Gerba (2015)
Cell wall	Lysozyme	Peptidoglycan hydrolysis and membrane perturbation	Masschalck & Michiels (2003)
Nucleic acids	Peracetic acid	DNA strand breaks	Maillard et al. (1996)
	GTA & OPA	Alkylation of nucleotides	McDonnell & Russell (1999)
Proteins	Peracetic acid	Oxidation of amino acids	Finnegan et al. (2010)
	GTA & OPA	Cross-linking amino acids	Simons et al. (2001)
	Silver	Reaction with thiol groups	Liau et al. (1997)
	Triclosan	Enzyme inhibition	Heath et al. (1999)

QACs: quaternary ammonium compounds | GTA: glutaraldehyde | OPA: o-phthalaldehyde

Elucidating the target of antimicrobial agents can be achieved through a variety of methods, dependent on the proposed target. For example, damage to the cytoplasmic membrane can be inferred through the loss of intracellular contents and penetration of exogenous agents whilst DNA damage can be visualised through agarose gel electrophoresis. These are described and contrasted in the following sections.

4.1.2 Markers of membrane damage

4.1.2.1 Loss of intracellular contents

The cytoplasm of bacterial cells contains a complex mixture of substances such as cations, amino acids and polymers, which are maintained at concentrations orders of magnitude greater than that which is present in the extracellular space. These can be detected in the event of damage to the cytoplasmic membrane. Potassium (K^+) is the principle intracellular cation in bacterial cells (Epstein, 2003). Due to its small size, K^+ is lost in the initial stages of membrane disruption and is a primary indicator of membrane damage (Johnston et al., 2003). Leakage of K^+ can be detected using a variety of methods including electrolyte probes (Orlov et al., 2002) and spectroscopic methods such as atomic emission spectroscopy (AES) and inductively coupled plasma-mass spectrometry (ICP-MS) (Johnston et al., 2003; Lopez-Romero et al., 2015). As previous research has already indicated that photodynamic treatment with methylene blue leads to loss of intracellular potassium (Sahu et al., 2009) in both *E. coli* and *S. aureus*, this study focused on studying other markers of damage.

ATP is the principle intracellular energy source which facilitates metabolic processes such as growth, nutrient transport, motility and genome replication (Lynch & Marinov, 2017). Like potassium, bacterial cells maintain an intracellular pool of ATP within the cytoplasm. However, ATP is a relatively large molecule compared to metal cations and is easily retained by the cytoplasmic membrane. Leakage of ATP into extracellular space is therefore indicative of membrane damage which exceeds the severity of that which results in the loss of cations (Johnston et al., 2003).

4.1.2.2 Membrane potential changes

Membrane potential is the result of uneven distribution of electrolytes across each side of a biological membrane, such as the cytoplasmic membrane of bacterial cells. This difference causes the membrane to be “polarised” and maintain a slightly negative membrane potential. Potassium, the primary intracellular cation, is maintained within cells at substantially higher concentrations than the surrounding environment. In *Escherichia coli* this results in a resting membrane potential of -85 to -142 mV, depending on the pH of the surrounding medium (Felle et al., 1980). Unlike eukaryotes, which contain mitochondrial networks, electron transport occurs on the cytoplasmic membrane of prokaryotes (Bonora et al., 2012; Lynch & Marinov, 2017). Upholding membrane potential is thus essential to bacterial survival as it maintains the proton motive force necessary to drive ATP synthesis (Dimroth et al., 2000). In addition to its role in energy production, membrane potential plays a vital role in directing cell division (Strahl & Hamoen, 2010). Depolarisation of the membrane is thus fatal due to its impact on both energy production and replication. Detecting whether exposure to a

biocide results in loss of membrane potential is therefore useful for determining its mechanism of action.

Changes in membrane potential as a result of exposure to antimicrobial agents can be examined using dyes which selectively interact with the cytoplasmic membrane depending on surface charge. Carbocyanine dyes such as 3,3'-diethyloxacarbocyanine iodide (DiOC2(3)) are considered to be slow-response voltage probes and are available as commercial kits (Thermo Fisher Scientific, 2019c). When not self-associated within cells, the dye exhibits green fluorescence. Conversely, the dye rapidly accumulates in depolarised membranes, which leads to the formation of dye aggregates and a shift toward red fluorescence as a result of self-association between dye monomers (Novo et al., 1999). Red/green fluorescence ratios of each cell ca be ascertained by flow cytometry, thus determining the extend of membrane depolarisation: healthy cells exhibit a high green/red ratio whilst the opposite is true of depolarised cells.

4.1.2.4 Penetration of exogenous agents

The fluorescent dye propidium iodide (PI) is a one of the most common methods for detecting damage to the cytoplasmic membrane. PI is a DNA intercalating fluorophore which is non-membrane permeable and is excluded from cells with intact membranes; disruption of membrane integrity facilitates PI entry into cells, facilitating its interaction with DNA and inducing an increase in red fluorescence (Stocks, 2004; Berney et al., 2008; Stiefel et al., 2015). In the “live/dead” stain, PI is used alongside SYTO9, a membrane permeable DNA probe which can permeate both live and dead cells. Penetration of PI into cells quenches SYTO9 fluorescence and so cells with damaged membranes exhibit a decrease in relative green/red fluorescence when examined by microscopy or flow cytometry (Stocks, 2004; Berney et al., 2008; Stiefel et al., 2015).

4.1.2.4 Microscopic examination

The effect of treatment on the surface structure of microbial cells can be investigated using scanning electron microscopy (SEM) or atomic force microscopy (AFM). Traditionally, SEM samples are prepared by fixing with a cross-linking agent such as glutaraldehyde and are then chemically dehydrated with ethanol and dried through a variety of approaches (Golding et al., 2016). Samples may be also fixed by specialised cryogenic techniques to avoid drying artefacts (Sriamornsak et al., 2008). The sample surface is then sputter coated with a layer of metal, such as gold and palladium, to improve electroconductivity and allow the electron beam to scan across the surface (Golding et al., 2016). In AFM, samples can be analysed *in situ* in the liquid phase with minimal preparation steps, allowing the effects of

antimicrobial exposure to be studied in real-time under physiological conditions (Dufrêne, 2014). AFM can also provide improved resolution as well as topographic information which can be used to characterise surface features such as pit and bumps (Russell, 2001). Changes in the internal ultrastructure of target cells following biocide exposure can also be investigated by transmission electron microscopy (TEM) after sectioning fixed samples (Thanomsub et al., 2002).

4.1.3 Indicators of DNA damage

Biocides such as peracetic acid and glutaraldehyde can have damaging effects on the nucleic acids of target cells (Maillard et al.,1996; McDonnell & Russell (1999). Whilst a range of methods exist for measuring DNA damage in eukaryotes, detecting DNA damage in prokaryotes is complicated by a limited number of suitable methodologies.

4.1.3.1 Transcriptomic approaches

DNA damage to prokaryotes causes transcriptomic changes in the expression of genes related to DNA repair. Single strand breaks are detected by RecA, which causes the LexA repressor protein to become degraded; this leads to the de-repression of numerous SOS regulon-associated genes, including *recA* itself (Kreuzer, 2013). mRNA transcribed during the SOS response is quantifiable using methods such as quantitative PCR (qPCR), though a sizable proportion of cells must survive treatment to allow changes in gene expression to be detected.

4.1.3.2 Terminal deoxynucleotidyl transferase deoxyuridine triphosphate (dUTP) nick end labelling (TUNEL) assay

The terminal deoxynucleotidyl transferase deoxyuridine triphosphate (dUTP) nick end labelling (TUNEL) assay facilitates identification of DNA damage and fragmentation by incorporating fluorescently-labelled nucleotides at exposed 3'-hydroxyl termini located at the site of strand breaks; the accompanying change in fluorescence and proportion of cells exhibiting genome fragmentation is quantifiable by flow cytometry (Loo, 2000). Whilst useful for detecting DNA fragmentation in spermatozoa and apoptotic cells (Loo, 2011; Sharma et al., 2013), the assay requires high yields of DNA and treated cells must retain protein synthesis and DNA repair functions. Inhibition of protein synthesis by chloramphenicol treatment prevents the detection of strand breaks following peroxide exposure (Rohwer & Azam, 2000) whilst Δ*recA E. coli* mutants appear TUNEL-negative following treatment with DNA-damaging norfloxacin (Dwyer et al., 2012). These requirements indicate that this approach would be unsuited for investigating DNA damage in cells treated with Formulation TCM+S.

4.1.3.3 Mutant strains

Mutants strains contain genetic defects which impair the expression or function of genes and are regularly utilised when investigating the mechanism of action of biocides. Mechanisms of biocide resistance in *Bacillus subtilis* endospores has been studied extensively using such an approach (Riesenman & Nicholson, 2000; Setlow et al., 2006; Ghosh et al., 2008) whilst Δ*recA* mutants have been used to investigate DNA damage by hydrogen peroxide and glutaraldehyde (Konola et al., 2000; Tennen et al., 2000). Differences in the susceptibility of mutants with impaired DNA damage responses could be used to infer whether DNA damage takes place following treatment with Formulation TCM+S.

4.1.3.6 Agarose gel electrophoresis

Agarose gel electrophoresis can be used to visualise damage to DNA by biocides. Intact whole DNA and enzymatically digested fragments exhibit distinct and well resolved banding patterns when separated by electrophoresis. Double strand break sites produce fragments at random points which results in poorly resolved and smeared bands following electrophoresis. This technique has been used previously to demonstrate damage to the genome of *Pseudomonas* bacteriophage F116 following treatment with PAA (Maillard et al., 1996). When used in the comet assay, electrophoresis can also be used to approximate the extent of genome fragmentation in isolated eukaryotic cells such as yeasts (Azevedo et al., 2011). The comet assay has also been adapted for use with prokaryotic cells though their smaller size and genome makes isolation and detection more challenging (Solanky & Haydel, 2012).

Native gel electrophoresis is insensitive to single strand DNA breaks as the gel conditions preserve hydrogen bonds between complementary nucleotides on each strand. Alkaline gel electrophoresis facilitates the detection of single strand breaks by disrupting these bonds, causing damaged DNA to denature and fragment at break sites. Alkaline gel electrophoresis is a sensitive method which allows identification of 2 lesions per 5 megabases of DNA (Sutherland *et al*., 2006).

It is unclear whether photosensitisation induces DNA strand breaks in target cells. Wagner et al. (1998) identified that methylene blue interacts with viral nucleic acids with high affinity and that these are targets of photosensitisation. However, Epe et al. (1993) did not observe large numbers of DNA stand breaks in a cell-free system following treating with methylene blue and red light, though detected extensive base modifications such as the oxidation of guanosine residues into 8-oxoguanine (Epe et al., 1993).

4.1.4 Damage to cellular macromolecules

Proteins, lipids, carbohydrates and nucleic acids can all become damaged following exposure to biocides. The effect of photosensitisers on proteins and amino acids has been extensively studied over the past half a century. Due to their catalytic activity, which can be easily monitored, enzymes are often used as model proteins. Photooxidation of lysozyme by methylene blue leads to loss of enzymatic activity and tryptophan appears to be the primary amino acid targeted (Silva et al., 2000). In contrast, inactivation of lipoamide and alcohol dehydrogenases appears to be the result of photooxidation of histidine residues (Tsai et al., 1985). Other amino acids, including tyrosine, cysteine and methionine, have long been established to be susceptible to photooxidation by methylene blue whilst peptide bonds between amino acids are not a target of photosensitisation (Weil et al., 1951). Negatively charged aspartic and glutamic acid do not appear to be major targets for oxidation (Weil et al., 1951), though it is plausible that they may facilitate initial interactions between proteins and cationic photosensitisers. TBO exhibits higher affinity for lysozyme compared to methylene blue and computational studies indicate that both photosensitisers interact with tryptophan residues within the enzyme active site (Saha et al., 2018).

The lipids of treated cells are also susceptible to damage by photosensitiser-derived singlet oxygen. Formation of lipid hydroperoxides during photosensitisation has been observed to destabilise lipid vesicles and the cytoplasmic membranes of eukaryotic cells (Girotti & Kriksha, 2004; Mertins et al., 2014). Bacterial and mammalian cytoplasmic membranes exhibit some differences which may affect susceptibility to photosensitisers. Bacterial membranes contain a high proportion of monounsaturated fatty acids, which contain a single C=C double bond, whilst mammalian cell phospholipids are dominated by polyunsaturated fatty acids containing many such bonds (Wang et al., 2017). As the C=C double bond is the target of peroxidation by ROS (Bielski et al., 1983), the cytoplasmic membranes of mammalian cells be may be more sensitive to peroxidation than those of bacteria.

4.1.5 Model organisms

Model organisms have distinct characteristics which can be used to tease apart the mechanism by which an antimicrobial interacts with target cells. These organisms can either occur naturally or be produced as the result of mutation or by culturing in conditions which result in phenotypic changes. These model organisms can then be compared to other species or wild-type variants to identify how their unique characteristics affect their susceptibility to biocides.

4.1.5.1 *Ureaplasma*

Ureaplasma are a genus of bacteria closely related to *Mycoplasma* within the Mycoplasmataceae family. *Ureaplasma* are characterised by using urea as a sole energy source and a pleomorphic appearance due to the absence of a cell wall (Jensen, 2017). The cytoplasmic membrane of *Ureaplasma* is instead supported by cholesterol, which forms a characteristic trilaminar membrane which maintains cell stability (Razin, 1996). Whilst *Ureaplasma* have not yet been described as a model organism to study the effect of biocides, they may be suited for determining whether the presence of a cell wall is required for bactericidal activity of Formulation TCM+S, or if the presence of cholesterol protects against photosensitisation.

Whilst culturable in the appropriate liquid media, *Ureaplasma* are difficult to quantify using traditional methods such as total viable counts. The production of self-toxic metabolites substantially limits their growth (Beeton & Spiller, 2017) and so *Ureaplasma* colonies are visible only by microscopy (Geissdörfer et al., 2008). The metabolism of urea into ammonia facilitates approximate quantification of cells by observing changes in the pH of the growth media, which can be detected by pH responsive dyes such as phenol red (Hillitt et al., 2017). Log_{10} changes in viability can be monitored by serially diluting survivors in a 96-well plate and recording the lowest dilution in which a colour change is observed (Glaser et al., 2017; Hillitt et al., 2017). This indicates that urea metabolism has taken place and facilitates quantification of *Ureaplasma* as colour changing units (CCUs).

4.1.5.2 *Deinococcus radiodurans*

Deinococcus radiodurans is a highly robust bacterial species with unparalleled resistance to DNA damage from exposure to ionising radiation, oxidising agents and desiccation. One factor responsible for the hardiness of *Deinococcus* is the highly condensed DNA packaging, which keeps DNA strands in close proximity in the event of double strand breaks; this prevents their separation and allows them to be quickly repaired by non-homologous end joining (Levin-Zaidman et al., 2003; Englander et al., 2004; Minsky et al., 2007). A polyploid genome of 4-10 copies per cell (Hansen, 1978), promotes genome stability by providing redundancy and a high intracellular manganese/iron ratio protects proteins from oxidative stress (Daly et al., 2004). Resistance of *D. radiodurans* to Formulation TCM+S may infer that DNA damage is the primary mechanism by which the formulation inactivates target cells. Conversely, susceptibility to photosensitisation would infer that damage to other targets such as the cytoplasmic membrane may play a significant role in cell death.

4.2 Chapter aims and objective

The objective of this chapter was to ascertain the mechanism by which Formulation TCM+S inactivates bacterial cells. We sought to study the effects of treatment on the integrity and function of the cytoplasmic membrane, integrity of DNA and whether specific model organisms were susceptible to its biocidal effects. The results of this chapter will be particularly useful for contextualising the results of Chapter 5, as it will allow us to identify how formulation interacts with target cells. This will allow us to identify its weaknesses and guide future product development.

4.3 Methods

4.3.1 Formulation

Formulation TCM+S was prepared on the day of testing and consisted of 40 μM TBO, 10 mM MGDA, 15 mM sodium hydrogen carbonate, 10 mM sodium carbonate, 0.01% Plurafac LF 901, 0.01% Praepagen TQ; pH 10.2.

4.3.2 *ΔrecA Bacillus subtilis* susceptibility test

4.3.2.1 Media

Overnight cultures of *Bacillus subtilis* were prepared in tryptone soya broth and counts were performed by enumerating control and test suspensions on tryptone sodium agar.

4.3.2.2 Bacterial strains

Stains of *B. subtilis* strains were kindly provided by Professor Peter Setlow of the University of Connecticut (UConn, USA). *B. subtilis* PS533 was used as a control strain whereas *B. subtilis* PS2318 was used as an isogenic mutant with a deletion in the *recA* gene. As *recA* is required to detect DNA damage and derepress the LexA-SOS response, PS2318 is more susceptible to death by DNA damage.

4.3.2.3 Preparation of test suspensions

Test suspensions of each strain of *B. subtilis* were prepared cultured as previously described (section 2.2.2) and adjusted to an A_{630} 1.0. This was equivalent to a cell density of 5×10^7 CFU/mL.

4.3.2.4 Test procedure

100 μL of *B. subtilis* suspensions was added to 900 μL of Formulation TCM+S and vortexed. 960 μL of test suspension was transferred to a 35 mm diameter tissue culture dish and placed under the light source for 0.5 minutes. To validate that endospores were not present, suspensions were also incubated at 95ºC for 5 minutes in a heat block. Following treatment and neutralisation, suspensions were serially diluted and survival was quantified by the Miles & Misra method (section 2.2.3).

4.3.3 Electrophoresis DNA damage assay

4.3.3.1 Reagents

Lambda DNA, HindIII, gel loading buffer and a Lambda-HindIII molecular weight marker were all obtained from Promega UK. DNAse and RNAse free Ultrapure water was obtained from Invitrogen. Lambda DNA was supplied at a concentration of 519 µg/mL. Tris-Acetate EDTA (TAE) was used as a buffer for the gel preparation and running buffer and contained 40 mM Tris, 20 mM acetic acid, and 2 mM EDTA (Cold Spring Harbor Laboratory Press, 2013). MULTI-CORE 10X restriction enzyme buffer was provided alongside HindIII and contained essential cofactors for restriction enzyme activity.

4.3.3.2 Digestion of lambda DNA

Before testing the effect of treatment on DNA integrity, DNA was enzymatically digested using the restriction enzyme HindIII. Digestion into smaller fragments would allow easier identification of DNA damage by electrophoresis as strand breaks would lead to loss of band resolution. 50 µL of undigested DNA was added to a microcentrifuge tube containin 825 µL sterile deionised water, 100 µL restriction enzyme buffer and 5 µL restriction enzyme buffer. After mixing by pipetting, 25 µL of 10 u/µL HindIII was subsequently added and the tube gently inverted several times to mix the components. The reaction mixture was incubated at 37ºC for 120 minutes to facilitate digestion.

4.3.3.3 DNA precipitation

Following digestion, Lambda DNA was purified and concentrated using the cold ethanol precipitation method (Green & Sambrook, 2016). 50 µL of 3 M sodium acetate (pH 5.2) was added to 400 µL of DNA digest. 900 µL of ice cold 95% ethanol was then added to the tube and mixed to precipitate DNA. After incubating on ice for 30 minutes, the sample was centrifuged at 12,000 G for 10 minutes at 0ºC. The supernatant was discarded and the pellet washed with 70% ethanol at 4ºC. After another centrifugation under the same conditions, the supernatant was discarded and the pellet allowed to dry at room temperature. The pellet was then resuspended in 25 µL of DNAse and RNAse free water to yield a concentration of 1000 µg/mL. DNA was stored at -20ºC until use.

4.3.3.4 DNA treatment with Formulation TCM+S

To ascertain whether the formulation caused DNA damage via double and single strand breaks, 2 µL of the digested DNA was added to 18 µL of formulation at a concentration of 100 µg/mL. The 20 µL droplet transferred to a sterile 35 mm tissue culture dish and placed under the light source for 5 minutes. After treatment, 10 µL of the droplet was transferred to a PCR tube and 2 µL of 6X loading buffer added. Controls consisted of DNA left in water

for 5 minutes (negative control), DNA exposed to formulation in the dark for 5 minutes (dark control) and DNA exposed to 3% hydrogen peroxide for 5 minutes (positive control). As with the treated DNA, loading buffer was added to each. Samples were then electrophoresed using both native and denaturing agarose gels.

4.3.3.5 Gel electrophoresis

For native gel electrophoresis, 5 µL of each sample was loaded into two lanes on a 1.5% agarose gel made up with TAE. The gel was electrophoresed for 120 minutes using a power of 5 V/cm and a current of 400 mA.

4.3.3.6 Staining and visualisation of bands

Following electrophoresis, DNA was stained using Invitrogen SYBR Gold (Thermo Fisher Scientific). SYBR Gold has a high fluorescence quantum yield and is substantially more sensitive compared to ethidium bromide (Thermo Fisher Scientific, 2019d) and so would be more capable of detecting smears of degraded DNA within in the lanes. 20 µL SYBR Gold concentrate was added to 200 mL TAE buffer and stirred to mix. Gels were then transferred to the staining solution and placed on an orbital shaker platform for 30 minutes. DNA was then visualised using a G:BOX Chemi XX6 transilluminator (Syngene) using the UV-C mode and the integrated camera module.

4.3.4 *Deinococcus radiodurans* indicator

4.3.4.1 Bacterial strains

Biocidal activity of the formulation was determined against *D. radiodurans* ATCC 13939, which was obtained from LGC Standards.

4.3.4.2 Media

Deinococcus radiodurans was cultured solely on tryptone sodium agar (TSA).

4.3.4.3 Preparation of test suspensions

As *D. radiodurans* grew to unsuitably low cell densities in liquid media, test suspensions were prepared by harvesting colonies from spread plates. Spread plates of *D. radiodurans* were prepared by adding 100 µL of -80ºC stock to the centre of a TSA plate and spreading with a sterile L-shaped spreader. Plates were incubated for 48 hours and the colonies harvested by scraping off with an inoculation loop and resuspending in a 50 mL centrifuge tube containing 5g of sterile borosilicate glass beads and 10 mL TSC. A_{630} was adjusted to 1.0, which was equivalent to a cell density of 5×10^7 CFU/mL.

4.3.4.4 Test procedure

100 µL of *D. radiodurans* test suspensions (5×10^7 CFU/mL) were added to 900 µL of treated Formulation TCM+S and vortexed. 960 µL aliquots of the resulting suspensions were transferred to sterile 35 mm tissue culture dishes and placed under the light source for 0.5, 1 and 5 minutes. Following treatment and neutralisation, suspensions were serially diluted and survival was quantified by the Miles & Misra method (section 2.2.3).

4.3.5 SYTO9-propidium iodide staining

Penetration of propidium iodide (PI) into treated cells was ascertained using an Invitrogen LIVE/DEAD BacLight Bacterial Viability Kit (Thermo Fisher Scientific, 2019a), which contains the fluorescent DNA intercalating probes SYTO9 and PI.

4.3.5.1 Stain preparation

2X Live/Dead stain was produced by diluting 10 µL of SYTO 9 and 3.5 µL of PI stocks to 3.5 mL of sterile deionised water; this yielded 9.5 µM SYTO 9 and 20 µM PI in the staining solution.

4.3.5.2 Sample preparation

Test suspensions of *Staphylococcus aureus* NCTC 10788 and *Escherichia coli* ATCC 10798 were prepared as previously described (section 2.2.2) and adjusted to A_{630} 1.0 (*S. aureus*; 5×10^8 CFU/mL) and A_{630} 0.5 (*E. coli*; 3×10^8 CFU/mL). 100 µL aliquots of these suspensions were added to 900 µL of Formulation TCM+S, vortexted and transferred to 35 mm sterile tissue culture dishes before being placed beneath the light source 0.5, 1 and 5 minutes. Following treatment, 500 µL of sample was added to an equal volume of double-strength universal neutraliser (section 2.2.5). Double-strength neutraliser was found to be necessary for maintaining a sufficiently high cell density for staining. A negative control of live cells was prepared by adding 100 µL of test suspension to sterile TSC whilst a positive control of dead cells was produced by adding 100 µL of cell suspension to 900 µL of 70% isopropanol. After incubating for 60 minutes, dead cells were pelleted by centrifuging at 10,000 G for 10 minutes; the resulting supernatants were discarded, and the pellet resuspended in 1 mL TSC. Control samples were also added to double-strength universal neutraliser.

4.3.5.3 Staining and fluorescence measurements

Following treatment ad neutralisation, 100 µL of sample was transferred to wells of a 96-well microtiter plate to which 100 µL of 2X stain was added. After gently mixing by pipetting, the samples were incubated in the dark at 20ºC for 15 minutes to allow the stain to equilibrate. Fluorescence was measured using a Tecan Infinite spectrophotometer. Fluorophores were excited at 460 nm whilst emission was measured from 500-700 nm. The intensities at 510-540 nm (green) and 620-650 nm (red) were integrated and the resulting numbers were divided to yield a red/green fluorescence ratio.

4.3.6 Membrane potential assay

Changes in membrane potential were determined using an Invitrogen BacLight Membrane Potential Kit (Thermo Fisher Scientific 2019b). This kit contains the carbocyanine dye 3,3'-diethyloxacarbocyanine iodide (DiOC2(3)), which is a slow-response probe for changes in membrane potential. A decrease in membrane potential (depolarisation) allows more dye to enter cells, whereby it binds to proteins leading to a change in fluorescence emission ratios.

4.3.6.1 Sample preparation

Suspensions of *Staphylococcus aureus* NCTC 10788 and *Escherichia coli* ATCC 10798 were prepared as previously described and adjusted to A_{630} 0.5, which was equivalent to a concentration of 2-3 × 10^8 CFU/mL. Suspensions were treated with a combination of Formulation TCM+S and red light for 0.5, 1 and 5 minutes (as in section 4.3.5.2) and then immediately diluted 10-fold in PBS and kept in the dark. A positive control of depolarised cells was prepared by adding the protonophore CCCP to a control suspension to a final concentration of 5 μM whilst a negative control of healthy cells was prepared by diluting the test suspension in TSC. Universal neutraliser was not used to quench residual biocidal activity after treatment as the polysorbate surfactants contained within interfere with the DiOC2(3) probe. Samples were instead stored in the dark to prevent any further excitation of the photosensitiser. In the case of *E. coli*, the PBS diluent was supplemented with 1 mM MGDA. This was necessary to permeabilise the outer membrane to ensure the dye was able to reach the cytoplasmic membrane interacting successfully with the bacteria in the negative and positive control groups.

DiOC2(3) was added to a concentration of 30 μM (1:100 volume) to each sample and vortexed. Samples were then incubated in the dark at 20ºC for 30 minutes before analysing by flow cytometry. An unstained control sample containing 1 × 10^6 CFU/mL was also prepared for gating purposes

4.3.6.2 Analysis of fluorescence by flow cytometry

Samples were analysed using a BD LSRFortessa flow cytometer using FITC-A (red) and PerCP-Cy5-5-A (green) channels, to detect green and red fluorescence respectively. The flow cytometer instrument was adjusted by using a population of undyed cells and adjusting the forward and side scatter so that the cells appeared in the centre of the data space. The central population was gated and remained unchanged throughout the experiment. For each sample, 50,000 events within the gated area were recorded to yield mean values for green and red fluorescence.

4.3.6.3 Calculation of relative membrane potential

Data obtained by flow cytometry were analysed using FlowJo version 10.5.3. The mean green (PerCP-Cy5-5-A) and red (FITC-A) values calculated for the whole population (i.e. not a gated subset) and relative green/red ratios calculated for graphing and statistical analysis purposes.

4.3.7 ATP leakage assay

Loss of intracellular ATP was ascertained using an Invitrogen ATP Determination Kit (Thermo Fisher Scientific, 2019c), which utilises the luciferase reaction to detect and quantify ATP by the production of light.

4.3.7.1 Chemicals and reaction mixture

Kit components were provided in a lyophilised state and were reconstituted in accordance with the manufacturer instructions using ultrapure deionised water (Alfa Aesar) and the reaction buffer provided. The concentration of each component in stock is included in table 4.2. On the day of testing, 10 mL of a standard reaction solution was prepared by combining the following: 8.9 mL of ultrapure deionised water; 0.5 mL 1X reaction buffer; 0.1 mL DTT; 0.5 mL D-luciferin; 2.5 µL firefly luciferase.

Table 4.2: Concentration of ATP determination kit components

Chemical	Kit component	Concentration of components
1X Reaction buffer	Component E, diluted 20-fold with ultrapure deionised water	25 mM tricine buffer (pH 7.8); 5 mM $MgSO_4$; 100 µM EDTA; 100 µM sodium azide
D-luciferin	Component A, reconstituted with 1X reaction buffer	10 mM D-luciferin; 25 mM tricine buffer (pH 7.8); 5 mM $MgSO_4$; 100 µM EDTA; 100 µM sodium azide
Dithiothreitol (DTT)	Component C, reconstituted in ultrapure deionised water	0.1 M DTT
Adenosine Triphosphate (ATP)	Component D	5 mM ATP; 5 mM tris EDTA buffer
Firefly luciferase	Component B	5 mg/mL luciferase; 25 mM tris acetate (pH 7.8); 0.2 M ammonium sulfate; 15% (v/v) glycerol; 30% (v/v) ethylene glycol

4.3.7.2 Sample preparation

Suspensions of *S. aureus* and *E. coli* cells prepared as previously described to a cell density of 1×10^8 CFU/mL (section 2.2.2). 100 µL of suspension and 100 µL of sterile deionised water were each added to 800 µL of Formulation TCM+S. After mixing by vortexing, 960 µL was transferred to 35 mm diameter tissue culture dishes (Greiner Bio-One International GmbH) and placed directly beneath the light source for 5 minutes. This was performed with three separately prepared biological replicates to facilitate statistical analysis.

Immediately following treatment, 800 µL of sample was added to an equal volume of 100 mM phosphate buffered saline (PBS). This resulted in a neutral pH of 7.2, which was important to ensure that the luciferase enzyme retained its catalytic activity. The resulting suspension was then filtered through a Minisart 0.45 µm-pore filter (Sartorius) to produce cell-free lysates which contained only ATP which leaked from cells.

To obtain a baseline luminescence value, the above protocol was repeated but 100 µL sterile TSC was added to the formulation rather than the cell suspensions. The background fluorescence was subtracted from all other luminescence readings. As a positive control, three test suspensions were placed in a 100ºC heat block for 5 minutes and then vortexed for 30 seconds; this convenient method sufficiently releases intracellular ATP stores (Yang et al., 2002).

4.3.7.3 Analysis of luminescence

To analyse luminescence, 20 µL of lysate was added to 180 µL of reaction mixture in a PCR tube. After gently mixing by pipetting, the full 200 µL contents were transferred to a 5 mL round bottomed polystyrene tube (Fisher Scientific). Total luminescence over 10 seconds was then determined using a Lumat LB 9507 luminometer (Berthold). Luminescence was read three times for each tube and the resulting relative luminescence units (RLUs) were averaged. The background luminescence was subtracted from each value to yield a final luminescence value.

4.3.7.4 Validation of method linearity

To validate that the assay offered a linear response to ATP concentration, a standard range of the following ATP concentrations was prepared: 1, 5, 25, 50, 125, 250, 500 & 1000 nM. 20 µL aliquots of standard were added to 180 µL of standard reaction solution and luminescence was measured (section 4.3.7.3). The standard curve obtained was not used to plot linear regressions as the values close to zero (e.g. in untreated cells) linearly regressed to negative values. Since absolute values were unnecessary for the purposes of this test, this was not seen as problematic.

4.3.8 Examination by scanning electron microscopy

Both *Staphylococcus aureus* NCTC 10788 and *Escherichia coli* ATCC 10798 cells were examined by scanning electron microscopy. Cells were either left untreated or were treated with Formulation TCM+S and red light for 5 minutes prior to fixation.

Following treatment, 960 µL of treated suspensions was transferred from tissue culture dishes to 9 mL of 2% glutaraldehyde (electron microscopy grade; Sigma Aldrich) in 0.1 M sodium cacodylate buffer (pH 7.4). Following a 2-hour incubation at 20°C, fixed cells were transferred to isopore 0.2-µm polycarbonate filter membranes (Merck) using a three-way manifold filtration system (Sartorius). Polycarbonate membranes were chosen due to their chemical resistance to ethanol and HMDS and their very smooth surface, which provided good contrast to facilitate easier identification of cells during microscopic examination.

To dehydrate and dry the samples, membranes were transferred into petri dishes containing an ascending series of ethanol and hexamethyldisilazane (HMDS; Sigma Aldrich), as illustrated in figure 4.1. This was performed slowly and with great care to ensure cells were not sheered from the membrane. HMDS is a drying agent which was used as a convenient alternative to critical point drying as it can preserve cell morphology by preventing damage due to the meniscus effect (Hazrin-Chong & Manefield, 2012). After the final 5-minute incubation in HMDS, membranes were placed in sterile petri dishes which were then placed in a bell jar containing silica gel packets and left overnight to allow HMDS to evaporate.

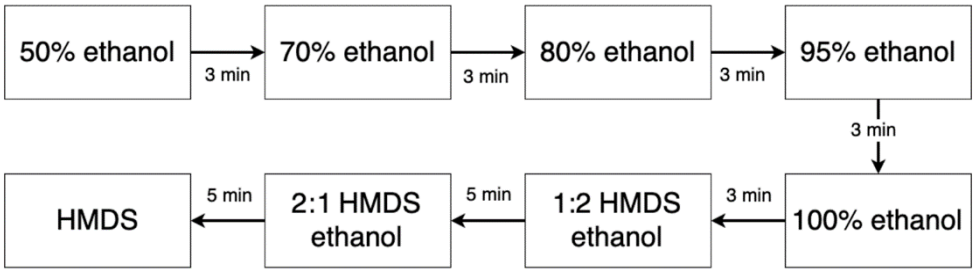

Figure 4.1: Dehydration and drying steps used for preparation of samples for scanning electron microscopy.

To prepare membranes for SEM analysis, small squares were cut from each and mounted onto 12.5 mm stainless steel stubs using Leit adhesive carbon tabs. A 7 nm layer of 80:20 Au/Pd was then deposited onto the samples using a Q150T ES turbo sputter coater (Quorum). After coating, samples were examined using a Triglav MAIA3 Field emission gun scanning electron microscope (Tescan) using a 15 kV forward voltage electron beam. For each sample, 10 fields of view were captured to assess changes in cell morphology.

4.3.8 *Ureaplasma urealyticum* susceptibility test

4.3.8.1 Media

Ureaplasma were cultured in *Ureaplasma* Medium, which was purchased from Mycoplasma Experience. This media is based on Urea Broth 10B and contains the pH indicator dye phenol red. Since *Ureaplasma spp*. produce ammonia as a result of urea metabolism, positive growth is indicated by the medium turning red.

4.3.8.2 Strains

Activity of the formulation was assessed against *Ureaplasma urealyticum* serovar 8 NCTC 10177, which was provided by Dr Mike Beeton of Cardiff Metropolitan University.

4.3.8.3 Preparation of test suspensions

In a 96-well plate, wells were filled with 90 µL of Ureaplasma Medium. Each well was then inoculated with 10 µL of *U. urealyticum* freezer stock. This was serially diluted down the wells. In a 10-fold dilution series. A film lid was placed over the top to seal wells and to prevent ammonia from leaching into adjacent wells. Plates were incubated overnight at 37ºC and wells corresponding to the lowest dilution with positive growth were harvested and pooled.

Pooling of these dilutions was necessary as *Ureaplasma* remain viable only for a few hours after reaching the log phase of growth due to ammonia toxicity. Therefore, the lowest dilution with positive growth would have been the latest to reach this phase of growth and would contain the highest titre of viable cells. The pooled suspensions contained 10^6 CCU/mL *U. urealyticum* and were used directly in suspension tests without any prior preparation steps such as washing.

4.3.8.4 Test procedure and quantification

100 µL aliquots of *U. urealyticum* (10^6 CCU/mL) were added to 900 µL of Formulation TCM+S. 960 µL of the resulting suspension was then transferred to 35 mm tissue culture dishes and illuminated for 1, 2.5 and 5 minutes. To determine whether the formulation exhibited dark toxicity against *U. urealyticum,* test suspension*s* were also exposed to the formulation in the dark for the same amount of time. After treatment, 20 µL of test suspensions was neutralised in 180 µL universal neutraliser for 5 minutes. The neutralised samples were then serially diluted in a 10-fold series in *Ureaplasma* Medium in a 96-well plate and the plate was covered with a film lid. Plates were incubated at 37ºC for 48 hours and CCUs were counted.

4.4 Results

4.4.1 *Bacillus subtilis recA* mutant

The *recA*-deficient strain of *Bacillus subtilis* (PS2318) was more susceptible to Formulation TCM+S compared to the wild-type strain PS533 (P <0.05; ANOVA Šidák) (Fig 4.2). After 30 seconds of treatment, a 1.5 $\log_{10}$ reduction in PS533 viability was observed whereas PS2318 viability decreased by 2.9 $\log_{10}$ (P <0.001; ANOVA, Šidák). In the case of the PS2318 mutant, viability was decreased to below the limit of detection and there was no difference in survivability when compared to the boiled control (P >0.05; ANOVA, Šidák). In contrast, significant numbers of PS533 remained viable when compared to the boiled control (P=<0.001; ANOVA, Šidák). In the case of both *B. subtilis* strains, total viable counts of the boiled controls were reduced to below the limit of detection, which validated that the cells tested were in a vegetative state, rather than endospores.

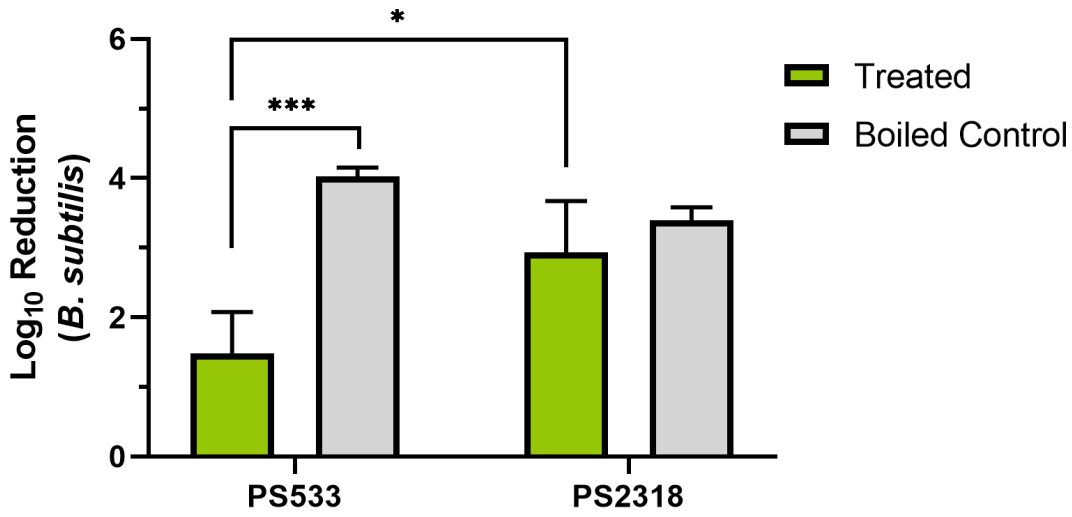

Figure 4.2: Susceptibility of *Bacillus subtilis* mutant strains to Formulation TCM+S. 0.5-minute contact time. PS533 corresponds to a wild-type phenotype whilst PS2318 is an isogenic strain containing a deletion in *recA,* which impairs DNA repair. * = P <0.05; *** = P <0.001.

4.4.2 DNA damage assay

Treatment of HindIII-digested Lambda DNA with Formulation TCM+S and red light did not appear to affect the DNA integrity upon examination by native gel electrophoresis (fig. 4.3). Bands corresponding to DNA treated with water, red light, Formulation TCM+S/red light and hydrogen peroxide all retained distinct banding patterns when resolved on the gel. This indicated that extensive double strand breaks do not occur in isolated DNA after 5 minutes.

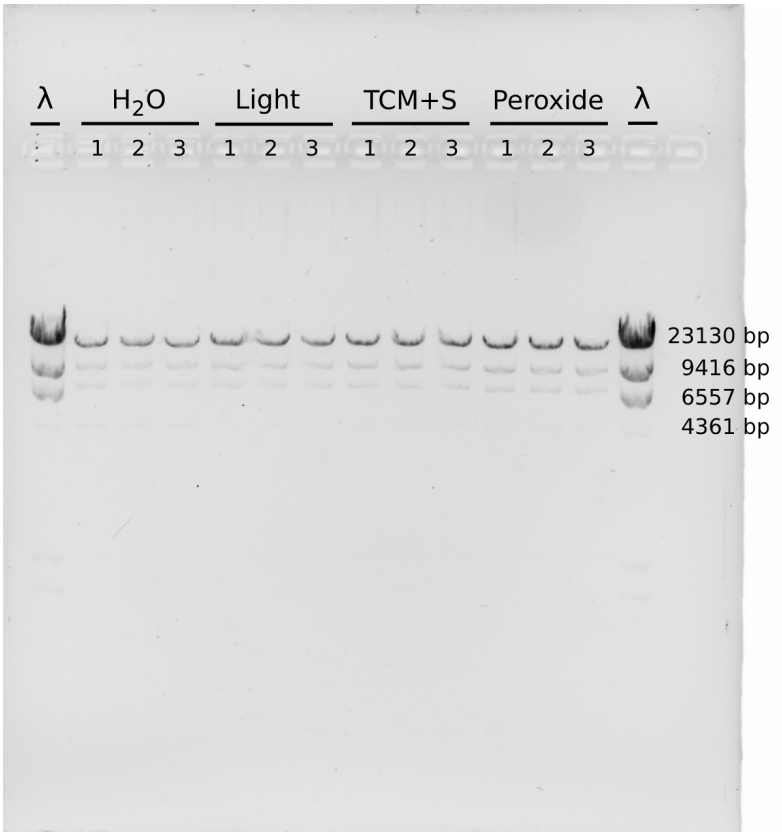

Figure 4.3: Native gel electrophoresis of HindIII-digested Lamda DNA. DNA was treated for 5 minutes contact with DNAse-free water (H_2O), red light (Light), Formulation TCM+S/red light (TCM+S) and 3% hydrogen peroxide (peroxide). Replicates are denoted by numbers 1-3. Lanes corresponding to a HindIII Lamda molecular weight marker are marked λ and corresponding molecular weights in base pairs (bp) are presented right of the gel.

4.4.3 *Deinococcus radiodurans*

Deinococcus radiodurans ATCC 13939 was highly susceptible to treatment with Formulation TCM+S. After only 1 minute of treatment, we observed a >4 log_{10} reduction in its viability (fig. 4.4). As total viable counts were below the lower limit of detection in the case of each time point, there were no statistically significant differences between the treatment groups (ANOVA, Tukey).

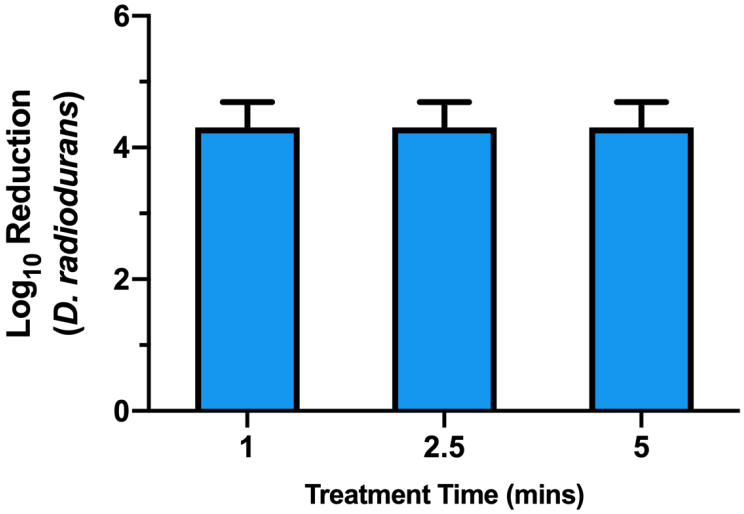

Figure 4.4: Log_{10} reductions in *Deinococcus radiodurans* viability following treatment with Formulation TCM+S and red light.

4.4.4 Propidium iodide/SYTO9 stain

S. aureus green/red fluorescence exhibited a gradual dose-response to Formulation TCM+S (fig. 4.5). Decreases in viability were observed between 0 to 0.5 minutes ($P < 0.0001$; ANOVA, Tukey), 0.5 to 1 minutes ($P < 0.001$; ANOVA, Tukey) and 1 to 5 minutes ($P < 0.01$; ANOVA, Tukey). Incubating with the formulation in the dark for 5 minutes also led to a decrease in green/red fluorescence ratios compared to the 0-minute control ($P < 0.01$; ANOVA, Tukey). In contrast, when observing changes in green/red fluorescence in *E. coli*, there was an immediate decrease between 0 and 0.5 minutes ($P < 0.0001$; ANOVA, Tukey). However, there were no further changes in fluorescence ratios upon further treatment for 1 or 5 minutes ($P > 0.05$; ANOVA, Tukey). These observations suggest that full penetration of propidium iodide into *E. coli* occurs within 0.5 minutes of treatment. It should be noted that incubation of *E. coli* with Formulation TCM+S in the dark for 5 minutes also results in propidium iodide fully entering cells ($P < 0.0001$).

When compared to one another, the two species exhibited differences in their green/red fluorescence 0.5 minutes ($P < 0.0001$; ANOVA, Šidák) and 1 minute ($P < 0.001$; ANOVA, Šidák. At 5 minutes, there were no differences in fluorescence ratios between the two species ($P > 0.05$; ANOVA, Šidák). The two species exhibited different susceptibilities to being incubated with Formulation TCM+S in the dark ($P < 0.0001$).

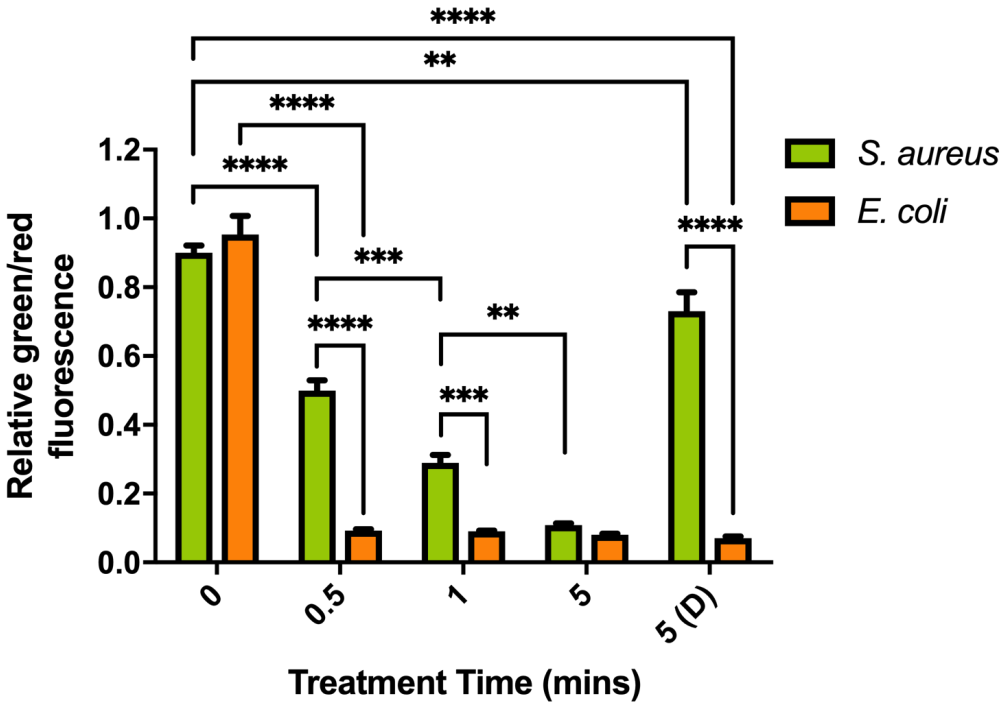

Figure 4.5: Changes in SYTO9-propidium iodide (green/red) fluorescence ratios of *Staphylococcus aureus* and *Escherichia coli* suspensions treated with Formulation TCM+S. 5 (D) indicates suspensions were incubated with the formulation for 5 minutes in the dark. Changes in fluorescence ratios between timepoints were compared with Tukey's multiple comparison tests whilst differences between the two species at each timepoint were analysed by Šidák's tests. ** P <0.01; *** P <0.001; **** P <0.0001.

4.4.5 ATP Leakage

Treatment of *S. aureus* NCTC 10788 with Formulation TCM+S resulted in a partial loss of intracellular ATP (fig. 4.6). Over time there appeared to be a dose response to continued treatment. However, there were no significant differences between 0 and 0.5 minutes ($P > 0.05$; ANOVA, Tukey) or between 0.5 and 1 minutes ($P > 0.05$; ANOVA, Tukey). After 5 minutes of treatment, there was an increase in relative luminescence units (RLUs) compared to the untreated (0-minute) control ($P < 0.01$; ANOVA, Tukey) and the previous 1-minute time point ($P < 0.01$; ANOVA, Tukey). Treatment for 5 minutes did not lead to complete release of intracellular ATP stores as samples from the boiled controls exhibited markedly greater luminescence ($P < 0.0001$; ANOVA, Tukey).

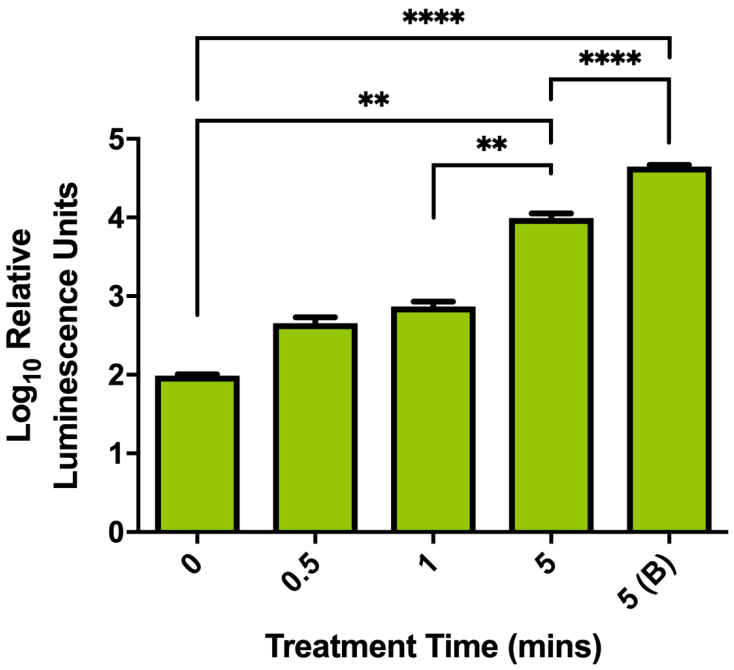

Figure 4.6: Changes in the ATP content of *S. aureus* supernatants following treatment with Formulation TCM+S, as indicated by relative luminescence units. 5 (B) corresponds to 5 minutes of boiling. ** = $P < 0.01$; **** = $P < 0.0001$.

Treatment of *Escherichia coli* ATCC 10798 with Formulation TCM+S resulted in a complete loss of intracellular ATP (fig. 4.7). Over time there appeared to be a dose response to continued treatment. Compared to the untreated (0-minute) control there was an increase in luminescence after only 0.5 minutes ($P < 0.001$; ANOVA, Tukey). Further treatment for 1 minute did not cause any more ATP to leak from cells compared to those treated for 0.5 minutes ($P > 0.05$; ANOVA, Tukey). Treatment for 5 minutes led to an increase in luminescence compared to those treated for 1 minute ($P < 0.0001$; ANOVA, Tukey). Boiling for 5 minutes did not lead to an additional luminescence when compared to those treated with Formulation TCM+S for 5 minutes ($P > 0.05$; ANOVA, Tukey); this indicated that the entire intracellular ATP stores had been lost after 5 minutes.

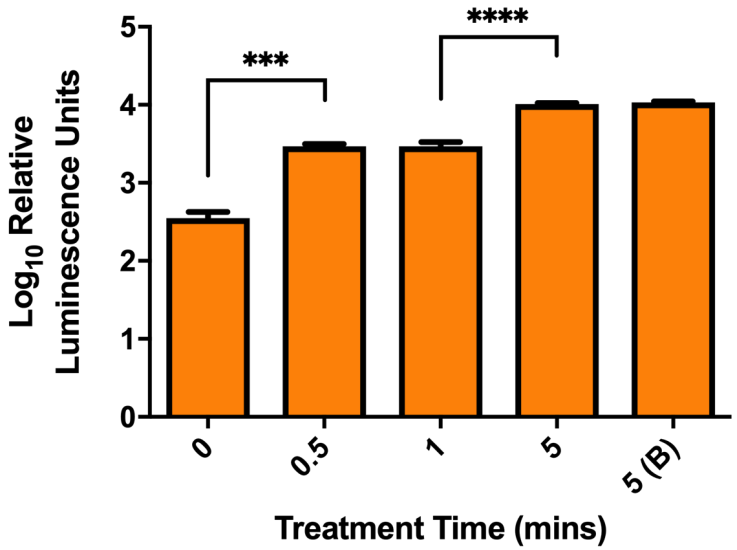

Figure 4.7: Changes in the ATP content of *E. coli* supernatants following treatment with Formulation TCM+S, as indicated by relative luminescence units. 5 (B) corresponds to 5 minutes of boiling. *** = $P < 0.001$; **** = $P < 0.0001$.

4.4.6 Membrane potential

Treatment of *Staphylococcus aureus* NCTC 10788 with Formulation TCM+S led to a gradual loss of membrane potential across the treatment period (fig. 4.8). Compared to the 0-minute control, there was a marked decrease in relative green/red fluorescence after only 0.5 minutes of treatment (P <0.0001; ANOVA, Tukey). Increasing the treatment time from 0.5 to 1 and from 1 to 5 minutes both led to further decreases (P <0.01; ANOVA, Tukey). At 1 minute, the decrease in relative red/green fluorescence was equal to that of cells treated with the protonophore carbonyl cyanide m-chlorophenyl hydrazine (CCCP) (P >00.5; ANOVA, Tukey) which confirmed that membrane potential had been lost. Curiously, the relative green/red fluorescence at 5 minutes was lower than the CCCP control (P <0.05; ANOVA, Tukey).

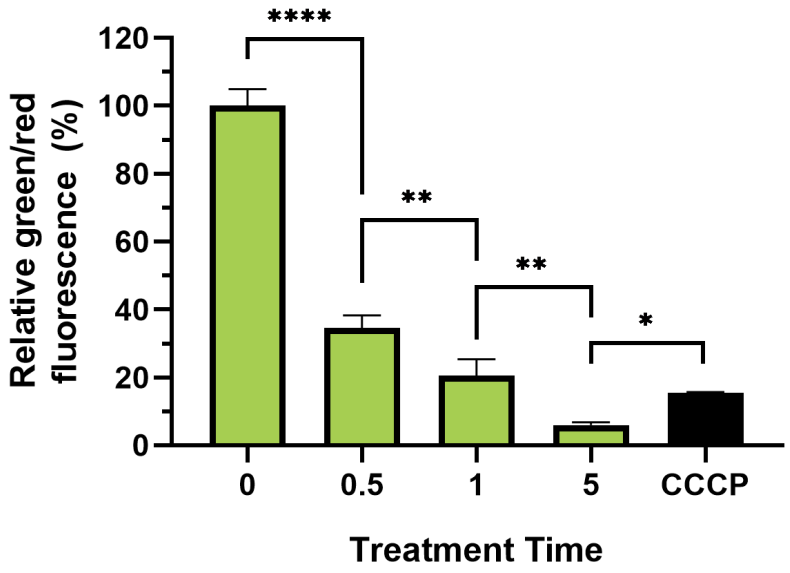

Figure 4.8: Decrease in DiOC2(3) relative red/green fluorescence in *Staphylococcus aureus* as a result of treatment with Formulation TCM+S and carbonyl cyanide m-chlorophenyl hydrazine (CCCP), as indicated by staining with 3,3'-diethyloxacarbocyanine iodide (DiOC2(3)). Decreased green/red fluorescence indicates loss of membrane potential. CCCP -; * P <0.05; ** P <0.01; *** P <0.001; **** P

Treatment of *E. coli* ATCC 10798 with Formulation TCM+S led to rapid loss of membrane potential (fig. 4.9). Compared to the 0-minute control, there was a marked decrease in relative green/red fluorescence after only 0.5 minutes of treatment (P <0.0001; ANOVA, Tukey). There were no further changes in fluorescence after increasing the treatment time from 1 and 5 minutes (P >0.05; ANOVA, Tukey). The decrease in relative red/green fluorescence at 0.5 minutes was equal to that of cells treated with CCCP (P >00.5; ANOVA, Tukey), indicating complete loss of membrane potential.

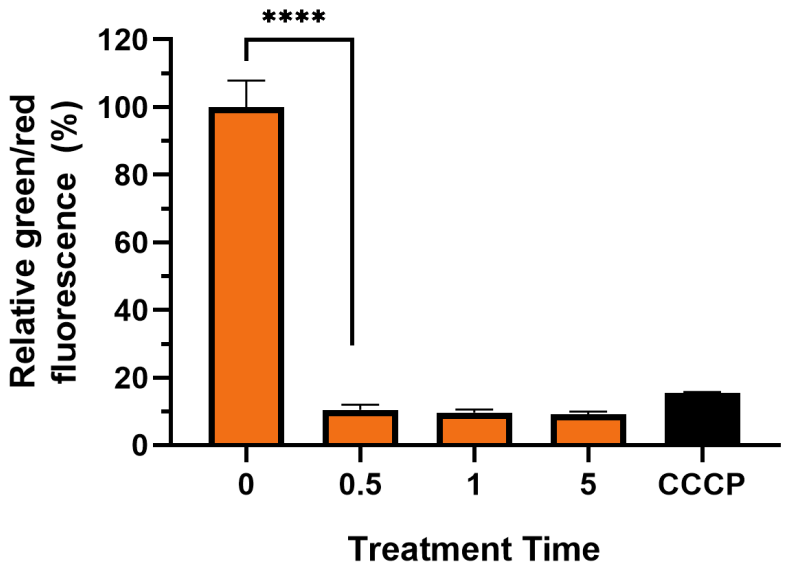

Figure 4.9: Changes in DiOC2(3) relative red/green fluorescence in *Escherichia coli* ATCC 10798 following treatment with Formulation TCM+S and carbonyl cyanide m-chlorophenyl hydrazine (CCCP), as indicated by staining with 3,3'-diethyloxacarbocyanine iodide (DiOC2(3)). Decreased green/red fluorescence indicates loss of membrane potential. **** P <0.0001.

4.4.7 Scanning electron microscopy

Treatment of *Staphylococcus aureus* NCTC 10788 with Formulation TCM+S for 5 minutes had a minor effect on their morphology (fig. 4.10). Cells remained intact though they appeared less rounded than their untreated counterparts. They appeared to form roughly hexagonal shapes when in proximity to other cells and their cytoplasmic membranes appeared to merge with those of adjacent cells.

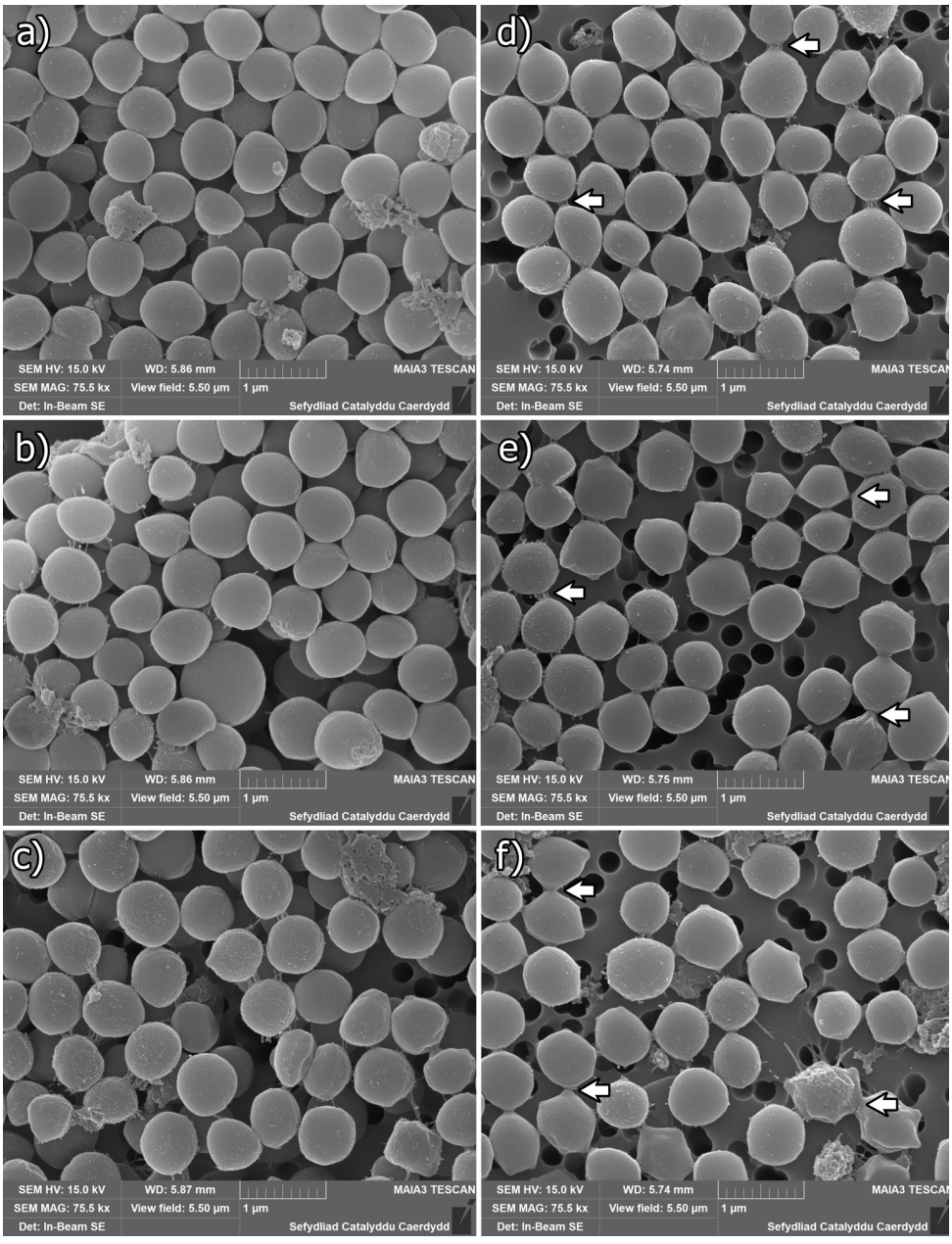

Figure 4.10: Scanning electron micrographs of cells of *Staphylococcus aureus.* Before (a-c) and after (d-f) 5 minutes treatment with Formulation TCM+S and red light. Each image shows a view field of 5.5 µm and the scale bars correspond to a distance of 1 µm. Arrows indicate examples of where the cytoplasmic membranes of adjacent cells appeared to merge.

Treatment of *Escherichia coli* ATCC 10798 with Formulation TCM+S did not lead to any obvious changes in morphological appearance when examined by scanning electron microscopy (fig. 4.11). Cells retained their rod shape and remained fully intact, with no changes to their surface texture.

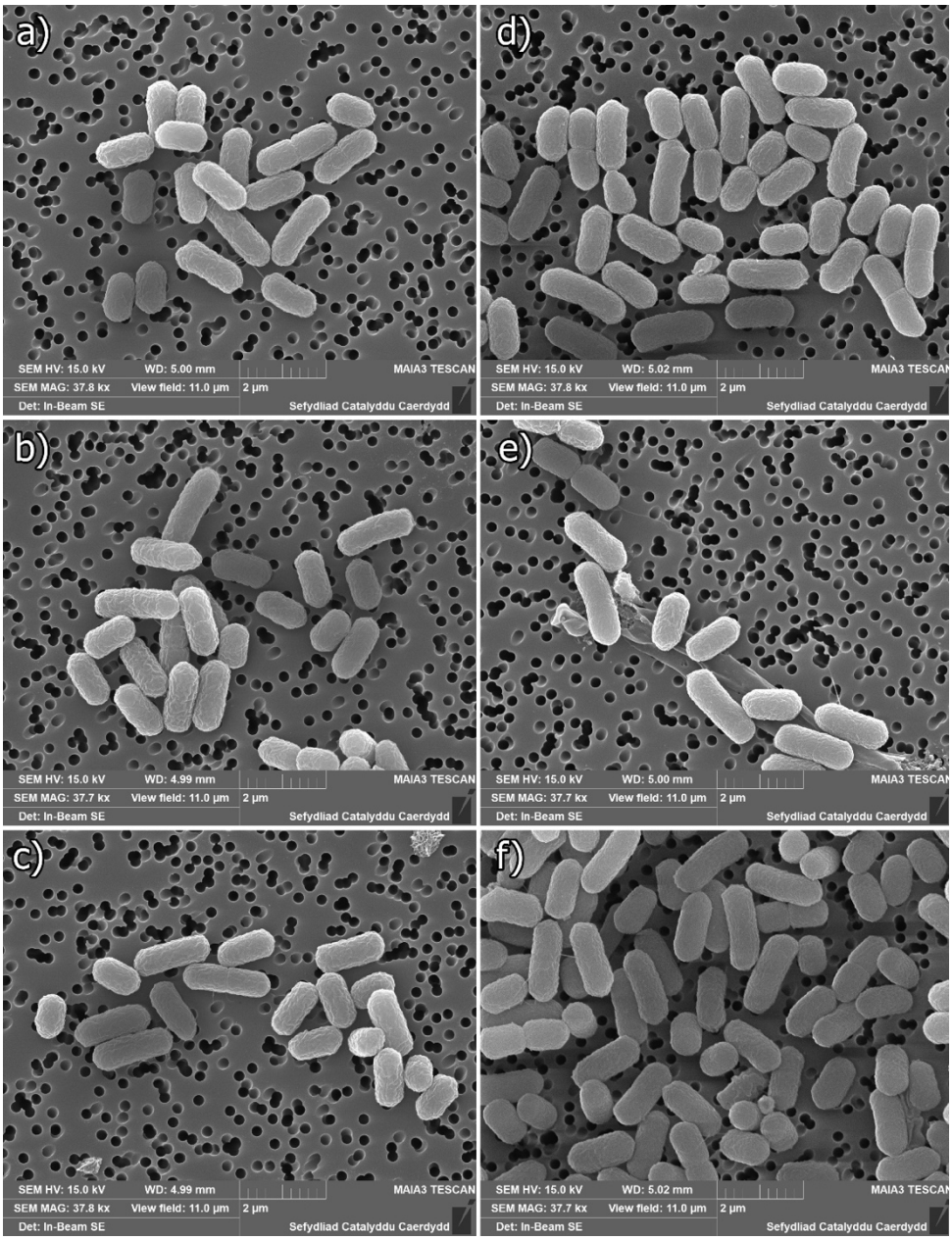

Figure 4.11: Scanning electron micrographs of cells of *Escherichia coli.* Before (a-c) and after (d-f) 5 minutes treatment with Formulation TCM+S and red light. Each image shows a view field of 11 µm and the scale bars correspond to a distance of 2 µm.

4.4.8 *Ureaplasma urealyticum*

Ureaplasma urealyticum serovar 8 NCTC 10177 was highly susceptible to Formulation TCM+S (fig. 4.12). After only 1 minute of treatment, we observed a 4 log_{10} reduction in cell viability when the formulation was used in combination with red light. This was the limit of detection for this test. Surprisingly, the formulation also exhibited some dark toxicity: at 1 and 2.5 minutes, we observed 2 log_{10} reductions in *U. urealyticum* viability, which increased to 3 log_{10} after 5 minutes. It should be noted that the differences between the light and dark treated groups were statistically significant at 1, 2.5 ($P < 0.001$; ANOVA, Šidák), and 5 minutes ($P < 0.05$).

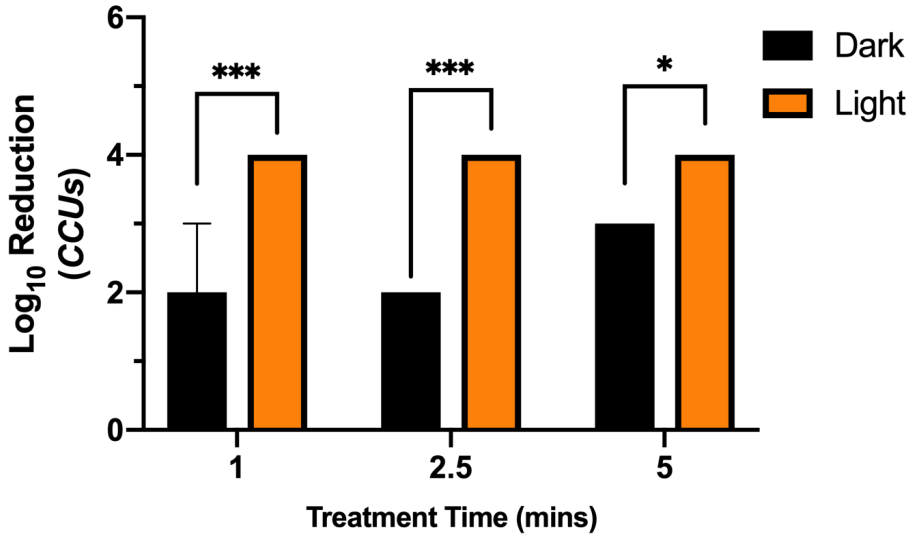

Figure 4.12: Log_{10} reductions in colour changing units (CCUs) of *Ureaplasma urealyticum* NCTC 10177 following treatment with Formulation TCM+S, in light and dark treatment conditions.

4.5 Discussion

4.5.1 Effects on nucleic acids

Our observations suggest that nucleic acids are targeted during photosensitisation by Formulation TCM+S. RecA is a protein involved in the sensing of DNA damage and induces DNA repair by derepression of LexA; deletion of *recA* impairs DNA repair functions (Maul & Sutton, 2005). The Δ*recA Bacillus subtilis* mutant (PS2318) exhibited increased sensitivity to inactivation by the Formulation TCM+S when compared to an isogenic wild-type strain carrying a functioning copy of *recA* (fig. 4.2). Whilst significant numbers of wild-type cells survived a 0.5-minute treatment, viability of the mutant strain was decreased to below the lower limit of detection. This strongly indicates that DNA damage occurs during photosensitisation with Formulation TCM+S and red light. Due to the 10-400 nm diffusion distance of singlet oxygen in macromolecule rich environments such as the cytoplasm (Baier et al., 2005), the ability to damage DNA in this mutant also infers that TBO enters the cytoplasm of treated cells.

Damage to nucleic acids can include base modifications and strand breaks due to cleavage of the deoxyribose backbone. Double strand breaks (DSBs) are considered an extreme form of DNA damage (Ayora et al., 2011). Whilst such breaks can be repaired effectively by homologous recombination, this requires an intact DNA template with similar sequence homology (Đermić, 2015). Many prokaryotes contain a single chromosome and so rely on non-homologous end-joining to repair DSBs, which is highly error prone and can lead to loss of gene function (Pitcher et al., 2007; Rodgers & McVay, 2016). Whilst extensive oxidation of guanosine into 8-oxoguanine by methylene blue has been observed in cell free systems (Epe et al., 1993), it is unclear whether photosensitisation causes DSBs.

To determine whether photosensitisation can induce DSBs, isolated HindIII-digested Lambda phage DNA was treated with Formulation TCM+S and electrophoresed on a native gel to assess its integrity. A native gel was utilised to preserve hydrogen bonding between complementary strands, allowing DNA to maintain its secondary structure and avoids the detection of single strand breaks. Hydrogen peroxide, which is known to induce DBSs (Driessens et al., 2009), was used as a positive control for DNA damage. Following electrophoresis and visualisation with a nucleic acid stain, lanes corresponding to DNA treated with Formulation TCM+S did not appear differently from control DNA incubated with water and exposed to red-light alone (fig. 4.3). This indicated that the DNA integrity was maintained and that extensive DSBs did occur not after 5 minutes of treatment. DNA treated with 3% hydrogen peroxide also retained highly resolved bands, indicating that double strand breaks do not appear to occur in DNA at this contact time. The method utilised

may be too insensitive to detect small numbers of double strand breaks. Alternatively, DNA damage may be limited to oxidative base modifications (Epe et al., 1993) or through single strand breaks, which are not detectable by native gel electrophoresis. Further investigations using an alkaline denaturing gel may provide further insights into whether single stand breaks occur in this time frame after treatment with Formulation TCM+S or hydrogen peroxide (Sutherland *et al*., 2006).

The most direct method current available for assessing strand break damage in prokaryotes involves microscopic observations alongside a DNA chelating dye such as SYBR Gold. Fernández et al. (2008) developed an *in-situ* method in which biocide-treated cells are trapped within an agarose droplet on a glass slide. After chemical lysis of cells, DNA is liberated and can be stained with SYBR Gold to visualise DNA migration. The authors reasoned that the degree of DNA damage correlated the extent of DNA diffusion as intact DNA appeared as dense branched structures around the lysed cells whereas damaged DNA manifested as large diffuse halos (Fernández et al., 2008). This method has since been used to identify DNA damage by fluoroquinolones (Tamayo et al., 2009) and so may be useful for direct detection of DNA damage in microorganisms without the need to extract, purify and prepare DNA for electrophoresis.

Deinococcus radiodurans is an extremely radiation tolerant bacterial species renowned for its ability to survive extreme DNA damaging events such as gamma irradiation, desiccation and treatment with DNA damaging biocides. The resilience of *D. radiodurans* is due to its armoury of DNA protection and repair systems which are able to resist even the most severe forms of DNA damage such as double strand breaks (Levin-Zaidman et al., 2003; Englander et al., 2004; Minsky et al., 2007). Consequently, *D. radiodurans* was used as an indicator organism to determine whether Formulation TCM+S killed cells via DNA damage alone or by alternative mechanisms. We theorised that a lack of susceptibility of *D. radiodurans* to photosensitisation would strongly indicate that DNA damage is the primary route by which target cells are inactivated. Conversely, sensitivity to the formulation would indicate that other structures such as the cytoplasmic membrane are targeted.

D. radiodurans was highly susceptible to photosensitisation by Formulation TCM+S and red light. Within 1 minute of treatment, >4 $\log_{10}$ reductions in *D. radiodurans* viability were observed and its viability was reduced to below the lower limit of detection (fig. 4.4). Whilst these observations do exclude damage of DNA, they strongly demonstrate that formulation inactivates cells by mechanisms other than through DNA damage alone. These observations corroborate those of other authors, who have described *D. radiodurans* as being susceptible to porphyrin-based photosensitisers (Nitzan & Ashkanezi, 2008).

4.5.2 Effect on the bacterial cytoplasmic membrane

Photosensitisation with Formulation TCM+S had a strong effect on the cytoplasmic membrane integrity of target cells. Propidium iodide (PI) penetrated the membranes of *Staphylococcus aureus* and *Escherichia coli* within 0.5 minutes of exposure (fig. 4.5). Whilst PI entered *E. coli* rapidly, penetration into *S. aureus* was observed to occur more gradually over the 5 minutes of treatment. In healthy cells with intact membranes, PI is excluded from the cytoplasm and exhibits low red fluorescence. In contrast, SYTO9 readily enters living cells whereby it intercalates with DNA and fluoresces green. The entry of PI into cells resulted in a quenching of green fluorescence and a concurrent increase in red fluorescence. This indicated that the integrity of target cell membranes was disrupted following treatment with Formulation TCM+S. These observations corroborate the findings of Sharma et al. (2008) who observed penetration of PI into *S. aureus* within biofilms following treatment with TBO and a 640-nm (red) laser.

Perturbation of membrane integrity can result in the loss of intracellular contents. The intracellular cation potassium is the primary indicator of membrane damage and its loss occurs early in response to membrane damage (Johnston et al., 2003). Potassium has been previously demonstrated to leak from photosensitised cells treated with methylene blue (Sahu et al., 2009). ATP is the universal intracellular energy source and has a larger molecular mass than potassium; its loss requires more extensive damage to the cytoplasmic membrane (Johnston et al., 2003). We observed that photosensitisation with Formulation TCM+S resulted in the leakage of ATP from *S. aureus* (fig. 4.6) and *E. coli* (fig. 4.7) within the 5-minute treatment window. There was a dose-response relationship between treatment time and the loss of ATP, as indicated by a gradual increase in luminescence. Intracellular stores of ATP were fully released from *E. coli* after 5 minutes of illumination with Formulation TCM+S, whilst ATP was only partially released from *S. aureus*. As cell-free lysates were prepared immediately after cessation of light, it is unclear whether ATP continued to leak from cells after this time.

In healthy bacterial cells, DNA damage is repairable via the SOS response. However, this process is energy intensive as the detection of DNA damage relies on RecA filament formation, which is facilitated by ATP hydrolysis (Zhao et al., 2017). The loss of the intracellular ATP would deprive target cells of the means to repair DNA damage which occurs during photosensitisation and so damage to the cytoplasmic membrane also impairs the ability of target cells to resist DNA-damaging effects of Formulation TCM+S.

It is unclear whether the entry of propidium iodide and loss of ATP occurs by simple diffusion through the membrane or via the formation of transmembrane pores. A dextran particle assay could be used as a follow up test to ascertain whether large pores form in the cytoplasmic membrane during photosensitisation. In this assay, cells are incubated with fluorescently-labelled dextran particles, which are available in a variety of sizes such as 4 to 40 kDa in diameter; the use of different sized particles can facilitate determination of the size of the transmembrane pores (O'Brien-Simpson et al., 2014).

Membrane potential is the result of a transmembrane ion gradient between the intracellular and extracellular space. In bacteria, membrane potential drives the protonmotive force utilised for ATP synthesis and facilitates cell division by controlling MinD localisation during septum formation (Dimroth et al., 2000; Strahl & Hamoen, 2010). Loss of membrane potential would therefore rob cells of the means to produce new energy and divide. Treatment of both bacterial species with Formulation TCM+S resulted in depletion of membrane potential, as determined by fluorometric measurement of DiOC2(3) fluorescence. In *E. coli*, membrane potential was lost extremely rapidly and had become equal to that of CCCP-treated cells after only 0.5 minutes (fig. 4.9). In contrast, loss of membrane potential in *S. aureus* occurred more slowly and full depletion of membrane potential was observed after 1 minute (fig. 4.9). When coupled with the loss of ATP which occurs in treated cells (section 4.4.5), the inability to produce and utilise energy appears to be a major process underlying bacterial inactivation by Formulation TCM+S.

Loss of membrane potential can occur due to leakage of potassium cations in the early-stages of membrane damage. Disruption of normal homeostatic mechanisms which maintain a potassium ion gradient (e.g. potassium ion channels) leads to free diffusion of potassium across the membrane in which the concentration becomes equalised. Leakage of potassium from cells can be measured using spectroscopic methods such as atomic emission or inductively coupled plasma mass spectrometry or by measuring changes in conductivity using K^+ probes (Johnston et al., 2002). Sahu et al. (2009) detected a loss of intracellular contents, including potassium, from *E. coli* and *S.* a*ureus* following treatment with TBO and determined that this process occurred faster in *E. coli*. This is concordant with our observations that membrane depolarisation occurs more rapidly in *E. coli* than *S. aureus*.

Examination by scanning electron microscopy (SEM) indicated that *E. coli* cells retained their normal morphology after 5 minutes of treatment with Formulation TCM+S (fig. 4.11). Despite this treatment time exceeding the time required to achieve total inactivation of these cells, treated cells remained indistinguishable from untreated cells. In contrast, *S. aureus* cells exhibited some minor morphological changes following treatment (fig. 4.10). Untreated

cells appeared round with well-defined borders whereas treated cells exhibited a hexagonal appearance and the borders between cells was less well defined; adjacent cells appeared to stick to one another as if the membranes had fused.

Loss of roundness and the development of a rough appearance has been previously observed in *S. aureus* following exposure to cationic surfactants such as quaternary ammonium compounds (Kawai & Yamagishi, 2009). In Chapter 3, the cationic surfactant Praepagen TQ was demonstrated to improve biocidal activity against *S. aureus*. It is plausible that the change in shape and fusion of membranes of adjacent cells occurred due to disruption of the intramolecular forces between phospholipids, either as a result of exposure to Praepagen TQ or due to the process of photosensitisation.

The morphology of rod-shaped bacterial cells such as *E. coli* is maintained by a rigid peptidoglycan cell wall, which is relatively thin in Gram-negative species. Exposure to cell wall-damaging agents can manifest as perturbations in cell morphology and the appearance of cracks and bulges at the cell surface (Huang et al., 2008). Upon examination by SEM, no discernible changes were observed in the cell morphology in *E. coli* cells treated with Formulation TCM+S for 5 minutes when compared to untreated control cells (fig. 4.7). This indicated that large scale destruction of the cell wall does not occur in inactivated cells and damage to the cytoplasmic membrane is not extensive enough to affect cell morphology visibly. Diogo et al. (2017) reported only minor damage to the cell wall following treatment of *Enterococcus faecalis,* a Gram-positive species, with TBO and suggested instead that surface damage is localised to proteins or lipids. Given that biocidal activity against *E. coli* decreased when TBO was replaced with lipophilic new methylene blue (Chapter 3, section 3.5.7), we suggest proteins are a more important cell surface target for photosensitisers.

The observations of Mertins et al. (2014) may offer an alternative explanation for our observations. By examining lipid vesicles by phase contrast microscopy *in situ* with light treatment, they reported that photosensitisation with methylene blue resulted in observable but transient damage in the form of membrane invaginations and pores. Cessation of excitatory light resulted in apparent restoration of vesicle stability in less than 1 minute. As the preparation time for SEM samples is lengthily (i.e. several hours), it is plausible that any cell surface perturbations would be restored prior to examination.

In the case of both bacterial species, we did not observe a change in the texture of the cell surface. Textural changes such as surface roughness accompany exposure to membrane active agents such as QACs (Kawai & Yamagishi, 2009) and so we expected to make similar observations in cells treated with Formulation TCM+S. It is possible that the long

preparation time and coating of treated cells with an electroconductive Au-Pd layer may have masked some of the changes to the surface texture of cells. Atomic force microscopy would circumvent coating of cells and could provide improved resolution and topographic information of treated bacteria (Braga & Ricci, 1998). As the only step of sample preparation is immobilisation, other artefacts associated with drying may also be avoided (Kirat et al., 2014). Other authors report observing surface blebbing in TBO-photosensitised *S. aureus* and *E. coli* cells upon examination by AFM and that the cytoplasmic membrane and cell wall can become detached (Sahu et al., 2009). In addition to AFM, transmission electron microscopy (TEM) could provide useful insights regarding how intracellular structures are affected by photodynamic treatment. For example, biocide-induced ultrastructural changes such as shifts in chromatin density, the coagulation of intracellular contents and detachment of membrane layers can be observed by TEM (Otto et al., 2010; Cheung et al., 2012).

Ureaplasma are a group of organisms which lack a cell wall. As previous experiments indicated that the cell wall was unlikely to be a major target for photosensitisation, *U. urealyticum* was used as an indicator organism in place of the more classic model of spheroplasts, which also lack a cell wall but must be maintained in hypertonic conditions to prevent cell lysis. *U. urealyticum* was highly susceptible to treatment with Formulation TCM+S and the viability of *U. urealyticum* decreased by >4 $\log_{10}$ within 1 minute of treatment (fig. 4.12). Exposure to the formulation without light was also able to achieve between 2 $\log_{10}$ in the same time frame which indicates that other formulation components such as MGDA, the surfactants or the pH may exhibit residual biocidal activity.

Whilst these observations indicate that the cell wall was unnecessary for the biocidal activity of Formulation TCM+S, the data obtained was of questionable value. Unlike spheroplasts, there is no cell wall-containing *Ureaplasma* species to which sensitivity can be compared. Furthermore, the assay format itself was highly quantal as it was only able to detect whole $\log_{10}$ changes in viability, depending on whether a colour change was observed in each dilution. Whilst resolution could be improved in the future by using a 2-fold dilution series rather than a 10-fold one, spheroplasts may be a more useful approach in future investigations.

4.6 Chapter conclusions

Treatment of target cells with Formulation TCM+S and red light had a strong effect on the cytoplasmic membrane of *S. aureus* and *E. coli* cells. Depolarisation of cell membranes occurred rapidly following treatment, allowing propidium iodide to enter cells and bind to DNA. This was accompanied by a concomitant loss of intracellular energy, as ATP leaked into the surrounding medium. Loss of stored ATP and the means to synthesise new energy was hypothesised to lead to cell inactivation. Examination by scanning electron microscopy determined that treated cells remained intact following treatment. Whilst *S. aureus* cells underwent slight morphological changes, *E. coli* cells retained their typical morphology. *Ureaplasma* were highly susceptible to photosensitisation by Formulation TCM+S, indicating that the cell wall was not necessary for biocidal activity. Δ*recA* mutants of *B. subtilis* were more sensitive to Formulation TCM+S than a wild-type isogenic strain, indicating that DNA is a targeted during photosensitisation and that DNA repair responses protect bacterial cells from inactivation. This observation supports the hypothesis that TBO enters target cells during treatment. Treatment of isolated DNA by Formulation TCM+S and red light did not induce double strand breaks when examined by gel electrophoresis. DNA damage may instead take the form of base modifications.

Chapter 5.

Extended Panel Testing

5.1 Introduction

5.1.1 Disinfectant requirements

The aim of this study was to develop a photosensitiser-based biocide which is suitable for high-level disinfection of medical surfaces, particularly those of an automated endoscope reprocessor (AER). In Chapter 3, Formulation TCM+S (40 µM TBO, 10 mM MGDA, 15 mM sodium hydrogen carbonate, 10 mM sodium carbonate, 0.01% Plurafac LF 901, 0.01% Praepagen TQ; pH 10.2) demonstrated biocidal activity against several bacterial species in suspension and dried onto PVC surfaces. Medical surfaces, including those of AERs, can be contaminated by a broad range of other organisms, including viruses, fungi, mycobacteria and bacterial endospores. A biocide suitable for high-level disinfection should demonstrate activity against each of these organism types (Centres for Disease Prevention and Control, 2008b).

5.1.2 Hierarchy of susceptibility to biocides

McDonnell & Burke (2011) assert that pathogenic microorganisms can be categorised into an ascending hierarchy based on their resistance to chemical disinfection (Fig. 5.1). This hierarchy can be a useful guide to determine the strengths and limitations of a biocide and determine whether it is suitable for the intended application. Identifying limitations at an early stage of development will provide future researchers a direction with which to focus their research, either to overcome these limitations or find a more suitable use. The following sections will address the specific issues of each of these organism types.

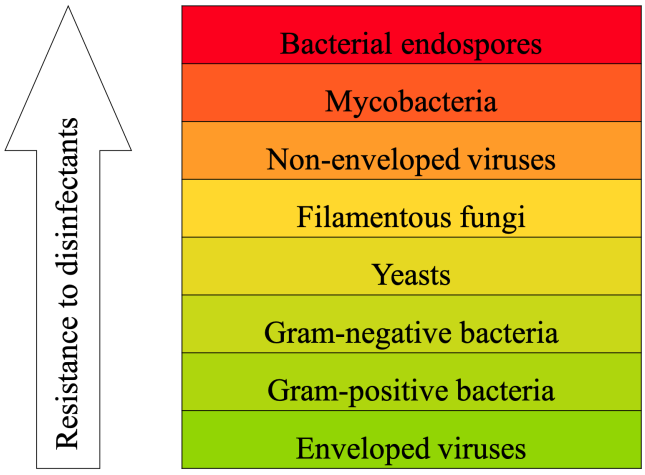

Figure 5.1: McDonnell & Burke's hierarchy of microbial resistance to disinfectants (McDonnell & Burke, 2011). Enveloped viruses exhibit the greatest susceptibility to biocides whilst bacterial endospores are the most resilient.

5.1.4 Fungi

5.1.4.1 Structural features of fungi

Fungi are a diverse clade of eukaryotic organisms, characterised by the presence of cell walls containing chitin amongst other components. Whilst many fungal species are non-pathogenic, many are opportunistic or true pathogens and infection is more common and severe in individuals with compromised immune systems. The major groups of fungi implicated in infectious disease include yeasts and moulds. Yeasts are capable of thriving as unicellular organisms whereas moulds exist in multicellular communities which form filamentous hyphae. Table 5.1 describes some of the most common fungal diseases known to affect humans. Assessment of claims of yeasticidal and fungicidal activity for disinfectant products used in medical areas is performed using the EN 13624 standard (British Standards Institute, 2013a).

Table 5.1: Common fungal diseases in humans

Disease	Area of infection	Causative organism
Candidiasis	Dermis (thrush); systemic circulation (invasive candidiasis)	*Candida albicans*, *C. auris*, *C. glabrata* etc
Aspergillosis	Respiratory tract	*Aspergillus fumigatus*, *A. flavus*
Pneumocystis pneumonia	Respiratory tract	*Pneumocystis jirovecii*
Cryptococcosis	Central nervous system	*Cryptococcus neoformans*
Tinea	Dermis	*Trichophyton mentagrophytes*

5.1.4.2 Yeasts

Yeasts such as *Candida albicans* are part of the normal dermal and gastrointestinal flora of humans. Consequently, they have a high potential to contaminate medical surfaces. Indeed, yeasts commonly contaminate AERs. In one study, 50% of positive swab cultures from contaminated AERs were due to *Candida* or yeast-like species (Lu et al., 2012). Whilst transmission of *C. albicans* to patients is generally uncomplicated and highly treatable, *C. auris* is a rapidly emerging pathogen which exhibits intrinsic non-susceptibility to many frontline antifungal drugs (Arendrup et al., 2017; Forsberg et al., 2019). Preventing the transmission of *C. auris* is therefore of paramount importance to protect patient safety. To borrow the adage *prevention is better than cure*, patient safety is best guaranteed by preventing its transmission in the first place. Whilst peracetic acid (PAA) is fairly effective at controlling *C. auris*, Kean et al. (2018) reported significant survival and regrowth after treatment which may be an issue for endoscope reprocessing

5.1.4.3 Filamentous fungi

In contrast to yeasts, filamentous fungi (moulds) develop only as multicellular communities and form branching hyphae across surfaces. Whilst also being responsible for food spoilage and damage to buildings, filamentous fungi can cause dermal and respiratory diseases such as tinea and aspergillosis. Infection of the airways by *Aspergillus spp.* can cause serious chronic recurring problems for cystic fibrosis patients due to persistence of hyphae inside the lungs (King et al., 2016). In the context of endoscopy, colonisation of the rinse water purification system of automated endoscope reprocessors by *Aspergillus fumigatus* has been reported (Khalsa et al., 2014).

Asexual reproduction of filamentous fungi occurs through the production of conidia. These small spores bud from specialised hyphal structures (conidiophores) and readily disperse in the air. This allows them to contaminate large areas where they can persist and can remain viable for months (Alshareef & Robson, 2014). Transmission can therefore occur through direct contact with contaminated surfaces or by inhalation of airborne conidia or aerosols. Claims for the fungicidal activity of biocides are substantiated by assessing the disinfectant product against conidia of *Aspergillus brasiliensis*.

5.1.4.4 Fungal susceptibility to photosensitisers

Yeasts are widely reported to be susceptible to the photodynamic inactivation by phenothiazines such as TBO and methylene blue (Souza et al., 2010, Pupo et al., 2011; Rodrigues et al., 2013). However, inactivation occurs at a relatively slow rate when compared to bacterial species (Zeina et al., 2001). Both TBO and methylene blue are capable of photodynamic inactivation of *Aspergillus nidulans* and *Metarhizium anisopliae* conidia (Gonzalez et al., 2010) and *Trichophyton* microconidia (Rodrigues et al., 2012). Friedberg et al. (2001) reported successful inactivation of *A. fumigatus* using the porphyrin-based photosensitiser *Green 2W*, though the reported culture conditions did not isolate conidia specifically. As of 2019, there have been no studies on the effect of photosensitisers on conidia of *A. brasiliensis*.

5.1.4.5 The role of melanin in fungal resistance to biocides

A. brasiliensis belongs to the *Aspergillus* section Nigri (i.e. black Aspergillus), which are characterised by strong pigmentation due to the production of melanin. This pigment is incorporated into the cell wall of conidia providing structural support and protection from a range of environmental stressors (Pihet et al., 2009; Bayry et al., 2013). Melanin granules are arranged in concentric layers within the cell wall of fungi; in some fungal species, such as *Cryptococcus neoformans,* this can form a barrier measuring over 200 nm thick

(Eisenman et al., 2005). Fungal melanins are negatively charged (Nosanchuk et al., 1997) and interact with positively charged, aromatic peptides with high affinity (Nosanchuk et al., 1999).

Melanin is a potent antioxidant which can quench reactive oxygen species including radicals and singlet oxygen (Hamilton & Holden, 1999; Tada et al., 2010). It has an established role in protection from UV-induced oxidative stress and melanin biosynthesis in *Aspergillus spp.* is induced by exposure to UV (Singaravelan et al., 2008; Esbelin et al., 2013). Melanin extracted from *Aspergillus nidulans* exhibits antioxidant properties against chlorine-releasing agents and hydrogen peroxide (de Cassia & Pombeiro-Sponchiado, 2005) and strains with impairments in melanin biosynthesis are considerably more susceptible to inactivation by hydrogen peroxide (Jackson et al., 2009).

Melanin may play a significant role in protecting fungi from Formulation TCM+S via three major mechanisms. TBO has a positively charged aromatic structure which would likely interact strongly with melanin within the outer layers of the cell wall. This would prevent it from reaching intracellular targets within the cytoplasmic membrane and cytoplasm. The strong antioxidant properties of melanin may then offer a second layer of chemical protection by quenching any singlet oxygen which forms. Finally, even if TBO successfully penetrates into deeper layers of the conidia, the dark colouration of melanin may optically quench the transmission of excitatory light to the photosensitiser, thus preventing TBO photoactivation. Due to these factors, we hypothesise that conidia of *Aspergillus brasiliensis* may resist inactivation by Formulation TCM+S.

5.1.4.6 *Aspergillus* melanin biosynthesis

In fungi, melanin biosynthesis is primarily achieved through the dihydroxy naphthalene (DHN) and L-dihydroxy phenylalanine (L-DOPA) pathways (Langfelder et al., 2003). Most *Aspergillus spp*. utilise the DHN pathway though *A. niger* appears to be an exception (Krijgsheld et al., 2012). Elliot (1995) established that sub-inhibitory concentrations of several antifungal compounds, including kojic acid and tricyclazole can be used to inhibit melanin biosynthesis in the plant pathogen *Gaeumannomyces*. Using these findings, Pal et al. (2014) reported success in using the same methodology against multiple *Aspergillus* species. Whilst *A. brasiliensis* was not included in this study, the closely related *A. niger* exhibited an albino phenotype after being cultured with kojic acid, an inhibitor of the L-DOPA biosynthesis pathway (Pal et al., 2014).

5.1.5 Viruses

5.1.5.1 Viral structure and physiology

Viruses are small obligate intracellular parasites which are the aetiological agents of many human diseases (table 5.2). Viruses are structurally simple compared to prokaryotes and eukaryotes and consists of a handful of proteins, replicative enzymes and minimal genetic material. Some viruses are encapsulated in a lipid envelope which surrounds the capsid and fuses with the membrane of host cells during the infection process. Due to their simplicity the targets for viral disinfection are more limited than with more complex organisms. Inactivation can occur through disruption of the envelope, damage to viral proteins or destruction of nucleic acids (Baillie & Theriault, 2013). As membranes are relatively fragile and susceptible to surfactants, biocides and desiccation, enveloped viruses are generally easier to inactivate when compared to their non-enveloped cousins. Non-enveloped viruses are particularly persistent on environmental surfaces (Firquet et al., 2015) and smaller variants are considered particularly difficult to inactivate (Sattar et al., 2007).

Table 5.2: Common viral diseases in humans

Viral Envelope	Virus	Disease
Non-enveloped	Adenovirus	Common cold
	Norovirus	Gastroenteritis
	Influenza	Influenza
Enveloped	Human immunodeficiency virus	Acquired immunodeficiency syndrome (AIDS)
	Hepatitis C	Viral hepatitis
	Herpes simplex virus 1	Cold sores (herpes)

5.1.5.4 Methods of assessing virucidal activity

In Europe, claims of efficacy against viruses must be substantiated by the EN 14476 standard. In this test, monolayers of host mammalian cells are infected with the virus and examined by light microscopy to quantify cytopathic effects. Surface disinfectants should be tested against poliovirus, adenovirus and murine norovirus at a concentration of 10^8 Median Tissue Culture Infectious Dose ($TCID_{50}$) per mL which facilitates detection of 4 $\log_{10}$ reductions in viral titre (British Standards Institute, 2013b). Whilst EN 14476 assesses activity of disinfectants against viral suspensions, it can also be adapted for use with surface carriers (Rabenau et al., 2014).

The technical expertise and expense required to perform the tests are a major drawback to their use (Cock & Kalt, 2010). Distinguishing cytopathic effects from biocide cytotoxicity to host cells can be difficult and the test must be validated to determine the maximum concentration of biocide able to be used. Biocide neutralisation is achieved by ice cold dilution and so it is not always possible to eliminate host cell cytotoxicity. These drawbacks add an additional layer of complication and expense to an already complex test procedure and makes it inefficient for screening (Cock & Kalt, 2010).

5.1.5.5 Bacteriophage surrogate testing

MS2 bacteriophage is a 27-nm diameter, icosahedral, non-enveloped RNA virus which infects *Escherichia coli* expressing fertility pili (Bollback & Huelsenbeck, 2001; Valegârd et al., 1997). Its structure is considered highly analogous to that of norovirus (Robilotti et al., 2015) and MS2 is commonly used as a surrogate for mammalian viruses in biocide testing (Horm & D'Souza, 2011; Schulz et al., 2012) The United States Environmental Protection Agency considers MS2 a safer and suitable surrogate for water purification technologies (Mapp et al., 2016) and MS2 has been used to assess the efficacy of surface disinfection technologies such as vaporized hydrogen peroxide (Pottage et al., 2010).

As it replicates in bacterial hosts, MS2 is considerably cheaper and faster to culture than mammalian viruses. This makes it a useful screening tool for antiviral compounds (Cock & Kalt, 2016). Virucidal activity against bacteriophages can be determined using a plaque reduction assay. Infection of host cells in a semi-solid agar overlay results in the formation of plaques where host cells have lysed. Changes in phage infectivity are inferred by the number of plaques present in the overlay. In contrast to mammalian viral CPEs, these plaques are visible without the aid of a microscope and are considerably easier to quantify (Cock & Kalt, 2016).

5.1.5.5 Viral susceptibility to photosensitisers

Given the strong interactions which occur between TBO and negatively charged residues, such as those which occur in amino acids, it seems logical that photosensitisers would be effective in inactivating non-enveloped viruses surrounded by a proteinaceous capsid. Numerous studies have confirmed the effectiveness of photosensitisers against both mammalian and bacterial non-enveloped viruses, including with phenothiazines such as TBO (Costa et al., 2012). It is therefore anticipated that Formulation TCM+S will be exhibit rapid virucidal activity against MS2 bacteriophage.

5.1.6 Mycobacteria

5.1.6.1 Physiology of mycobacteria

Whilst phylogenetically classified as a Gram-positive species, bacteria of the *Mycobacterium* genus represent a distinct category of organisms in disinfection. The cell wall of mycobacteria is uniquely rich in hydrophobic mycolic acid residues, which are anchored to the peptidoglycan cell wall via arabinogalactan as a mycolyl-arabinogalactan-peptidoglycan (mAGP) complex (Alderwick *et al.,* 2015; Jankute et al., 2015). Mycobacteria are the causative agents of several diseases (table 5.3) and can be sub grouped by growth characteristics and pigment production. Slow-growing mycobacteria (e.g. *Mycobacterium avium*) can take several weeks to culture *in vitro* whilst fast growing species (e.g. *Mycobacterium smegmatis*) may be propagated in only a few days.

Table 5.3: Mycobacterial diseases

Species	Disease
Mycobacterium tuberculosis	Tuberculosis
Mycobacterium avium	Nontuberculous mycobacterial (NTM) pulmonary disease
Mycobacterium leprae	Hansen's disease (leprosy)
Mycobacterium chelonae	Opportunistic pulmonary and dermal infections
Mycobacterium bovis	Bovine tuberculosis

5.1.6.2 Mycobacterial resistance to antimicrobials

Second only to bacterial endospores, mycobacteria exhibit considerable intrinsic resistance to chemical disinfectants (McDonnell & Burke, 2011). The cell wall-mAGP complex plays a vital role in facilitating resistance by forming a permeability barrier which functions analogously to the outer membrane of Gram-negative bacteria (Hett & Rubin, 2008). The high density of hydrophobic residues makes the cell wall of mycobacteria extremely impermeable to hydrophilic solutes: compared to *E. coli* and *P. aeruginosa,* mycobacteria can be 100-1000 times less permeable to such compounds (Jarlier & Nikaido, 1990; Trias & Benz, 1994). Akin to the Gram-negative organisms, mycobacteria utilise porins to transport nutrients across this permeability barrier. However, these porins are longer and considerably fewer in number compared to those of Gram-negative species, which limits diffusion of nutrients and other solutes into mycobacterial cells (Niederweis, 2003).

Several species of mycobacteria, including *M. chelonae* and *M. abscessus*, have been isolated from AERs and exhibit decreased susceptibility to the high-level disinfectants glutaraldehyde (GTA) and ortho-phthalaldehyde (OPA) (Griffiths et al., 1997; De Groot et al., 2014). Resistance to these agents appears to be fairly prevalent; in a random sampling of endoscopy units a startlingly high number of resistant organisms were able to be isolated from those which primarily utilise GTA or OPA (Fisher et al., 2012). Resistance to GTA and OPA in mycobacteria is associated with changes in the expression of porins (Svetlíková et al., 2009).

Frenzel et al. (2011) determined that that relatively large susceptibility of *M. smegmatis* to biocides is due to the relatively prolific expression of porins compared to other *Mycobacterium* species. Deletion of the *mspA* gene, which encodes the major porin in *M. smegmatis*, resulted in 100 times lower susceptibility to a range of biocides, including formaldehyde and isothiazolinones (Frenzel et al., 2011). Susceptibility of biocide-resistant *Mycobacterium* strains can be restored by the removal of the cell wall, which can be experimentally achieved through the preparation of spheroplasts (Fraud et al., 2003) and the heterologous expression of *mspA* in *M. tuberculosis* increases its susceptibility to copper and antibiotics (Mailaender et al., 2004; Speer et al., 2013). In light of these studies, porins play a key role in mediating mycobacterial susceptibility and resistance to antimicrobials.

Since porins facilitate the transport of hydrophilic solutes including antimicrobial drugs, concerns have been raised that the continued use of alkylating agents may drive the development of mycobacterial antibiotic resistance. (Svetlíková et al., 2009). Switching to oxidative agents has therefore been recommended to reduce the occurrence of outbreaks associated with GTA/OPA resistance (Burgess et al., 2017). As photosensitisers exert their biocidal activity through the production of oxidative species, they may be a suitable alternative.

5.1.6.3 Photosensitiser-based disinfection of mycobacteria

Previous studies have reported that *Mycobacterium smegmatis* is susceptible to several photosensitisers, including porphyrin and phenothiazine derivatives (Feese & Ghiladi, 2009; Shim et al., 2016). Moreover, several other photosensitiser derivatives have been utilised successfully against *M. bovis* (O'Riordan et al., 2007). It is unclear whether photosensitisers are effective against slow growing species such as *Mycobacterium tuberculosis*. Since these species lack an *mspA* homologue (Kartmann et al., 1999) their low permeability may facilitate resistance to photosensitisation by Formulation TCM+S.

5.1.6.4 Lipophilic antimicrobials and mycobacteria

The lipophilicity of antimicrobials appears to play an important role in their efficacy against mycobacteria. *In vitro* studies suggest that lipophilicity is an essential property of effective anti-tuberculosis drugs, particularly when targeting mycobacteria in a non-replicative stage of the life cycle (Picarro et al., 2013; Picarro et al., 2015). Whilst less effective as a cross-linking agent, OPA exhibits greater biocidal activity than GTA against *M. chelonae* (Fraud et al., 2001). Increased lipophilicity of OPA due to the presence of an aromatic moiety has been proposed to underlie this difference in activity (Simons et al., 2001). More lipophilic photosensitisers such as new methylene blue may therefore be more capable of increased uptake through the lipophilic cell wall of mycobacteria and exhibit improved activity.

5.1.7 Bacterial endospores

Bacterial endospores (spores) are highly resilient structures produced by *Bacillus* and *Clostridium* species when subjected to environmental stress. Endospores are metabolically inactive, exceptionally hardy and can even survive in harsh simulated Martian environments (Cortesão et al., 2019). Spores are considered the hardiest type of organism in the hierarchy of disinfection (McDonnell & Burke, 2011) and high-level disinfection should achieve a reduction in the viability of spores contaminating a surface, though some spores may still survive (Centers for Disease Control and Prevention, 2008b). The persistence of endospores in healthcare environments is problematic as they may contaminate surfaces for prolonged periods of time, do not respond to normal infection control interventions such as hand sanitisers and are easily spread to patients.

5.1.7.1 Endospore formation and resistance to biocides

The formation of spores (sporulation) occurs in response to environmental stressors such as nutrient limitation and is reviewed in detail by Tan & Ramamurthi (2014). In contrast to binary fission, sporulation in an asymmetric process which occurs within the mother cell. After separation of genetic material and formation of a septum, the mother cell envelops the daughter forespore with a second lipid bilayer, resulting in the formation of an inner and outer membrane, which are highly impermeable to exogenous agents (Cortezzo & Setlow, 2005). A thick peptidoglycan cortex is synthesised in the space between these membranes, which provides thermal protection. The outer membrane is then surrounded by a proteinaceous basement layer, inner and outer coats and finally a crust (McKenny et al., 2010; Tan & Ramamurthi, 2014). This multi-layered structure protects endospores from enzymatic and chemical attack by being a barrier to diffusion and by detoxifying agents. Disruption of *cotE* leads to a marked loss in the outer coat proteins and a concurrent increase in susceptibility to disinfection by peroxide, hypochlorite and UV radiation (Riesenman & Nicholson, 2000; Ghosh et al., 2008).

After formation of the outer protective layers, the endospore core is saturated with dipicolinic acid and α/β-type small acid soluble proteins (SASPs). These complex with calcium and double stranded DNA respectively and confer resistance to chemical agents and physical insults such as ionising radiation and desiccation (Setlow et al., 1992; Setlow et al., 2006; Moeller et al., 2009). A low water content in the core further protects endospores from damage. Whilst a small amount of damage may still occur, an array of integrity scanning and repair proteins become active upon spore germination and can rectify the damage which does occur (Setlow & Setlow, 1996). The structure of a spore and its resistance mechanisms are illustrated in figure 5.2.

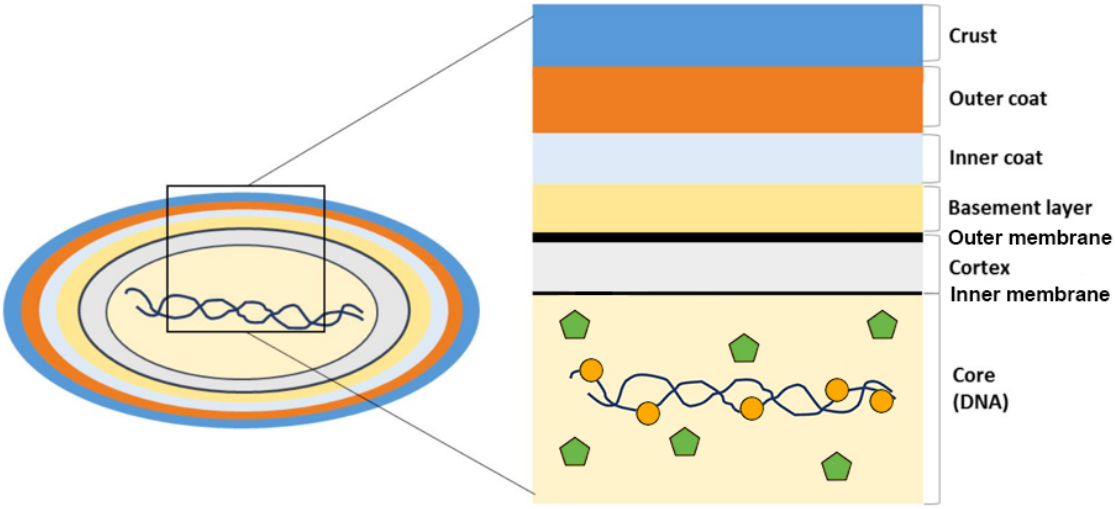

Figure 5.2: Bacterial endospore structure. In contrast to vegetative cells, endospores contain many additional outer layers which confer protection from biocides and other damage. The core is saturated with small acid soluble proteins (orange circles) and dipicolinic acid (green pentagons) to protect its DNA. Adapted from Cortesão et al. (2019). © reproduced under a Creative Commons Attribution license.

5.1.7.2 Sporicidal biocides and photosensitisers

Alkylating and oxidising agents such as glutaraldehyde and peracetic acid (PAA) exhibit sporicidal activity. Combinations of Quaternary ammonium compounds are sporistatic and inhibit spore germination; this can result in false positives for sporicidal activity under standardised test conditions if improperly neutralised (Leggett et al., 2016b). Whilst alkylating agents can take several hours to achieve sufficient reductions in spore viability, disinfection with PAA can be achieved within minutes (Martin et al., 2008; Maillard, 2011). The reactive oxygen species produced by photosensitisers may also exhibit rapid sporicidal activity.

Compared to other groups of microorganisms, relatively few studies have assessed the efficacy of photosensitisers against bacterial endospores. In a landmark study in 2005, Demidova & Hamblin (2005) reported sporicidal activity of TBO and methylene blue against *B. subtilis*. This protocol utilised 50 µM of photosensitiser and a 3-hour pre-incubation step prior to illumination to be effective; shorter incubation periods resulted in markedly reduced sporicidal activity (Demidova & Hamblin, 2005). A similar study by Oliveira et al. (2009) reported similar activity with TBO and several cationic porphyrin derivatives but also incorporated a 3-hour incubation step to facilitate adsorption of the photosensitiser to spores.

In contrast to the aforementioned studies, Eichner et al. (2015) reported rapid sporicidal activity against spores of *Bacillus atrophaeus* without the need of a prolonged pre-incubation step. After a 15 second incubation and 10 second light excitation, they observed 4.4 $\log_{10}$ reductions in spore viability when using photosensitisers derived from riboflavin. They reported the greatest success using a derivative possessing a side chain containing 8 cationic $-NH_3^+$ groups. This indicated that increased cationic charge is associated with greater sporicidal activity. In contrast to other authors, who used photosensitisers in a micromolar concentration range (Demidova & Hamblin, 2005; Oliveira et al., 2009), this group reportedly used a relatively high concentration of 4 mM (Eichner et al., 2015). It is unknown whether the Formulation TCM+S will demonstrate similarly rapid sporicidal activity considering the steps taken to optimise its activity in previous chapters.

5.1.7.3 Enhancement of biocidal activity with hydrogen peroxide

Hydrogen peroxide is an oxidative biocide which exhibits sporicidal activity. It is utilised as a high-level disinfectant and has a favourable environmental profile since it decomposes into oxygen and water. Hydrogen peroxide and PAA exhibit synergy when used against spores and are found co-formulated in a range of commercial products. Pre-treatment with 0.1% peroxide primes spores to the effects of PAA whilst the opposite doesn't have an effect (Leggett et al., 2016a). Proposed mechanisms for this synergy include the peroxide permeabilising the spore to enhance penetration of PAA or the reacting with sites in upper layers of the spore (such as the coat proteins) which reduces quenching of PAA activity. Cortezzo et al. (2004) deduced that exposure to oxidising agents primes spores for future biocide exposure by damaging the inner membrane, even when the initial exposure was non-lethal. Whilst some studies indicate that a combination of photosensitiser and peroxide enhances activity against biofilms (Decker et al., 2017; Yang et al., 2018), nobody has looked at whether this combination is synergistic against bacterial spores.

5.1.8 Surface biofilms

Biofilms are complex communities of sessile microorganisms, most commonly associated with surfaces. They exhibit distinct phenotypic characteristics from their planktonic counterparts and can resist chemical disinfection through several complementary mechanisms. These include the production of an extracellular polymeric substance (EPS) matrix, degradative enzymes and the presence of metabolically inert persister cells (Lewis, 2005; Bridier et al., 2011). EPS is primarily composed of proteins but also contains nucleic acids and carbohydrates; this acts as a permeability barrier which excludes exogenous agents (Mah & O'Toole, 2001) and can quench the activity of biocides (Stewart et al., 2001). These factors facilitate the survival of biofilm organisms following exposure to commonly used healthcare disinfectants (Smith & Hunter, 2008). Removal of biofilms can be achieved by mechanical processes though this complicates decontamination procedures.

5.1.8.1 Biofilms in automated endoscope reprocessors

Automated endoscope reprocessors are susceptible to colonisation by biofilms. Colonisation by *Pseudomonas* and *Mycobacterium* can cause recontamination of endoscopes post-processing and has been implicated in numerous nosocomial outbreaks over the past decades (Alvarado et al., 1991; Schelenz & French, 2000; Kressel & Kidd, 2001; Shimono et al., 2008). Colonisation can occur in many different AER components, including the filtration system, detergent tank and fluid channels. Fluid channel colonisation can result from design flaws which prevent full evacuation of water following use (Roberts, 2013). According to the ISO 15883 standard, AER self-disinfection cycles should be capable of eliminating biofilm organisms (British Standards Institute, 2018).

5.1.8.1 Dry surface biofilms

As well as growing under moist conditions, biofilms can develop over time with alternating periods of hydration and desiccation. In endoscopy units, biofilm build up is particularly problematic when alkylating agents such as glutaraldehyde are used, as fixation of EPS proteins creates a robust crust which can protect microbial communities from high-level disinfection (Alfa & Howie, 2009). These biofilms can be described as dry surface biofilms (DSBs) and are highly resistant to terminal cleaning regimens (Vickery et al., 2012; Hu et al., 2015; Johani et al., 2018). DSBs can persist on surfaces over prolonged periods (Costa et al., 2019) and viable organisms have even been recovered after autoclaving at 121ºC for 2 hours (Almatroudi et al., 2018). DSBs are also readily transferred between surfaces and patients in the healthcare environment through contact with contaminated surfaces (Chowdhury et al., 2018). Developing biocides which are effective against DSBs would be a valuable contribution to the antimicrobial armamentarium.

5.1.8.2 Assessment of biocidal efficacy against biofilms

Despite the threats posed by biofilms in healthcare settings, there are limited options for standardised disinfectant testing against these bacterial structures. This is partly due to the huge diversity of culture methods employed in biofilm research, which can affect biofilm susceptibility to biocides. Whilst enriched media can enhance the rate of biofilm formation (Seneviratne et al., 2013), biofilms produced under nutrient-poor conditions are more stable and less susceptible to removal (Dewanti & Wong, 1995).

Currently, the only standardised testing method for the assessment of biocidal efficacy against biofilms is the Minimum Biofilm Eradication Concentration (MBEC) assay, described by the E2799–17 standard (ASTM International; 2017b). Using a specially designed MBEC plate (formerly referred to as a Calgary device), biofilms of *P. aeruginosa* are cultured on small polystyrene pegs under minimal shearing force provided by an orbital shaker platform. Whilst it offers high-throughput and reproducible results (Parker et al., 2014), this assay has only been developed for testing against *P. aeruginosa* and has not been adapted to produce DSBs.

Alternative test methods have been proposed against DSBs which more closely mirror the tests used against surface dried bacteria in the EN 13697 and ASTM E2197 standards. In these tests, biofilms are cultured on surface carriers and are then subjected to a biocide challenge; after dislodging cells from the carriers, $\log_{10}$ reductions in biofilm viability may then be calculated to assess efficacy (Almatroudi et al., 2015; Ledwoch et al., 2019). In specific applications such as antimicrobial wipes, metrics such as the time required for regrowth and transferability of the biofilm may also be useful when assessing product efficacy (Ledwoch & Maillard, 2018).

DSBs for biocidal testing can be produced using two different methods (table 5.4). The Melbourne-based Vickery research group utilises a Centers for Disease Control biofilm reactor and use polycarbonate coupons as surface carriers (Almatroudi et al., 2015) whereas the Cardiff-based Maillard research group utilises stainless steel coupons in tissue culture plates placed on an orbital shaker (Ledwoch et al., 2019). In both cases, biofilms are subjected to recurring 2-day cycles of desiccation and hydration over the course of 12 days, after which DSBs may be tested. Whilst both methods yield a surprisingly similar cell density per coupon (~7 $\log_{10}$ CFU), the protein content of each differs by a considerable margin. As proteins interfere with many biocides, the greater protein content in DSBs produced by Ledwoch et al. (2019) may facilitate more robust testing.

Table 5.4: Dry surface biofilm culture methods

	Almatroudi et al. (2015)	Ledwoch et al. (2019)
Species/strain	*S. aureus* ATCC 25923	*S. aureus* NCTC 10788
Culture method	CDC Biofilm reactor	Orbital shaker plate
Coupon material	Polycarbonate	AISI 430 stainless steel
Growth Medium	5 % tryptone soya broth	100% tryptone soya broth
Cell number (Log_{10} CFU)	7.13 ± 0.04	7.38 ± 0.58
Relative protein content %	56	95

5.1.8.3 Current state of photodisinfection against biofilms

Phenothiazines including MB and TBO have been demonstrated to be effective against biofilms of several species, including *Staphylococcus aureus*, *Streptococcus mutans*, *Aggregatibacter actinomycetemcomitans* and *Candida albicans* (Zanin et al., 2005; Sharma et al., 2008; Misba et al., 2011). Gad et al. (2004) observed that EPS is a protective factor in biofilms, though noted that cationic photosensitisers such as TBO were able to overcome this barrier. No studies have yet addressed the biocidal activity of photosensitisers against dry surface biofilms. The thick layer of EPS may protect DSBs from Formulation TCM+S, though rehydration upon exposure to the formulation may facilitate enhanced penetration into the biofilm compared to hydrated biofilms.

5.2 Chapter aims and objectives

The aim of this chapter was to evaluate the biocidal activity of Formulation TCM+S (40 μM TBO, 10 mM MGDA, 15 mM sodium hydrogen carbonate, 10 mM sodium carbonate, 0.01% Plurafac LF 901, 0.01% Praepagen TQ; pH 10.2) against an extended spectrum of organisms encompassing the major groups described in McDonnell & Burke's hierarchy of disinfection (McDonnell & Burke; 2011). These groups include yeasts, fungi, viruses, mycobacteria, bacterial endospores and bacterial biofilms. The results of these tests will be used to determine the limitations of the current formulation and photosensitiser technology and to guide future development.

5.3 Methods

5.3.1 General test procedure

5.3.1.1 Formulation & neutraliser

Unless noted otherwise, the formulation used in this chapter was Formulation TCM+S, which consisted of: 40 μM TBO, 10 mM MGDA, 15 mM sodium hydrogen carbonate, 10 mM sodium carbonate, 0.01% Plurafac LF 901, 0.01% Praepagen TQ (pH 10.2).

Following exposure to the disinfection procedure for a defined contact time, residual biocidal activity was quenched by turning off the light source and by diluting the suspension 10-fold in universal neutraliser (section 2.2.5).

5.3.1.2 Test format and organic load

With the exception of experiments on surface biofilms, all efficacy tests described in this chapter were performed in suspension. Light soiling conditions were simulated by the addition of 0.3 g/L BSA to test suspensions immediately prior to testing (Section 2.2.7.2).

To perform testing, 800 μL aliquots of formulation were added to microcentrifuge tubes. 100 μL of 0.3 g/L BSA was then added to each tube, followed by 100 μL of test suspension (density described below). After vortexing to mix, 960 μL was transferred to sterile 35 mm diameter petri dishes (Greiner Bio-one International), which were placed directly underneath the light source for the defined contact time. The light intensity at this point is described in Chapter 2, Section 2.1.9.

5.3.1.3 Microbial cell density of test suspensions

Test suspensions were adjusted to various cell densities depending on the organism type (table 5.5). The preparation of suspensions is described in their relevant subsections.

Table 5.5: Cell density of test suspensions

Organism type	CFU /mL	Section
Candida spp.	1.5-5 × 10^7	5.3.2.3
Aspergillus brasiliensis conidia	1.5-5 × 10^7	5.3.2.4
MS2 bacteriophage	2 × 10^{8*}	5.3.4.3
Mycobacterium smegmatis	1-2 × 10^7	5.3.5.3
M. avium/M. terrae	1-2 × 10^6	5.3.5.3
B. subtilis endospores	1-5 × 10^8	5.3.6.3

*PFU/mL

5.3.2 Determination of yeasticidal and fungicidal activity

The yeasticidal activity of the formulation was evaluated against *Candida albicans* and *C. auris*. The fungicidal activity of the formulation was determined against mature conidia of *Aspergillus brasiliensis*. Tests were performed in accordance with the EN 13624 standard, which is considered a phase 1 test for determining activity against fungal species.

5.3.2.1 Media and chemicals

Fungi were cultured on malt extract agar (MEA), which was obtained as a dried powder from Oxoid. *Candida* suspensions were prepared and diluted using sterile TSC whilst suspensions of *Aspergillus* conidia were prepared in a dilutent of sterile deionised water containing 0.1% polysorbate 80, which prevented aggregation of conidia.

5.3.2.2 Organisms

Yeasticidal activity was determined against *Candida albicans* ATCC 10231 and *Candida auris* DSM 21092. Fungicidal activity was determined against mature conidia of *Aspergillus brasiliensis* NCTC 16404.

5.3.2.3 Preparation of *Candida* test suspensions

Spread plates of *C. albicans* and *C. auris* were prepared by adding 100 µL of freezer stock to the centre of MEA plates and spreading with a sterile L-shaped spreader. After incubating plates for two days at 30ºC, test suspensions were prepared by harvesting colonies from the plates using a sterile inoculation loop and resuspending in centrifuge tubes containing 5g sterile glass beads and 10 mL TSC. Absorbance A_{630} was adjusted to 1.5, which was equivalent to a cell density of 1.5-5 × 10^7 CFU/mL. Candida suspensions were tested in accordance with section 5.3.1.

5.3.2.4 Preparation of *A. brasiliensis* test suspensions

20 µL aliquots of *A. brasiliensis* freezer stock were dropped into the centre of MEA plates. Plates were incubated at 30ºC for 8 days, after which the surface of the agar had become covered in a hyphae and black conidiophores were visible. Ensuring not to disturb the spores, 5 mL of polysorbate diluent was gently added to each plate and the conidia harvested by scraping with a sterile L-shaped spreader. The resulting suspension was filtered through a sterile glass fritted filter to remove hyphae. To validate conidia were suitable for testing, the suspension was examined under a light microscope to ensure hyphae were not present and that conidia were spiny, indicating maturity. The cell density was adjusted to 1-5 × 10^7 CFU/mL and tested in accordance with section 5.3.1.

5.3.2.5 Recovery and quantification

Following testing, neutralisation and serial dilution, surviving microorganisms were recovered by preparing spread plates using 250 µL aliquots of diluted suspension; two technical replicates were prepared from each suspension. *Candida spp.* were incubated for two days at 30°C and *A. brasiliensis* for three days, after which colonies were counted and survival quantified.

5.3.2.6 Effect of melanin biosynthesis inhibitors on conidial susceptibility to photosensitisation

There are two melanin biosynthesis pathways in *Aspergillus* species which are inhibited by kojic acid (DOPA-pathway) and tricyclazole (DHN-pathway). Exposure to these agents during propagation yields an albino phenotype whose conidia lack melanin (Pal et al., 2014).

15X chemical stocks of each antifungal agent were prepared: kojic acid was dissolved in 70% DMSO whilst tricyclazole was dissolved in 100% ethanol. Each was added to centrifuge tubes containing 15 mL sterile molten malt extract agar (cooled to 50°C) so that the final concentration of each inhibitor in the agar was 100 µg/mL. The resulting agar was used to pour plates, which were set and dried in an isolation hood. Plates were inoculated with 20 µL of *A. brasiliensis* freezer stock and conidia test suspensions were prepared as described previously (section 5.3.2.4); due to slower growth, plates were incubated for 10 days instead of 8 prior to harvesting conidia. The biocidal activity of Formulation TCM+S was then tested against these conidia.

5.3.4 Determination of virucidal activity by plaque reduction assay

5.3.4.1 Media and chemicals

A 200X stock of 0.1 M $CaCl_2$ was prepared by dissolving in deionised water and sterilising by filtration. Semi-solid agar was prepared from nutrient agar (Oxoid) at 65% of the normal concentration. Following sterilisation by autoclaving, flasks were placed in a water bath set to 50°C. After equilibrating to temperature, $CaCl_2$ was added to a final concentration of 500 µM. Serial dilutions were performed in SM buffer, which was prepared as described in table 5.6.

Table 5.6: Preparation of SM buffer (Cold Spring Harbour Protocols, 2018).

Component	Amount	Final Concentration
NaCl	5.8 g	100 mM
$MgSO_4.7H_2O$	2g	8 mM
Tris-Cl (1 M, pH 7.5)	50 mL	50 mM
Deionised H_2O	To 1L	-

5.3.4.2 Species and strains

MS2 bacteriophage ATCC 15597-B1 was used as the surrogate virus and *Escherichia coli* ATCC 15597 was used as the host organism to propagate MS2.

5.3.4.3 Preparation of host organism and bacteriophage

Host organisms were prepared by adding 100 µL of freezer stock to 10 mL TSB in sterile 50 mL centrifuge tubes and incubating for 18 hours at 37°C. Samples were centrifuged at 3500 G for 10 minutes, washed and resuspended in sterile TSB to an A_{630} of 0.2 (section 2.2.2); this yielded a cell density of 5×10^7 CFU/mL.

Bacteriophage were propagated by adding 100 µL of host and 100 µL of MS2 to 10 mL of TSB. Following incubation for 18 hours at 37°C, cultures were centrifuged at 3500 G for 10 minutes, and the supernatant was harvested and filtered through a 0.2-micron filter to remove any bacterial cells. This yielded 5 x 10^9 plaque forming units (PFU)/mL of MS2 so was diluted 25-fold to obtain a viral titre of 2 x 10^8 PFU/mL; this mirrors the titre used for testing against mammalian viruses in the EN 14476 standard (British Standards Institute, 2013). Viral suspensions were used within 2 hours of preparation.

5.3.4.4 Test protocol and phage recovery

100 µL of 0.3 g/L BSA and 100 µL of viral suspensions were added to 800 µL of formulation. After vortexing, 960 µL was transferred to 35 mm petri dishes and the samples were illuminated for 1 and 5 minutes. As a control, 100 µL was also transferred to 900 µL of sterile deionised water for 5 minutes. After treatment, 100 µL of each sample was transferred to 900 µL of neutraliser for 5 minutes and then serially diluted in SM buffer.

To quantify the survival of phage, 4 mL of molten semi-solid agar was transferred to sterile 7 mL bijou tubes. 100 µL of host cell suspension and 100 µL of serially diluted phage were added to tubes, which was mixed gently by inversion. The contents of the tubes were then poured onto the surface of TSA plates, which were rocked to ensure the semi-solid agar completely overlaid the surface. To ensure the agar remained molten, this process was carried out with one tube at a time.

After allowing the agar to set for 30 minutes, plates were and incubated for 18 hours at 37°C. The plaques which formed due to infection by viable MS2 virions appeared as clear zones where host bacteria did not grow. Plaques were quantified, and PFU/mL values were calculated using the following equation:

$$\text{PFU/mL} = \text{plaque count} \times \text{dilution factor} \times 10$$

5.3.5 Determination of biocidal activity against mycobacteria

Biocidal activity of Formulation TCM+S against mycobacteria was determined using a modified version of the EN 14348 standard (British Standards Institute, 2005). In this test, the threshold for substantiating efficacy claims is achieving 4 $\log_{10}$ reductions in viability.

5.3.5.1 Media and chemicals

Mycobacterium spp. were cultured on Middlebrook 7H10 agar (Oxoid) enriched with 10% Middlebrook Oleic Albumin Dextrose Catalase (OADC) growth supplement (Remel; San Diego). The medium was prepared by first adding 900 mL deionised water to 19 g of 7H10 powder. After autoclaving, the agar was cooled to 50ºC, after which 100 mL of OADC was added. After inverting the flask to mix, 20 mL aliquots were used to prepare agar plates.

5.3.5.2 Species and strains

Mycobactericidal activity of the formulation was investigated using three *Mycobacterium* species: *M. terrae* NCTC 15769 (tuberculocidal), *M. avium* NCTC 15755 (mycobactericidal) and *M smegmatis* NCTC 8159. *M smegmatis* was used due to its faster growth rate compared to other species, which allows it to be cultured in three days rather than three weeks.

5.3.5.3 Propagation and preparation of test suspensions

For each organism, 50 µL of freezer stock was added to six Middlebook 7H10 plates, spread with an L-shaped spreader and placed in an ICH110 incubator (Memmert) at 37ºC and 80% relative. *M. smegmatis* was grown for 72 hours whilst *M. terrae* and *M. avium* were grown for 21 days.

Following incubation, cells were harvested by scraping colonies of each of the six plates using an inoculation loop. Loopfuls of bacteria were added to 50 mL centrifuge tubes (two plates per tube) containing 5 g sterile borosilicate glass beads and vortexed dry for 5 minutes to separate cell aggregates. 10 mL of sterile deionised water was then added dropwise to each tube, alternating with the vortex; this method minimised aggregation of cells. After all water added, tubes were left for 20 minutes to allow any large aggregates to settle. The top fraction containing separated cells was removed by pipette and transferred to a fresh centrifuge tube containing 5 g sterile borosilicate glass beads. Using this method, *M. smegmatis* suspensions were prepared to a cell density of 10^7 CFU/mL whilst *M. terrae* and *M. avium* to 10^6 CFU/mL. The biocidal activity of Formulation TCM+S was then tested against these suspensions (section 5.3.1) using contact times of 5 and 15 minutes.

5.3.5.4 Effect of new methylene blue on mycobactericidal activity

To determine whether new methylene blue (NMB) would exhibit greater biocidal activity against mycobacteria, alternative versions of Formulation TCM+S were prepared by substituting the TBO component either entirely with NMB or by preparing a 50:50 mix of both 20 μM TBO and 20 μM NMB. Each formulation was tested against suspensions of *M. smegmatis*.

5.3.6 Determination of Sporicidal Activity

Determination of sporicidal activity was performed using the ASTM E2197−17$^{\varepsilon 1}$ standard (ASTM International, 2017a). This test is more stringent than EN 14347 (Wesgate et al., 2016) and was favoured over EN 13704 standard as batches of spores could be prepared in three days, rather than 32. The threshold for passing this test is to demonstrate greater than 4 $\log_{10}$ reductions in spore viability.

5.3.6.1 Media and Chemicals

Bacillus subtilis spores were propagated in dilute (1:10) Columbia broth (Oxoid), supplemented with 100 μM $MnSO_4$. $MnSO_4$ was obtained from Sigma and was prepared as a 10 mM stock in deionised water, which was sterilised by filtration. Supplementation with manganese aided sporulation as it is an essential cofactor for the enzyme phosphoglycerate phosphomutase (Oh & Freese, 1976). For quantification, spores were recovered using tryptone soya agar.

Hydrogen peroxide was obtained from Fisher Scientific as a 35% concentrate. It was diluted to 1% immediately prior to use with sterile deionised water.

5.3.6.2 Strains

Spores from three strains of *B. subtilis* were used in this study. They were produced using isogenic derivatives of *B. subtilis* strain 168. Each strain was provided by Professor Peter Setlow of the University of Connecticut (UConn Health; Farmington, Connecticut). These strains were chosen over *B. subtilis* ATCC 19659 (as recommended in the E2197 standard) to facilitate the investigation of resistance mechanisms. PS533 was used as a wild-type strain. PS578 has large base pair deletions in genes *sspA* and *sspB* (α and β SASPs) whilst PS3394 contains a defect in *cotE* (outer coat protein) due to insertion of a tetracycline resistance cassette into the coding regions (Leggett et al., 2016b).

5.3.6.3 Spore propagation

99 mL of Columbia broth and 1 mL of $MnSO_4$ was added to pre-sterilised 500 mL Erlenmeyer flasks. Each flask was subsequently inoculated with *B. subtilis* and the opening was closed with a sterile foam stopper and aluminium foil. Flasks were incubated for 72 hours at 37^{o}C on an orbital shaker. After 72 hours, 10 μL of suspension was transferred to a glass slide, air dried and then examined by phase contrast microscopy. Suspensions were validated as suitable if >80% of cells exhibited a phase bright appearance, indicating that spores had reached maturity.

Spores were harvested by transferring the contents of flasks into 50 mL centrifuge tubes and centrifuging at 5000 G for 20 minutes. After discarding the supernatant and resuspending the spores and cells in sterile deionised water, tubes were placed in a water bath (80ºC) for 60 minutes to inactivate any remaining vegetative *B. subtilis* cells whilst leaving spores viable. Suspensions were centrifuged and washed a further 3 times in deionised water. After the final centrifugation step, pellets were resuspended in $1/10^{th}$ of the original volume of each (i.e. 5 mL per centrifuge tube).

Spore suspension were then quantified by recovery using the serial dilution/drop count method, allowing the plates 3 days to incubate at 30ºC. Upon quantification, suspensions were determined to have a spore density of 1-5 × 10^8 CFU/mL. Spore suspensions were stored for up to 2 weeks prior to testing.

5.3.6.4 Sporicidal Testing

ASTM E2197 states that the sporicidal activity of disinfectants should be determined against spore suspensions at a density of 1.5-5 × 10^6 CFU/mL. Suspensions were therefore diluted in sterile deionised water to yield a final concentration of 5 × 10^6 CFU/mL and tested as described in section 5.3.1 using illuminated treatment times up to 30 minutes.

5.3.6.5 Effect of hydrogen peroxide pre-treatment on sporicidal activity

To assess whether pre-treatment with hydrogen peroxide could increase the sporicidal activity of the formulation, spores were first diluted to a concentration of 5 × 10^7 CFU/mL. 100 µL aliquots of spore suspension were then added to 900 µL of 1% hydrogen peroxide and incubated for 1, 5 10, 30 and 60 minutes. Following incubation, 100 µL of peroxide pre-treated spores were treated with Formulation TCM+S (section 5.3.1) for 30 minutes. To compare the combined disinfection efficacy to peroxide treatment alone, 100 µL aliquots of primed spores were also transferred to 900 µL of deionised water and incubated for 30 minutes.

5.3.7 Determination of bactericidal activity against surface biofilms

5.3.7.1 Test organisms and biofilms

S. aureus NCTC 10788 and *E. coli* ATCC 10798 were used to prepare biofilms. Wet and dry surface biofilms were prepared for each species.

5.3.7.2 Preparation of test surfaces

Surface biofilms were grown on 10 mm diameter AISI 430 stainless steel coupons. Coupons were cleaned prior to use in accordance with EN 13697 by soaking in 0.1% polysorbate 80 for 60 minutes. They were then rinsed with deionised water, dried using paper towels and sterilised by autoclaving (section 2.1.6). Using sterile forceps, sterilised coupons were placed into wells of 24-well tissue culture plates.

5.3.7.3 Preparation of wet surface biofilms

Overnight cultures of *S. aureus* or *E. coli* were prepared and used to inoculate Reasoner's 2A (R2A) broth with 10^6 CFU/mL of organisms. 1 mL of inoculated broth was transferred to each well containing a disc and plates were incubated for three days at 20ºC at 150 RPM using an Orbit P4 digital shaker (Labnet). This resulted in 1-5 × 10^7 CFU organisms growing on each coupon.

5.3.7.4 Preparation of dry surface biofilms

Dry surface biofilms were produced using the procedure described by Ledwoch et al. (2019). Using this protocol, biofilms were grown over a 12-day period with alternating 2-day phases of hydration and desiccation. In this case, R2A broth was used instead of TSB to maintain continuity with the growth conditions of the hydrated biofilm.

The same initial inoculation procedure was followed as with the hydrated biofilm but plates were incubated for two days. Liquid media was removed and plates dried for two days in a stationary incubator at 37ºC (desiccation phase). To re-enter the hydration phase, 1 mL of sterile R2A broth was then added to each disc and incubated for a further two days at 20ºC on the orbital shaker. The biofilms continued to be hydrated and desiccated in two-day intervals for a total of 12-days, after which dry biofilms were formed on each coupon. Each coupon contained approximately 1-5 × 10^7 CFU of organism.

5.3.7.5 Test Procedure

To determine the biocidal activity of the formulation and disinfection procedure against biofilms, coupons were carefully removed from each well and placed in a 35 mm petri dish. 1 mL of formulation was added to the dish, which was sufficient to ensure the coupons were completely submerged in the formulation. Samples were illuminated 5 & 15 minutes, as previously described. As a negative control, some biofilms were placed in 1 mL sterile deionised water.

After testing, each coupon was transferred to flasks containing 9 mL universal neutraliser and 5 g glass beads using sterile forceps. The 1 mL contents of each petri dish were also transferred to ensure any dislodged cells would also be quantified to assess survival. Each sample was vortexed for 2 minutes to dislodge biofilms from the discs and to disperse cells. Samples were then serially diluted, and cells quantified using the Miles & Misra method (section 2.2.3).

5.4 Results

5.4.1 Yeasticidal and fungicidal activity

Table 5.7 outlines the biocidal activity of Formulation TCM+S against various species of yeast and filamentous fungi. Formulation TCM+S was highly biocidal against suspensions of *Candida albicans* and *C. auris* as ≥5 log_{10} reductions in viability were observed for both species after a contact time of 1 minute. In contrast, conidia of *Aspergillus brasiliensis* were not susceptible to Formulation TCM+S as only a 0.5 log_{10} reduction in viability was observed after a contact time of 15 minutes.

Table 5.7: Yeasticidal and fungicidal activity of Formulation TCM+S. EN 13624 test conditions.

Species	Contact time (mins)	Log_{10} CFU reduction	SD	Pass/Fail*
C. albicans	1	≥5.0	0.02	Pass
	5	≥5.0	0.02	Pass
C. auris	1	≥5.3	0.04	Pass
	5	≥5.3	0.04	Pass
A. brasiliensis	5	0.3	0.08	Fail
conidia	15	0.5	0.10	Fail

*Pass threshold = 4 log_{10} reduction; SD = standard deviation.

Propagation of *A. brasiliensis* in the presence of 100 µg/mL of the melanin biosynthesis inhibitors, kojic acid and tricyclazole, led to a distinct change in the phenotype of the colonies compared to those grown in the absence of an inhibitor (figure 5.3). Tricyclazole, which inhibits the DHN melanin pathway caused colonies to exhibit a dark green coloration. In contrast, the L-DOPA melanin pathway inhibitor kojic acid caused colonies to exhibit an albino phenotype. Whilst this indicates that *A. brasiliensis* utilises both melanin biosynthesis pathways, the L-DOPA pathway is dominant.

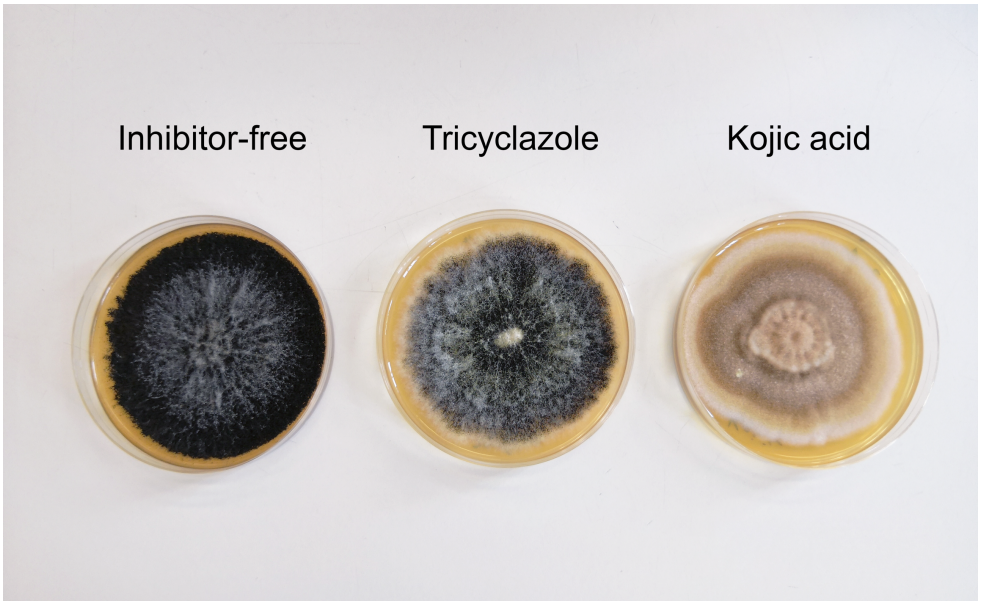

Figure 5.3: Effect of of melanin biosynthesis inhibitors on *Aspergillus brasiliensis* colony pigmentation. Propagation in the presence of tricyclazole resulted in the colonies exhibiting a green-white phenotype. In contrast, kojic acid caused the colonies to exhibit an albino phenotype.

Microscopic examination of the conidia produced by non-inhibited and kojic acid-treated *A. brasiliensis* demonstrated a distinct difference in conidial morphology (fig. 5.4). In the absence of an inhibitor of L-DOPA melanin biosynthesis, conidia exhibited a dark colouration and spiny morphology. This indicates the conidia were matured and contained melanin. In contrast, conidia produced by *A. brasiliensis* propagated in the presence of kojic acid exhibited an immature phenotype. They appeared as rounded structures which were considerably lighter in appearance than their uninhibited counterparts.

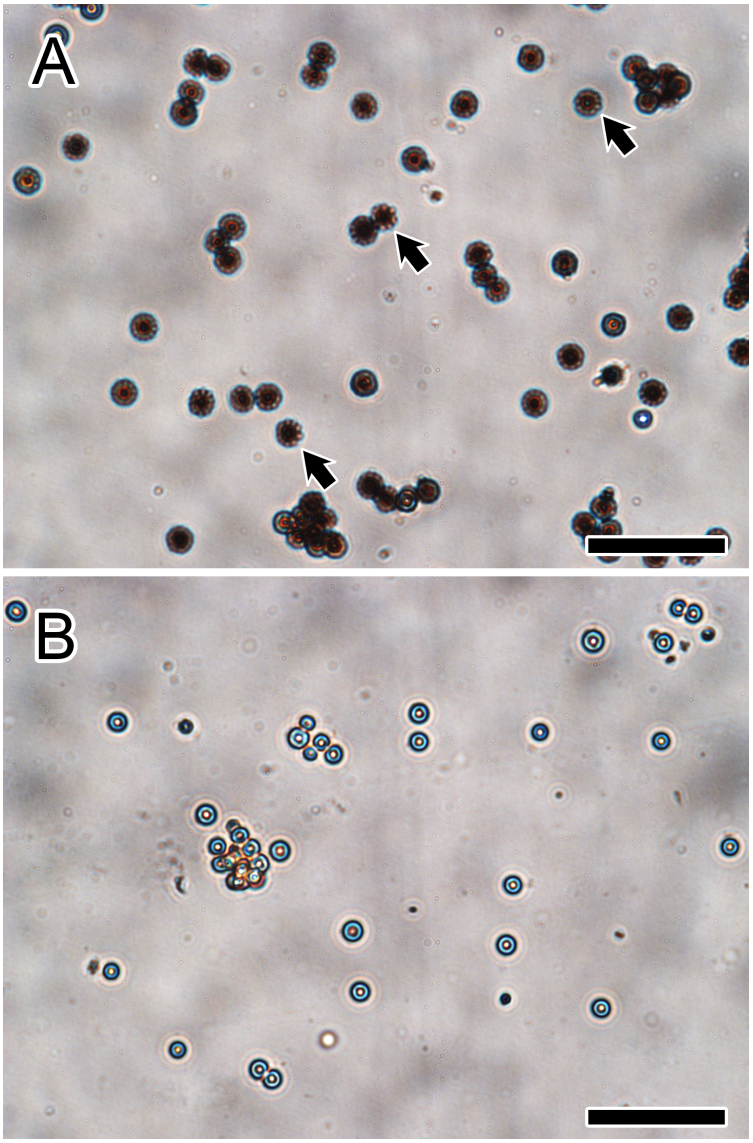

Figure 5.4: Conidia of *Aspergillus brasiliensis* propagated in the absence (A) and presence (B) of the L-DOPA melanin biosynthesis inhibitor, kojic acid. Non-inhibited conidia exhibit a dark colouration and undulate (spiny) morphology (arrows). In contrast, *A. brasiliensis* conidia grown in the presence of kojic acid possess a light and rounded appearance. Black bars (bottom left) correspond to a scale of 50 μm.

Biocidal efficacy tests using Formulation TCM+S demonstrated that *A. brasiliensis* conidia propagated in the presence of kojic acid were considerably more susceptible to inactivation (figure 5.5). Aspergillus conidia propagated in the presence of kojic acid were considerably more susceptible to Formulation TCM+S ($P < 0.0001$; ANOVA, Dunnett). Viability decreased by 2.4 $\log_{10}$ in 1 minute and was reduced to below the limit of detection within 5 minutes. In contrast, tricyclazole-treated conidia maintained their resistance to photosensitisation and there were no differences in susceptibility compared to the inhibitor-free control ($P > 0.05$; ANOVA, Dunnett).

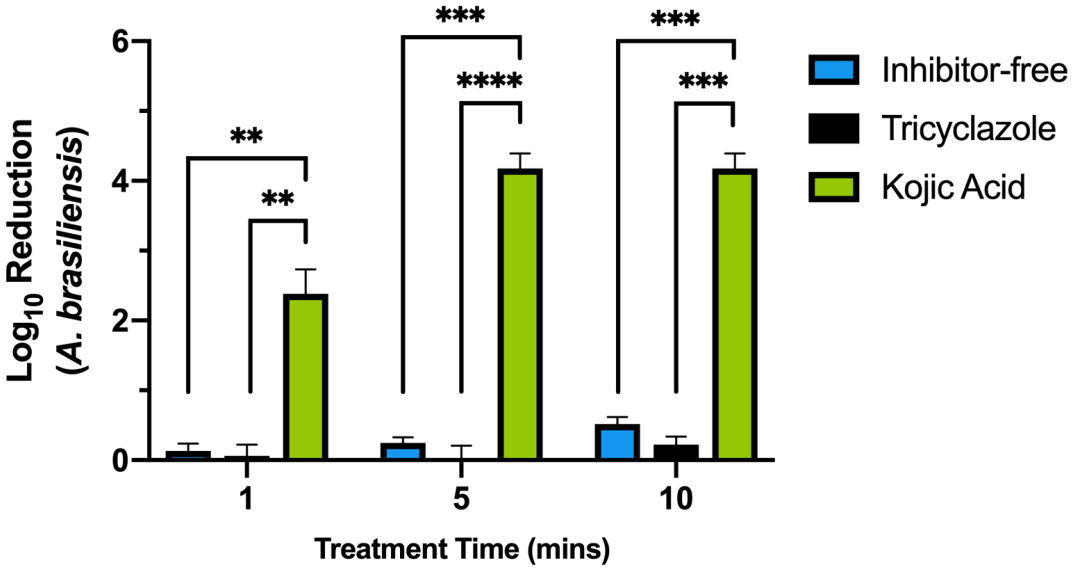

Figure 5.5: Biocidal activity of Formulation TCM+S against conidia of *Aspergillus brasiliensis.* Conidia were propagated in the presence or absence of various inhibitors of melanin biosynthesis.

5.4.2 Virucidal activity against MS2 bacteriophage

Formulation TCM+S performed extremely well against MS2 bacteriophage. After 1 minute of contact, viral infectivity decreased by 5.6 log_{10}; this rose to 6.1 log_{10} after 5 minutes (table 5.8). In both cases, this exceeded the 4 log_{10} requirement of the EN 14476 standard.

Table 5.8: Virucidal activity of Formulation TCM+S against suspensions of MS2 bacteriophage. EN 14476 test conditions, modified for use with bacteriophage.

Organism	Contact time (mins)	Log_{10} reduction	**SD**	**Pass/Fail***
MS2 bacteriophage	1	5.6	0.16	Pass
	5	6.1	0.34	Pass

*Pass threshold = 4 log_{10} reduction; SD = standard deviation.

5.4.3 Mycobactericidal and tuberculocidal activity

Mycobacterium species exhibited varying levels of susceptibility to Formulation TCM+S . After a contact time of 5 minutes, the viability of fast-growing *M. smegmatis* decreased by ≥5.3 $\log_{10}$. In contrast, slow-growing *M. terrae* and *M. avium* were resistant to disinfection and viability decreased by 0.4 and 0.3 $\log_{10}$ respectively after a 15-minute contact time (table 5.9). Partial or complete substitution of TBO with new methylene blue was ineffective at improving biocidal activity against *M. smegmatis* (fig. 5.6). The 50:50 mixture of TBO and NMB performed slightly worse than TBO ($P < 0.01$; ANOVA, Tukey) whilst complete substitution of TBO with NMB led to a marked decrease in biocidal activity compared to both TBO and the 50:50 mix ($P < 0.0001$; ANOVA, Tukey).

Table 5.9: Biocidal activity of Formulation TCM+S against *Mycobacterium* species. EN 14348 test conditions.

Species	Contact time (mins)	Log_{10} reduction	St Dev	Pass/Fail*
Mycobacterium	5	≥ 5.3	0.04	Pass
smegmatis	-	-	-	-
Mycobacterium	5	0.3	0.08	Fail
terrae	15	0.4	0.11	Fail
Mycobacterium	5	0.1	0.07	Fail
avium	15	0.3	0.10	Fail

*Pass threshold = 4 $\log_{10}$ reduction; SD = standard deviation.

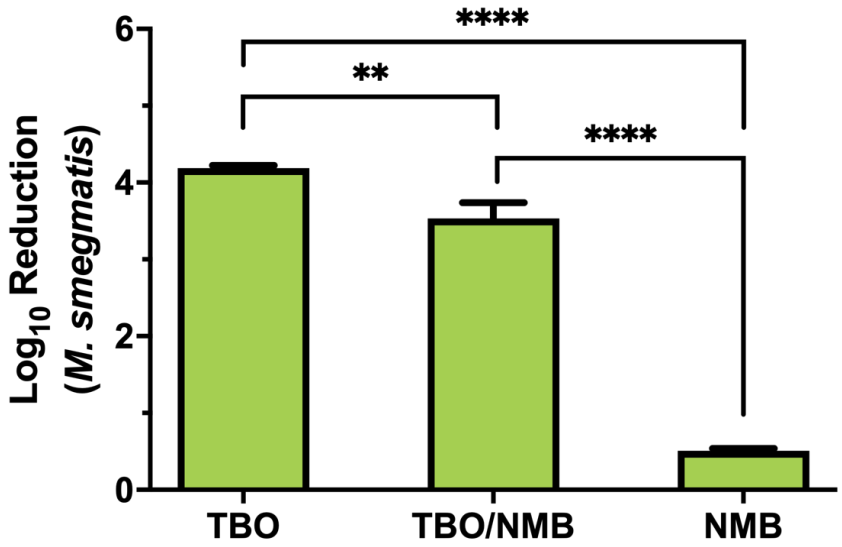

Figure 5.6: Biocidal activity of alternative photosensitiser combinations on *Mycobacterium smegmatis*. 1-minute contact time. TBO = toluidine blue O; NMB = new methylene blue; ** = $p<0.01$; **** = $p<0.0001$.

5.4.4 Sporicidal activity against *B. subtilis* spores

The viability of the wild-type *B. subtilis* (PS533) was reduced by 0.2 $\log_{10}$ following a 30-minute contact time (table 5.10). Strains defective in the outer coat (PS3394) and SASPs (PS578) were more susceptible to inactivation as their viability was reduced by 2.1 $\log_{10}$ and 1.1 $\log_{10}$ respectively. These reductions were still below the 4 $\log_{10}$ threshold necessitated by the ASTM E2197 standard.

Table 5.10: Biocidal activity of Formulation TCM+S against *Bacillus subtilis* endospores. ASTM E2197 test conditions.

Strain	Contact time (mins)	Log_{10} reduction	SD	Pass/Fail*
PS533	1	0.0	0.14	Fail
(wild-type)	5	0.0	0.17	Fail
	30	0.2	0.32	Fail

*Pass threshold = 4 $\log_{10}$ reduction; SD = standard deviation.

Spore mutants were markedly more susceptible to treatment with Formulation TCM+S (fig. 5.7). After 30 minutes, the viability of small acid soluble protein (SASP)-deficient spores (PS578) decreased by 1.1 $\log_{10}$, which was a fivefold improvement from the wild-type ($P < 0.05$; ANOVA, Tukey). Outer coat (*coteE*)-deficient spores (PS3394) were even more susceptible and viability decreased by 2.1 $\log_{10}$ after 30 minutes; this was a large increase in susceptibility compared to both the wild-type ($P < 0.001$; ANOVA, Tukey) and the SASP-deficient mutant ($P < 0.01$; ANOVA, Tukey).

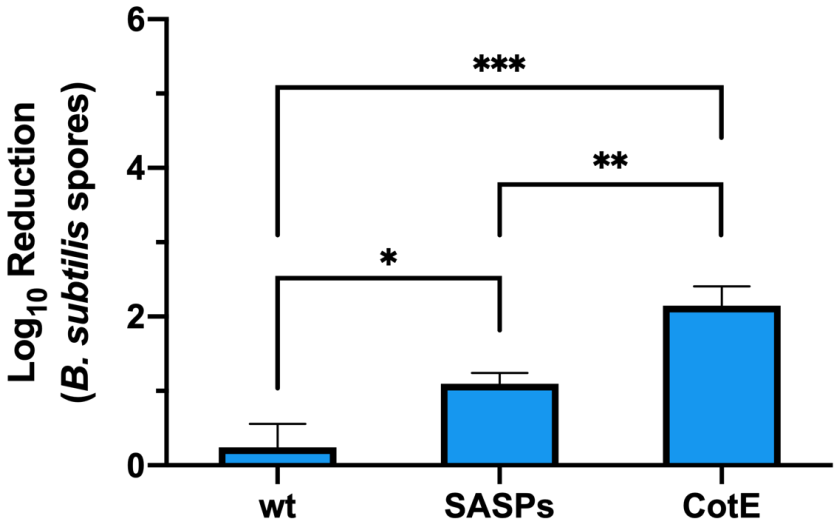

Figure 5.7: Susceptibility of *B. subtilis* spore mutants to Formulation TCM+S. Contact time: 30 minutes. wt: wild-type strain (PS533); SASPs: small acid soluble protein-deficient mutant (PS578); CotE: outer coat-deficient mutant (PS3394).

Pre-treatment of PS533 spores with 1% hydrogen peroxide did not improve the sporicidal activity of Formulation TCM+S (fig. 5.8). There were no differences in sporicidal activity between non-treated and pre-treated spores at any of the pre-treatment timepoints, even when pre-treated for 30 minutes (P >0.05; ANOVA).

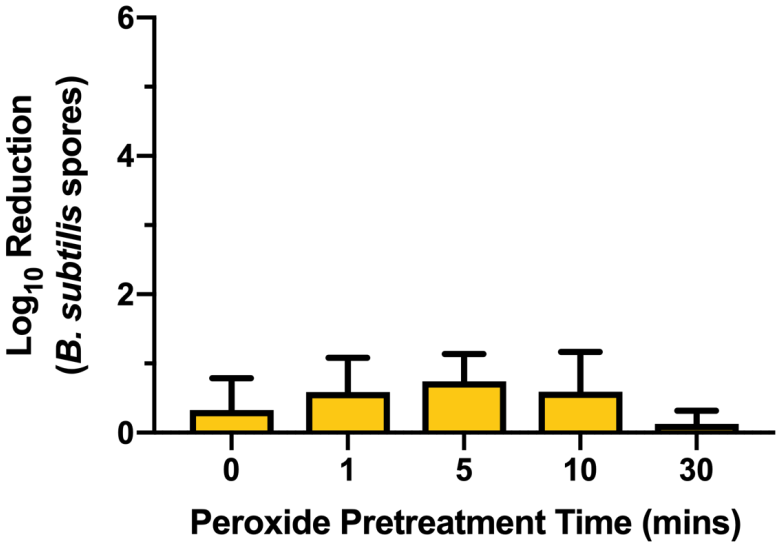

Figure 5.8: Sporicidal activity of Formulation TCM+S after pre-treatment of *B. subtilis* spores with 1% peroxide. After pre-treatment, primed spores were added to Formulation TCM+S and treated for 30 minutes.

5.4.5 Bactericidal activity against surface biofilms

Formulation TCM+S exhibited moderate bactericidal activity against both wet and dry biofilms of *Staphylococcus aureus* NCTC 10788 (figure 5.9). After 5 minutes of contact, the viability of *S. aureus* wet and dry biofilms decreased by 3.5 and 2.6 log_{10} respectively; this increased to 4.2 (wet) and 4.0 log_{10} (dry) at 15 minutes. The formulation performed equally well against both types of biofilm (P >0.05; ANOVA, Šidák). In contrast, biofilms of *E. coli* ATCC 10798 were less susceptible to Formulation TCM+S. After 5 minutes of contact, viability of wet and dry biofilms decreased by 0.9 and 1.9 log_{10} respectively; this increased to 1.8 (wet) and 3.6 log_{10} (dry) after 15 minutes. At 5 minutes, hydrated biofilms of *E. coli* were markedly less susceptible to Formulation TCM+S than wet (P <0.01; ANOVA, Šidák) and dry (P <0.05; ANOVA, Šidák) biofilms of *S. aureus.* Dry biofilms of *E. coli* were less susceptible than hydrated biofilms of *S. aureus* (P <0.05; ANOVA, Šidák) but equally susceptible as dry biofilms of *S. aureus* (P>0.05; ANOVA, Šidák). At 15 minutes, hydrated biofilms of *E. coli* were considerably less susceptible to inactivation when compared to dry biofilms of *E. coli* (P <0.05; ANOVA, Šidák).

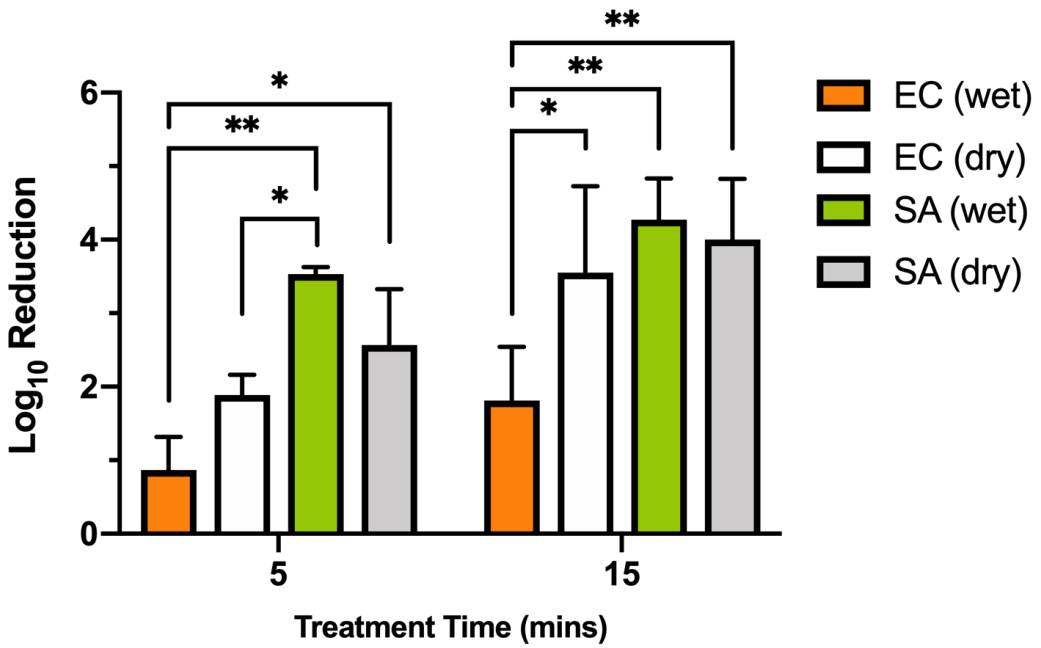

Figure 5.9: Biocidal activity of Formulation TCM+S against hydrated (wet) and dry biofilms of *E. coli* (EC) and *S. aureus* (SA). * = P <0.05; ** = P <0.01.

5.5 Discussion

5.5.1 Fungicidal activity

Previous studies have established that oxidising agents including peroxygen compounds and photosensitisers are highly effective against yeast species (Pupo et al., 2011; Rodrigues et al., 2013; Cadnum et al., 2017). Formulation TCM+S demonstrated that the formulation was yeasticidal against *Candida albicans* and *C. auris* as greater than 5 $\log_{10}$ reductions in viability were observed in both species after only 1 minute of contact (table 5.7). This fulfils the requirement of substantiating product efficacy claims for yeasticidal activity, as outlined in the EN 13624 standard. As this is considered a phase I test these results should be followed up using surface carriers under EN 13697 conditions to better simulate real-world use.

These observations are the first time a photosensitiser-based formulation has demonstrated efficacy against *C. auris*. Since this emerging species is intrinsically resistant to many antifungal drugs and disinfectants (Forsberg et al., 2019), this may indicate that there is a potential role for TBO-based formulations in infection control pertaining to *C. auris*. Photosensitisers have been previously suggested for therapeutic use against azole-resistant *Candida* strains (Paz-Critstobal et al., 2014).

Conidia facilitate dispersal of fungi in the environment and are responsible for transmitting fungal diseases such as aspergillosis. Product claims of fungicidal activity are based on the biocidal activity of disinfectants against conidia of *A. brasiliensis.* After a 15-minute contact time, we observed only 0.5 $\log_{10}$ reductions in conidia viability (table 5.7). This was far below the required 4 $\log_{10}$ threshold for efficacy and demonstrates that Formulation TCM+S is ineffective against *A. brasiliensis* conidia.

A major structural difference between yeasts and *Aspergillus* conidia is the high density of melanin present in the cell walls. Melanin is negatively charged (Nosanchuk et al., 1997) and protects conidia from oxidative damage related to biocide exposure and UV radiation (Singaravelan et al., 2008; Jackson et al., 2009). This negatively charged layer is rich in anionic residues which was anticipated to interact with TBO. Since this layer is up to 200 nm thick and the diffusion distance of singlet oxygen is 10-400 nm (Baier et al., 2005), trapping of TBO in the melanin layer was hypothesised to protect conidia from photosensitisation by Formulation TCM+S. As melanin exhibits strong absorbance across the visible spectrum, melanin may also act as a strong optical quencher and inhibit photoactivation of TBO adsorbed to conidia.

Previous authors report that conidia of *Penicillium chrysogenum* (Gomes et al., 2011) and *Aspergillus flavus* (Temba et al., 2019) are susceptible to photosensitisation. However, colonies of these species exhibit lighter pigmentation than *A. brasiliensis*, which belongs to the *Aspergillus* section Nigri (i.e. black aspergilli) group (D'hooge et al., 2011). The lighter pigmentation of these species is likely is a result of reduced melanin content, which would reduce their resistance to photosensitisation. It is interesting to note that one group reported curcumin as an effective photosensitiser against conidia of *A. niger,* which is a phylogenetic cousin of *A. brasiliensis* (Al-Asmari et al., 2011). However, they were only able to achieve a maximum of 2 $\log_{10}$ reductions in viability which was still significantly below the required level of efficacy required to make claims of fungicidal activity. Within section Nigri there are significant inter-species differences in susceptibility to antifungal compounds such as azoles (Hashimoto et al., 2011). It is unknown whether these differences may further contribute to the discrepancies between previous findings and our observations.

Propagation of *A. brasiliensis* in the presence of tricyclazole and kojic acid had a marked effect on the colony phenotype. Tricyclazole is a potent inhibitor of DHN melanin whilst kojic acid is effective in blocking synthesis of L-DOPA melanin (Pal et al., 2014). Whilst tricyclazole slowed the growth of colonies, they retained a dark pigmentation. In contrast, kojic acid was highly effective in inhibiting melanin production; colonies grown in the presence of this compound exhibited an albino phenotype (fig. 5.3). Microscopic examination of the conidia indicated that they were light in colouration and had a smooth appearance. (fig. 5.4). These observations demonstrate that L-DOPA melanin is the dominant pigment in *A. brasiliensis*, which is also the case for the phylogenetically close *A. niger* (Pal et al., 2014).

Inhibition of melanin biosynthesis by kojic acid had a profound effect on the susceptibility of *A. brasiliensis* conidia to Formulation TCM+S. A contact time of 5 minutes resulted in >4 $\log_{10}$ reductions in viability which indicated that albino conidia were readily inactivated by the formulation (fig. 5.5). These results clearly demonstrate that melanin is the primary mechanism of intrinsic resistance of *Aspergillus* conidia to toluidine blue O photosensitisation. This is the first time that this mechanism has been described for photosensitisers. The inability to inactivate wild-type conidia of *A. brasiliensis* is a significant barrier in the development of a photosensitiser-based high-level disinfectant formulation. Many antifungal formulations are based on oxidising agents, such as chorine releasing agents, which would be incompatible with formulations TCM+S due to oxidation of the photosensitiser. Further development is necessary to identify potential excipients and co-actives to improve fungicidal activity.

5.5.3 Virucidal activity against non-enveloped bacteriophage

Non-enveloped viruses pose specific challenges to disinfection due to their environmental persistence and resistance to some biocides. As a small, non-enveloped virus, MS2 bacteriophage is a useful surrogate for mammalian viruses. Previous results suggested that proteins and nucleic acids may be target sites for Formulation TCM+S and so it was anticipated that virucidal activity would be observed against MS2. Formulation TCM+S was highly virucidal and 5.1 $\log_{10}$ reductions in viability were observed after a 1-minute contact time, increasing to 6.1 $\log_{10}$ after 5 minutes (table 5.8). These reductions exceeded the 4 $\log_{10}$ reduction in viability required in the EN 14476 standard to substantiate claims of virucidal activity.

Despite their structural similarity, other authors have questioned the validity of generalising the results of bacteriophage studies to mammalian viruses. Su et al. (2009) observed a poor correlation between MS2 and norovirus susceptibility to the antimicrobial polysaccharide chitosan. Methylene blue has previously been demonstrated to be highly effective against adenovirus and 7 $\log_{10}$ reductions in viral infectivity were observed after 1 minute of photodynamic treatment with 2.7 μM methylene blue at pH 7.4 (Schagen et al., 1999). Due to the structural similarities between methylene blue and TBO, which are both phenothiazines, it is likely that Formulation TCM+S will also be effective against mammalian non-enveloped viruses. Before being validated as suitable for use in an AER, addition testing should be performed against poliovirus and adenovirus.

The effectiveness of Formulation TCM+S against MS2 bacteriophage further supports the conclusions of Chapter 4, which identified proteins and nucleic acids as major intracellular target. Indeed, a literature search revealed that the A (attachment) protein of MS2 is a target for photodynamic inactivation by TBO (Majiya et al., 2018). Due to the small size of MS2 phage, viral nucleic acids are well within the 10-400 nm diffusion distance of singlet oxygen (Baier et al., 2005). Further studies on the effect of photosensitisation on MS2 genome integrity would provide useful insights into whether nucleic acids are also affected during treatment and determine whether our observations are generalisable to other small non-enveloped viruses.

5.5.4 Mycobactericidal activity

Formulation TCM+S was highly effective against suspensions of *Mycobacterium smegmatis* and decreased the viability of this species by more than 5.3 $\log_{10}$ after a contact time of 5 minutes (table 5.9). Our observations support those of Feese & Ghiladi (2009), who reported that several cationic photosensitisers are biocidal against *M. smegmatis*. *M. smegmatis* shares its rapid growth characteristics with *M. abscessus* and *M. chelonae*, which are commonly isolated from AERs in endoscopy units where alkylating agents are utilised (Fisher et al., 2012). In contrast to these observations, Formulation TCM+S exhibited poor biocidal activity against the slow-growing mycobacterial species *M. terrae* and *M. avium*. After a contact time of 15 minutes, the viability of *M. terrae* and *M. avium* decreased by only 0.4 and 0.3 $\log_{10}$ respectively (table 5.9). This was substantially beneath the 4 $\log_{10}$ threshold required by the EN 14348 standard to substantiate product claims of tuberculocidal and mycobacterial activity. In light of these observations, Formulation TCM+S cannot be classed as tuberculocidal or mycobactericidal.

Cationic photosensitisers are capable of self-promoted uptake into target cells via porins (George et al., 2009). The rapid growth rate of *M. smegmatis* is dependent on the Msp porin, which facilitates diffusion of hydrophilic solutes. Loss of Msp results in considerably longer generation times and a concurrent increase in resistance to antimicrobial agents (Stephan et al., 2004; Stephan et al., 2005). As slow-growing mycobacteria lack an Msp homologue (Kartmann et al., 1999) and are resistant to photosensitisation by Formulation TCM+S, we propose that porin expression may play a key role in determining mycobacterial susceptibility to hydrophilic photosensitisers such as TBO.

Lipophilic biocides such as OPA exhibit increased mycobactericidal activity compared to hydrophilic alternatives such as GTA (Fraud et al., 2001; Simons et al., 2001). The photosensitiser new methylene blue is considerably more lipophilic than TBO and so it was hypothesised that replacement of TBO with new methylene blue (NMB) in Formulation TCM+S would improve activity against mycobacteria. Two alternative formulations were prepared in which TBO was partly or wholly replaced with NMB. These alternative formulations both exhibited reduced biocidal activity against *M. smegmatis* and the NMB-only formulation was almost inactive by comparison (fig. 5.6). Whilst this disproved the hypothesis, these observations support the proposed hydrophilic uptake route for TBO via cell wall porins.

Our observations suggest that *M. smegmatis* is a poor surrogate for slow-growing species in the study of anti-mycobacterial compounds. The distinct phenotypic differences between species necessitates caution when generalising *M. smegmatis* results to members of the broader genus. As an example, Shim et al. (2016) reported high sensitivity of M. smegmatis to photosensitisation and proposed photodynamic therapy could be used as an alternative treatment for multidrug resistant *Mycobacterium tuberculosis* infections. However, our observations suggest their results are unlikely to translate well to *M. tuberculosis* and that *M. terrae* would have been a more appropriate choice of surrogate.

The EN 14348 standard states that mycobacterial tests suspensions should be prepared to a cell density of of 1.5-5 × 10^9 CFU/mL (British Standards Institute, 2005). Despite following the methodology closely, we were only able to achieve a cell density of between 10^6 and 10^7 CFU/mL; this continued to be the case after harvesting cells from several spread plates and vortexing for a prolonged period with glass beads. It is plausible that there were a sufficient number of cells but their propensity to form aggregates greatly reduced the apparent cell density by causing cells to cluster and settle out of the suspension. This would have significantly decreased their relative surface area and reduced their susceptibility to disinfection. Other groups have also highlighted the problem of aggregation in mycobacterial suspensions and have critiqued the unclear specifications for homogenisation in European testing standards (Woelk et al., 2003). Frenzel et al. (2011) reported success homogenising and dispersing aggregates through the use of a cooled pestle and were able to achieve a high titre of 2-5 × 10^9 CFU/mL and so this method may be preferable in future iterations of the EN 14348 standard.

5.5.4 Sporicidal activity

Previous studies have indicated that cationic photosensitisers such as TBO can be effective for the disinfection of *Bacillus spp*. endospores (Demidova & Hamblin, 2005; Oliveira et al., 2009). Whilst this indicates that such spores are susceptibility to the biocidal effects of singlet oxygen, both studies reported using a long pre-incubation phase for several hours prior to exposure to excitatory light in order to achieve efficacy. Whilst it was unclear whether Formulation TCM+S would be effective if used for shorter contact times, without this step, rapid sporicidal activity has been reported for a riboflavin-based photosensitiser with a high density of positively charged residues (Eichner et al., 2015). Due to the rapid bactericidal activity of Formulation TCM+S compared to simple solutions of TBO, we anticipated that the formulation may be effective against spores without the need of a long pre-incubation.

Following a 30-minute contact time, a 0.2 $\log_{10}$ reduction in endospore viability was observed (table 5.10). This was far below the 4 $\log_{10}$ requirement of the ASTM E2197 standard and so Formulation TCM+S was ineffective against *B. subtilis* endospores. After this contact time we also observed complete decolourisation of the formulation, which indicated that the TBO component had autooxidised and that the formulation had produced its full yield of singlet oxygen.

Due to their roles in restricting permeability and protecting DNA, we hypothesised that the outer coat and small acid soluble proteins (SASPs) may be responsible for endospore resistance to Formulation TCM+S. Spores with defects in the genes encoding outer coat protein (*cotE*) and α/β SASPs (*sspA*/*sspB*) were markedly more susceptible to Formulation TCM+S. After a contact time of 30 minutes, the viability of the *cotE* mutant decreased by 2.1 $\log_{10}$ and the *sspA*/*sspB* by 1.1 $\log_{10}$ (fig. 5.7). This indicated that both spore impermeability and DNA protection both confer protection against photosensitisation by Formulation TCM+S

The 1.1 $\log_{10}$ reduction in the viability of spores with defective SASPs indicates DNA is an intracellular target for photosensitisation, supporting the conclusions of Chapter 4. Even when the spores had a functional outer coat, at least some singlet oxygen was able to exert its biocidal effects against DNA. In protein-rich environments such as the outer coat, singlet oxygen has a diffusion distance of only 10 nm (Baier et al., 2005). As this is far below the diameter of a spore, the observed biocidal activity against the SASP-deficient mutants indicates some TBO is able to naturally penetrate the outer spore coat and exert activity against intracellular target sites.

Hydrogen peroxide and peracetic acid (PAA) can be co-formulated in disinfectant products to improve sporicidal activity. Peroxide sensitises spores to PAA by weakening the coat and enhancing biocide penetration (Cortezzo et al., 2004; Leggett et al., 2016a). As the outer coat was a significant protective factor against photosensitisation with Formulation TCM+S, we hypothesised that pre-treating spores with 1% peroxide may provide synergistic activity against *B. subtilis*. After pre-treating spores for 60 minutes in 1% peroxide prior to photosensitisation, we did not observe an increase in biocidal activity. This indicates that peroxide does not sensitise spores to photosensitiser-based formulations.

Whilst other authors reported success when incubating spores with photosensitisers for several hours prior to illumination (Demidova & Hamblin, 2005; Oliveira et al., 2009), this time-frame is not feasible for a rapid AER self-disinfection cycle. Existing high-level disinfectants such as peracetic acid are able to achieve sufficient reductions in spore viability within several minutes (Maillard, 2011) and so Formulation TCM+S cannot compete in efficacy or rapidity. Given the reported success of an octo-cationic photosensitiser against spores (Eichner et al., 2015), it may be possible to develop a superior product based on this photosensitiser instead.

5.5.5 Biocidal activity against bacterial biofilms

Several previous studies have described biofilms of various species as being susceptible to photosensitisation by phenothiazines including TBO (Zanin et al., 2005; Sharma et al., 2008; Misba et al., 2011). Whilst a threshold level of bactericidal activity against biofilms has not yet been established, we used a 4 $\log_{10}$ reduction in viability as a benchmark analogous to the requirements of the EN 13697 surface carrier test (British Standards Institute, 2015a). We hypothesised that wet and dry surface biofilms of *S. aureus* and *E. coli* would be susceptible to treatment with Formulation TCM+S.

The biocidal activity of the formulation against biofilms was mixed. After a contact time of 5 minutes, reductions in viability ranged from a minimum of 0.9 $\log_{10}$ (*E. coli* hydrated biofilm) to a maximum of 3.5 $\log_{10}$ (*S. aureus* hydrated biofilm), which were both below the selected 4 $\log_{10}$ threshold (fig. 5.9). After a contact time of 15 minutes, reductions in viability increased from a minimum of 1.8 $\log_{10}$ (*E. coli* hydrated biofilm) to a maximum of 4.2 $\log_{10}$ (*S. aureus* hydrated biofilm). After 15 minutes, the viability of *S. aureus* dry surface biofilms (DSBs) decreased by 4.0 $\log_{10}$, which was at the threshold of efficacy, whilst *E. coli* DSBs were reduced by 3.6 $\log_{10}$. In all cases, significant numbers of biofilm cells survived treatment, which indicates that Formulation TCM+S is not effective at eliminating biofilm organisms. The survival of biofilm organisms may be due to protection of a subpopulation of cells embedded deep within the biofilm structure. This could be investigated in the future by staining with SYTO9 and propidium iodide and using confocal laser scanning microscopy to determine the distribution and special arrangement of live cells within treated biofilms (Drago et al., 2016).

Interestingly, both *S. aureus* biofilm types were equally susceptible to photosensitisation and *E. coli* DSBs were more susceptible than their hydrated counterparts. This observation was unexpected as DSBs are considered to be more resistant than hydrated biofilms to terminal disinfection processes (Vickery et al., 2012; Hu et al., 2015; Johani et al., 2018). The increased susceptibility of *E. coli* DSBs may be due to their desiccated nature, which may improve penetration of the formulation as it rehydrates the biofilm. In contrast, hydrated biofilms already contain water and so diffusion of the formulation components into the biofilm structure may occur at a reduced rate.

Compared to single species, polymicrobial biofilms are more resistant to a range of biocides including chlorine dioxide, QACs and glutaraldehyde (Lindsay et al., 2002; Simões et al., 2009). Biofilms which colonise medical surfaces such as AERs are likely to be comprised of multiple species and so development of future biofilm disinfection standards should therefore consider the effects of multiple species.

5.6 Chapter conclusions

Testing of Formulation TCM+S against an extended panel of challenge organisms provided valuable insights into its strengths and limitations which must be addressed in future stages of development. Whilst yeasts, *M. smegmatis* and the MS2 bacteriophage were highly susceptible to the formulation, fungal conidia of *A. brasiliensis*, slow growing *Mycobacterium spp*. and *B. subtilis* endospores of were highly resistant to disinfection. Whilst the formulation performed moderately well against some bacterial biofilms, its weakness against biofilms of *E. coli* was of some concern.

Resistance to the formulation appeared to occur through several separate mechanisms. Melanin was determined to offer a high degree of protection to fungal conidia, most likely due to its negative charge and antioxidant properties. In the case of mycobacteria, cell wall impermeability and porins were proposed to determine susceptibility to the formulation and lipophilic photosensitisers were less effective than TBO; this indicated that uptake of the photosensitiser through hydrophilic routes is necessary for mycobactericidal activity. Endospore resistance to the formulation was facilitated through mechanisms including impermeability of the outer coat and protection of nucleic acids by small acid soluble proteins (SASPs). Pre-treatment of spores with hydrogen peroxide did not improve sporicidal activity. Overcoming these mechanisms of resistance will require substantial improvements to the formulation and disinfection parameters.

Chapter 6.

Assessment of Technological Scalability

6.1 Introduction

As outlined in Chapter 1, this project aimed to develop a photosensitiser-based formulation suitable for disinfecting medical surfaces such as those of AERs. In addition to performing microbiological research, commercialisation necessitates exploring and addressing other concerns including regulatory requirements, production costs, consideration of environmental impacts and how easily the product can be utilised in a real-world setting.

6.1.1 Regulatory requirements

Novel biocides must fulfil specific regulatory requirements to be sold. Under the European Union Biocides Regulation 528/2012 (EU BPR) and Review Regulation 1062/2014, "active substances" must be registered with the European Chemicals Agency (ECHA) in order to be used in biocides sold within the EU (European Parliament & Council of the European Union, 2012). Article 3 of the EU BPR defines an active substance as "a substance or a micro-organism that has an action on or against harmful organisms". The legislaton further defines a biocidal product as:

> "Any substance or mixture, in the form in which it is supplied to the user, consisting of, containing or generating one or more active substances, with the intention of destroying, deterring, rendering harmless, preventing the action of, or otherwise exerting a controlling effect on, any harmful organism by any means other than mere physical or mechanical action."

Under these definitions, active substances generated *in situ* are covered by this legislation. For example, active chlorine generated from sodium chloride by electrolysis and free radicals generated *in situ* from ambient air or water are contained within the Article 95 list of active substances (European Chemicals Agency, 2019a). In the case of Formulation TCM+S (40 μM TBO, 10 mM MGDA, 15 mM sodium hydrogen carbonate, 10 mM sodium carbonate, 0.01% Plurafac LF 901, 0.01% Praepagen TQ; pH 10.2), the active substance could be described as "singlet oxygen generated from a photosensitiser by photoexcitation". Currently, singlet oxygen is not listed within the Article 95 list of active substances and so is unable to be sold as a biocide within the European Union.

The process of registering an active substance with the ECHA requires the applying body to submit evidence of efficacy to a national regulatory body such as the UK's Health and Safety Executive. Included in this application should be a dossier which addresses several endpoints, including the active substance chemistry, its efficacy against microorganisms, human health impacts and environmental data (Health and Safety Executive, 2019). In addition to registering the active substance with the ECHA, individual products containing

the active must also be registered. It is been estimated that the total cost of bringing a novel product to market exceeds £1 million (Gander, 2016).

6.1.2 Chemical safety

Biocidal products which are effective against microorganisms can be hazardous to human health. Under the 2002 Control of Substances Hazardous to Health (COSHH) regulations, employers must take reasonable steps to prevent employees from being injured as a result of exposure to hazardous substances. Whilst this can be achieved through the use of personal protective equipment such as gloves and safety glasses, UK guidelines suggest it desirable to seek less toxic alternatives where possible (Health and Safety Executive, 2013). Separate to these requirements, developing safer alternatives to traditional disinfectants can be useful for product marketing. For example, the United States Environmental Protection Agency (EPA) produces the Safer Choice Standard, which allows a product to carry a label certifying it is a "safer choice", which can affect consumer purchasing choices (Environmental Protection Agency, 2009).

In addition to UK guidelines, Article 5 of the EU BPR outlines specific exclusion criteria which would result in a rejected application for an active substance to be added to the ECHA's Article 95 list. These include: having endocrine disrupting properties or having persistent, bioaccumulative and toxic (PBT) properties or being a known (category 1A) or presumed (category 1B) human carcinogen, mutagen or reproductive toxin (European Parliament & Council of the European Union, 2012). Suspected (category 2) carcinogens, mutagens and reproductive toxins are not included within these exclusion criteria.

6.1.2.1 Cytotoxicity, irritancy and corrosiveness

A common route of chemical exposure is dermal contact as a result of splashes and spills. The health risks associated with dermal contact can be acute, in the case of irritating or corrosive substances, or chronic, such as in the case of substances which induce hypersensitivity reactions. Numerous models exist to assess the irritation potential of chemical exposure. More simplistic tests determine whether a substance is cytotoxic and affects the viability of a monolayer of epithelial cells following exposure. For example, in their investigations of the antimicrobial ebselen, Thangamani et al. (2015) utilised an in-house protocol to observe whether a 24-hour exposure to the compound affected HaCAT cell viability. Standardised tests for topical safety also exist. OECD Test No. 491 assesses the potential of substances to cause eye damage by exposing a monolayer of Statens Seruminstitut Rabbit Cornea (SIRC) cells to a substance for 5 minutes and assessing whether this leads to a change in cell viability using the colorimetric MTT assay (OECD, 2018).

Whilst these methods are rapid, relatively low cost and effective for ruling out cytotoxicity, they are limited in their ability to model dermal exposure. Histologically, the dermis consists of several distinct layers, or strata. The outermost layer of the stratum corneum consists of non-viable, flattened keratinised cells (corneocytes) which overlap to form a tightly packed stratified epithelium. The stratum corneum is coated in an acidic mantle containing lipids such as squalene; together these form a non-porous barrier which prevents water loss from the epidermis whilst protecting underlying layers of the epithelium from toxic agents (Elias & Feingold, 2006). The stratum corneum is continuously shed via the process of desquamation and so it must constantly be regenerated through the maturation of viable cells, which are located in the lower layers of the stratum granulosum, stratum spinosum and stratum basale. Tests such as the OECD Test No. 491 are limited in their applicability to dermal exposure since the protective effects of the stratum corneum and mantle are not taken into consideration.

Numerous animal models can be used to determine irritancy and corrosivity by assessing effects on cell viability, such as OECD Test No. 404 (OECD, 2015). Compounds which induce dermal hypersensitivity can also be detected using rodents, in accordance with OECD Test. No. 406 (Buehler test) (OECD, 1992b), though a negative result in the Buehler test does not rule out sensitising properties (Scientific Committee on Consumer Products, 2005). In the case of irritants and corrosive compounds, *in vitro* options are also available. OECD Test No. 439 and Test No. 431 both utilise advanced dermal models such as reconstructed human epidermis (RHE) to assess damage (OECD, 2019a; OECD, 2019b) and offer a less expensive and more ethically sound alternative to animal testing.

Volatile disinfectants can pose occupational exposure risks to the respiratory system due to the evaporation of biocide residues into the air. Breathing peracetic acid vapour can cause severe irritation to the nose, throat and lungs and cause breathing difficulties whilst long-term exposure to glutaraldehyde vapours can cause occupational asthma in humans and the development of non-neoplastic lesions in the respiratory tract of animal models (Di Stefano et al., 1998; van Birgelen et al., 2000). Odour is a hallmark sign of product volatility and the volatility of compounds from an aqueous solution is dependent on factors including product concentration, vapour pressure and water solubility (Seuvre & Voilley, 2017). As the components of Formulation TCM+S are highly water soluble and the formulation is non-odorous, it was posited that the risks posed to the respiratory system are low relative to those of other disinfectants. Consequently, this aspect of chemical exposure risk was not addressed in this chapter.

6.1.2.2 Genotoxicity

Genotoxic substances induce genetic damage which can lead to the development of cancers (carcinogenesis) or damage reproductive health. Carcinogenicity can be investigated in vivo using models such as the Syrian golden hamster cheek pouch (Gimenez-Conti & Slaga, 1993; Vitale-Cross et al., 2009), as well as a range of in vivo methods. The Ames test is a popular method for screening compounds for mutagenicity by studying populations of Salmonella typhimurium with genetic impairments histidine biosynthesis (Zeiger & Mortelmans, 1999). Normal growth of these populations requires supplementation of growth media with histidine and so they will not grow on minimal media lacking this amino acid. However, exposure to mutagenic agents promotes reversion to genotypes which are capable of synthesising their own histidine and thus allow growth on minimal media. Whilst fast and convenient, this test can create false positives. Compounds which are mutagenic to prokaryotes may not be carcinogenic to mammalian cells due to differences in cell permeability and superior gene repair mechanisms in eukaryotes. Indeed, the International Commission for Protection against Environmental Mutagens and Carcinogens has long recognised that as many at 50% of compounds identified as clastogenic by *in vitro* methods fail to demonstrate the same properties when tested *in vivo* (Scott et al., 1991).

6.1.3 Environmental safety

6.1.3.1 Regulatory Requirements

Article 8 of the Biocidal Products Regulations requires that dossiers for registering a new active product should include a risk assessment of the environmental impacts posed by the new product (European Parliament & Council of the European Union, 2012). This should account for the specific hazards posed by the product, the dose/concentration required to elicit a hazardous response, an exposure assessment of the fate of an active substance in the environment and a risk characterisation on the likelihood of hazards occurring as a result of a release of the substance into an environmental compartment (European Chemicals Agency, 2017). Under these criteria, a product which is toxic to aquatic life at low concentrations, accumulates in the environment over time and is likely to be released under normal parameters would be regarded unfavourably. Conversely, a product which poses few hazards, readily degrades and enters the environment via a wastewater treatment plant, where it is detoxified, would pose a low environmental risk.

Formulation TCM+S was developed for use in automated endoscope reprocessors. Guidance suggests that liquid waste from AERs should be discharged directly into the wastewater system (British Society for Gastroenterology, 2016). In the European Union, urban wastewater must be treated in several stages to reduce the risks of discharging hazardous substances into the environment (Council Directive 91/271/EEC, 1991). In most wastewater treatment plants, primary treatment removes solid waste by sedimentation whilst secondary treatment results in the aerobic degradation of dissolved or suspended organic components by microorganisms in aeration tanks (Das et al., 2017). The sewage sludge produced as a by-product of treatment should then be recycled for agricultural use by anaerobic digestion (Council Directive 91/271/EEC, 1991). As it is likely to be discharged into wastewater systems following use in an AER, environmental compartments most likely to be affected by Formulation TCM+S include microorganisms in the aeration tanks of treatment plants, aquatic ecosystems, including sediments, and terrestrial ecosystems. The effect of formulation components in these environmental compartments will be the focus of the environmental review of the formulation.

6.1.3.2 Commercial benefits to environmentalism

In addition to regulatory requirements, developing environmentally such products can afford commercial advantages to manufacturers. As social awareness of the environmental impacts of human activities grows, products with favourable ecological profiles can gain an edge in marketability. Whilst companies can be accused of greenwashing when marketting products as environmentally friendly, several schemes allow manufacturers to substantiate such claims with scientific data.

The United States Environmental Protection Agency (EPA) operates the Safer Products labelling scheme so that consumers can identify products which pose a low-risk to health and the environment. The EPA maintains a list of trusted chemicals which are registered for use under this scheme, which can be consulted to verify whether a formulation component is suitably safe in the environment. Similar to the Safer Products scheme, manufacturers of products sold within the EU can apply to use the EU Ecolabel on the product packaging. Whilst Ecolabel requirements do not yet exist for disinfectant products, guidelines do exist for sanitary hard-surface cleaners (Commission Decision 2017/1217, 2017). The criteria used to assess hard-surface cleaners can be useful as a surrogate methodology for determining whether Formulation TCM+S is environmentally friendly. Relevant assessment criteria include: toxicity to aquatic organisms, biodegradability and the presence of excluded and restricted substances (Commission Decision 2017/1217, 2017). Examination of the

database of excluded substances will be useful in determining whether Formulation TCM+S may be suitable for future recognition if disinfectant products are added to the scheme.

6.1.4.2 Biodegradability

Biodegradability is a crucial factor in the environmental hazards posed by chemical substances. Biodegradation prevents accumulation of environmental pollutants by breaking them down into less hazardous compounds, such as CO_2 and water. The OECD Test No. 301 is a six-panel standardised test which can be used to assess whether a product is readily biodegradable. Test substances are exposed to a microbial inoculum under different conditions of oxygenation. Parameters such as oxygen consumption, CO_2 production and the dissolved organic content are measured over a 28-day period to monitor the extent of test substance biodegradation (OECD, 1992a). The six sub-methods of OECD Test. No. 301 are included in table 6.1. Chemicals used in EU Ecolabel-compliant products must be readily biodegradable under aerobic conditions and biodegradable under anaerobic conditions (Commission Decision 2017/1217, 2017).

Table 6.1: OECD Test No. 301 sub-methods. Adapted from OECD (1992a).

Sub-methods	Measurement parameter	Analytical method
301 A: DOC die away	DOC	DOC analyser
301 B: CO_2 evolution	CO_2 production	Respirometry
301 C: MITI (I)	Oxygen consumption Intermediate formation	Respirometry Substrate-specific chemical analysis
301 D: Closed bottle test	Dissolved oxygen	Respirometry
301 E: Modified OECD test	DOC	DOC analyser
301 F: Manometric respirometry	Oxygen consumption	Respirometry

DOC: Dissolved organic carbon; MITI: Ministry of International Trade and Industry, Japan

6.1.4 Requirements of an AER self-disinfection cycle

Modern AERs have the capacity to self-disinfect to maintain hygiene and to address contamination issues such as colonisation due to a failure in water purification. The requirements of a self-disinfection cycle are outlined in section 4.8 of the ISO 15883 standard (British Standards Institution, 2018). ISO 15883 states that a self-disinfection cycle should be capable of disinfecting all parts of the machine which come into contact with water and solutions used in the endoscope disinfection cycle; this includes the basin,

channels, connectors and tank. Self-disinfection should also be achieved using a different high-level disinfectant to that which is used to disinfect endoscopes or using different parameters to what is used for endoscopes. For example, using a significantly increased contact time is considered sufficient in fulfilling this requirement (British Standards Institution, 2018). In endoscopy units, self-disinfection cycles are typically completed once-daily and are programmed to run during the night to minimise downtime; a cycle lasts an hour and machines stagger their start times so that several machines are always available (Personal communication; Dr J Turner, Consultant Gastroenterologist at University Hospital Llandough). By performing AER disinfection only once daily, there is an opportunity for biofilms to develop within the machine and lead to disinfection failure. Performing more regular self-disinfection cycles may reduce this risk.

6.1.5 Soluscope Serie 4 AER

Soluscope is a subsidiary company of Laboratoires Anios which designs and manufactures automated endoscope reprocessors. Their latest development is the Serie 4 Washer Disinfector, which is yet to be released on the market. Unlike previous AERs in the series, the Serie 4 integrates a high-pressure showerhead to facilitate mechanical removal of soil and biofilms from endoscopes and the AER basin. Laboratoires Anios have expressed an interest in using Formulation TCM+S for rapid disinfection cycles into future version of the Serie 4 design. Rather than running a self-disinfection only once per day, Laboratoires Anios have expressed interest in developing the means for rapid self-disinfection cycles following the reprocessing of each endoscope. This would improve machine hygiene and prevent biofilm build up over the course of the day.

6.1.6 Commercial viability

The cost of producing a biocide product can have a strong impact on its commercial viability. The global disinfection market is highly competitive, and a large variety of comparable products are available from competing manufacturers. A biocide should offer value-for-money to purchasers whilst also providing appropriate profit margins to manufacturers. In competitive markets, firms can gain market share by offering products at a low price compared to competitors or by pursuing quality and offering unique product benefits (Dransfield & Needham, 2005). With appropriate marketing support, a product which offers similar performance to existing products at a fraction of the cost can disrupt the market and attain market share (Dransfield & Needham, 2005). Performance factors relevant to the disinfection market include product efficacy, safety and price. As efficacy and safety have already been addressed in this thesis, it is important to calculate the manufacturing costs of Formulation TCM+S and compare this to competing products. In endoscopy, the

major competitor products include peracetic acid, hydrogen peroxide and glutaraldehyde (Centers for Disease Prevention and Control, 2008).

6.2 Chapter Aims and Objectives

This chapter sought to address some of the major considerations for bringing a photosensitiser-based biocidal product to market. The toxicological and environmental properties of Formulation TCM+S (40 μM TBO, 10 mM MGDA, 15 mM sodium hydrogen carbonate, 10 mM sodium carbonate, 0.01% Plurafac LF 901, 0.01% Praepagen TQ; pH 10.2) were considered, as well as its production costs and design considerations of an AER which utilises this formulation.

6.3 Methods

6.3.1 Chemical safety evaluation by literature view and database search

An evaluation of the chemical safety of Formulation TCM+S was conducted by reviewing published data on the ecological and toxicological properties of each of the components. The Chemical Abstract Service (CAS) numbers associated with each component (table 6.2) were used to search numerous databases maintained by chemical safety authorities (table 6.3). As the chemical composition of surfactants are proprietary information (trade secrets) their ecotoxicological properties were assessed using information provided by the manufacturers. To supplement the information from database searching, a literature review was also performed.

Table 6.2: CAS numbers of Formulation TCM+S components

Component	Chemical class	IUPAC* name	CAS number
Toluidine blue O	Phenothiazine dye	(7-amino-8-methylphenothiazin-3-ylidene)-dimethylammonium chloride	92-31-9
MGDA	Chelator	Trisodium;2-[bis(carboxylate-methyl)amino]propanoate	164462-16-2
Sodium carbonate	Inorganic salt	Sodium carbonate	497-19-8
Sodium hydrogen carbonate	Inorganic salt	Sodium hydrogen carbonate	144-55-8
Plurafac LF 901	Fatty alcohol alkoxylate	Formula unknown	-
Praepagen TQ	Triethanolamine esterquat:	C16-C18-dialkanoyloxyethyl-hydroxyethyl-methyl-ammonium methyl sulphate	91995-81-2

*IUPAC: International Union of Pure and Applied Chemistry

Table 6.3: Databases searched to identify chemical and environmental hazards

Database Name	Description
European Chemicals Agency (ECHA)	Lists active substances and suppliers of biocides registered for use within the European Union. Allows searching by CAS number.
Human and Environmental Risk Assessment (HERA) Project	Voluntary European initiative founded by the International Association for Soaps, Detergents and Maintenance Products (AISE) and the European Chemical Industry Council (Cefic). Produces risk assessments for ingredients used in household cleaning products.
Proposition 65 list	List maintained by California Office of Environmental Health Hazard Assessment. Lists synthetic and natural chemicals known to cause carcinogenesis, birth defects and other reproductive harms. Products containing these chemicals must be labelled as such to be sold in the state of California.
United States Environmental Protection Agency Safer Chemicals List (SCLI)	Electronically updated list of substances which qualify as “Safer Chemicals”. Substances can be searched by CAS number.

6.3.2 Determination of formulation cytotoxicity

The cytotoxicity of Formulation TCM+S and its constituent components was investigated experimentally by measuring changes in the viability of human keratinocytes cells using a cell viability stain, following exposure to these compounds.

6.3.2.1 Cell line and storage conditions

HaCaTs are an immortalised keratinocyte cell line which is popularly used to model the effect of biocides on the skin. HaCaT cells were obtained from the ATCC and were stored in vapour phase liquid nitrogen until use.

6.3.2.2 Media, diluents and incubation conditions

HaCaT cells were cultured in EMEM-FBS-PS media consisting of Eagle's Minimum Essential Medium ATCC 30-2003 (EMEM; ATCC), supplemented with 10% foetal bovine serum (FBS; Gibco) and 1% penicillin/streptomycin (PS; Gibco). All media components were certified for tissue culture use. Phosphate buffered saline (PBS) was used as a diluent and was prepared by dissolving PBS tablets (Sigma) in deionised water and sterilising by autoclave (Chapter 3; section 2.1.4). Cells were cultured in sterile, non-pyrogenic 25 cm^2 tissue culture flasks (Conning) containing 8 mL of media. Cells were cultured in a dedicated tissue culture incubator which was maintained at 37^oC and 5% CO_2.

6.3.2.3 Formulations

A selection of formulations were prepared, as described in table 6.4, using sterile deionised water as a diluent. To examine the effect of electrolyte balance on formulation biocompatibility, a variation of Formulation TCM+S was also prepared with the addition of 0.9% saline; which is physiologically isotonic. To compare cytotoxicity with other disinfectants, peracetic acid and hydrogen peroxide were prepared at their standard use concentrations of 0.2% and 3% respectively. For an additional comparison, a competitor product was also tested to determine its effects on cell viability. This formulation is pH neutral, dermatologically tested and marketed as skin friendly (Gama Healthcare, 2019). To extract the formulation, a single prewetted wipe was aseptically placed inside a sterile syringe barrel using sterile forceps. The plunger was then pressed to squeeze the formulation out of the wipe and into a sterile 7 mL bijou tube.

Table 6.4: Contents of formulations prepared for cytotoxicity testing

Formulation	Contents	Notes
Saline	0.9% w/v NaCl	Isotonic medium to assess total viability
Water	Sterile deionised water	Hypotonic medium to determine effect of osmotic pressure on cell viability
TBO	40 μM TBO	Photosensitiser in hypotonic medium
Formulation 1 (TCM+S)	40 μM TBO; 10 mM MGDA; 15 mM Na2CO3; 10 mM NaHCO3; 0.01% v/v Plurafac LF 901; 0.01% v/v Praepagen TQ; pH 10.2	Optimised photosensitiser formulation containing co-actives and excipients
Formulation 2 (TCM+S with saline)	40 μM TBO; 10 mM MGDA; 15 mM Na2CO3; 10 mM NaHCO3; 0.01% v/v Plurafac LF 901; 0.01% v/v Praepagen TQ; 0.9% w/v NaCl; pH 10.2	Saline added to reduce damage hypotonic osmotic pressure
Hydrogen peroxide	Hydrogen peroxide 3%	Commonly used high-level disinfectant
Peracetic acid	Peracetic acid 0.2%	Commonly used high-level disinfectant
Skin-safe competitor product	Benzalkonium chloride ≤ 0.5%; didecyl dimethyl ammonium chloride ≤ 0.5%; polyhexamethylene biguanide ≤ 0.1%*	Dermatologically tested mid-level disinfect; marketed as "skin-safe".

*Contents based on declarable components listed on safety data sheet.

6.3.2.4 Passage of cells

After revival, cell lines were maintained using 48-hour passages. To passage cells, spent media was gently poured out of the flask and cells were washed twice with sterile PBS. After removing the final wash of PBS, 2 mL of Trypsin-EDTA (0.25% Trypsin / 0.53 mM EDTA) in Hank's balanced salt solution (HBBS) was added to each flask to detach the cell monolayer. After incubating at 37°C/5% CO_2 for 10 minutes, flasks were agitated by tapping to detach cells. Detachment was confirmed by examination under a Ceti TC inverted light

microscope (Medline Scientific) and by observing turbidity in the media. 6 mL of EMEM-FBS-PS media was then added to each flask to quench trypsin activity and to provide new nutrients for cell growth. Two 2 mL aliquots of cell suspension were then transferred to two fresh tissue culture flasks and each was topped up with 6 mL of EMEM-FBS-PS media. Flasks were then placed in the incubator to begin the next 48-hour passage.

6.3.2.5 Quantification of cells

Cell density was determined through trypan blue staining and microscopy (Abcam, 2019). Trypan blue is excluded from live cells and so cells appear as bright white objects on a blue field. Following 48 hours of incubation, tissue culture flasks were examined by microscopy to confirm the monolayer had reached 80% confluency. Cells were then washed twice with PBS and detached by the addition of 2mL Trypsin-EDTA and the resulting cell suspension diluted with 6 mL EMEM-FBS-PS media (section 6.3.2.4). 100 µL of cell suspension was transferred to a microcentrifuge tube containing 400 µL of 0.4% trypan blue (Sigma Aldrich) to obtain a 1:4 dilution and incubated for 1 minute. After gentle mixing, 10 µL of stained suspension was transferred to a haemocytometer and cover slip. Live cells were counted in each of the four 16-square quadrants; cells were only counted when within squares or on the right-hand or bottom boundary lines. The average cell count of the four quadrants was calculated, multiplied by 5 to correct for the 1:4 staining procedure and then multiplied by 10^4 to account for the dilution factor. Using this method, it was determined that tissue culture flasks at 80% confluency contained a total of 3 x 10^6 cells.

6.3.2.6 Exposure to formulations and constituents

Exposure to biocides formulations followed an adaption of the protocol reported by Thangamani et al. (2015). Following 48 hours of incubation, cells were washed twice with PBS and detached by the addition of 2 mL Trypsin-EDTA to detach cells (section 6.3.2.4). The resulting cell suspension was diluted with 28 mL EMEM-FBS-PS media to yield a cell suspension of 1×10^5 cells/mL. 100 µL aliquots of this suspension were then used to seed wells of a sterile 96-well microtiter plate with 10,000 cells per well. After incubating for 18 hours (37ºC; 5% CO_2), media was removed from each well and cells were washed twice with sterile PBS. 20 µL of various formulations and constituents (table 6.4) were added to cells and incubated for 15 minutes in a tissue culture incubator (37ºC/5% CO_2). The well contents were then removed, cells were washed three times with PBS to remove any residual formulation and stained to determine cell viability.

6.3.2.7 Viability staining

The viability of treated cells was determined using the CellTiter-Blue viability assay. In this assay, viable cells metabolise resazurin into resorufin, which emits fluorescence at 590 nm, and so fluorescence at 590 nm is proportional to cell viability. CellTiter-Blue was obtained from Promega and a master mix of stain was prepared by diluting 1-part CellTiter-Blue to 5-parts EMEM-FBS-PS. Following the treatment and washing of cells, 100 µL of viability stain was added to each well and placed in an incubator for 2 hours. 100 µL of stain was also added to an empty well as a blank control. Following incubation, plates were placed in a Tecan F1000 spectrophotometer and the 590 nm fluorescence of each well was measured, using an excitation wavelength of 570 nm. The fluorescence of the blank control well was subtracted from the other wells to yield fluorescence values.

6.3.3 Estimated formulation production costs

The production costs of the formulation were calculated under the guidance of Gaétan Rauwel (Director of Research and Development), and Jean-Noël Bertho (Formulation Manager) at Laboratoires Anios. Laboratoires Anios is a French disinfection specialist which produces a range of disinfectants, including peracetic acid (5%) and glutaraldehyde (20%).

To estimate the batch production cost of Formulation TCM+S, the quantity of each component required to produce a 5-tonne batch was calculated. The raw materials cost per batch was then calculated using wholesale prices provided by Laboratoires Anios, which was then used to calculate the cost per kg. The calculation assumed production at use-concentration, rather than as a concentrate.

6.3.4 Calculation of required light output for case study devices

6.3.4.1 Case study schematics

The Serie 4 Endoscope Washer Disinfector from Soluscope was used as case study device. Schematics for the Serie 4 were kindly provided by Gaétan Rauwel, Director of Research and Development at Laboratoires Anios.

6.3.4.2 Inverse square law equation

The power requirements of the light excitation source for the two devices were calculated using the inverse-square law equation. This law dictates that the intensity of radiation from a point source is inversely proportional to the square of distance. As distance from the source doubles, irradiance decreases by a factor of 4. Likewise, a 5-times increase in distance would decrease irradiance by a factor of 25.

6.3.4.2 Calculation of indirect light path length

In accordance with the law of reflection, light is reflected from a surface at the same angle of incidence (Katz, 1994). The pathway of first order indirect light (i.e. light which is reflected from a surface once) thus represents two equal sides of an isosceles triangle. An isosceles triangle can be expressed as two symmetric right-angle triangles and so Pythagorus theorem ($A^2+B^2=C^2$) can be used to calculate the length of the hypotenuse of each of these triangles. This yields the length of indirect light paths.

6.3.4.4 Calculation assumptions

To achieve sufficient photoactivation of the formulation, it was first assumed that surfaces of an AER should receive a similar dose of light over the same period of time as was used in the experiments described in this thesis. Accordingly, increasing the distance between the light source and illuminated AER surface would require a proportional increase in light output. The second assumption for this calculation was that the most simple method for illuminating the AER basin would be to place the light source on a single facet of the basin, such as the ceiling. This configuration would require the minimum amount of redesign to accommodate the light source and associated heat dissipation system. To calculate an absolute maximum lighting requirement, the addititive effect of indirect illumination of surfaces was not taken into account. To approximate the potential contribution of indirect illumination, the minimum and maximum contributory effect was calculated relative to the direct path. The reflectance of the grey PVC used in the Serie 4 basin is unknown. However, white PVC reflects up to 90% of 630 nm light whilst black PVC reflects less than 10% (Masoumi et al., 2012); 50% reflectance was therefore selected for the purposes of this calculation.

6.3.4.5 Known values

At a distance of 55 mm from the light source, irradiance was measured as 5 mW/cm^2. In the Serie 4 basin, the widest distance between the top and bottom facets of the basin measures 388 mm (fig. 6.1). In the schematic, this same point is 83.5 mm from the left wall of the basin and 336.5 mm from the right. Indirect light paths due to light reflected from the walls of the basin thus measure between 442.3 mm (shortest path) to 776.9 mm (longest path).

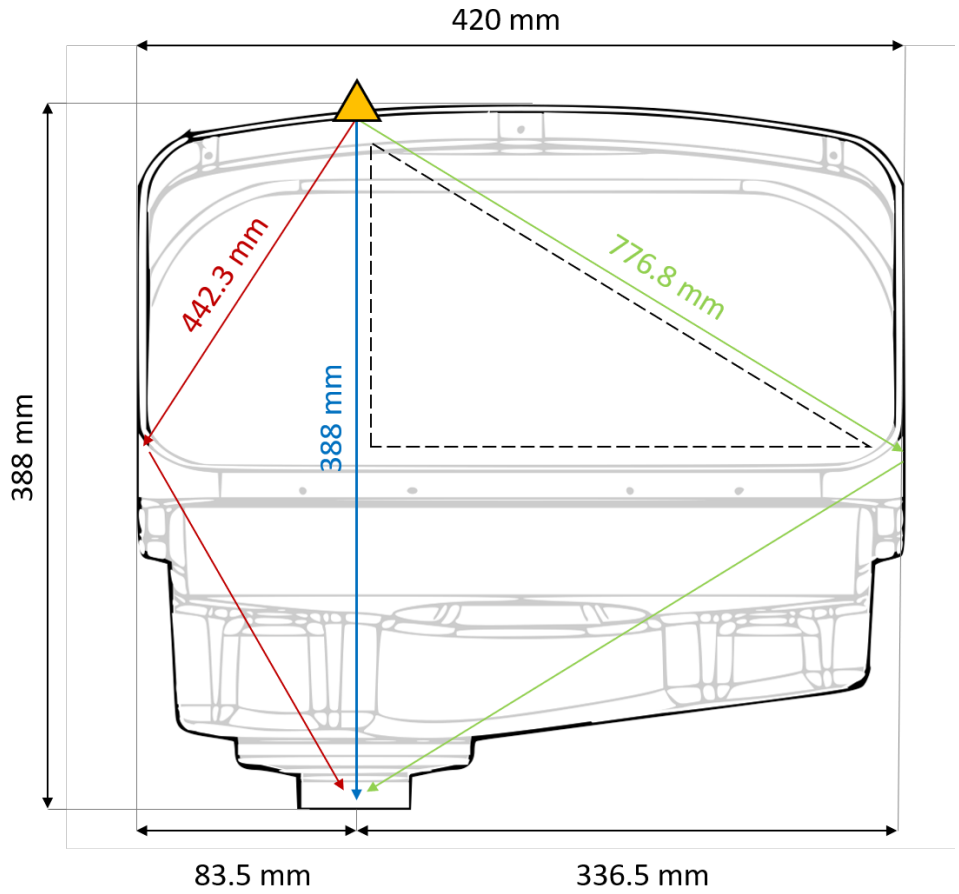

Figure 6.1: Schematic frontal view of the Soluscope Serie 4 Washer-Disinfector basin. A theoretical LED light source is indicated by a yellow triangle. A direct light path to the far side of the basin. A direct light path (blue line) from the apex of the basin to its lowest point measures 388 mm. First-order indirect light paths to the same point comprise a minimum distance of 442.3 mm (red line) and a maximum distance of 776.9 mm (green line). A right-angle triangle, used to calculate the length of indirect light paths, is represented by a dashed line. Note that there is a loss in light intensity transmitted from reflected surfaces due to partial absorbance by the PVC.

6.4 Results

6.4.1 Hazards identified through ECHA database search

Several hazards relating to components of Formulation TCM+S were identified through the ECHA database (table 6.5). None of the components were included in the Proposition 65 list of known carcinogens. In the case of the two surfactant components, it was not possible to find information through database searching.

Table 6.5: Potential hazards identified by ECHA database search

Component	Identified Hazards
Toluidine blue O	Harmful if swallowed
MGDA	Corrosive to metals
Sodium carbonate	Causes severe eye irritation
Sodium hydrogen carbonate	No hazards identified
Alkoxylated fatty alcohol*	No hazards identified
TEA Esterquat**	Causes dermal and eye irritation

*Same class as Plurafac LF 901; **Same class as Praepagen TQ

6.4.2 Cell cytotoxicity

Exposure of HaCAT cells to Formulation TCM+S caused a large decrease in cell viability compared to saline (P <0.0001; ANOVA, Tukey), as indicated by resorufin fluorescence (fig. 6.2). Exposure to water lead to a statistically significant change in cell viability compared to saline (P >0.05 ANOVA, Tukey), though cells remained largely viable. The skin-safe competitor formulation, 3% hydrogen peroxide and 0.2% peracetic acid all led to large decreases in viability compared to both controls (P <0.001; ANOVA, Tukey). There were no differences in viability between Formulation TCM+S or the other disinfectants tested (P >0.05; ANOVA, Tukey). The addition of saline to Formulation TCM+S led to a slight increase in cell viability compared to the competitor product, peroxide and peracetic acid (P <0.05; ANOVA, Tukey), though this was significantly below the saline and water controls (P <0.0001; ANOVA, Tukey).

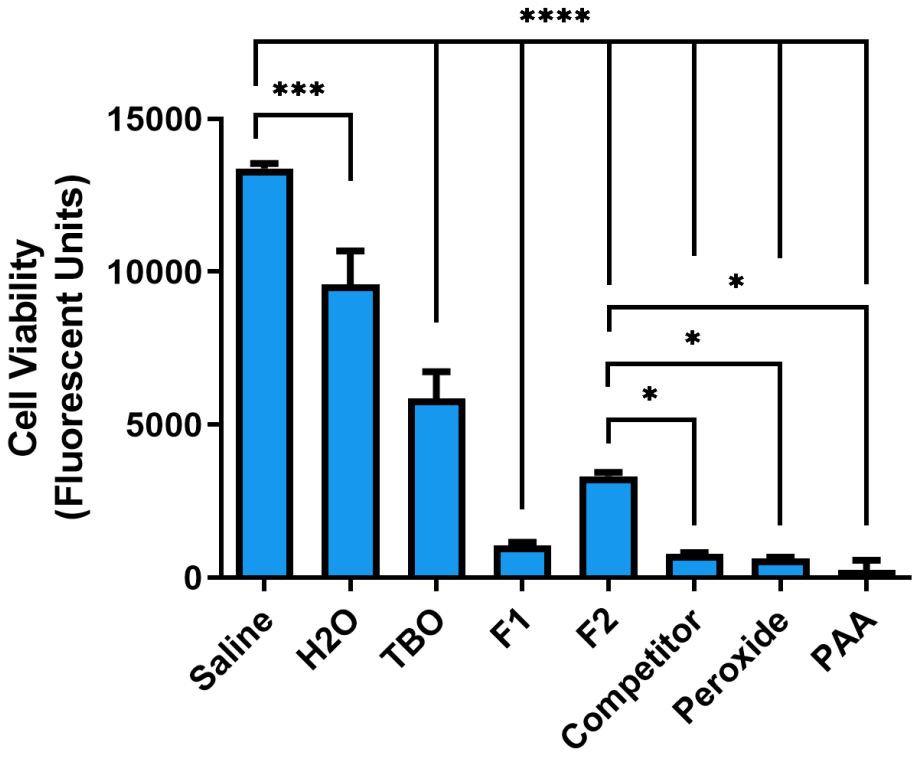

Figure 6.2: Cytotoxicity of a range of formulations and disinfectants against HaCAT cells, as determined by the CellTiter-Blue resazurin-resorufin assay. H20 = Water; F1 = Formulation TCM+S; F2 = Formulation TCM+S supplemented with saline; Competitor = skin-safe competitor product; peroxide = 3% hydrogen peroxide; PAA = 0.2% peracetic acid. * P <0.05; *** P <0.001; **** P <0.0001.

6.4.3 Raw materials production costs

Laboratoires Anios produce disinfectants in 5 tonne batches. Peracetic acid (PAA; 5%) and glutaraldehyde (GTA; 20%) are produced at raw materials costs of 0.7 €/kg and 1.4 €/kg respectively (Personal communication; Gaétan Rauwel, Director of Research and Development at Laboratoires Anios; 10/10/2019). This is equivalent to a batch cost of €3500 (PAA) and €7500 (GTA).

Toluidine blue O was not available to purchase at wholesale cost. To minimise the presence of chemical impurities, TBO should be purchased at a high purity grade. As of October 2019, this can be purchased from VWR (cat no: 0672-50G) at a cost of £136.40 per 50 g, which is equivalent to a cost of £2728 per kilogram. Converted into Euros at an exchange rate of 1 GBP to 1.11 EUR, this is equal to €3025.

Plurafac LF 901 has a density of 1.01 (BASF, 2019a) though the density of Praepagen TQ is non-disclosed. For the purposes of the calculation, 1 L of each surfactant was assumed to be equivalent to 1 kg.

Water is a negligible contributor to the raw material costs. 1 cubic meter of water (1000 kg), costs less than €3. The mass of water required to produce a 5-tonne batch was calculated by subtracting the total mass of all other components from 5000 kg.

Using wholesale costs provided by Laboratoires Anios, the raw materials costs of Formulation TCM+S were determined (table 6.6). This yielded a final cost of 0.08 €/kg and a batch cost of €401.52.

Table 6.6: Raw materials cost to produce 5-tonne batch of Formulation TCM+S.

Component	Molar mass	Concentration	Mass for 5000 L (kg)	Wholesale cost per kilo (€)	Cost for 5000 L (€)
TBO	270.37	40 µM	0.05	3025	151.25
MGDA	271.11	10 mM	3.56	1.30	4.63
Sodium carbonate	105.99	10 mM	5.30	0.40	2.12
Sodium hydrogen carbonate	84.007	15 mM	6.30	0.40	2.52
Plurafac LF 901	-	0.01% v/v	50.00	2.50	125
Praepagen TQ	-	0.01% v/v	50.00	2.20	110
Water	-	-	4885.00	0.003	15
Total batch cost (€)					410.52
Cost per litre (€)					0.082

6.4.4 Light power calculations

6.4.4.1 Maximum light power requirements for AER basin

In the experiments described in previous chapters, bacteria-loaded surface carriers and suspensions of microorganisms were treated at a distance of 55 mm from the LED light source; at this distance, light intensity was measured at 5 mW/cm (table 2.2). In a Serie 4 endoscope washer disinfector, there is a distance of 378 mm at the widest point between the top and bottom of the basin using a direct light path. This is a 7.05 times greater distance between the source and surface compared to the experiments described in this thesis. In accordance with the inverse square law, this would reduce lumination of the surface by a factor of 49.70. Sufficient illumination of the basin surfaces through a direct light path can thus be achieved in the same time by increasing the light output of the LED source by a factor of 49.70.

6.4.4.2 Calculation of secondary illumination by reflection from basin surfaces

Relative to direct illumination, indirect light reflected from AER basin surfaces was calculated to contribute an additional 1-11.5% illumination to the target surface of a Serie 4 Washer-Disinfector basin (table 6.7).

Table 6.7: Calculation of reflected light to target surface

	Illumination path		
	Direct	Shortest indirect**	Longest indirect**
Light power at 55 mm (%)	100	100	100
Distance to reflection surface (mm)	-	211	378
Doubling distance to reflection point	-	3.84	7.06
Relative power at reflection point (%)	-	6.78	2.01
Light transmitted from reflection point* (%)	-	3.39	1.00
Distance to target area (mm)	388	211	378
Doubling distance to target area	7.05	3.84	7.06
Light power at target site (%)	2.01	0.23	0.02
Relative illumination compared to direct path (%)	100.0	11.5	1.0

* Calculation assumes 50% reflection efficiency from grey PVC; ** indirect paths from a single reflection point.

6.5 Discussion

6.5.1 Toxicological profile

6.5.1.1 Toluidine blue O

Recent studies on the toxicological effects of TBO are sparse. The ECHA database notes that TBO may be harmful if ingested (European Chemicals Agency, 2019b). Data suggests that the quantity of TBO which would need to be ingested to achieve an acutely toxic response in humans are unrealistic from exposure to Formulation TCM+S. The lethal dose (LD_{50}) of TBO in sheep is 10 mg/kg (Cudd et al., 1990) whilst the toxic low dose (TLDo) in humans is reportedly as high as 43 mg/kg (Toxicology Data Network, 2019). Extrapolated to an average human mass of 60 kg, an individual could ingest 600-2400 mg of TBO without experiencing toxic effects. Since Formulation TCM+S contains 40 μM TBO, which is approximately equivalent to 11 mg/L, this would equate to more than 50 litres of the formulation.

Several preparations containing TBO are already licensed for direct use in humans (Sweetman, 2009). ORABLU is used to visualise oral lesions and contains TBO at a concentration of 0.5% w/v (Addent, 2019). This is equivalent to 16.5 mM and so contains 40 times more TBO than Formulation TCM+S. A TBO-based oromucosal gel for the photodynamic treatment of dental and soft tissue infections has also been approved for paediatric use in the EU (European Medicines Agency, 2017) which suggests that TBO is of acceptable toxicological tolerability to regulators.

Using the Ames test, Dunipace et al. (1992) observed that TBO exposure could induce mutagenesis in a prokaryote model. However, it is controversial whether mutagens identified through bacterial mutation assays exhibit the same properties in mammalian hosts. Bartsch (1976) contends that the predictive value of mutagenicity assays for identifying potential carcinogens is limited and that substances identified through the Ames test should not be assumed to be carcinogenic without accompanying animal studies. *In vivo* investigations using the hamster cheek pouch model have determined that TBO does not promote carcinogenesis in mammals, nor does it promote co-carcinogenesis with other compounds (Redman et al., 1992). The closely related phenothiazine, methylene blue, also promotes mutagenesis in prokaryotes without causing *in vivo* carcinogenesis (Wagner et al., 1995). Accordingly, TBO is not classified as a known or presumed human carcinogen and so would not be excluded from consideration as part of an active substance registration under Article 5 of the EU BPR.

Synthetic dyes can pose environmental hazards due to inherent toxicity and by blocking light transmission through contaminated water (Hassaan & El Nemr, 2017). Globally, large quantities of synthetic dyes are discharged into water systems due to their widespread use in the textile industry. The environmental fate of TBO is unclear from the literature review. However, TBO is capable of being biodegraded under aerobic and anaerobic conditions by microorganisms isolated from terrestrial and aquatic environments, including *Sphingomonas* and *Brevibacillus* species (Alhassani et al., 2007; Ali et al., 2014). This suggests that the TBO component of Formulation TCM+S would be degraded during both primary and secondary wastewater treatment processes. Furthermore, TBO autooxidises rapidly when exposed to visible light. It is therefore anticipated that the low quantity of TBO which would be discharged into the wastewater system following use would have negligible effects on the environment. UV/TiO_2-based technologies are gaining traction as a suitable tertiary wastewater treatment (Thiruvenkatachari, 2008) and are known to efficiently degrade synthetic dyes such as TBO and methylene blue (Houas et al., 2001; Zhang et al., 2019). Increased use of tertiary wastewater treatments such as these are likely to further reduce the potential hazards of TBO in the environment.

The EU Ecolabel scheme for hard surface cleaners requires that organic components which are not classed as “ready biodegradable” should be used at concentrations of less than 0.01% w/w (European Commission, 2017). A TBO concentration of 40 μM, as used in Formulation TCM+S, is three orders of magnitude beneath this threshold and so should be considered non-hazardous.

6.5.1.2 MGDA

Chelators can pose hazards to the environment. Despite its poor biodegradability, EDTA is utilised widely in many domestic and industrial products and enters wastewater in copious quantities. Poor removal from wastewater facilitates its entry into the environment, where it persists and aids in the mobilisation of metals which contaminate the food chain (Sillanpää, 1997; Soltan, 2006). EDTA has come under increased scrutiny and product developers have been urged to seek less persistent alternatives (Oviedo & Rodríguez, 2003). Accordingly, MGDA was selected for use as a chelator in Formulation TCM+S.

According to the manufacturer BASF, MGDA is readily biodegradable under all 6 test parameters of OECD Test No. 301 and is non-toxic to marine organisms at concentrations below 100 mg/L (BASF, 2019b). Whilst Formulation TCM+S contains MGDA at a concentration of 10 mM, which is equivalent to a content of approximately 2800 mg/L, discharge into the wastewater system would dilute the MGDA in the formulation to non-hazardous levels. In support of the product claims made by BASF, MGDA is included in the

United States Environmental Protection Agency Safer Chemical Ingredients List (SCLI), which verifies that it is of low concern based on experimental and model data (Environmental Protection Agency, 2019). Due to its chelating properties concentrated solutions of MGDA can be corrosive to metals (PubChem, 2019).

MGDA poses a low-risk to human health. Whilst public data is sparse, the manufacturer BASF claims that is does not cause mutagenesis in the Ames test, is non-irritating to the skin (OECD Test No 404) or eyes (OECD Test no. 405) of rabbits and does not cause skin sensitisation in the Guinea pigs maximisation test (BASF, 2019b). The favourable ecotoxicological profile of MGDA supports its inclusion in Formulation TCM+S.

6.5.1.3 pH buffering agents

The pH of Formulation TCM+S is 10.2. This is within the boundary requirements of pH ≥ 2 and ≤ 11.5 of section 4.2.2 of the EPA Safer Products standard (Environmental Protection Agency, 2015). The pH of Formulation TCM+S is modified and buffered by the inclusion of sodium hydrogen carbonate and sodium carbonate. Sodium hydrogen carbonate is non-hazardous according to ECHA and is commonly used in food products, where it is known as bicarbonate of soda. Whilst sodium carbonate can cause severe eye irritation in powdered form (European Chemicals Agency, 2019c) it is included on the EPA Safer Chemicals List (Environmental Protection Agency, 2019). HERA estimate that the concentration of sodium carbonate in laundry detergents was 3.0 g/L and that this concentration is non-irritating (HERA, 2005). In Formulation TCM+S, sodium carbonate is used at a concentration of 15 mM, which is equivalent to 1.6 g/L and so lower than that of laundry detergents. It is therefore reasonable to conclude that the sodium carbonate component of Formulation TCM+S poses little hazard to human health.

Sodium carbonate and sodium hydrogen carbonate pose low environmental risk. HERA have estimated that over 5 million tonnes of sodium carbonate are already used in cleaning products in the European Union and that is readily neutralised during wastewater treatment processes (HERA, 2005). Therefore, this choice of buffering agents was suitable for the objectives of this project.

6.5.1.4 Surfactants

In the absence of a CAS number for Plurafac LF 901, assessment of its ecotoxicological properties was based on a literature review on the broader family of compounds. BASF vaguely describes Plurafac LF 901 as a "fatty alcohol alkoxylate" (BASF, 2014). Alcohol alkoxylates include alcohol ethoxylates (AEs), as well as propoxylates and butoxylates. These compounds are classed as high production volume chemicals and comprise a large proportion of non-ionic surfactants used in Europe and North American (HERA, 2009a; Cowan-Ellsberry et al., 2014). The majority of published literature addresses AEs specifically and so this class was used as the basis for the ecotoxicological risk assessment.

HERA (2009a) determined that AEs pose a low-risk to the environment and human health. AEs are not mutagenic, genotoxic nor carcinogenic and do not induce skin sensitisation; they also have a low irritation potential when diluted to in-use concentrations (HERA, 2009a). Oral administration of AEs to rats in doses up to 500 mg/kg body weight per day for 14 days reportedly led to no observable toxicological effects other than mild gastric irritation whilst marine organisms tolerate AE concentrations in excess of 100 mg/L (HERA 2009a). AEs are readily degraded in the environment by aerobic microbial metabolism (Nielsen et al., 2002) and are also efficiently metabolised and eliminated by fish (Newsome et al., 1995). Plurafac LF 901 is certified as compliant with the EU Ecolabel scheme (BASF, 2019a) and a large number of alcohol alkoxylates of variable carbon chain lengths are included in the EPA Safer Chemicals List (Environmental Protection Agency, 2019).

The cationic surfactant, Praepagen TQ, is a triethanolamine quat (TEAQ) which exhibits an acceptable ecotoxicological profile. Whilst concentrated esterquat solutions can cause eye and skin irritation in rabbits, the concentration of Praepagen TQ in Formulation TCM+S is only 0.01% v/v, which is far below the levels used in consumer products such as fabric softeners (>5%) (HERA, 2009b). TEA esterquats are non-mutagenic and do not produce genotoxic effects in mice and Praepagen TQ has not been found to induce hypersensitivity in guinea pigs under Buehler test conditions (HERA, 2009b). As of writing, Praepagen TQ is included in the EPA Safer Chemicals List (Environmental Protection Agency, 2019).

Esterquats such as Praepagen TQ contain at least one ester linkage between the triethanolamine hydroxyl chain and long alkyl side chains. This bond is readily cleaved by hydrolytic enzymes and spontaneous hydrolysis in both aerobic and anaerobic conditions, yielding methyl-trihydroxyethyl-ammonium and fatty acid by-products which are readily biodegradable in turn (Puchta et al., 1993). Vast quantities of esterquats already enter the wastewater system due to their widespread domestic and industrial uses as fabric softeners. Of the 130,000 tonnes of esterquats sold in the EU market, 99% are estimated to be used as

fabric softening agents (HERA, 2008). Due to their low toxicity to microorganisms, aquatic and terrestrial organisms, HERA (2008) determined triethanolamine esterquats as of no environmental concern.

The production of esterquats requires the use of dimethyl sulfate as a precursor. This compound is a suspected human carcinogen (European Commission Joint Research Centre, 2002) and reacts with water during synthesis to produce methanol, which is also hazardous (Murphy, 2014). However, the manufacturing process developed for the production of Praepagen TQ renders the dimethyl sulfate safe due to full quaternisation into the triethanolamine moiety; this process also results in a considerably lower methanol content in the final product (<1500 ppm) compared to previous generations of esterquat products (Köhle et al., 2016). Due to considerable dilution of the esterquat component in the final formulation (0.01% v/v) the methanol content is anticipated to be extremely low at 0.15 ppm. Praepagen TQ is therefore a particularly toxicologically friendly choice of cationic surfactant in Formulation TCM+S.

To fulfil the requirements of the EU Ecolabel scheme, the surfactant content of hard-surface cleaning products must be below 0.01% (Commission Decision 2017/1217, 2017). Due to the inclusion of two surfactants both at a concentration of 0.01%, the content of surfactants in Formulation TCM+S exceeds this threshold and would not satisfy this criterion. To develop the product further, re-formulation should be attempted to bring under this level. For example, reducing the content of both surfactants to 0.049% would yield a total concentration of 0.098%, which is below the threshold.

6.5.1.5 Limitations of method

The approach used to assess the ecotoxicological hazards of Formulation TCM+S did not consider the cumulative or negative synergistic effects of multiple components interacting with one another, or with other chemicals present in the sewerage system. This is a recognised limitation of theoretical assessments and can be partially addressed by calculating the additive effects of each ingredient (Steber, 2007). More detailed information could be gathered experimentally by performing tests for ready biodegradability (i.e. OECD Test No. 301) on the formulation.

It should also be noted that the assessment of the toxicity of surfactants was reliant on secondary sources, particularly reports by HERA. HERA is a voluntary initiative which describes itself as "A unique European partnership established in 1999 between the makers of household cleaning products (A.I.S.E.) and the chemical industry (Cefic) who supplies the raw materials." (HERA, 2019). As the toxicological data used to compile these reports is not publicly available, it was not possible to independently scrutinise the safety of these formulation components.

6.5.2 Experimental toxicity of Formulation TCM+S

Exposure of human keratinocytes to selected biocides led to a decrease in HaCAT cell viability, as indicated by the CellTiter-Blue resazurin assay (fig. 6.2). Cells exposed to Formulation TCM+S, hydrogen peroxide (3%), peracetic acid (0.2%) and the competitor product for 15 minutes all exhibited sharp decreases in viability.

Whilst cells treated with deionised water and with 40 μM TBO retained a substantial degree of viability compared with the saline-treated control, both exhibited a slight decrease in viability. Whilst Soukos et al. (1996) previously observed mild cytotoxic effects in keratinocytes and fibroblasts exposed to TBO at a concentration of 5 μg/mL (approximately 4 μM), we did not detect a statistically significant difference between TBO and water (fig. 6.2). Instead, it was hypothesised that this decrease in viability may have been a result of exposure to hypotonic stress. On this basis, Formulation TCM+S was supplemented with 0.85% w/v saline to maintain isotonic conditions. However, this only led to a marginal recovery of the viability of treated cells.

Based on these observations, Formulation TCM+S may have cytotoxic properties. Whilst TBO itself is not cytotoxic, cumulative or synergistic effects between other components may contribute to an overall cytotoxic profile (i.e. death by many cuts). This could be explored through more in-depth testing by exposing cells to each of the formulation's components and in different combinations.

It was notably observed that cell viability also decreased in the case of cells exposed to the competitor product, which has been dermatologically tested and marketed as skin safe. Dermatological tests follow alternative standards to cytotoxicity testing. For example, OECD Test No. 439 identifies irritancy by exposing reconstructed human epidermis (RHE) models to a substance and then assessing its effects on the viability of cells in the deeper epidermal layers (OECD, 2019b). Whilst many substances could impact cell viability when directly applied to viable cells, they may also be unable to penetrate the stratum corneum. In this sense, chemicals with cytotoxic effects may pose a low-risk to health as the epidermis is a sufficient barrier of protection in case of accidental exposure. Further investigation with RHE or *in vivo* models would be necessary to provide more information on the risks of Formulation TCM+S.

6.5.3 Production costs

Formulation TCM+S is an economically viable option for mass production. At a cost of €401.82 per 5-tonne batch, the costs of production are significantly lower than those of peracetic acid (€3500) and glutaraldehyde (€7000). Whilst cheaper to produce on a batch basis, it should be noted that both peracetic acid and glutaraldehyde are produced in concentrated forms and are diluted prior to use. In contrast, the cost of producing Formulation TCM+S was made on the assumption of it being produced as a ready-to-use product. Peracetic acid is produced at a concentration of 5% and is used at a concentration of 0.3% (15-times dilution) whilst glutaraldehyde is produced at 20% and diluted to 2% prior to use (10-times dilution). By producing as a concentrate, transportation costs are reduced considerably and larger volumes of biocide can be prepared by the end user from a single purchase. Formulation TCM+S could also be produced as a 10-times concentrate at a batch cost of €4018.20; this would make production comparable to those of peracetic acid and glutaraldehyde.

6.5.4 AER design considerations for LED integration

Results of the inverse square power calculation suggest that an LED of up to 49.70 times the intensity of that used in this project would be needed to directly illuminate the Serie 4 Washer-Disinfector basin surface with a sufficient intensity of light to obtain similar rates of inactivation to those described in chapters 3 and 5. The Eagle L330F/FW LED used in the experiments is a 30 W light source when all three colour LEDs (red, green and blue) are utilised simultaneously to produce white light (Electrovision, 2019). Since the red LEDs in this device emits a third of this energy (i.e. 10 W), it can be concluded that a suitably powerful LED array must emit at an intensity of 476 W to sufficiently light the AER cavity.

Compared to traditional lighting technologies, such as halogen or incandescent bulbs, LEDs are considered energy efficient as they produce a relatively low amount of heat per unit of light emitted (Mironyuk et al., 2019). Despite this, LEDs still produce a significant amount of heat which must be dissipated with a heat sink to maintain efficiency and avoid damage during use (Pecht et al., 2014). A heat sink is comprised of a thermally conductive material such as aluminium or copper, which can absorb and dissipate the heat built up during use (Lasance, 2014). In the case of an array with 49.70 times the output, a significantly larger heat sink would be necessary to ensure component longevity.

The VIPARSPECTRA DS600 is a 600 W LED array developed for the hydroponic plant growing; this unit utilises an active cooling system of an aluminium heat sink in tandem with high speed fans in order to provide sufficient thermal dissipation to the LEDs (VIPARSPECTRA, 2019). As the light output is similar to that which would be required in an AER, a similar cooling system would therefore be necessary. Due to its large thermal capacity, water cooling is considered an efficient method of LED heat management (Lasance, 2014). AERs contain a tank of rinse water which is used at several stages during the disinfection cycle to remove biocide residues. It is plausible that excess thermal energy held by the heat sink could be transferred to the rinse water tank to efficiently dissipate the heat without the need of fans.

LEDs have a lifetime of approximately 100,000 hours (Mironyuk et al., 2019). Even under continuous usage, this would equate to a lifetime of over 4000 days (>11 years). Since an auto-disinfection cycle would only be used for 5 minutes after each endoscope disinfection cycle, which lasts approximately 20 minutes in a Soluscope AERs (Soluscope, 2019), the LEDs would only be active for a small portion of the device use-time. Consequently, the LED component of an AER is unlikely to require replacement during the lifetime of the device.

The equation used to determine the light output required to illuminate the Serie 4 AER basin has notable limitations. LEDs have a viewing angle which affects the directionality of the light path. Whilst some have a very narrow viewing angle and illuminate with a very tight cone, others have a wider angle and produce more diffuse light. The viewing angle would affect how light emitted from a source illuminates the walls of the AER cavity, particularly towards the top side of the cavity. The equation used to calculate maximum lighting requirements did not take account for secondary indirect illumination of the same surface by light reflected from other sides of the basin. From the shortest path, indirect light could follow a path as short as 442.3 mm from the light source; this can increase to a maximum of 776.8 mm for the longest indirect path (fig. 6.1). This can contribute an additional 1% (longest path) to 11.5% (shortest path) illumination to the target surface (table 6.7). The additional lighting provided by reflectance would theoretically reduce the overall light power needed to sufficiently illuminate the basin and so the calculation used in section 6.3.4 should be consired a maximum requirement. The amount of light reflected from the basin walls is dependent on the color of PVC.

The distribution of light throughout an illuminated basin can be computationally modelled using finite element analysis (FEA). The geometry of the basin can be rendered as a meshwork of finite shapes and a set of linear equations can be used to produce an

approximation of light distribution (Giraldo, 2019). Point light sources, such as an LED, can be added with different viewing angles and in various positions to map potential dark spots and ensure sufficient illumination in all areas. This approach could be used to optimise the position of LEDs in the basin. Material properties such as reflectance can be added to FEA parameters which can allow a designer to determine the effect of different material finishes on basin illumination. Designing a basin with white PVC or a mirrored surface should further improve illumination and reduce power requirements.

6.5.5 Other scalability considerations

Due to the inherent reactivity of photosensitisers in the presence of visible light, it should be noted that any photosensitiser-based formulations, including Formulation TCM+S, should be packaged in light-impervious containers. Such containers are already widely used for the storage of hydrogen peroxide-based formulations, which must be protected from light, and so should not pose a major challenge for commercialisation.

The ISO 15883 standard regulates the requirements of AER self-disinfection cycles. Self-disinfection cycles should be capable of disinfecting the basin, connectors, channels and tank and efficacy must be demonstrated against *Pseudomonas aeruginosa*, which commonly colonises AERs through failures in the water purification system (Nelson & Muscarella, 2006; British Standards Institution, 2018). Whilst the results of Chapter 3 demonstrated efficacy of TBO-based formulations against *P. aeruginosa*, additional considerations must be made about a real-world device. Disinfection of the basin, connectors, channels and tank using a photosensitiser-based formulation would require sufficient illumination in each of these areas. Ensuring light can reach the lumen of channels would require the use of transparent plumbing; for example, transparent PVC. Considerations should also be given as to how the tank and channels could be illuminated. For example, flexible LED lighting strips and electroluminescent wire are commercially available products which could run parallel to the transparent tubing to ensure lighting is sufficient for disinfection. Developing this solution would require additional experimentation to ensure lighting is sufficient to disinfect the channels.

The long-term effects of AER exposure to Formulation TCM+S are unknown. Whilst the Formulation itself is unlikely to cause damage, it is plausible that singlet oxygen may have an effect on the lifetime of polymer-based components. Experimentally, singlet oxygen has been shown to degrade PVC (Rabek et al., 1979), which comprises the Serie 4 basin and several other parts. It remains unclear whether this would occur under conditions of real-world use and to how this might affect device longevity.

6.6 Chapter conclusions

Formulation TCM+S (40 μM TBO, 10 mM MGDA, 15 mM sodium hydrogen carbonate, 10 mM sodium carbonate, 0.01% Plurafac LF 901, 0.01% Praepagen TQ; pH 10.2) is a commercially viable product. Whilst photosensitiser-generated singlet oxygen is not currently a registered active substance within the EU, examination of the environmental profile of each of the formulation components suggests that the formulation is highly biodegradable and would pose low risks to the environment if discharged into the wastewater system. The toxicological profile of the components also suggests that the formulation would be non-hazardous to end-users. Registration should therefore not be a barrier to commercialisation. The formulation is cost effective to produce in bulk compared to other disinfectants though the difficulties in ensuring adequate lighting complicates its utilisation. Whilst difficult to utilise for AER self-disinfection cycles, the rapid bactericidal activity of Formulation TCM+S may be useful for alternative applications;these will be discussed in the following chapter.

Chapter 7.

General Discussion and Conclusions

7.1 Summary of project findings

This thesis sought to identify whether a photosensitiser-based formulation is a feasible alternative to high-level disinfectants for decontaminating medical surfaces. The primary objectives were to develop a low cost and ecotoxicologically safe formulation which exhibits rapid, broad-spectrum biocidal activity against all major groups of microorganisms. The formulation should also be usable in real-world applications, such in an automated endoscope reprocessor, and meet the criteria for new active substance registration, as required under EU biocidal product regulations. The objectives, measures and major findings of this work are summarised below in Table 7.1.

Table 7.1: Summary of project findings

Objective	Specific measures	Summary of findings
Develop photosensitiser-based biocide formulation	Ascertain requirements for optimal biocidal activity	Optimal activity successfully achieved through modifying concentration of photosensitiser and excipients
	Determine mechanism of action	Formulation disrupts bacterial membrane, leading to loss of intracellular contents and depletion of membrane potential, and induces double strand breaks in nucleic acid isolates.
Demonstrate broad spectrum activity against extended panel of required microorganisms	Vegetative bacteria	Biocidal against suspensions of *Staphylococcus aureus*, *Enterococcus hirae*, *Pseudomonas aeruginosa* and *Escherichia coli* within 1 minute. Biocidal against surface-dried *S. aureus* and *E. coli* within 1 and 2.5 minutes respectively.
	Non-enveloped viruses	Biocidal against MS2 bacteriophage within 1 minute.
	Fungi	Biocidal against *Candida albicans* and *C. auris* within 1 minute. Non-biocidal against wild-type conidia of *Aspergillus brasiliensis* due to cell wall melanins.
	Mycobacteria	Biocidal against *Mycobacterium smegmatis* within 5 minutes. Non-biocidal against *M. avium* and *M. terrae* in 15 minutes.

	Bacterial endospores	Non-biocidal against wild-type *Bacillus subtilis* endospores in 15 minutes. Partially active against outer coat and SASP-deficient mutants.
	Biofilms	Biocidal against wet and dry biofilms of *S. aureus* within 15 minutes. Partially biocidal against wet and dry biofilms of E. coli within 15 minutes.
Determine scalability of technology	Identify regulatory requirements for registering new active substance	Active substance feasible to register within EU as "i*n situ* production of singlet oxygen via excitation of a photosensitiser".
	Assess ecotoxicology safety of formulation	Formulation non-hazardous to human health or environment and fulfils safety requirements for active substance registration.
	Determine commercial viability of manufacture	Formulation is commercially viable to produce.
	Consider design requirements of real-world device	Feasible to achieve sufficient illumination of surfaces within an AER basin. Considerations must be made as to how rinse water tank and channels can be sufficiently illuminated during self-disinfection cycle.

7.2 Biocidal activity of Formulation TCM+S

Photosensitisers such as TBO produce high yields of reactive oxygen species (ROS), primarily singlet oxygen, following light excitation. As other oxidising agents exhibit broad spectrum activity, including against bacterial endospores and mycobacteria (table 7.2), it was anticipated that an optimised photosensitiser formulation would demonstrate biocidal activity against all major groups of challenge organisms. Whilst the formulation exhibited strong biocidal activity against a range of vegetative bacteria, yeasts and a non-enveloped virus, it was completely ineffective against fungal conidia, slow growing mycobacteria and endospores (Chapter 5). As high-level disinfectants must demonstrate biocidal efficacy against these microorganisms, the photosensitiser-based formulation developed here is unsuitable for the envisaged application.

Table 7.2: Advantages and disadvantages of commonly used biocides

Disinfectant	Type	Advantages	Disadvantages
Peracetic acid/hydrogen peroxide	Oxidising agent	Rapid broad-spectrum activity against endospores and mycobacteria.	Corrosive and irritating. Must be stabilised to prevent decomposition. Efficacy reduced by soiling.
Sodium hypochlorite	Oxidising agent	Broad spectrum activity against endospores and mycobacteria. Low production cost and available in anhydrous preparations.	Corrosive to metals. Can form chlorine gas when mixed with other cleaning agents. Chlorines reacts to form ecologically persistent organochloride compounds.
Glutaraldehyde	Cross-linking agent	Broad spectrum activity. Low production cost and shelf stable. Can be reused.	Relatively slow sporicidal and mycobactericidal activity. Resistance in mycobacteria reported. Occupational exposure hazard due to irritating vapours.
Benzalkonium chloride	Quaternary ammonium compound	Highly biocompatible and shelf stable.	Non-sporicidal and poor activity against mycobacteria. Only suitable for mid-level disinfection.

The observations of Chapter 5 suggest several factors protect microorganisms from TBO photosensitisation (table 7.3). Limited cell permeability by various means conferred a high degree of resistance to TBO photosensitisation in several organism types. Whilst the addition of a chelator negated this mechanism in the case of *Pseudomonas aeruginosa*, the intrinsic impermeability of slow growing mycobacteria and *Bacillus subtilis* endospores cannot be so easily resolved by adjustments to the formulation. In *Aspergillus* conidia, melanin may confer resistance through several mechanisms, such as limiting access to intracellular targets, quenching ROS activity and impeding activation of the photosensitiser. Whilst other authors have reported rapid sporicidal activity using an octo-cationic riboflavin derivative (Eichner et al., 2015), melanin will likely continue to offer protection to *Aspergillus* conidia and so would also be unsuited to high-level disinfection.

Table 7.3: Mechanisms of resistance to TBO photosensitisation

Mechanism of Resistance	Resistance factor	Organism
Permeability barrier/limited access to intracellular targets	Lipopolysaccharide outer membrane	*Pseudomonas aeruginosa*
	Mycolyl-arabinogalactan-peptidoglycan cell wall	Slow-growing mycobacteria
	Outer spore coat	*Bacillus subtilis* endospores
	Melanin (negative charge)	*Aspergillus* conidia
DNA protection	Small acid soluble proteins	*Bacillus subtilis* endospores
Intrinsic ROS quencher	Melanin (antioxidant)	*Aspergillus* conidia
Reduced excitation of the photosensitiser	Melanin (dark pigmentation)	*Aspergillus* conidia

Whilst singlet oxygen is an ROS, it's activity as a biocide is acutely limited by its diffusion distance within cellular environments; in protein-rich settings, it may diffuse only 10 nm (Baier et al., 2005). Our observations suggest that the biocidal activity of photosensitisers is contingent on the photosensitiser being located proximal to target sites, namely the cytoplasmic membrane and DNA which are rapidly damaged during the photosensitisation process (Chapter 4). Singlet oxygen-producing photosensitisers must therefore penetrate microbial structures to exert antimicrobial activity and this activity can be easily thwarted by numerous mechanisms which limit their interaction with target sites.

Whilst the experiments reported here were limited to the use of a single photosensitiser, it is anticipated that other cationic photosensitisers such as fullerenes and porphyrins would suffer from similar drawbacks. Whilst TBO has a molar mass of 270 g/mol, the molar mass of fullerenes and porphyrins exceed 700 and 1150 g/mol respectively (Tegos et al., 2011). This larger size would be expected to impede penetration into target cells and so reduce their efficacy. Whilst anionic photosensitisers differ in their routes of intracellular uptake (George et al., 2009), they are less potent antimicrobials and must still reach target sites to exert a biocidal effect (Minnock et al., 1996). As such, it is anticipated that these alternatives would remain ineffective against mycobacteria, melanin-rich fungal conidia and endospores.

In contrast to organic photosensitisers, inorganic quantum dots and titanium dioxide nanoparticles are semi-conductors which produce hydroxyl and superoxide radicals during the photoexcitation process. These species are longer lived than singlet oxygen and induce a cascade of radical formation upon reacting with microbial targets. This can improve their effective range of activity and may offer superior biocidal activity. Unlike organic photosensitisers, they do not contain conjugated chromophores which are susceptible to cleavage by ROS. Inorganic alternatives thus do not suffer from photobleaching and are capable of being used over longer contact times. Titanium oxide nanoparticles co-doped with other metals, sulphur and carbon have also been observed to possess light-independent sporicidal activity (Hamal et al., 2011), which highlights their potential utility as an alternative high-level disinfection technology. Despite these strengths, it should be noted that there are concerns about the ecological impacts of nanoparticles (Simonin et al., 2016). Furthermore, UV light is required for photoexcitation and is efficiently blocked by melanin which may render inorganic alternatives as unsuitable.

7.3 Practical considerations

One of the major scalability obstacles faced by photosensitisers is the requirement for photoactivation by light. The illumination of surfaces such as those within an automated endoscope reprocessor is possible but distinctive considerations must be made during the design of devices which wish to utilise this technology. Whilst an AER basin is relatively simple to illuminate, a self-disinfection cycle is also required to disinfect components such as the plumbing and rinse water tank. Whilst this is theoretically achievable, this adds a large element of complexity into the design of such machines. The technology is much more suitable for applications where lighting requirements are more simplistic, such as flat surfaces or where light is manually applied, such as during endodontic procedures. These factors should be considered by other researchers developing antimicrobial photosensitiser technologies.

7.4 Alternative applications for photosensitiser-based biocides

Whilst unsuitable for high-level disinfection applications, Formulation TCM+S fulfilled several other objectives of the project. The formulation exhibited rapid bactericidal, virucidal and yeasticidal activity, is cheap to produce and presents minimal risks to human health and the environment. These strengths make considerations of alternative uses worthwhile.

7.4.1 Food preparation surfaces

In Chapter 3, assessment of the biocidal activity of Formulation TCM+S against surface-dried bacteria (EN 13697) determined that the formulation was suitable for the disinfection of contaminated surfaces. Alternative surfaces which could be disinfected with the formulation include industrial food preparation surfaces. Factory production of food items utilises conveyors during manufacturing process. Due to their direct contact with contaminated food items, food conveyors are a critical control point and must be disinfected regularly to ensure compliance with food hygiene standards. *Listeria monocytogenes* is a psychrotrophic organism which is particularly burdensome in in seafood production plants due to its ability to thrive in refrigerated environments (Di Ciccio et al., 2012; Leong et al., 2015). Food conveyors have been noted as a vector for direct *Listeria* contamination of foodstuffs (Jami et al., 2014).

Currently, hot water and sodium hypochlorite are widely used to decontaminate these surfaces. However, this procedure leads to hydrolytic degradation of the conveyor surface which can compromise decontamination and necessitate replacement of the conveyor (Food Processing Technology, 2011). The widespread use of hypochlorite has also raised concerns of the contamination of foodstuffs with perchlorate residues and alternatives are sought (Nelter, 2017). Whilst UV-C decontamination is a possible solution, this requires large upfront capital investment to implement and bulky shielding is required to protect workers from the hazards of ionizing radiation (Gordon, 2018). Moreover, conventional UV sources are inefficient in cold environments, which limits their use (Gordon, 2018).

As conveyors are flat, a light source can be placed in close proximity to the surface to minimise energy loss by the inverse square law. LED sources can be installed at low cost, operate efficiently at low temperatures and present minimal risk to workers. Photosensitisers may therefore be useful for continuous decontamination of conveyor surfaces. Moreover, since Formulation TCM+S was found to be more active at lower temperatures, it may be well suited for use in chilled environments to control the spread of *L. monocytogenes*.

7.4.2 Medical applications

As discussed in Chapter 6, Formulation TCM+S poses minimal risks to human health. The formulation may thus be useful for medical applications in which targeted destruction of microorganisms is desirable. Even without specific optimisation, the formulation demonstrated good bactericidal activity against biofilms. Biofilms are problematic in areas such as endodontic procedures and chronic wound healing. Whilst TBO is already being investigated for the disinfection of root canals (Lee et al., 2004), Formulation TCM+S is highly optimised for rapid bactericidal activity and has improved wettability due to the inclusion of surfactants. This may improve its penetration into deeper recesses of the endodontic canal and so Formulation TCM+S may offer superior performance to current photosensitiser products registered for endodontic use.

Photosensitisers including TBO and methylene blue have also been investigated for the photodynamic management of chronic wounds such as diabetic foot ulcers. Chronic wounds develop as a result of poor perfusion of the wound bed and the formation of microbial biofilms; these biofilms contribute to persistent inflammation and are recalcitrant to treatment (Malone, 2017). Photodynamic treatment has already been shown to rapidly improve the healing of diabetic foot ulcers without debridement and with low rates of relapse (Tardivo et al., 2017) and Formulation TCM+S demonstrated bactericidal activity against mature biofilms (Chapter 5). Photosensitisers also supress the expression of bacterial virulence factors (Tseng et al., 2017) and neutralise the activity of those already present in extracellular environments (Kömerik et al., 2000). Formulation TCM+S may therefore be successfully utilised for photodynamic management of chronic wounds.

7.5 Future developments of formulation and disinfection parameters

Whilst unsuited for high-level disinfection, the formulation and disinfection parameters can be developed further to improve its usability in other applications. Changes to the formulation should consider the specific requirements of these applications and can include changes to the photosensitiser itself, as well as the addition of excipients to the formulation.

7.5.1 Alternative photosensitisers

In applications such as the control of microorganisms in food production lines, it may be desirable to develop a food-safe photosensitiser formulation. Xanthene dyes and natural products such as curcumin are widely used food colourants and have photosensitising properties (Ghorbani et al., 2018). Their use would not contaminate food preparation surfaces with hazardous residues. There has already been interest in using curcumin for the control of *L. monocytogenes* in food preservation, though as a non-formulated solution (Bonifácio et al., 2018), and the xanthene dye erythrosine B is effective against microbial biofilms (Wood et al., 2006). Utilising the same approach used to develop Formulation TCM+S may yield photosensitiser-based formulations appropriate for use in food areas.

7.5.2 Additional excipients

Pre-treatment of bacterial cells with sodium azide, a quencher of singlet oxygen, has been experimentally demonstrated to improve activity of phenothiazines such as TBO; this paradoxical observation was posited to be due to promoting ROS production through a type-I photosensitisation mechanism, which yields radical species rather than singlet oxygen (Kasimova et al., 2014). Due to the larger diffusion distance, pre-treatment of mycobacteria and endospores with azide may improve activity against these species.

Co-formulation of photosensitisers with cationic polymers such as chitosan and poly-lysine can improve their bactericidal activity (Tsai et al., 2011). Both chitosan and poly-lysine exert their bactericidal effects through permeablisation of the cytoplasmic membrane (Liu et al., 2004; Hyldgaard et al., 2014). Poly-lysine has been investigated for a range of applications, including food preservation (Li et al., 2014) and possesses bactericidal activity, including against slow growing mycobacteria (Delihas et al., 1995). Other authors have successfully produced photosensitiser-poly-lysine conjugates which exhibit excellent bactericidal activity (Demidova & Hamblin, 2005). Targeted improvements to the mycobactericidal activity of the formulation may thus be attainable through the addition of poly-lysine.

Microemulsion preparations of TBO have been demonstrated to considerably improve its biocidal activity against *P. aeruginosa* and biofilms of *S. aureus* (Rout et al., 2016; Rout et al., 2018). These emulsions can be prepared relatively simply using an aqueous solution of TBO, polysorbate-80 and an organic phase such as eucalyptus oil (Rout et al., 2016). The biocidal activity of such preparations would be an avenue worth exploring in future formulation development, particularly for applications such as food preparation surfaces and endodontics, in which biofilms are likely to pose additional challenges. Many essential oils possess quorum sensing disrupting properties (Poli et al., 2018) and so their addition to a formulation may provide additional anti-biofilm properties.

Thickening agents may be useful in applications where the formulation is to be applied to inclined surfaces in order to improve adherence. Anionic thickeners may be incompatible with cationic components of Formulation TCM+S (TBO and Praepagen TQ) as the addition of sodium alginate to TBO solutions leads to decolourisation (Vleugels et al., 2017), similar to our observations with SDS in Chapter 3. Non-ionic polyurethane-based polymers are compatible with other cationic disinfectants and so would be suited for addition to the formulation (Mahfouz et al., 2017). Amine oxides and naturally derived thickening agents (e.g. xanthan gum) may provide suitable thickening properties whilst offering an excellent ecotoxicological profile through being readily biodegraded (García et al., 2007).

7.4.3 Alternative light wavelengths and co-treatment with blue light

A limitation of this study was the use of a single wavelength of light (620 nm) to photoactivate the formulation. The formation of TBO dimers at bacterial target sites is purported to play a key in contributing toward the photodynamic inactivation of Gram-negative species (Usacheva et al., 2003). As dimers are excited by 590 nm light, the biocidal activity of Formulation TCM+S may be potentiated by utilising a 590 nm-emitting light source, either separately or in tandem with 620 nm light. Blue light has also been demonstrated to exert photosensitiser-independent antimicrobial activity against vegetative bacteria (Hönes et al., 2015), bacterial biofilms (Wang et al., 2014) and endospores of the *Clostridioides* and *Bacillus* genera (MacClean et al. (2012). MacClean et al. (2012) report that treatment of *B. subtilis* endospores with 405 nm blue light yielded 4 $\log_{10}$ reductions in viability after a 110 J/cm^2 dose of light; such illumination would be attainable within 10 minutes using the light source used during this study (section 2.1.9). Blue light offers substantially greater antimicrobial activity at shorter wavelengths which are close to the UV electromagnetic region (Hönes et al., 2015). Blue light also acts synergistically with other microbicides, such as chlorinated compounds (Moorhead et al., 2016) and so may improve the biocidal activity if used in combination with Formulation TCM+S.

7.6 Considerations of the methodology

The overall methodological approach used during this research was useful for exploring the use of photosensitisers as alternative disinfectants. After developing an optimised TBO-based formulation through methodical improvements, its biocidal activity was benchmarked against the requirements of a high-level disinfectant. Shortfalls in biocidal activity against specific species were explored by comparing to observations on its mechanism of action and effects on target cells. This provided valuable and generalisable insights into the limitations of photosensitisers as a biocide. By exploring the requirements for commercialising the formulation and applying it to a real-world device, the strengths and weaknesses of this approach to disinfection were fully determined. Whilst the formulation developed here did not meet the requirements of a high-level disinfectant, our observations indicate that photosensitisers are a feasible alternative to mid-level disinfectants in other surface-disinfection applications.

Working with an industrial partner offered unique opportunities to explore the research question holistically. Providing access to company data, including machine schematics, and offering information on batch production methods proved essential for determining whether a photosensitiser-based approach to surface disinfection is commercially viable. Moreover, considering the statutory requirements of registering a novel active substance indicated that photosensitiser-based formulations are likely to be accepted by European regulators.

Whilst other researchers have examined the role of photosensitisers in inactivating surface-associated bacteria, this is the first time a photosensitiser-based formulation has been examined using adaptions of standardised testing protocols. This facilitated development of the formulation using parameters relevant to the real-world requirements of a biocide whilst also allowing comparisons to be drawn with existing biocidal products. The main adaptation which was considered in this project was standardising photoexcitation conditions and using a light source which can be readily scaled to real-world use. With growing interest in the use of photosensitisers for a range of applications, a standardised protocol for illuminating substances should be developed.

7.7 Alternative approaches to disinfection in endoscopy units

Improvements to AER disinfection can be achieved through engineering-led approaches, such as better engineering. For example, designing heat-resistant AERs opens the door to thermal self-disinfection. Competitors of Soluscope have favoured this approach in the design of their AERs, which can self-disinfect by circulating >80^{o}C water through throughout the basin, connectors and filtration systems for 20 minutes (Cantel, 2019; Steelco, 2019). Such systems confer significant advantages over chemical approaches since hazardous waste is not produced and errors in biocide dilution are avoided. The current iteration of the ISO 15883 standard, which outlines statutory requirements of AER design, indicates that thermal processes are favoured for self-disinfection cycles (British Standards Institute, 2018).

Double-hatch systems such as RapidAER offer further advantages to traditional AER design as they can be integrated into the space between cleaning and drying areas. This further limits the likelihood of unintentional recontamination of endoscopes since contaminated instruments can be loaded into one side and removed from the other to be dried in a clean area. In contrast, single door designs such as the Soluscope Serie 4 are less able to be integrated into an aseptic workflow and operators risk recontamination. Technical memoranda from the Department of Health (2016) suggest using two-way hatch designs to ensure best practice and maintain a suitably hygienic workflow.

The development of capsule endoscopy is an example of another engineering innovation which may address the issues of throughput and microbiological safety within endoscopy units. These devices are swallowed by the patient and traverse the entire length of the gastrointestinal tract. The procedure is able to be performed on an outpatient basis and, as single-use items, capsules forgo the need for reprocessing between patients (Hale et al., 2014). Increased adoption of capsules can improve throughput and patient safety whilst also reducing pressures on reprocessing units. Capsule endoscopes can be a cost-effective alternative to endoscopy in the management of upper gastrointestinal bleeding and for bowel cancer screening (Hassan et al., 2011; Meltzer et al., 2014). With rapid advances in the technology and improved patient acceptability, these devices are likely to supersede diagnostic endoscopy procedures and relieve some of the pressures faced by endoscope reprocessing units.

7.8 Conclusions and recommendations

Our observations suggest that photosensitisers can be utilised in a limited capacity for the disinfection of medical surfaces. Using standardised testing methods, Formulation TCM+S (40 μM TBO, 15mM Na_2CO_3, 10 mM $NaHCO_3$, 10 mM MGDA, 0.01% v/v Plurafac LF 901, 0.01% v/v Praepagen TQ, pH 10.2) demonstrated effective biocidal activity against vegetative bacteria, biofilms, non-enveloped viruses and yeasts, though was ineffective against slow-growing mycobacteria, fungal conidia and bacterial endospores. The intrinsic resistance of these organisms to disinfection would be likely to protect these organisms from other classes of photosensitisers. Photosensitisers are therefore unsuitable replacements for existing high-level disinfectants, though could be used as alternative mid-level disinfectants. Disinfection of automated endoscope reprocessors can be better achieved through existing technologies, such as thermal processes, and improvements to the control of microorganisms in endoscopy units may be better addressed through alternative developments. Due to their excellent ecotoxicological profile and low production costs, further investigations are warranted to better understand the suitability of photosensitisers for alternative applications such as disinfection of food preparation areas and wound management.

References

Abcam. (2019). Counting cells using a hemocytometer. Available from: https://www.abcam.com/protocols/counting-cells-using-a-haemocytometer [*Last accessed: 13/11/2019*].

Addent. (2019). ORABLU. Available from: https://www.addent.com/orablu/ [*Last accessed: 01/11/2019*].

Akram FE, El-Tayeb T, Abou-Aisha K, El-Azizi M. (2016). A combination of silver nanoparticles and visible blue light enhances the antibacterial efficacy of ineffective antibiotics against methicillin-resistant *Staphylococcus aureus* (MRSA). Ann Clin Microbiol Antimicrob. 15 (1), 48.

Al-Adham A, Haddadin R, Collier P. (2013). Types of microbicide and microbistatic agents. In: Fraise AP, Maillard J, Sattar SA Russell, Hugo & Ayliffe's Principles and Practice of Disinfection, Preservation and Sterilization. 5th ed. Chichester; UK: Wiley-Blackwell. 24-6, 38-9.

Al-Asmari F, Mereddy R, Sultanbawa Y. (2017). A novel photosensitization treatment for the inactivation of fungal spores and cells mediated by curcumin. J Photochem Photobiol B. 173, 301-6.

Alderwick LJ, Harrison J, Lloyd GS, Birch HL. (2015). The mycobacterial cell wall--peptidoglycan and arabinogalactan. Cold Spring Harb Perspect Med. 5 (8), a021113.

Alexander C, Rietschel ET. (2001). Bacterial lipopolysaccharides and innate immunity. J Endotoxin Res. 7 (3), 167-202.

Alfa MJ, Howie R. (2009). Modeling microbial survival in buildup biofilm for complex medical devices. BMC Infect Dis. 9 (56).

Alhassani HA, Rauf MA, Ashraf S. (2007). Efficient microbial degradation of toluidine blue dye by *Brevibacillus* sp. Dyes Pigments. 75 (2), 395-400.

Ali L, Alhassani H, Karuvantevida N, Rauf MA, Ashraf S. (2014). Efficient aerobic degradation of various azo dyes by a *Sphingomonas* sp isolated from petroleum sludge. J Bioremed Biodeg. 5 (3).

Alkawareek MY, Bahlool A, Abulateefeh SR, Alkilany AM. (2019). Synergistic antibacterial activity of silver nanoparticles and hydrogen peroxide. PLoS One. 14 (8), e0220575.

Almatroudi A, Hu H, Deva A, Gosbell IB, Jacombs A, Jensen SO, Whiteley G, Glasbey T, Vickery K. (2015). A new dry-surface biofilm model: An essential tool for efficacy testing of hospital surface decontamination procedures. J Microbiol Methods. 177, 171-6.

Almatroudi A, Tahir S, Hu H, Chowdhury D, Gosbell IB, Jensen SO, Whiteley GS, Deva AK, Glasbey T, Vickery K. (2018). Staphylococcus aureus dry-surface biofilms are more resistant to heat treatment than traditional hydrated biofilms. J Hosp Infect. 98 (2), 161-7.

Alshareef F, Robson GD. (2014). Prevalence, persistence, and phenotypic variation of *Aspergillus fumigatus* in the outdoor environment in Manchester, UK, over a 2-year period. Med Mycol. 52 (4), 367-75.

Alvarado CJ, Stolz SM, Maki DG. (1991). Nosocomial infections from contaminated endoscopes: a flawed automated endoscope washer. An investigation using molecular epidemiology. Am J Med. 91 (3B), 272-80.

ASTM International (2017a). E2197-17$^{\varepsilon 1}$. Standard quantitative disk carrier test method for determining bactericidal, virucidal, fungicidal, mycobactericidal, and sporicidal activities of chemicals.

Arendrup MC, Prakash A, Meletiadis J, Sharma C, Chowdhary A. (2017). Comparison of EUCAST and CLSI reference microdilution MICs of eight antifungal compounds for *Candida auris* and associated tentative epidemiological cutoff values. Antimicrob Agents Chemother. 61 (6), e00485-17.

ASGE Quality Assurance in Endoscopy Committee, Petersen BT, Chennat J, Cohen J, Cotton PB, Greenwald DA, Kowalski TE, Krinsky ML, Park WG, Pike IM, Romagnuolo J; Society for Healthcare Epidemiology of America, Rutala, W.A. (2011). Multisociety guideline on reprocessing flexible gastrointestinal endoscopes: 2011. Gastrointest Endosc. 73 (6), 1075-84.

ASGE Technology Committee. (2016). Status evaluation report. Automated endoscope reprocessors. Gastrointest Endosc. 84 (6), 885-92.

ASTM International. (2017b). ASTM E2799-17, Standard test method for testing disinfectant efficacy against *Pseudomonas aeruginosa* biofilm using the MBEC assay. ASTM International; West Conshohocken, PA, USA.

Atkins P, Friedman R. (2011). Molecular Electronic Transitions. In Molecular Quantum Mechanics, (New York, USA: Oxford University Press), 382–98.

Ayora S, Carrasco B, Cárdenas PP, César CE, Cañas C, Yadav T, Marchisone C, Alonso JC. (2011). Double-strand break repair in bacteria: a view from *Bacillus subtilis*. FEMS Microbiol Rev. 35 (6), 1055-81.

Azevedo F, Marques F, Fokt H, Oliveira R, Johansson B. (2011). Measuring oxidative DNA damage and DNA repair using the yeast comet assay. Yeast. 28 (1), 55-61.

Bacellar IO, Pavani C, Sales EM, Itri R, Wainwright M, Baptista MS. (2014). Membrane damage efficiency of phenothiazinium photosensitizers. Photochem Photobiol. 90 (4), 801-13.

Baillie L, Theriault S. (2013). Control of infectious bioagents. In: Fraise AP, Maillard J, Sattar SA Russell, Hugo & Ayliffe's Principles and Practice of Disinfection, Preservation and Sterilization. 5th ed. Chichester; UK: Wiley-Blackwell. 581.

Banin E, Brady KM, Greenberg EP. (2006). Chelator-induced dispersal and killing of *Pseudomonas aeruginosa* cells in a biofilm. Appl Environ Microbiol. 72 (3), 2064-9.

Bartsch H. (1976). Predictive value of mutagenicity tests in chemical carcinogenesis. Mutat Res. 38 (3), 177-90.

BASF (2007) Technical Information Ti/EVD 1418 e - Trilon® M types

BASF. (2019a). Plurafac® LF 901. Available from: https://www.homecare-and-i-and-i.basf.com/products/products-detail/Plurafac%20LF%20901/30273371 [*Last accessed: 03/11/2019*].

BASF. (2019b). EU Ecolabel. Available from: https://www.homecare-and-i-and-i.basf.com/products/product-labels/eu-ecolabel [*Last accessed 29/08/2019*].

Bayry J, Beaussart A, Dufrêne YF, Sharma M, Bansal K, Kniemeyer O, Aimanianda V, Brakhage AA, Kaveri SV, Kwon-Chung KJ, Latgé JP, Beauvais A. (2014). Surface structure characterization of *Aspergillus fumigatus* conidia mutated in the melanin synthesis pathway and their human cellular immune response. Infect Immun. 82 (8), 3141-53.

Beeton ML, Spiller OB. (2017). Antibiotic resistance among *Ureaplasma spp*. isolates: cause for concern? J Antimicrob Chemother. 72 (2), 330-7.

Beilenhoff U, Biering H, Blum R, Brljak J, Cimbro M, Dumonceau JM, Hassan C, Jung M, Kampf B, Neumann C, Pietsch M, Pineau L, Ponchon T, Rejchrt S, Rey JF, Schmidt V, Tillett J, van Hooft JE. (2018). Reprocessing of flexible endoscopes and endoscopic accessories used in gastrointestinal endoscopy: Position Statement of the European Society of Gastrointestinal Endoscopy (ESGE) and European Society. Endoscopy. 50 (12), 1205-34.

Berney M, Hammes F, Bosshard F, Weilenmann HU, Egli T. (2007). Assessment and interpretation of bacterial viability by using the LIVE/DEAD BacLight Kit in combination with flow cytometry. Appl Environ Microbiol. 73 (10), 3283-90.

Bertoloni G, Rossi F, Valduga G, Jori G, van Lier J. (1990). Photosensitizing activity of water- and lipid-soluble phthalocyanines on Escherichia coli. FEMS Microbiol Lett. 59 (1-2), 149-55.

Bielski BH, Arudi RL, Sutherland MW. (1983). A study of the reactivity of HO_2/O_2^- with unsaturated fatty acids. J Biol Chem. 258 (8), 4759-61.

Bollback JP, Huelsenbeck JP. (2001). Phylogeny, genome evolution, and host specificity of single-stranded RNA bacteriophage (family Leviviridae). J Mol Evol. 52 (2), 117-28.

Bonifácio D, Martins C, David B, Lemos C, Neves MGPMS, Almeida A, Pinto DCGA, Faustino MAF, Cunha Â. (2018). Photodynamic inactivation of *Listeria innocua* biofilms with food-grade photosensitizers: a curcumin-rich extract of *Curcuma longa* vs commercial curcumin. J Appl Microbiol. 125 (1), 282-294.

Bonora M, Patergnani S, Rimessi A, De Marchi E, Suski JM, Bononi A, Giorgi C, Marchi S, Missiroli S, Poletti F, Wieckowski MR, Pinton P. (2012). ATP synthesis and storage. Purinergic Signal. 8 (3), 343-57.

Bonsor SJ, Nichol R, Reid TM, Pearson GJ. (2006). An alternative regimen for root canal disinfection. Br Dent J. 201 (2), 101-5.

Braga PC, Ricci D. (1998). Atomic force microscopy: application to investigation of *Escherichia coli* morphology before and after exposure to cefodizime. Antimicrob Agents Chemother. 42 (1), 18-22.

Bridier A, Briandet R, Thomas V, Dubois-Brissonnet F. (2011). Resistance of bacterial biofilms to disinfectants: a review. Biofouling. 27 (9), 1017-32.

British Pharmacoepia Commission (2008). Appendix XVIII Methods of Sterilisation (Methods of Preparation of Sterile Products). British Pharmacoepia 2008: volume IV appendices. London; TSO.

British Society of Gastroenterology. 2016. BSG guidance for decontamination of equipment for gastrointestinal endoscopy. Available from: https://www.bsg.org.uk/asset/F28EDCE3-11FC-45B7-B204D3034251D6B9/ [*Last accessed: 07/10/2019*].

British Standards Institute (2005). BS EN 14348:2005. Chemical disinfectants and antiseptics. Quantitative suspension test for the evaluation of mycobactericidal activity of chemical

disinfectants in the medical area including instrument disinfectants. Test methods and requirements (phase 2, step 1). BSI Standards Limited; London, UK.

British Standards Institute (2006). BS EN 14561:2005. Chemical disinfectants and antiseptics. Quantitative carrier test for the evaluation of bactericidal activity for instruments used in the medical area. Test method and requirements (phase 2, step 2). BSI Standards Limited; London, UK.

British Standards Institute (2012). BS EN 13727:2012+A2:2015. Chemical disinfectants and antiseptics. Quantitative suspension test for the evaluation of bactericidal activity in the medical area - test method and requirements (phase 2, step 1). BSI Standards Limited; London, UK.

British Standards Institute (2013a). BS EN 13624:2005. Chemical disinfectants and antiseptics. Quantitative suspension test for the evaluation of fungicidal or yeasticidal activity in the medical area. Test method and requirements (phase 2, step 1). BSI Standards Limited; London, UK.

British Standards Institute (2013b). BS EN 14476:2013+A2:2019. Chemical disinfectants and antiseptics. Quantitative suspension test for the evaluation of virucidal activity in the medical area. Test method and requirements (Phase 2/Step 1). BSI Standards Limited; London, UK.

British Standards Institute (2015a). BS EN 13697:2015. Chemical disinfectants and antiseptics. Quantitative non-porous surface test for the evaluation of bactericidal and/or fungicidal activity of chemical disinfectants used in food, industrial, domestic and institutional areas — Test method and requirements without mechanical action (phase 2, step 2). BSI Standards Limited; London, UK.

British Standards Institute (2015b). BS EN 16615:2015. Chemical disinfectants and antiseptics. Quantitative test method for the evaluation of bactericidal and yeasticidal activity on non-porous surfaces with mechanical action employing wipes in the medical area (4- field test). Test method and requirements (phase 2, step 2). BSI Standards Limited; London, UK.

British Standards Institute. (2018). BS EN ISO 15883-4:2018. Washer-disinfectors. Requirements and tests for washer-disinfectors employing chemical disinfection for thermolabile endoscopes. BSI Standards Limited; London, UK.

BSG Endoscopy Committee Working Party. (1998). Cleaning and disinfection of equipment for gastrointestinal endoscopy. Report of a Working Party of the British Society of Gastroenterology Endoscopy Committee. Gut. 42 (4), 585-93.

Burgess W, Margolis A, Gibbs S, Duarte RS, Jackson M. (2017). Disinfectant susceptibility profiling of glutaraldehyde-resistant nontuberculous mycobacteria. Infect Control Hosp Epidemiol. 38 (7), 784-91.

Byers JP, Sarver JG. (2009). Chapter 10. Pharmacokinetic Measurements. In: Hacker M, Bachmann K, Messer M. Pharmacology: Principles and Practice. Burlington; Massachusetts: Academic Press. 207.

Cadnum JL, Shaikh AA, Piedrahita CT, Sankar T, Jencson AL, Larkin EL, Ghannoum MA, Donskey CJ. (2017). Effectiveness of disinfectants against *Candida auris* and other Candida species. Infect Control Hosp Epidemiol. 38 (10), 1240-3.

Campos-Martin JM, Blanco-Brieva G, Fierro JLG. (2006). Hydrogen peroxide synthesis: an outlook beyond the anthraquinone process. Angew. 45 (42), 6962-84.

Cantel. (2019). RapidAER. Available from: https://www.cantelmedical.co.uk/product/rapidaer/ [*Last accessed: 21/10/2019*].

Cavaliere R, Ball JL, Turnbull L, Whitchurch CB. (2014). The biofilm matrix destabilizers, EDTA and DNaseI, enhance the susceptibility of nontypeable *Hemophilus influenzae* biofilms to treatment with ampicillin and ciprofloxacin. Microbiologyopen. 3 (4), 557-67.

Centers for Disease Control and Prevention. (2008a). Peracetic acid sterilization: guideline for disinfection and sterilization in healthcare facilities. Available from: https://www.cdc.gov/infectioncontrol/guidelines/disinfection/sterilization/peracetic-acid.html [*Last accessed: 22/10/2019*].

Centers for Disease Control and Prevention. (2008b). Introduction, methods, definition of terms: guideline for disinfection and sterilization in healthcare facilities. Available from: https://www.cdc.gov/infectioncontrol/guidelines/disinfection/introduction.html [*Last accessed: 02/10/2019*].

Chen J, Cesario TC, Rentzepis PM. (2011). Effect of pH on methylene blue transient states and kinetics and bacteria photoinactivation. J Phys Chem A. 115 (13), 2702-7.

Cheung HY, Wong MM, Cheung SH, Liang LY, Lam YW, Chiu SK. (2012). Differential actions of chlorhexidine on the cell wall of *Bacillus subtilis* and *Escherichia coli*. PLoS One. 7 (5), e36659.

Chevalier S, Bouffartigues E, Bodilis J, Maillot O, Lesouhaitier O, Feuilloley MGJ, Orange N, Dufour A, Cornelis P. (2017). Structure, function and regulation of *Pseudomonas aeruginosa* porins. FEMS Microbiol Rev. 41 (5), 698-722.

Chowdhury D, Rahman A, Hu H, Jensen SO, Deva AK, Vickery K. (2019). Effect of disinfectant formulation and organic soil on the efficacy of oxidizing disinfectants against biofilms. J Hosp Infect. 103 (1), e33-e41.

Chowdhury D, Tahir S, Legge M, Hu H, Prvan T, Johani K, Whiteley GS, Glasbey TO, Deva AK, Vickery K. (2013). Transfer of dry surface biofilm in the healthcare environment: the role of healthcare workers' hands as vehicles. J Hosp Infect. 100 (3), e85-e90.

Clifton LA, Skoda MW, Le Brun AP, Ciesielski F, Kuzmenko I, Holt SA, Lakey JH. (2015). Effect of divalent cation removal on the structure of Gram-negative bacterial outer membrane models. Langmuir. 31 (1), 404-12.

Cock I, Kalt FR. (2010). A modified MS2 bacteriophage plaque reduction assay for the rapid screening of antiviral plant extracts. Pharmacognosy Res. 2 (4), 221-8.

Cold Spring Harbor Laboratory Press. (2013). Recipe. Tris-Acetate-EDTA (TAE) Buffer (50×). Available from: http://cshprotocols.cshlp.org/content/2013/5/pdb.rec074294.full [*Last accessed: 30/10/2019*].

Cold Spring Harbour Protocols. (2006). Recipe. SM buffer. Available from: http://cshprotocols.cshlp.org/content/2006/1/pdb.rec8111.full?text_only=true [*Last accessed: 25/10/2019*].

Commission Decision 2017/1217. (2017). Commission Decision (EU) of 23 June 2017 establishing the EU Ecolabel criteria for hard surface cleaning products. Available from: https://eur-lex.europa.eu/eli/dec/2017/1217/oj [*Last accessed: 21/10/2019*].

Cortesão M, Fuchs FM, Commichau FM, Eichenberger P, Schuerger AC, Nicholson WL, Setlow P, Moeller RR1. (2019). *Bacillus subtilis* spore resistance to simulated Mars surface conditions. Front Microbiol. 10 (333).

Cortezzo DE, Koziol-Dube K, Setlow B, Setlow P. (2004). Treatment with oxidizing agents damages the inner membrane of spores of *Bacillus subtilis* and sensitizes spores to subsequent stress. J Appl Microbiol. 97 (4), 838-52.

Cortezzo DE, Setlow P. (2005). Analysis of factors that influence the sensitivity of spores of *Bacillus subtilis* to DNA damaging chemicals. J Appl Microbiol. 98 (3), 606-17.

Costa DM, Johani K, Melo DS, Lopes LKO, Lopes Lima LKO, Tipple AFV, Hu H, Vickery K. (2018). Biofilm contamination of high-touched surfaces in intensive care units: epidemiology and potential impacts. Lett Appl Microbiol. 68 (4), 269-76.

Costa L, Faustino MA, Neves MG, Cunha A, Almeida A. (2012). Photodynamic inactivation of mammalian viruses and bacteriophages. Viruses. 4 (7), 1034-74.

Council Directive 91/271/EEC. (1991). Council Directive of 21 May 1991 concerning urban waste water treatment. Available from: https://eur-lex.europa.eu/legal-content/EN/TXT/?uri=CELEX:01991L0271-20140101 [*Last accessed: 21/10/2019*].

Cowan-Ellsberry C, Belanger S, Dorn P, Dyer S, McAvoy D, Sanderson H, Versteeg D, Ferrer D, Stanton K. (2014). Environmental safety of the use of major surfactant classes in North America. Crit Rev Environ Sci Technol. 44 (17), 1893-993.

Cowles PB. (1940). The disinfection concentration exponent. Yale J Biol Med. 12 (6), 697-704.

Craig RA, McCoy CP, Gorman SP, Jones DS. (2015). Photosensitisers – the progression from photodynamic therapy to anti-infective surfaces. Expert Opin. Drug Deliv. 12, 85–101.

Cristofari-Marquand E, Kacel M, Milhe F, Magnan A, Lehucher-Michel MP. (2007). Asthma caused by peracetic acid-hydrogen peroxide mixture. J. Occup. Health 49, 155–158.

Cudd LA, Burrows GE, Clarke CR. (1996). Pharmacokinetics and toxicity of tolonium chloride in sheep. Vet Hum Toxicol. 38 (5), 329-32.

D'hooge E, Becker P, Stubbe D, Normand AC, Piarroux R, Hendrickx M. (2018). Black aspergilli: A remaining challenge in fungal taxonomy? Med Mycol. 57 (6), 773–80.

Daly MJ, Gaidamakova EK, Matrosova VY, Vasilenko A, Zhai M, Venkateswaran A, Hess M, Omelchenko MV, Kostandarithes HM, Makarova KS, Wackett LP, Fredrickson JK, Ghosal D. (2004). Accumulation of Mn (II) in *Deinococcus radiodurans* facilitates gamma-radiation resistance. Science. 306 (5698), 1025-8.

Das S, Ray NM, Wan J, Khan A, Chakraborty T, Ray MB. (2017). Micropollutants in wastewater: fate and removal. In: Farroq Z, Ahmad F. Physico-Chemical Wastewater treatment and resource recovery. Rijeka: InTech. 81-2.

De Groote MA, Gibbs S, de Moura VC, Burgess W, Richardson K, Kasperbauer S, Madinger N, Jackson M. (2014). Analysis of a panel of rapidly growing mycobacteria for resistance to aldehyde-based disinfectants. Am J Infect Control. 42 (8), 932-4.

Decker EM, Bartha V, von Ohle C. (2017). Improvement of antibacterial efficacy through synergistic effect in photodynamic therapy based on thiazinium chromophores against planktonic and biofilm-associated periodontopathogens. Photomed Laser Surg. 35 (4), 195-205.

Delihas N, Riley LW, Loo W, Berkowitz J, Poltoratskaia N. (1995). High sensitivity of *Mycobacterium* species to the bactericidal activity by polylysine. FEMS Microbiol Lett. 132 (3), 233-7.

Delory, G. E., King, E., J. (1945). A sodium carbonate-bicarbonate buffer for alkaline phosphatases. Biochem J. 39 (3), 245.

Demidova TN, Hamblin MR. (2005a). Photodynamic inactivation of *Bacillus* spores, mediated by phenothiazinium dyes. Appl Environ Microbiol. 71 (11), 6918-25.

Demidova TN, Hamblin MR. (2005b). Effect of cell-photosensitizer binding and cell density on microbial photoinactivation. Antimicrob Agents Chemother. 49 (6), 2329-35.

Denyer SP, Maillard JY. (2002). Cellular impermeability and uptake of biocides and antibiotics in Gram-negative bacteria. J Appl Microbiol. 92, 35S-45S.

Denyer SP, Stewart GSAB. (1998). Mechanisms of action of disinfectants. Int. Biodeterior. Biodegradation 41, 261–268.

Denyer SP. (1990). Mechanisms of action of biocides. International Biodeterioration. 26 (2-4), 89-100.

Department of Health. (2016). Health technical memorandum 01-06: decontamination of flexible endoscopes. Part B: design and installation. Department of Health; London, UK.

Đermić D. (2015). Double-strand break repair mechanisms in *Escherichia coli*: recent insights. Adv Genomics Genet. 5, 35—42.

DeRosa MC, Crutchley RJ. (2002). Photosensitized singlet oxygen and its applications. Coord. Chem. Rev. 233, 351–71.

Dewanti R, Wong AC. (1995). Influence of culture conditions on biofilm formation by *Escherichia coli* O157:H7. Int J Food Microbiol. 62 (2), 147-64.

Di Ciccio P, Meloni D, Festino AR, Conter M, Zanardi E, Ghidini S, Vergara A, Mazzette R, Ianieri A. (2012). Longitudinal study on the sources of *Listeria monocytogenes* contamination in cold-smoked salmon and its processing environment in Italy. Int J Food Microbio. 158 (1), 79-84.

Di Stefano F, Siriruttanapruk S, McCoach JS, Burge PS. (1998). Occupational asthma due to glutaraldehyde. Monaldi Arch Chest Dis. 53 (1), 50-5.

Dimroth P, Kaim G, Matthey U. (2000). Crucial role of the membrane potential for ATP synthesis by F(1)F(o) ATP synthases. J Exp Biol. 203 (1), 51-9.

Diogo P, Fernandes C, Caramelo F, Mota M, Miranda IM5, Faustino MAF, Neves MGPMS, Uliana MP, de Oliveira KT, Santos JM, Gonçalves T. (2017). Antimicrobial photodynamic therapy against endodontic *Enterococcus faecalis* and *Candida albicans* mono and mixed biofilms in the presence of photosensitizers: a comparative study with classical endodontic irrigants. Front Microbiol. 8 (498).

dos Santos MM, Queiroz MJ, Baptista PV. (20). Enhancement of antibiotic effect via gold: silver-alloy nanoparticles. J Nanoparticle Res. 14, 859.

Drago L, Agrappi S, Bortolin M, Toscano M, Romanò CL, De Vecchi E. (2016). How to study biofilms after microbial colonization of materials used in orthopaedic implants. Int J Mol Sci. 17 (3), 293.

Dransfield R, Needham D. (2005). Applied Business. Oxford: Heineman Educational Publishers. 171.

Dreaden EC, Austin LA, Mackey MA, El-Sayed MA. (2012). Size matters: gold nanoparticles in targeted cancer drug delivery. Ther Deliv. 3 (4), 457-78.

Driessens N, Versteyhe S, Ghaddhab C, Burniat A, De Deken X, Van Sande J, Dumont JE, Miot F, Corvilain B. (2009). Hydrogen peroxide induces DNA single- and double-strand breaks in thyroid cells and is therefore a potential mutagen for this organ. Endocr Relat Cancer. 16 (3), 845-56.

Dufrêne YF. (2014). Atomic force microscopy in microbiology: new structural and functional insights into the microbial cell surface. MBio. 5 (4), e01363-14.

Dunipace AJ, Beaven R, Noblitt T, Li Y, Zunt S, Stookey G. (1992). Mutagenic potential of toluidine blue evaluated in the Ames test. Mutat Res. 279 (4), 255-9.

Durmuş M. (2011). Photochemical and Photophysical Characterization. In: Photosensitizers in Medicine, Environment, and Security. Dordrecht: Springer Netherlands. 135–266.

Durmuş Y, Büyükgüzel K. (2008). Biological and immune response of *Galleria mellonella* (Lepidoptera: Pyralidae) to sodium tetraborate. J Econ Entomol. 101 (3), 777-83.

Dwyer DJ, Camacho DM, Kohanski MA, Callura JM, Collins JJ. (2012). Antibiotic-induced bacterial cell death exhibits physiological and biochemical hallmarks of apoptosis. Mol Cell. 46 (5), 561-72.

Edbey K, Bader N, Eltaboni FB, Elabidi A, Albaba S, Ahmed M. (2015). Interactions Study between methyl violet and sodium dodecyl sulfate by conductometric and spectrophotometric methods. Int Res J Pure Appl Chem. 9 (4), 1-7.

Eichner A, Gollmer A, Späth A, Bäumler W, Regensburger J, König B, Maisch T. (2015). Fast and effective inactivation of *Bacillus atrophaeus* endospores using light-activated derivatives of vitamin B2. Photochem Photobiol Sci. 14 (2), 387-96.

Eisenman HC, Nosanchuk JD, Webber JB, Emerson RJ, Camesano TA, Casadevall A. (2005). Microstructure of cell wall-associated melanin in the human pathogenic fungus *Cryptococcus neoformans*. Biochemistry. 44 (10), 3683-93.

El Kirat K, Burton I, Dupres V, Dufrene YF. (2005). Sample preparation procedures for biological atomic force microscopy. J Microsc. 218 (3), 199-207.

Electrovision. (2019). LED RGB flood light with wireless infrared controller. Available from: https://www.electrovision.co.uk/homepage.aspx?com=product&productid=3409&pg=2962&tl=1187 [*Last accessed: 04/11/2019*].

Elias P. M., Feingold K. R. (2006). Stratum corneum barrier function: definitions and broad concepts. In: Elias P. M., Feingold K. R. Skin Barrier. New York: Taylor & Francis. 1-3.

Elliott ML. (1995). Effect of melanin biosynthesis inhibiting compounds on *Gaeumannomyces* species. Mycologia. 87 (3), 370-4.

Engelmann MD, Bobier RT, Hiatt T, Cheng IF. (2003). Variability of the Fenton reaction characteristics of the EDTA, DTPA, and citrate complexes of iron. Biometals. 16 (42), 519-27.

Englander J, Klein E, Brumfeld V, Sharma AK, Doherty AJ, Minsky A. (2004). DNA toroids: framework for DNA repair in *Deinococcus radiodurans* and in germinating bacterial spores. J Bacteriol. 186 (18), 5973-7.

Environmental Protection Agency. (2009). EPA's Safer Choice standard. February 2015 revision. Available from: https://www.epa.gov/sites/production/files/2013-12/documents/standard-for-safer-products.pdf [*Last accessed: 21/10/2019*].

Environmental Protection Agency. (2019). Safer Chemical Ingredients List. Available from: https://www.epa.gov/saferchoice/safer-ingredients [*Last accessed: 21/10/2019*].

Epe B, Pflaum M, Boiteux S. (1993). DNA damage induced by photosensitizers in cellular and cell-free systems. Mutat Res. 299 (3-4), 135-45.

Epstein W. (2003). The roles and regulation of potassium in bacteria. Prog Nucleic Acid Res Mol Biol. 75, 293-320.

Esbelin J, Mallea S, Ram AF, Carlin F. (2013). Role of pigmentation in protecting *Aspergillus niger* conidiospores against pulsed light radiation. Photochem Photobiol. 89 (3), 758-61.

European Chemicals Agency. (2017). Guidance on the Biocidal Products Regulation. Volume IV Environment - Assessment and Evaluation (Parts B + C). Version 2.0. European Chemicals Agency; Helsinki.

European Chemicals Agency. (2019a). List of active substances and suppliers. Information on biocides. Available from: https://echa.europa.eu/information-on-chemicals/active-substance-suppliers [*Last accessed: 25/10/2019*].

European Chemicals Agency. (2019b). Substance information. Tolonium chloride. Available from: https://echa.europa.eu/substance-information/-/substanceinfo/100.001.952 [*Last accessed*: 04/11/2019].

European Chemicals Agency. (2019c). Substance information. Sodium carbonate. Available from: https://echa.europa.eu/substance-information/-/substanceinfo/100.007.127 [*Last accessed*: 04/11/2019].

European Commission Joint Research Centre. (2002). European Union Risk Assessment Report: dimethyl sulphate. Available from: https://op.europa.eu/en/publication-detail/-/publication/d45d72f1-a7e6-11e7-837e-01aa75ed71a1 [*Last accessed: 21/10/2019*].

European Commission. (2017). Commission Decision (EU) 2017/1217 of 23 June 2017 establishing the EU Ecolabel criteria for hard surface cleaning products. Available from: https://eur-lex.europa.eu/eli/dec/2017/1217/oj [*Last accessed: 05/10/2019*]

European Medicines Agency. (2017). European Medicines Agency decision P/0370/2017. Available from: https://www.ema.europa.eu/en/medicines/human/paediatric-investigation-plans/emea-002170-pip01-17 [*Last accessed: 21/10/2019*].

European Parliament, Council of the European Union. (2012). Regulation (EU) no 528/2012 of the European Parliament and of the Council of 22 May 2012 concerning the making available on the market and use of biocidal products. Available from: https://eur-lex.europa.eu/legal-content/EN/TXT/?uri=CELEX%3A32012R0528 [*Last accessed*: *04/11/2019*]

Eustis S, el-Sayed MA. (2006). Why gold nanoparticles are more precious than pretty gold: noble metal surface plasmon resonance and its enhancement of the radiative and nonradiative properties of nanocrystals of different shapes. Chem Soc Rev. 35 (3), 209-17.

Faller M, Niederweis M, Schulz GE. (2004). The structure of a mycobacterial outer-membrane channel. Science. 303 (5661), 1189-92.

Feese E, Ghiladi RA. (2009). Highly efficient in vitro photodynamic inactivation of *Mycobacterium smegmatis*. J Antimicrob Chemother. 64 (4), 782-5.

Felle H, Porter JS, Slayman CL, Kaback HR. (1980). Quantitative measurements of membrane potential in *Escherichia coli*. Biochemistry. 19 (15), 3585-90.

Finnegan M, Linley E, Denyer SP, McDonnell G, Simons C, Maillard JY. (2010). Mode of action of hydrogen peroxide and other oxidizing agents: differences between liquid and gas forms. J Antimicrob Chemother. 65 (10), 2108-15.

Firquet S, Beaujard S, Lobert PE, Sané F, Caloone D, Izard D, Hober D. (2015). Survival of enveloped and non-enveloped viruses on inanimate surfaces. Microbes Environ. 30 (2), 140-4.

Fisher CW, Fiorello A, Shaffer D, Jackson M, McDonnell GE. (2012). Aldehyde-resistant mycobacteria bacteria associated with the use of endoscope reprocessing systems. Am. J. Infect. Control 40, 880–882.

Fitt B, Thornley J. (2002). Light Measurements. In: Lighting Technology. 2nd ed. Oxford: Focal Press. 42-3.

Food Processing Technology. (2011). Handle with care: conveyors and food handling. Available online: https://www.foodprocessing-technology.com/features/feature123151/. [*Last accessed: 20/10/2019*]

Forsberg K, Woodworth K, Walters M, Berkow EL, Jackson B, Chiller T, Vallabhaneni S. (2019). *Candida auris*: the recent emergence of a multidrug-resistant fungal pathogen. Med Mycol. 57 (1), 1-12.

Fraise AP. (2013). Chapter 2: Types of microbicidal and microbistatic agents. In: Fraise AP, Maillard J, Sattar SA Russell, Hugo & Ayliffe's: principles and practice of disinfection, preservation and sterilization. 5th ed. Chichester; UK: Blackwell Publishing Ltd. 24.

Fraud S, Hann AC, Maillard JY, Russell AD. (2003). Effects of ortho-phthalaldehyde, glutaraldehyde and chlorhexidine diacetate on *Mycobacterium chelonae* and *Mycobacterium abscessus* strains with modified permeability. J Antimicrob Chemother. 51 (3), 575-84.

Fraud S, Maillard JY, Russell AD. (2001). Comparison of the mycobactericidal activity of ortho- phthalaldehyde, glutaraldehyde and other dialdehydes by a quantitative suspension test. J Hosp Infect. 48 (3), 214-21.

Fraud S, Rees EL, Mahenthiralingam E, Russell AD, Maillard JY. (2003). Aromatic alcohols and their effect on Gram-negative bacteria, cocci and mycobacteria. J Antimicrob Chemother. 51 (6), 1435-6.

Frenzel E, Schmidt S, Niederweis M, Steinhauer K. (2011). Importance of porins for biocide efficacy against *Mycobacterium smegmatis*. Appl Environ Microbiol. 77 (9), 3068-73.

Friedberg JS, Skema C, Baum ED, Burdick J, Vinogradov SA, Wilson DF, Horan AD, Nachamkin I. (2001). In vitro effects of photodynamic therapy on *Aspergillus fumigatus*. J Antimicrob Chemother. 48 (1), 105-7.

Gad F, Zahra T, Hasan T, Hamblin MR. (2004). Effects of growth phase and extracellular slime on photodynamic inactivation of gram-positive pathogenic bacteria. Antimicrob Agents Chemother. 48 (6), 2173-8.

Gander P. (2016). Food safety update: biocides defy clean definition. Food manufacture. Available from: https://www.foodmanufacture.co.uk/Article/2016/09/13/Food-safety-update-biocides-in-focus [*Last accessed 21/10/2019*].

García MT, Campos E, Ribosa I. (2007). Biodegradability and ecotoxicity of amine oxide based surfactants. Chemosphere. 69 (10), 1574-8.

García MT, Campos E, Sánchez-Leal J, Ribosa I. (2000). Anaerobic degradation and toxicity of commercial cationic surfactants in anaerobic screening tests. Chemosphere. 41 (5), 705-10.

Geissdörfer W, Sandner G, John S, Gessner A, Schoerner C, Schröppel K. (2008). *Ureaplasma urealyticum* meningitis in an adult patient. J Clin Microbiol. 46 (3), 1141-3.

Gélinas P, Goulet J. (1983). Neutralization of the activity of eight disinfectants by organic matter. J Appl Bacteriol. 54 (2), 243-7.

George S, Hamblin MR, Kishen A. (2009). Uptake pathways of anionic and cationic photosensitizers into bacteria. Photochem Photobiol Sci. 8 (6), 788-95.

Gerba CP. (2015). Quaternary ammonium biocides: efficacy in application. Appl Environ Microbiol. 81 (2), 464-9.

Ghorbani J, Rahban D, Aghamiri S, Teymouri A, Bahador A. (2018). Photosensitizers in antibacterial photodynamic therapy: an overview. Laser Ther. 27 (4), 293-302.

Ghosh S, Setlow B, Wahome PG, Cowan AE, Plomp M, Malkin AJ, Setlow P. (2008). Characterization of spores of *Bacillus subtilis* that lack most coat layers. J Bacteriol. 190 (20), 6741-8.

Gimenez-Conti IB, Slaga TJ. (1993). The hamster cheek pouch carcinogenesis model. J Cell Biochem Suppl. 17F, 83-90.

Giraldo G. (2019). FEA for beginners. Available from: https://www.simscale.com/blog/2019/05/fea-for-beginners/ [Last accessed: 13/11/2019].

Girotti AW, Kriska T. (2004). Role of lipid hydroperoxides in photo-oxidative stress signaling. Antioxid Redox Signal. 6 (2), 301-10.

Glaser K, Silwedel C, Fehrholz M, Waaga-Gasser AM, Henrich B, Claus H, Speer CP. (2017). *Ureaplasma* species differentially modulate pro- and anti-inflammatory cytokine responses in newborn and adult human monocytes pushing the state toward pro-inflammation. Front Cell Infect Microbiol. 7 (484).

Golding CG, Lamboo LL, Beniac DR, Booth TF. (2016). The scanning electron microscope in microbiology and diagnosis of infectious disease. Sci Rep. 6 (26516).

Gomes MC, Woranovicz-Barreira SM, Faustino MA, Fernandes R, Neves MG, Tomé AC, Gomes NC, Almeida A, Cavaleiro JA, Cunha A, Tomé JP. (2011). Photodynamic inactivation of *Penicillium chrysogenum* conidia by cationic porphyrins. Photochem Photobiol Sci. 10 (11), 1735-43.

Gonzales FP, da Silva SH, Roberts DW, Braga GU. (2010). Photodynamic inactivation of conidia of the fungi *Metarhizium anisopliae* and *Aspergillus nidulans* with methylene blue and toluidine blue. Photochem Photobiol. 86 (3), 653-61.

Gordon P. 2018. UV-C LEDs for Food Safety. IUVA News. 20 (2). Available online: https://iuvanews.com/stories/pdf/IUVA_2018_Quarter2_full_Gordon_links.pdf [*Last accessed: 22/10/2019*].

Gorman SP, Scott EM. (1979). Potentiation and stabilization of glutaraldehyde biocidal activity utilizing surfactant-divalent cation combinations. Int J Pharm. 4 (1), 57-65.

Green MR, Sambrook J. (2016). Precipitation of DNA with ethanol. Cold Spring Harb Protoc. 2016 (12).

Griffiths PA, Babb JR, Bradley CR, Fraise AP. (1997). Glutaraldehyde-resistant Mycobacterium chelonae from endoscope washer disinfectors. J Appl Microbiol. 82 (4), 519-26.

Gubler JG, Salfinger M, von Graevenitz A. (1992). Pseudoepidemic of nontuberculous mycobacteria due to a contaminated bronchoscope cleaning machine. Report of an outbreak and review of the literature. Chest. 101 (5), 1245-9.

Hale MF, Sidhu R, McAlindon ME. (2014). Capsule endoscopy: current practice and future directions. World J Gastroenterol. 20 (24), 7752-9.

Hamal DB, Haggstrom JA, Marchin GL, Ikenberry MA, Hohn K, Klabunde KJ. (2010). A multifunctional biocide/sporocide and photocatalyst based on titanium dioxide (TiO2) codoped with silver, carbon, and sulfur. Langmuir. 26 (4), 2805-10.

Hamblin MR, Hasan T. (2004). Photodynamic therapy: a new antimicrobial approach to infectious disease? Photochem Photobiol Sci. 3 (5), 436-50.

Hamilton AJ, Holdom MD. (1999). Antioxidant systems in the pathogenic fungi of man and their role in virulence. Med Mycol. 37 (6), 375-89.

Hansen MT. (1978). Multiplicity of genome equivalents in the radiation-resistant bacterium *Micrococcus radiodurans*. J Bacteriol. 134 (1), 71-5.

Harrison JJ, Turner RJ, Joo DA, Stan MA, Chan CS, Allan ND, Vrionis HA, Olson ME, Ceri H. (2008). Copper and quaternary ammonium cations exert synergistic bactericidal and antibiofilm activity against *Pseudomonas aeruginosa*. Antimicrob Agents Chemother. 52 (8), 2870-81.

Hashimoto A, Hagiwara D, Watanabe A, Yahiro M, Yikelamu A, Yaguchi T, Kamei K. (2017). Drug sensitivity and resistance mechanism in *Aspergillus* section nigri strains from Japan. Antimicrob Agents Chemother. 61 (8), e02583-16.

Hassaan M, El Nemr A. (2017). Health and environmental impacts of dyes: mini review. Am J Environ Sci. 1 (3), 64-7.

Hassan C, Benamouzig R, Spada C, Ponchon T, Zullo A, Saurin JC, Costamagna G. (2011). Cost effectiveness and projected national impact of colorectal cancer screening in France. Endoscopy. 43 (9), 780-93.

Hazrin-Chong NH, Manefield M. (2012). An alternative SEM drying method using hexamethyldisilazane (HMDS) for microbial cell attachment studies on sub-bituminous coal. J Microbiol Methods. 90 (2), 96-9.

Health and Safety Executive (2013). Control of substances hazardous to health. The control of substances hazardous to health regulations 2002 (as amended). Approved code of practice and guidance. 6th ed. 20-28

Health and Safety Executive. (2019). An Introduction to Active Substance Approval and Product Authorisation. Available from: http://www.hse.gov.uk/pesticides/topics/pesticide-approvals/pesticides-registration/general/introduction-to-active-substance-approval.htm [*Last accessed: 02/11/2019*].

Heath RJ, Rubin JR, Holland DR, Zhang E, Snow ME, Rock CO. (1999). Mechanism of triclosan inhibition of bacterial fatty acid synthesis. J Biol Chem. 274 (16), 11110-4.

Henn SA, Boiano JM, Steege AL. (2015). Precautionary Practices of Healthcare Workers Who Disinfect Medical and Dental Devices Using High-Level Disinfectants. Infect. Control Hosp. Epidemiol. 36, 180–185.

Henoun Loukili N, Lemaitre N, Guery B, Gaillot O, Chevalier D, Mortuaire G. (2017). Is a chlorine dioxide wiping procedure suitable for the high-level disinfection of nasendoscopes? J Infect Prev. 18 (2), 78-83.

HERA. 2005. Human and Environmental Risk Assessment on Ingredients of Household Cleaning Products. Sodium carbonate: edition 2.0. Available from: https://www.heraproject.com/RiskAssessment.cfm?SUBID=10 [*Last accessed: 10/10/2019*].

HERA. 2008. Human and Environmental Risk Assessment on Ingredients of Household Cleaning Products. Esterquats: Environmental Risk Assessment Report. Available from: https://www.heraproject.com/RiskAssessment.cfm?SUBID=17 [*Last accessed: 21/10/2019*].

HERA. 2009a. Human and Environmental Risk Assessment on Ingredients of Household Cleaning Products. Alcohol Ethoxylates: version 2.0. Available from: https://www.heraproject.com/RiskAssessment.cfm?SUBID=34 [*Last accessed: 21/10/2019*].

HERA. 2009b. Human and Environmental Risk Assessment on Ingredients of Household Cleaning Products. Esterquats: Human Health Risk Assessment Report. Available from: https://www.heraproject.com/RiskAssessment.cfm?SUBID=17 [*Last accessed: 21/10/2019*].

HERA. 2019. HERA Initiative. Available from: https://www.heraproject.com/Initiative.cfm [*Last accessed: 10/10/2019*].

Hett EC, Rubin EJ. (2008). Bacterial growth and cell division: a mycobacterial perspective. Microbiol Mol Biol Rev. 72 (1), 126-56.

Hillitt KL, Jenkins RE, Spiller OB, Beeton ML. (2017). Antimicrobial activity of Manuka honey against antibiotic-resistant strains of the cell wall-free bacteria *Ureaplasma parvum* and *Ureaplasma urealyticum*. Lett Appl Microbiol. 64 (3), 198-202.

Hönes K, Stangl F, Sift M, Hessling M. (2015). Visible optical radiation generates bactericidal effect applicable for inactivation of health care associated germs demonstrated by inactivation of *E. coli* and *B. subtilis* using 405-nm and 460-nm light emitting diodes. Proc SPIE. 9540, 95400T.

Horm KM, D'Souza DH. (2011). Survival of human norovirus surrogates in milk, orange, and pomegranate juice, and juice blends at refrigeration (4 °C). Food Microbiol. 28 (5), 1054-61.

Houas A, Lachheb H, Ksibi M, Elaloui E, Guillard C, Herrmann JM. (2001). Photocatalytic degradation pathway of methylene blue in water. Appl Catal B Environ. 31 (2), 145-57.

Hu H, Johani K, Gosbell IB, Jacombs AS, Almatroudi A, Whiteley GS, Deva AK, Jensen S, Vickery K. (2015). Intensive care unit environmental surfaces are contaminated by multidrug-resistant bacteria in biofilms: combined results of conventional culture, pyrosequencing, scanning electron microscopy, and confocal laser microscopy. J Hosp Infect. 91 (1), 35-44.

Huang KC, Mukhopadhyay R, Wen B, Gitai Z, Wingreen NS. (2008). Cell shape and cell-wall organization in Gram-negative bacteria. Proc Natl Acad Sci USA. 105 (49), 19282-7.

Hutcheson R, Engelmann MD, Cheng IF. (2004). A hypothesis for the basis of the pro-oxidant nature of calcium ions. Biometals. 17 (6), 605-13.

Hyldgaard M, Mygind T, Vad BS, Stenvang M, Otzen DE, Meyer RL. (2014). The antimicrobial mechanism of action of epsilon-poly-l-lysine. Appl Environ Microbiol. 80 (24), 7758-70.

Ioannou CJ, Hanlon GW, Denyer SP. (2007). Action of disinfectant quaternary ammonium compounds against *Staphylococcus aureus*. Antimicrob Agents Chemother. 51 (1), 296-306.

Jackson JC, Higgins LA, Lin X. (2009). Conidiation color mutants of *Aspergillus fumigatus* are highly pathogenic to the heterologous insect host Galleria mellonella. PLoS One. 4 (1), e4224.

Jami M, Ghanbari M, Zunabovic M, Domig KJ, Kneifel W. (2014). *Listeria monocytogenes* in aquatic food products-a review. Compr Rev Food Sci Food Saf. 13 (5), 798–813.

Jankute M, Cox JA, Harrison J, Besra GS. (2015). Assembly of the Mycobacterial Cell Wall. Annu Rev Microbiol. 69, 405-23.

Jarlier V, Nikaido H. (1990). Permeability barrier to hydrophilic solutes in *Mycobacterium chelonei*. J Bacteriol. 172 (3), 1418-23.

Jebaramya J, Ilanchelian M, Prabahar S. (2009). Spectral studies of toluidine blue O in the presence of sodium dodecyl sulfate. Dig J Nanomater Bios. 4 (4), 789-97.

Jeevanandam J, Barhoum A, Chan YS, Dufresne A, Danquah MK. (2018). Review on nanoparticles and nanostructured materials: history, sources, toxicity and regulations. Beilstein J Nanotechnol. 9, 1050-74.

Jensen JS. (2016). 186 - Mycoplasma and Ureaplasma. In: Cohen J, Powderly WG, Opal SM Infectious Diseases. 4th ed. Elsevier. 1660-5.

Jeonga Y, Kook YM, Lee K, Koh WG. (2018). Metal enhanced fluorescence (MEF) for biosensors: General approaches and a review of recent developments. Biosens Bioelectron. 111, 102-116.

Johani K, Abualsaud D, Costa DM, Hu H, Whiteley G, Deva A, Vickery K. (2018). Characterization of microbial community composition, antimicrobial resistance and biofilm on intensive care surfaces. J Infect Public Health. 11 (3), 418-24.

Johnston MD, Hanlon GW, Denyer SP, Lambert RJ. (2003). Membrane damage to bacteria caused by single and combined biocides. J Appl Microbiol. 94 (6), 1015-23.

Kartmann B, Stenger S, Niederweis M. (1999). Porins in the cell wall of *Mycobacterium tuberculosis*. J Bacteriol. 181 (20), 6543-6.

Kashef N, Ravaei Sharif Abadi G, Djavid GE. (2012). Phototoxicity of phenothiazinium dyes against methicillin-resistant Staphylococcus aureus and multi-drug resistant Escherichia coli. Photodiagnosis Photodyn Ther. 9 (1), 11-5.

Kasimova KR, Sadasivam M, Landi G, Sarna T, Hamblin MR. (2014). Potentiation of photoinactivation of Gram-positive and Gram-negative bacteria mediated by six phenothiazinium dyes by addition of azide ion. Photochem Photobiol Sci. 13 (11), 1541-8.

Katz M. (1994). Introduction to Geometrical Optics. Singapore: World Scientific. 15.

Kawai M, Yamagishi J. (2009). Mechanisms of action of acriflavine: electron microscopic study of cell wall changes induced in *Staphylococcus aureus* by acriflavine. Microbiol Immunol. 53 (9), 481-6.

Kean R, Sherry L, Townsend E, McKloud E, Short B, Akinbobola A, Mackay WG, Williams C, Jones BL, Ramage G. (2018). Surface disinfection challenges for *Candida auris*: an in-vitro study. J Hosp Infect. 98 (4), 433-6.

Khalsa K, Smith A, Morrison P, Shaw D, Peat M, Howard P, Hamilton K, Stewart A.. (2014). Contamination of a purified water system by *Aspergillus fumigatus* in a new endoscopy reprocessing unit. Am J Infect Control. 42 (12), 1337-9.

Kibbe, A.H. (2009). Benzalkonium Chloride Monograph. In: Handbook of Pharmaceutical Excipients. 6th ed. London: Pharmaceutical Press. 56-8.

Kim SJ, Baek IH. (2012). Colonic Mucosal Pseudolipomatosis. Gastroenterol. Nurs. 35, 208–213.

King J, Brunel SF, Warris A. (2016). *Aspergillus* infections in cystic fibrosis.. J Infect. 72, S50-5.

Kinsella TJ, Colussi VC, Oleinick NL, Sibata CH. (2001). Photodynamic therapy in oncology. Expert Opin. Pharmacother. 2, 917–27.

Kirstensen A, Yang JKW, Bozhevolnyi SI, Link S, Nordlander P, Halas NJ, Mortensen A. (2016). Plasmonic colour generation. Nat Rev Mater. 2 (16008).

Köhle H, Kottke U, Dirk K, Dietmar T, Kurt S, Axel E. (2016). Fabric softener active composition and method for making it. Patent No. EP2847307. Available from: http://www.freepatentsonline.com/EP2847307.html [*Last accessed: 18/10/2019*].

Kömerik N, Wilson M, Poole S. (2000). The effect of photodynamic action on two virulence factors of gram-negative bacteria. Photochem Photobiol. 72 (5), 676-80.

Kömerik N, Wilson M. (2002). Factors influencing the susceptibility of Gram-negative bacteria to toluidine blue O-mediated lethal photosensitization. J Appl Microbiol. 92 (4), 618-23.

Konola JT, Sargent KE, Gow JB. (2000). Efficient repair of hydrogen peroxide-induced DNA damage by *Escherichia coli* requires SOS induction of RecA and RuvA proteins. Mutat Res. 459 (3), 187-94.

Konopka K, Goslinski T. (2007). Photodynamic therapy in dentistry. J. Dent. Res. 86, 694–707.

Kostka, M., Zimcik, P., Miletin, M., Klemera, P., Kopecky, K., and Musil, Z. (2006). Comparison of aggregation properties and photodynamic activity of phthalocyanines and azaphthalocyanines. J. Photochem. Photobiol. A Chem. 178, 16–25.

Kotiaho A, Lahtinen R, Efimov A, Metsberg HK, Sariola E, Lehtivuori H, Tkachenko NV, Lemmetyinen H. (2009). photoinduced charge and energy transfer in phthalocyanine-functionalized gold nanoparticles. J Phys Chem C. 114 (1), 162-8.

Kressel AB, Kidd F. (2001). Pseudo-outbreak of Mycobacterium chelonae and Methylobacterium mesophilicum caused by contamination of an automated endoscopy washer. Infect Control Hosp Epidemiol. 22 (7), 414-8.

Kreuzer KN. (2013). DNA damage responses in prokaryotes: regulating gene expression, modulating growth patterns, and manipulating replication forks. Cold Spring Harb Perspect Biol. 5 (11), a012674.

Krijgsheld P, Bleichrodt R, van Veluw GJ, Wang F, Müller WH, Dijksterhuis J, Wösten HA. (2013). Development in *Aspergillus*. Stud Mycol. 74 (1), 1-29.

Kronberg B, Holmberg K, Lindman B (2014). Surface Chemistry of Surfactants and Polymers. Chichester; UK: John Wiley & Sons. 2.

Kubacka A, Diez MS, Rojo D, Bargiela R, Ciodia S, Zapico I, Albar JP, Barbas C, Martins dos Santos, VAP, Fernández-García M, Ferrer M. (2014). Understanding the antimicrobial mechanism of TiO2-based nanocomposite films in a pathogenic bacterium. Sci Rep. 4 (4134).

Lambert RJ, Hanlon GW, Denyer SP. (2004). The synergistic effect of EDTA/antimicrobial combinations on *Pseudomonas aeruginosa*. J Appl Microbiol. 96 (2), 244-53.

Langfelder K, Streibel M, Jahn B, Haase G, Brakhage AA. (2003). Biosynthesis of fungal melanins and their importance for human pathogenic fungi. Fungal Genet Biol. 38 (2), 143-58.

Lasance CJM. (2014). Heat sinks from an industrial point of view. In: Lasance CJM, Poppe A. Thermal Management for LED Applications. New York: Springer. 347-8.

Laube T. (2017). Sourcing PAA for poultry processing in the wake of Hurricane Harvey. Poultry Health Today. 7. Available from https://poultryhealthtoday.com/wp-content/uploads/2017/11/Hurricane-Harvey-Poultry-Health-Today-Toolbox-7-FINAL.pdf [*Last accessed: 22/10/2019*].

Ledwoch K, Maillard JY. (2018). *Candida auris* dry surface biofilm (dsb) for disinfectant efficacy testing. Materials (Basel). 12 (1), E18.

Ledwoch K, Said J, Norville P, Maillard JY. (2019). Artificial dry surface biofilm models for testing the efficacy of cleaning and disinfection. Lett Appl Microbiol. 68 (4), 329-36.

Lee MT, Bird PS, Walsh LJ. (2004). Photo-activated disinfection of the root canal: a new role for lasers in endodontics. Aust Endod J. 30 (4), 93-8.

Leggett MJ, Schwarz JS, Burke PA, McDonnell G, Denyer SP, Maillard JY. (2016a). Mechanism of sporicidal activity for the synergistic combination of peracetic acid and hydrogen peroxide. Appl. Environ. Microbiol. 82, 1035–1039.

Leggett MJ, Setlow P, Sattar SA, Maillard JY. (2016b). Assessing the activity of microbicides against bacterial spores: knowledge and pitfalls. J Appl Microbiol. 120 (5), 1174-80.

Lejoy A, Arpita R, Krishna B, Venkatesh N. (2016). Methylene blue as a diagnostic aid in the early detection of potentially malignant and malignant lesions of oral mucosa. Ethiop J Health Sci. 26 (3), 201-8.

Leong D, Alvarez-Ordóñez A, Zaouali S, Jordan K. (2015). Examination of *Listeria monocytogenes* in seafood processing facilities and smoked salmon in the Republic of Ireland. J Food Prot. 78 (12), 2184-90.

Levin-Zaidman S, Englander J, Shimoni E, Sharma AK, Minton KW, Minsky A. (2003). Ringlike structure of the *Deinococcus radiodurans* genome: a key to radioresistance? Science. 299 (5604), 254-6.

Lewis K. (2005). Persister cells and the riddle of biofilm survival. Biochemistry (Mosc). 70 (2), 267-74.

Li F, Weir MD, Xu HH. (2013). Effects of quaternary ammonium chain length on antibacterial bonding agents. J Dent Res. 92 (10), 932-8.

Li Y, Han Q, Jian-Ling F, Tian WL, Mo HZ. (2011). Antibacterial characteristics and mechanisms of ε-poly-lysine against *Escherichia coli* and *Staphylococcus aureus*. Food Control. 43, 22-7.

Liau SY, Read DC, Pugh WJ, Furr JR, Russell AD. (1997). Interaction of silver nitrate with readily identifiable groups: relationship to the antibacterial action of silver ions. Lett Appl Microbiol. 25 (4), 279-83.

Lindsay D, Brözel VS, Mostert JF, von Holy A. (2002). Differential efficacy of a chlorine dioxide-containing sanitizer against single species and binary biofilms of a dairy-associated *Bacillus cereus* and a *Pseudomonas fluorescens* isolate. J Appl Microbiol. 92 (2), 352-61.

Lindstedt M, Allenmark S, Thompson RA, Edebo L. (1990). Antimicrobial activity of betaine esters, quaternary ammonium amphiphiles which spontaneously hydrolyze into nontoxic components. Antimicrob Agents Chemother. 34 (10), 1949-54.

Linley E, Denyer SP, McDonnell G, Simons C, Maillard JY. (2012). Use of hydrogen peroxide as a biocide: new consideration of its mechanisms of biocidal action. J Antimicrob Chemother. 67 (7), 1589–96.

Liu H, Du Y, Wang X, Sun L. (2002). Chitosan kills bacteria through cell membrane damage. Int J Food Microbiol. 95 (2), 147-55.

Liu Z, Lin Y, Lu Q, Li F, Yu J, Wang Z, He Y, Song C. (2017). In vitro and in vivo activity of EDTA and antibacterial agents against the biofilm of mucoid *Pseudomonas aeruginosa*. Infection. 45 (1), 23-31.

Loo DT. (2002) TUNEL Assay. In: Didenko VV In Situ Detection of DNA Damage. Methods in Molecular Biology, vol 203. Humana Press. 21-30.

Loo DT. (2011). In situ detection of apoptosis by the TUNEL assay: an overview of techniques. Methods Mol Biol. 682, 3-13.

Lu LS, Wu KL, Chiu YC, Lin MT, Hu TH, Chiu KW. (2012). Swab culture monitoring of automated endoscope reprocessors after high-level disinfection. World J Gastroenterol. 18 (14), 1660-3.

Luksiene Z, Brovko L. (2013). Antibacterial photosensitization-based treatment for food safety. Food Eng Rev. 5 (4), 185-99.

Luppens SB, Abee T, Oosterom J. (2001). Effect of benzalkonium chloride on viability and energy metabolism in exponential- and stationary-growth-phase cells of *Listeria monocytogenes*. J Food Prot. 64 (3), 476-82.

Lynch M, Marinov GK. (2017). Membranes, energetics, and evolution across the prokaryote-eukaryote divide. Elife. 6 (2), e20437.

Maclean M, Murdoch LE, MacGregor SJ, Anderson JG. (2013). Sporicidal effects of high-intensity 405 nm visible light on endospore-forming bacteria. Photochem Photobiol. 89 (1), 120-6.

Mah TF, O'Toole GA. (2001). Mechanisms of biofilm resistance to antimicrobial agents. Trends Microbiol. 9 (1), 34-9.

Mahfouz GN, Brijmohan S, Paczkowski M, Belock C. 2017. Thickener for cationic disinfectants. Patent: 000249345D. Available from: https://priorart.ip.com/IPCOM/000249345 [*Last accessed: 21/10/2019*].

Maibaum L, Dinner AR, Chandler D. (2004). Micelle formation and the hydrophobic effect. J Phys Chem B. 107 (21), 6778-81.

Maillard JY, Beggs TS, Day MJ, Hudson RA, Russell AD. (1996). Damage to *Pseudomonas aeruginosa* PAO1 bacteriophage F116 DNA by biocides. J Appl Bacteriol. 80 (5), 540-4.

Maillard JY. (2011). Innate resistance to sporicides and potential failure to decontaminate. J Hosp Infect. 77 (3), 204-9.

Maillard JY. (2013). Factors affecting the activities of microbicides. In: Fraise AP, Maillard J, Sattar SA Russell, Hugo & Ayliffe's Principles and Practice of Disinfection, Preservation and Sterilization. 5th ed. Chichester; UK: Wiley-Blackwell. 71-107.

Majiya H, Adeyemi OO, Stonehouse NJ, Millner P. (2018). Photodynamic inactivation of bacteriophage MS2: The A-protein is the target of virus inactivation. J Photochem Photobiol B. 178, 404-11.

Malone M. (2017). Chapter 3 - The microbiome of diabetic foot ulcers and the role of biofilms. In: Kon K, Rai M, The microbiology of skin, soft tissue, bone and joint infections. London: Academic Press. 41-56.

Mapp L, Chambers Y, Takundwa P, Hill VR, Schneeberger C, Knee J, Raynor M, Klonicki P, Miller K, Pope M, Hwang N. (2016). Inter-laboratory evaluation and successful implementation of MS2 coliphage as a surrogate to establish proficiency using a BSL-3 procedure. Water. 8 (248).

Marian CM. (2012). Spin-orbit coupling and intersystem crossing in molecules. Wiley Interdiscip. Rev. Comput. Mol. Sci. 2, 187–203.

Martin DJH, Denyer SP, McDonnell G, Maillard JY. (2008). Resistance and cross-resistance to oxidising agents of bacterial isolates from endoscope washer disinfectors. J. Hosp. Infect. 69, 377–383.

Masoumi H, Safavi SM, Khani Z. (2012). Identification and classification of plastic resins using near infrared reflectance spectroscopy. IJMME. 6 (5), 877-84.

Masschalck B, Michiels CW. (2003). Antimicrobial properties of lysozyme in relation to foodborne vegetative bacteria. Crit Rev Microbiol. 29 (3), 191-214.

Maul RW, Sutton MD. (2005). Roles of the *Escherichia coli* RecA protein and the global SOS response in effecting DNA polymerase selection in vivo. J Bacteriol. 187 (22), 7607-18.

McDonnell G, Burke P. (2011). Disinfection: is it time to reconsider Spaulding? J Hosp Infect. 78 (3), 163-70.

McDonnell G, Russell AD. (1991). Antiseptics and disinfectants: activity, action, and resistance. Clin Microbiol Rev. 12 (1), 147-79.

McHugh ML. (2011). Multiple comparison analysis testing in ANOVA. Biochem Med (Zagreb). 21 (3), 203-9.

McKenney PT, Driks A, Eskandarian HA, Grabowski P, Guberman J, Wang KH, Gitai Z, Eichenberger P. (2010). A distance-weighted interaction map reveals a previously uncharacterized layer of the *Bacillus subtilis* spore coat. Curr Biol. 20 (10), 934-8.

Meltzer AC, Ward MJ, Gralnek IM, Pines JM. (2014). The cost-effectiveness analysis of video capsule endoscopy compared to other strategies to manage acute upper gastrointestinal hemorrhage in the ED. Am J Emerg Med. 32 (8), 823-32.

Mertins O, Bacellar IO, Thalmann F, Marques CM, Baptista MS, Itri R. (2014). Physical damage on giant vesicles membrane as a result of methylene blue photoirradiation. Biophys J. 106 (1), 162-71.

Migneault I, Dartiguenave C, Bertrand MJ, Waldron KC. (2004). Glutaraldehyde: Behavior in aqueous solution, reaction with proteins, and application to enzyme crosslinking. Biotechniques 37, 790–802.

Miles AA, Misra SS, Irwin JO. (1938). The estimation of the bactericidal power of the blood. J Hyg (Lond). 38 (6), 732-49.

Minnock A, Vernon DI, Schofield J, Griffiths J, Parish JH, Brown ST. (1996). Photoinactivation of bacteria. Use of a cationic water-soluble zinc phthalocyanine to photoinactivate both gram-negative and gram-positive bacteria. J Photochem Photobiol B. 32 (3), 159-64.

Minsky A, Shimoni E, Englander J. (2006). Ring-like nucleoids and DNA repair through error-free nonhomologous end joining in *Deinococcus radiodurans*. J Bacteriol. 188 (17), 6047-51.

Mironyuk S, Smirnov S, Sokolov AV, Proshkin Y. (2019). Optimisation of spectral composition and energy economy effectiveness of phyto-irradiators with digital technologies. In: Kharchenko, V., Vasant, P. Handbook of Research on Energy-Saving Technologies for Environmentally-Friendly Agricultural Development. Hershey: IGI Global. 191.

Misba L, Zaidi S, Khan AU. (2018). Efficacy of photodynamic therapy against *Streptococcus mutans* biofilm: Role of singlet oxygen. J Photochem Photobiol B. 183, 16-21.

Mishra S, Tyagi VK. (2007). Esterquats: the novel class of cationic fabric softeners. J Oleo Sci. 56 (6), 269-76.

Modenez IA, Sastre DE, Moares FC, Marques Netto CGC. (2018). Influence of Glutaraldehyde Cross-Linking Modes on the Recyclability of Immobilized Lipase B from Candida antarctica for Transesterification of Soy Bean Oil. Molecules. 23 (9), E2230.

Moeller R, Setlow P, Reitz G, Nicholson WL. (2009). Roles of small, acid-soluble spore proteins and core water content in survival of *Bacillus subtilis* spores exposed to environmental solar UV radiation. Appl Environ Microbiol. 75 (16), 5202-8.

Moorhead S, Maclean M, Coia JE, MacGregor SJ, Anderson JG. (2016). Synergistic efficacy of 405 nm light and chlorinated disinfectants for the enhanced decontamination of Clostridium difficile spores.. Anaerobe. 37, 72-7.

Murphy DS. (2014). Fabric softener technology: a review. J Surfactants Deterg . 18 (2), 199-204.

National Transportation Safety Board. (1989). Accident report detail: collision and derailment of Montana rail link freight train with locomotive units and hazardous materials release. Available from: https://www.ntsb.gov/investigations/AccidentReports/Pages/RAR8905.aspx [*Last accessed: 22/10/2019*].

Nelson DB, Muscarella LF. (2006). Current issues in endoscope reprocessing and infection control during gastrointestinal endoscopy. World J Gastroenterol. 12 (25), 3953-64.

Nelter J. (2017). EPA to consider perchlorate risks from degradation of hypochlorite bleach. Environmental Defence Fund. Available online: http://blogs.edf.org/health/2017/02/03/perchlorate-risks-from-bleach/ [*Last accessed: 21/10/2019*].

Newsome C, Howes D, Marshall SJ, van Egmond RA. 1995. Fate of some anionic and alcohol ethoxylate surfactants in Crassius auratus. Tenside Surf. Det. 32: 498-503.

Niederweis M. (2003). Mycobacterial porins--new channel proteins in unique outer membranes. Mol Microbiol. 49 (5), 1167-77.

Nielsen AM, DeCarvalho AJ, McAvoy DC, Kravetz L, Cano ML. 2002. Investigation of an onsite wastewater treatment system in sandy soil: site characterization and fate of anionic and nonionic surfactants. Environ. Toxicol. Chem. 21: 2606-2616.

Nitzan Y, Ashkenazi H. (2008). Photoinactivation of *Deinococcus radiodurans*: an unusual Gram-positive microorganism. Photochem Photobiol. 69 (4), 505-10.

Noïk C, Bavière M, Defives D. (1987). Anionic surfactant precipitation in hard water. J Colloid Interface Sci. 115 (1), 36-45.

Nosanchuk JD, Casadevall A. (1997). Cellular charge of *Cryptococcus neoformans*: contributions from the capsular polysaccharide, melanin, and monoclonal antibody binding. Infect Immun. 65 (5), 1836-41.

Nosanchuk JD, Valadon P, Feldmesser M, Casadevall A. (1999). Melanization of *Cryptococcus neoformans* in murine infection. Mol Cell Biol. 19 (1), 745-50.

Novo D, Perlmutter NG, Hunt RH, Shapiro HM. (1999). Accurate flow cytometric membrane potential measurement in bacteria using diethyloxacarbocyanine and a ratiometric technique. Cytometry. 35 (1), 55-63.

O'Riordan K, Akilov OE, Chang SK, Foley JW, Hasan T. (2007). Real-time fluorescence monitoring of phenothiazinium photosensitizers and their anti-mycobacterial photodynamic activity against *Mycobacterium bovis* BCG in in vitro and in vivo models of localized infection. Photochem Photobiol Sci. 6 (10), 1117-23.

O'Brien-Simpson NM, Pantarat N, A. Walsh KA, Reynolds EC, Marc-Antoine S, Separovic F. (2014). Bacterial fluorescent-dextran diffusion assay. Bio Protoc. 4 (14), e1191.

OECD. (1992a). Test No. 301: Ready Biodegradability. Section 3. OECD Publishing; Paris.

OECD. (1992b). Test No. 406: Skin Sensitisation. OECD Publishing; Paris.

OECD. (2015). Test No. 404: Acute Dermal Irritation/Corrosion. OECD Publishing; Paris.

OECD. (2018). Test No. 491: short time exposure in vitro test method for identifying i) chemicals inducing serious eye damage and ii) chemicals not requiring classification for eye irritation or serious eye damage, OECD guidelines for the testing of chemicals, Section 4, OECD Publishing, Paris, https://doi.org/10.1787/9789264242432-en.

OECD. (2019a). Test No. 431: In vitro skin corrosion: reconstructed human epidermis (RHE) test method, OECD Guidelines for the Testing of Chemicals, Section 4, OECD Publishing, Paris, https://doi.org/10.1787/9789264264618-en.

OECD. (2019b). Test No. 439: In vitro skin irritation: reconstructed human epidermis test method, OECD Guidelines for the Testing of Chemicals, Section 4, OECD Publishing, Paris, https://doi.org/10.1787/9789264242845-en.

Oh YK, Freese EWesgate R, Rauwel G, Criquelion J, Maillard JY. (2016). Impact of standard test protocols on sporicidal efficacy. J Hosp Infect. 93 (3), 256-62.

Okuda K, Urabe I, Yamada Y, Okada H. (1991). Reaction of glutaraldehyde with amino and thiol compounds. J Biosci Bioeng. 71 (2), 100-5.

Oliveira A, Almeida A, Carvalho CM, Tomé JP, Faustino MA, Neves MG, Tomé AC, Cavaleiro JA, Cunha A. (2009). Porphyrin derivatives as photosensitizers for the inactivation of *Bacillus cereus* endospores. J Appl Microbiol. 106 (6), 1986-95.

Olympus KeyMed (2012). Compatibility statement Olympus flexible endoscopes. Issue 8. Available online from: https://olympus.co.uk/medical/en/medical_systems/hidden/download_jsp.jsp?link=/medical/rmt/media /en/content/content_1/documents_1/data_sheets/Flexible-Endoscope-Compatibility.pdf [*Last accessed 14/11/2018*].

Orlov DS, Nguyen T, Lehrer RI. (2002). Potassium release, a useful tool for studying antimicrobial peptides. J Microbiol Methods. 49 (3), 325-8.

Otto CC, Cunningham TM, Hansen MR, Haydel SE. (2010). Effects of antibacterial mineral leachates on the cellular ultrastructure, morphology, and membrane integrity of *Escherichia coli* and methicillin-resistant *Staphylococcus aureus*. Ann Clin Microbiol Antimicrob. 9 (26).

Oviedo C, Rodríguez J. (2003). EDTA: the chelating agent under environmental scrutiny. Quím Nova. 26 (6), 901-5.

Ozerdem Akpolat N, Elçi S, Atmaca S, Akbayin H, Gül K. (2003). The effects of magnesium, calcium and EDTA on slime production by *Staphylococcus epidermidis* strains. Folia Microbiol (Praha). 48 (5), 649-53.

Pal AK, Gajjar DU, Vasavada AR. (2014). DOPA and DHN pathway orchestrate melanin synthesis in *Aspergillus* species. Med Mycol. 52 (1), 10-8.

Pan X, Ushio H, Ohshima T. (2005). Effects of molecular configurations of food colorants on their efficacies as photosensitizers in lipid oxidation. Food Chem. 92 (1), 37-44.

Parker AE, Walker DK, Goeres DM, Allan N, Olson ME, Omar A. (2014). Ruggedness and reproducibility of the MBEC biofilm disinfectant efficacy test. J Microbiol Methods. 102, 55-64.

Paz-Cristobal MP, Royo D, Rezusta A, Andrés-Ciriano E, Alejandre MC, Meis JF, Revillo MJ, Aspiroz C, Nonell S, Gilaberte Y. (2014). Photodynamic fungicidal efficacy of hypericin and dimethyl methylene blue against azole-resistant *Candida albicans* strains. Mycoses. 57 (1), 35-42.

Pecht M, Das D, Chang M. (2014). Introduction to LED thermal management and reliability. In: Lasance, C., J., M., Poppe, A. Thermal Management for LED Applications. New York: Springer. 3-5.

Pena Luengas SL, Marin GH, Aviles K, Cruz Acuña R, Roque G, Rodríguez Nieto F, Sanchez F, Tarditi A, Rivera L, Mansilla E. (2014). Enhanced singlet oxygen production by photodynamic therapy and a novel method for its intracellular measurement. Cancer Biother Radiopharm. 29 (10), 435-43.

Phoenix DA, Sayed Z, Hussain S, Harris F, Wainwright M. (2003). The phototoxicity of phenothiazinium derivatives against *Escherichia coli* and *Staphylococcus aureus*. FEMS Immunol Med Microbiol. 39 (1), 17-22.

Piccaro G, Giannoni F, Filippini P, Mustazzolu A, Fattorini L. (2013). Activities of drug combinations against *Mycobacterium tuberculosis* grown in aerobic and hypoxic acidic conditions. Antimicrob Agents Chemother. 57 (3), 1428-33.

Piccaro G, Poce G, Biava M, Giannoni F, Fattorini L. (2015). Activity of lipophilic and hydrophilic drugs against dormant and replicating *Mycobacterium tuberculosis*. J Antibiot (Tokyo). 68 (11), 711-4.

Pihet M, Vandeputte P, Tronchin G, Renier G, Saulnier P, Georgeault S, Mallet R, Chabasse D, Symoens F, Bouchara JP. (2009). Melanin is an essential component for the integrity of the cell wall of *Aspergillus fumigatus* conidia. BMC Microbiol. 9 (177).

Pinto IS, Neto IF, Soares HM. (2014). Biodegradable chelating agents for industrial, domestic, and agricultural applications--a review. Environ Sci Pollut Res Int. 21 (20), 11893-906.

Pitcher RS, Brissett NC, Doherty AJ. (2007). Nonhomologous end-joining in bacteria: a microbial perspective. Annu Rev Microbiol. 61, 259-82.

Pottage T, Richardson C, Parks S, Walker JT, Bennett AM. (2010). Evaluation of hydrogen peroxide gaseous disinfection systems to decontaminate viruses. J Hosp Infect. 74 (1), 55-61.

PubChem. (2019). Compound Summary: TrisodiuM N-(1-Carboxylatoethyl)iMinodiacetate Hydrate. Available: https://pubchem.ncbi.nlm.nih.gov/compound/70699979 [*Last accessed 09/10/2019*].

Puchta R, Krings P, Sandkuhler P. (1993). A new generation of softeners, Tenside Surf. Det. 30:186 (1993).

Pupo YM, Gomes GM, Santos EB, Chaves L, Michel MD, Kozlowski VA Jr, Gomes OM, Gomes JC. (2011). Susceptibility of *Candida albicans* to photodynamic therapy using methylene blue and toluidine blue as photosensitizing dyes. Acta Odontol Latinoam. 24 (2), 188-92.

Rabek JF, Rånby B, Östensson B, Flodin P. (1979). Oxidation of polyene structures in poly(vinyl chloride) by molecular oxygen and singlet oxygen. J Appl Polym Sci. 24 (12), 2407-13.

Rabenau HF, Steinmann J, Rapp I, Schwebke I, Eggers M. (2014). Evaluation of a virucidal quantitative carrier test for surface disinfectants. PLoS One. 9 (1), e86128.

Razin S. (1996). Chapter 37. Mycoplasmas. In: Baron S Medical Microbiology. 4th ed. The University of Texas Medical Branch.

Redman RS, Krasnow SH, Sniffen RA. (1992). Evaluation of the carcinogenic potential of toluidine blue O in the hamster cheek pouch. Oral Surg Oral Med Oral Pathol. 74 (4), 473-80.

Rideout K, Teschke K, Dimich-Ward H, Kennedy SM. (2005). Considering risks to healthcare workers from glutaraldehyde alternatives in high-level disinfection. J. Hosp. Infect. 59, 4–11.

Riesenman PJ, Nicholson WL. (2000). Role of the spore coat layers in *Bacillus subtilis* spore resistance to hydrogen peroxide, artificial UV-C, UV-B, and solar UV radiation. Appl Environ Microbiol. 66 (2), 620-6.

Roberts CG. (2013). The role of biofilms in reprocessing medical devices. Am J Infect Control. 41 (5), S77-80.

Robertson P, Smith A, Mead A, Smith I, Khanna N, Wright P, Joannidis P, Boyd S, Anderson M, Hamilton A, Shaw D, Stewart A. (2015). Risk-assessment-based approach to patients exposed to endoscopes contaminated with *Pseudomonas spp*. J Hosp Infect. 90 (1), 66-9.

Robilotti E, Deresinski S, Pinsky BA. (2015). Norovirus. Clin Microbiol Rev. 28 (1), 134-64.

Rodgers K, McVey M. (2016). Error-prone repair of DNA double-strand breaks. J Cell Physiol. 231 (1), 15-24.

Rodrigues GB, Dias-Baruffi M, Holman N, Wainwright M, Braga GU. (2013). In vitro photodynamic inactivation of *Candida* species and mouse fibroblasts with phenothiazinium photosensitisers and red light. Photodiagnosis Photodyn Ther. 10 (2), 141-9.

Rodrigues GB, Ferreira LK, Wainwright M, Braga GU. (2012). Susceptibilities of the dermatophytes *Trichophyton mentagrophytes* and *T. rubrum* microconidia to photodynamic antimicrobial chemotherapy with novel phenothiazinium photosensitizers and red light. J Photochem Photobiol B. 116, 89-94.

Rodriguez CH, Scamehorn JF. (2001). Kinetics of precipitation of surfactants. II. Anionic surfactant mixtures. J Surfactants Deterg. 4 (1), 15–26.

Rogers WJ. (2014). Healthcare Sterilisation: Challenging Practices, Volume 2. Shrewsbury; UK: Smithers Rapra Technology. 70.

Rohwer F, Azam F. (2000). Detection of DNA damage in prokaryotes by terminal deoxyribonucleotide transferase-mediated dUTP nick end labeling. Appl Environ Microbiol. 66 (3), 1001-6.

Rout B, Liu CH, Wu WC. (2016). Enhancement of photodynamic inactivation against *Pseudomonas aeruginosa* by a nano-carrier approach. Colloids Surf B Biointerfaces. 140, 472-80.

Rout B, Liu CH, Wu WC. (2018). Increased anti-biofilm efficacy of toluidine blue on *Staphylococcus* species after nano-encapsulation. Photodiagnosis Photodyn Ther. 28, 190-200.

Russell PE. (2001). SEM and AFM: Complementary techniques for surface investigations. microscopy and analysis. Available from: https://microscopy-analysis.com/sites/default/files/magazine_pdfs/mag%20203_2001_Jul_Russell_1.pdf [*Last accessed: 28/10/2019].*

Rutala WA, Weber DJ. (2004). Disinfection and sterilization in health care facilities: what clinicians need to know. Clin Infect Dis. 39 (5), 702-9.

Rutala WA, Weber DJ. (2011). Sterilization, high-level disinfection, and environmental cleaning. Infect Dis Clin North Am. 25 (1), 45-76.

Sabnis RW. (2010). Handbook of Biological Dyes and Stains: Synthesis and Industrial Applications. Hoboken, New Jersey: John Wiley & Sons. 470.

Saha B, Chowdhury S, Sanyal D, Chattopadhyay K, Suresh Kumar G. (2018). Comparative study of toluidine blue O and methylene blue binding to lysozyme and their inhibitory effects on protein aggregation. ACS Omega. 3 (3), 2588-601.

Sahu K, Bansal H, Mukherjee C, Sharma M, Gupta PK. (2009). Atomic force microscopic study on morphological alterations induced by photodynamic action of toluidine blue O in *Staphylococcus aureus* and *Escherichia coli*. J Photochem Photobiol B. 96 (1), 9-16.

Sattar SA. (2007). Hierarchy of susceptibility of viruses to environmental surface disinfectants: a predictor of activity against new and emerging viral pathogens. J AOAC Int. 90 (6), 1655-8.

Schagen FH, Moor AC, Cheong SC, Cramer SJ, van Ormondt H, van der Eb AJ, Dubbelman TM, Hoeben RC. (1999). Photodynamic treatment of adenoviral vectors with visible light: an easy and convenient method for viral inactivation. Gene Ther. 6 (5), 873-81.

Schelenz S, French G. (2000). An outbreak of multidrug-resistant *Pseudomonas aeruginosa* infection associated with contamination of bronchoscopes and an endoscope washer-disinfector. J Hosp Infect. 46 (1), 23-30.

Schreck A, Knorr A, Wehrstedt KD, Wandrey PA, Gmeinwieser T, Steinbach J. (2004). Investigation of the explosive hazard of mixtures containing hydrogen peroxide and different alcohols. J Hazard Mater. 108 (1-2), 1-7.

Scientific Committee on Consumer Products. (2005). SCCP/0919/05. Memorandum on the classification and categorization of skin sensitisers and grading of test reactions. Available from: https://ec.europa.eu/health/ph_risk/committees/04_sccp/docs/sccp_s_01.pdf [*Last accessed: 21/10/2019*].

Scott D, Galloway SM, Marshall RR, Ishidate M Jr, Brusick D, Ashby J, Myhr BC. (1991). International commission for protection against environmental mutagens and carcinogens. Genotoxicity under extreme culture conditions. A report from ICPEMC Task Group 9. Mutat Res. 257 (2), 147-205.

Seneviratne CJ, Yip JW, Chang JW, Zhang CF, Samaranayake LP. (2013). Effect of culture media and nutrients on biofilm growth kinetics of laboratory and clinical strains of *Enterococcus faecalis*. Arch Oral Biol. 58 (10), 1327-34.

Setlow B, Atluri S, Kitchel R, Koziol-Dube K, Setlow P. (2006). Role of dipicolinic acid in resistance and stability of spores of *Bacillus subtilis* with or without DNA-protective alpha/beta-type small acid-soluble proteins. J Bacteriol. 188 (11), 3740-7.

Setlow B, Setlow P. (1996). Role of DNA repair in *Bacillus subtilis* spore resistance. J Bacteriol. 178 (12), 3486-95.

Setlow B, Sun D, Setlow P. (1992). Interaction between DNA and alpha/beta-type small, acid-soluble spore proteins: a new class of DNA-binding protein. J Bacteriol. 174 (7), 2312-22.

Seuvre A, Voilley A. (2017). Physio-chemical interactions in the flavour release process. In: Buettner A. Springer Handbook of Odor. New York: Springer. 279.

Shaffer MP, Belsito DV. (2000). Allergic contact dermatitis from glutaraldehyde in health-care workers. Contact Dermatitis 43, 150–156.

Sharma M, Visai L, Bragheri F, Cristiani I, Gupta PK, Speziale P. (2008). Toluidine blue-mediated photodynamic effects on staphylococcal biofilms. Antimicrob Agents Chemother. 52 (1), 299-305.

Sharma R, Masaki J, Agarwal A. (2013). Sperm DNA fragmentation analysis using the TUNEL assay. Methods Mol Biol. 927, 121-36.

Shim I, Choi M, Min Y, Seok K, Kim J, Jeong JY, Oak CH, Park I . (2016). Effect of methylene blue-mediated photodynamic therapy on wild-type and ciprofloxacin-resistant *Mycobacterium smegmatis*. J Bacteriol Virol. 46 (1), 27.

Shimono N, Takuma T, Tsuchimochi N, Shiose A, Murata M, Kanamoto Y, Uchida Y, Morita S, Matsumoto H, Hayashi J. (2008). An outbreak of *Pseudomonas aeruginosa* infections following thoracic surgeries occurring via the contamination of bronchoscopes and an automatic endoscope reprocessor. J Infect Chemother. 14 (6), 418-23.

Sillanpää M. (1997). Environmental fate of EDTA and DTPA. Rev Environ Contam Toxicol. 152, 85-111.

Silva E, De Landea C, Edwards AM, Lissi E. (2000). Lysozyme photo-oxidation by singlet oxygen: properties of the partially inactivated enzyme. J Photochem Photobiol B. 55 (2-3), 196-200.

Simões M, Simões LC, Vieira MJ. (2009). Species association increases biofilm resistance to chemical and mechanical treatments. Water Res. 43 (1), 229-37.

Simonin M, Richaume A, Guyonnet JP, Dubost A, Martins JM, Pommier T. (2016). Titanium dioxide nanoparticles strongly impact soil microbial function by affecting archaeal nitrifiers. Sci Rep. 6, 33643.

Simons C, Walsh SE, Maillard JY, Russell AD. (2000). A note: ortho-phthalaldehyde: proposed mechanism of action of a new antimicrobial agent. Lett Appl Microbiol. 31 (4), 299-302.

Simons C, Walsh SE, Maillard JY, Russell AD. (2000). A note: ortho-phthalaldehyde: proposed mechanism of action of a new antimicrobial agent. *Lett. Appl. Microbiol*. 31, 299–302.

Singaravelan N, Grishkan I, Beharav A, Wakamatsu K, Ito S, Nevo E. (2008). Adaptive melanin response of the soil fungus *Aspergillus niger* to UV radiation stress at "Evolution Canyon", Mount Carmel, Israel. PLoS One. 3 (8), e2993.

Singh P, Pandit S, Mokkapati VRSS, Garg A, Ravikumar V, Mijakovic I. (2018). Gold nanoparticles in diagnostics and therapeutics for human cancer. Int J Mol Sci. 19 (7), E1979.

Smith K, Hunter IS. (2008). Efficacy of common hospital biocides with biofilms of multi-drug resistant clinical isolates. J Med Microbiol. 57 (8), 966-73.

Solanky D, Haydel SE. (2012). Adaptation of the neutral bacterial comet assay to assess antimicrobial-mediated DNA double-strand breaks in *Escherichia coli*. J Microbiol Methods. 91 (2), 257-61.

Soltan ME. (2006). Remobilization of selected metal ions from Nile sediment (Egypt) according to sequential extraction and metal–EDTA complex. J Chem Ecol. 22 (5), 359-78.

Soluscope. (2019). Serie 3. Available from: https://www.soluscope.com/eng/page/endoscope-washer-disinfector-serie-3-0 [*Last accessed 18/08/2019*].

Soukos NS, Wilson M, Burns T, Speight PM. (1996). Photodynamic effects of toluidine blue on human oral keratinocytes and fibroblasts and Streptococcus sanguis evaluated in vitro. Lasers Surg Med. 18 (3), 253-9.

Souza RC, Junqueira JC, Rossoni RD, Pereira CA, Munin E, Jorge AO. (2010). Comparison of the photodynamic fungicidal efficacy of methylene blue, toluidine blue, malachite green and low-power laser irradiation alone against *Candida albicans*. Lasers Med Sci. 25 (3), 385-9.

Sriamornsak P, Thirawong N, Cheewatanakornkool K, Burapapadh K, Sae-Ngow W. (2008). Cryo-scanning electron microscopy (cryo-SEM) as a tool for studying the ultrastructure during bead formation by ionotropic gelation of calcium pectinate. Int J Pharm. 352 (1-2), 115-22.

St Laurent JB, de Buzzaccarini F, De Clerk K, Demeyere H, Labeque R, Lodewick R, van Langenhove L. (2007). Chapter B.1.I: Laundry Cleaning of Textiles. In: Johansson Somasundaran IJP. Handbook for Cleaning/Decontamination of Surfaces. Amsterdam; Netherlands: Elsevier. 57-99.

Steber J. (2007). The ecotoxicity of cleaning product ingredients. In: Johansson I, Somasundaran P Handbook for cleaning/decontamination of surfaces. Amsterdam: Elsevier. 727-8.

Steelco. (2019). EW2. Available from: https://www.steelcogroup.com/en/products-catalogue/medical-products/flexible-endoscopes-reprocessing-and-storage/item/ew-2-flexible-endoscopes-reprocessor?category_id=2006 [*Last accessed 21/10/2019*].

Stephan J, Bender J, Wolschendorf F, Hoffmann C, Roth E, Mailänder C, Engelhardt H, Niederweis M. (2005). The growth rate of *Mycobacterium smegmatis* depends on sufficient porin-mediated influx of nutrients. Mol Microbiol. 58 (3), 714-30.

Stephan J, Mailaender C, Etienne G, Daffé M, Niederweis M. (2004). Multidrug resistance of a porin deletion mutant of *Mycobacterium smegmatis*. Antimicrob Agents Chemother. 48 (11), 4163-70.

Stewart PS, Rayner J, Roe F, Rees WM. (2001). Biofilm penetration and disinfection efficacy of alkaline hypochlorite and chlorosulfamates. J Appl Microbiol. 91 (3), 525-32.

Stewart PS, Roe F, Rayner J, Elkins JG, Lewandowski Z, Ochsner UA, Hassett DJ. (2000). Effect of catalase on hydrogen peroxide penetration into Pseudomonas aeruginosa biofilms. Appl. Environ. Microbiol. 66, 836–838.

Stiefel P, Schmidt-Emrich S, Maniura-Weber K, Ren Q. (2015). Critical aspects of using bacterial cell viability assays with the fluorophores SYTO9 and propidium iodide. BMC Microbiol. 15 (36).

Stocks SM. (2004). Mechanism and use of the commercially available viability stain, BacLight. Cytometry A. 61 (2), 189-95.

Strahl H, Hamoen LW. (2010). Membrane potential is important for bacterial cell division. Proc Natl Acad Sci USA. 107 (27), 12281-6.

Su X, Zivanovic S, D'Souza DH. (2009). Effect of chitosan on the infectivity of murine norovirus, feline calicivirus, and bacteriophage MS2. J Food Prot. 72 (12), 2623-8.

Sutherland BM, Bennett PV, Sutherland JC. (2006). DNA damage quantitation by alkaline gel electrophoresis. Methods Mol Biol. 314 (.), 251-73.

Sutton S, Jimenez L. (2012). A review of reported recalls involving microbiological control 2004-2011 with emphasis on FDA considerations of “objectionable organisms”. Am Pharmaceut Rev. 15 (1), 42-57.

Svetlíková Z, Skovierová H, Niederweis M, Gaillard JL, McDonnell G, Jackson M. (2009). Role of porins in the susceptibility of *Mycobacterium smegmatis* and *Mycobacterium chelonae* to aldehyde-based disinfectants and drugs. Antimicrob Agents Chemother. 53 (9), 4015-8.

Sweetman SC (2009). Martindale: the complete drug reference. 15th ed. London: Pharmaceutical Press. 2403.

Sylvain D, Gibbins J. (2009). Evaluation of Worker Exposures to Peracetic Acid-Based Sterilant during Endoscope Reprocessing (Buffalo, USA; National Institute for Occupational Health and Safety).

Tada M, Kohno M, Niwano Y. (2010). Scavenging or quenching effect of melanin on superoxide anion and singlet oxygen. J Clin Biochem Nutr. 46 (3), 224-8.

Tan IS, Ramamurthi KS. (2014). Spore formation in *Bacillus subtilis*. Environ Microbiol Rep. 6 (3), 212-25.

Tang HM, Hamblin MR, Yow CM. (2007). A comparative in vitro photoinactivation study of clinical isolates of multidrug-resistant pathogens. J Infect Chemother. 13 (2), 87-91.

Tardivo JP, Serrano R, Zimmermann LM, Matos LL, Baptista MS, Pinhal MAS, Atallah ÁN. (2017). Is surgical debridement necessary in the diabetic foot treated with photodynamic therapy? Diabet Foot Ankle. 8 (1), 1373552.

Tegos GP, Demidova TN, Arcila-Lopez D, Lee H, Wharton T, Gali H, Hamblin MR. (2006). Phenothiazinium antimicrobial photosensitizers are substrates of bacterial multidrug resistance pumps. Antimicrob Agents Chemother. 50 (1), 196-203.

Tegos GP, Demidova TN, Arcila-Lopez D, Lee H, Wharton T, Gali H, Hamblin MR. (2005). Cationic fullerenes are effective and selective antimicrobial photosensitizers. Chem Biol. 12 (10), 1127-35.

Tegos GP, Masago K, Aziz F, Higginbotham A, Stermitz FR, Hamblin MR. (2008). Inhibitors of bacterial multidrug efflux pumps potentiate antimicrobial photoinactivation. Antimicrob Agents Chemother. 52 (9), 3202-9.

Temba BA, Fletcher MT, Fox GP, Harvey J, Okoth SA, Sultanbawa Y. (2019). Curcumin-based photosensitization inactivates *Aspergillus flavus* and reduces aflatoxin B1 in maize kernels. Food Microbiol. 82, 82-8.

Tennen R, Setlow B, Davis KL, Loshon CA, Setlow P. (2000). Mechanisms of killing of spores of *Bacillus subtilis* by iodine, glutaraldehyde and nitrous acid. J Appl Microbiol. 89 (2), 330-8.

Thangamani S, Younis W, Seleem MN. (2015). Repurposing ebselen for treatment of multidrug-resistant staphylococcal infections. Sci Rep. 5, 11596.

Thanomsub B, Anupunpisit V, Chanphetch S, Watcharachaipong T, Poonkhum R, Srisukonth C. (2002). Effects of ozone treatment on cell growth and ultrastructural changes in bacteria. J Gen Appl Microbiol. 48 (4), 193-9.

Thermo Fisher Scientific. (2019). Chapter 22. Probes for membrane potential. Slow-response probes. Section 22.3. In: The Molecular Probes Handbook. Available from: https://www.thermofisher.com/uk/en/home/references/molecular-probes-the-handbook/probes-for-membrane-potential/slow-response-probes.html [*Last accessed: 25/10/2019*].

Thermo Fisher Scientific. (2019a). LIVE/DEAD™ BacLight™ bacterial viability kit for microscopy & quantitative assays. Available from: https://www.thermofisher.com/order/catalog/product/L7012?SID=srch-srp-L7012#/L7012?SID=srch-srp-L7012 [*Last accessed: 30/10/2019*].

Thermo Fisher Scientific. (2019b). ATP determination kit, 200-1,000 assays. Available from: https://www.thermofisher.com/order/catalog/product/A22066?SID=srch-srp-A22066#/A22066?SID=srch-srp-A22066 [*Last accessed: 30/10/2019*].

Thermo Fisher Scientific. (2019c). BacLight™ Bacterial membrane potential kit. Available from: https://www.thermofisher.com/order/catalog/product/B34950#/B34950 [*Last accessed: 30/10/2019*].

Thermo Fisher Scientific. (2019d). SYBR™ Gold Nucleic Acid Gel Stain (10,000X Concentrate in DMSO). Available from: https://www.thermofisher.com/order/catalog/product/S11494#/S11494 [*Last accessed: 30/10/2019*].

Thiruvenkatachari R, Vigneswaran S, Moon IS. (2008). A review on UV/TiO2 photocatalytic oxidation process. Korean J Chem Eng. 25 (1), 64–72.

Toxicology Data Network. (2019). Tolonium chloride. Available from: https://chem.nlm.nih.gov/chemidplus/sid/0000092319 [*Last accessed: 01/11/2019*].

Trias J, Benz R. (1994). Permeability of the cell wall of *Mycobacterium smegmatis*. Mol Microbiol. 14 (2), 283-90.

Tsai CS, Godin JR, Wand AJ. (1985). Dye-sensitized photo-oxidation of enzymes. Biochem J. 225 (1), 203-8.

Tsai T, Chien HF, Wang TH, Huang CT, Ker YB, Chen CT. (2011). Chitosan augments photodynamic inactivation of gram-positive and gram-negative bacteria. Antimicrob Agents Chemother. 55 (5), 1883-90.

Tseng SP, Hung WC, Chen HJ, Lin YT, Jiang HS, Chiu HC, Hsueh PR, Teng LJ, Tsai JC. (2017). Effects of toluidine blue O (TBO)-photodynamic inactivation on community-associated methicillin-resistant *Staphylococcus aureus* isolates. J Microbiol Immunol Infect. 50 (1), 46-54.

Tseng SP, Teng LJ, Chen CT, Lo TH, Hung WC, Chen HJ, Hsueh PR, Tsai JC. (2009). Toluidine blue O photodynamic inactivation on multidrug-resistant *Pseudomonas aeruginosa*. Lasers Surg Med. 41 (5), 391-7.

Umerska A, Strandh M, Cassisa V, Matougui N, Eveillard M, Saulnier P. (2018). Synergistic effect of combinations containing EDTA and the antimicrobial peptide AA230, an arenicin-3 derivative, on Gram-negative bacteria. Biomolecules. 8 (4), E122.

Usacheva MN, Teichert MC, Biel MA. (2003). The role of the methylene blue and toluidine blue monomers and dimers in the photoinactivation of bacteria. J Photochem Photobiol B. 71 (1-3), 87-98.

Usacheva MN, Teichert MC, Sievert CE, Biel MA. (2006). Effect of Ca^{+} on the photobactericidal efficacy of methylene blue and toluidine blue against Gram-negative bacteria and the dye affinity for lipopolysaccharides. Lasers Surg Med. 38 (10), 946-54.

Valegård K, Murray JB, Stonehouse NJ, van den Worm S, Stockley PG, Liljas L. (1997). The three-dimensional structures of two complexes between recombinant MS2 capsids and RNA operator fragments reveal sequence-specific protein-RNA interactions. J Mol Biol. 270 (5), 724-38.

van Birgelen AP, Chou BJ, Renne RA, Grumbein SL, Roycroft JH, Hailey JR, Bucher JR. (2000). Effects of glutaraldehyde in a 2-year inhalation study in rats and mice. Toxicol Sci. 55 (1), 195-205.

Varga B, Csonka Á, Csonka A, Molnár J, Amaral L, Spengler G. (2017). Possible Biological and Clinical Applications of Phenothiazines. Anticancer Res. 37 (11), 5983-93.

Vickery K, Deva A, Jacombs A, Allan J, Valente P, Gosbell IB. (2012). Presence of biofilm containing viable multiresistant organisms despite terminal cleaning on clinical surfaces in an intensive care unit. J Hosp Infect. 80 (1), 52-5.

Vickery K, Pajkos A, Cossart Y. (2004). Removal of biofilm from endoscopes: evaluation of detergent efficiency. Am. J. Infect. Control 32, 170–176.

VIPARSPECTRA. (2019). VIPARSPECTRA DS600 600W. Available from: https://www.viparspectra.com/goods.php?id=104 [*Last accessed 04/11/2019*].

Vitale-Cross L, Czerninski R, Amornphimoltham P, Patel V, Molinolo AA, Gutkind JS. (2009). Chemical carcinogenesis models for evaluating molecular-targeted prevention and treatment of oral cancer. Cancer Prev Res (Phila). 2 (5), 419-22.

Vleugels LFW, Ricois S, Voets IK, Tuinier R. (2017). Reversal of metachromasy revisited; displacement of toluidine-blue from alginate by surfactants. Colloids Surf. 529, 454-61.

Wagner SJ, Cifone MA, Murli H, Dodd RY, Myhr B. (1995). Mammalian genotoxicity assessment of methylene blue in plasma: implications for virus inactivation. Transfusion. 35 (5), 407-13.

Wagner SJ, Skripchenko A, Robinette D, Foley JW, Cincotta L. (1998). Factors affecting virus photoinactivation by a series of phenothiazine dyes. Photochem Photobiol. 67 (3), 343-9.

Wainwright, M. (2009). Photosensitisers in Biomedicine (Chichester; UK: John Wiley & Sons). 1–12, 27–41, 237–57.

Walker SE, Sander JE, Cheng IH, Wooley RE. (2002). The in vitro efficacy of a quaternary ammonia disinfectant and/or ethylenediaminetetraacetic acid-tris against commercial broiler hatchery isolates of *Pseudomonas aeruginosa*. Avian Dis. 46 (4), 826-30.

Wang TY, Libardo MDJ, Angeles-Boza AM, Pellois JP. (2017). Membrane oxidation in cell delivery and cell killing applications. ACS Chem Biol. 12 (5), 1170-82.

Wang Y, Wu X, Chen J, Amin R, Lu M, Bhayana B, Zhao J, Murray CK, Hamblin MR, Hooper DC, Dai T. (2016). Antimicrobial blue light inactivation of gram-negative pathogens in biofilms: in vitro and in vivo studies. J Infect Dis. 213 (9), 1380-7.

Weil L, Gordon WG, Buchert AR. (1951). Photoöxidation of amino acids in the presence of methylene blue. Arch Biochem Biophys. 33 (1), 90-109.

Weir RJ Jr, Fisher RS. (1972). Toxicologic studies on borax and boric acid. Toxicol Appl Pharmacol. 23 (3), 351-64.

Wickham G. (2017). An investigation into the relative resistances of common bacterial pathogens to quaternary ammonium cation disinfectants. Biosci Horiz. 10.

Wilkinson LJ, White RJ, Chipman JK. (2011). Silver and nanoparticles of silver in wound dressings: a review of efficacy and safety. J Wound Care. 20 (11), 543-9.

Woelk E, Goroncy-Bermes P, Sand W.. (2003). Influence of storage on monodispersed cells of *Mycobacterium terrae* used for quantitative carrier test prEN 14563. Appl Environ Microbiol. 69 (11), 6932-4.

Wood S, Metcalf D, Devine D, Robinson C. (2004). Erythrosine is a potential photosensitizer for the photodynamic therapy of oral plaque biofilms. J Antimicrob Chemother. 57 (4), 680-4.

Working Party of the British Society of Gastroenterology Endoscopy Committee (2017). BSG Guidance for Decontamination of Endoscopes Available online from: https://www.bsg.org.uk/resource/guidance-on-decontamination-of-equipment-for-gastrointestinal-endoscopy-2017-edition.html *[Last accessed 22/10/2019].*

World Health Organisation (2016). Global guidelines on the prevention of surgical site infection. 2nd ed. Geneva: World Health Organisation. 50.

Wu EL, Engström O, Jo S, Stuhlsatz D, Yeom MS, Klauda JB, Widmalm G, Im W. (2013). Molecular dynamics and NMR spectroscopy studies of *E. coli* lipopolysaccharide structure and dynamics. Biophys J. 105 (6), 1444-55.

Yang NC, Ho WM, Chen YH, Hu ML. (2002). A convenient one-step extraction of cellular ATP using boiling water for the luciferin-luciferase assay of ATP. Anal Biochem. 306 (2), 323-7.

Yang SM, Lee DW, Park HJ, Kwak MH, Park JM, Choi MG. (2019). Hydrogen peroxide enhances the antibacterial effect of methylene blue-based photodynamic therapy on biofilm-forming bacteria. Photochem Photobiol. 95 (3), 833-8.

Yoo JH. (2018). Review of disinfection and sterilization - back to the basics. Infect Chemother. 50 (2), 101-9.

Yoshimura F, Nikaido H. (1982). Permeability of *Pseudomonas aeruginosa* outer membrane to hydrophilic solutes. J Bacteriol. 152 (2), 636-42.

Zanin IC, Gonçalves RB, Junior AB, Hope CK, Pratten J. (2005). Susceptibility of *Streptococcus mutans* biofilms to photodynamic therapy: an in vitro study. J Antimicrob Chemother. 56 (2), 324-30.

Zeiger E, Mortelmans K. (1999). The *Salmonella* (Ames) test for mutagenicity. Curr Protoc Toxicol. 00 (1), 3.1.1-29.

Zeina B, Greenman J, Purcell WM, Das B. (2001). Killing of cutaneous microbial species by photodynamic therapy. Br J Dermatol. 144 (2), 274-8.

Zhang C, Cui F, Zeng GM, Jiang M, Yang ZZ, Yu ZG, Zhu MY, Shen LQ. (2015). Quaternary ammonium compounds (QACs): a review on occurrence, fate and toxicity in the environment. Sci Total Environ. 518-9, 352-62.

Zhang R, Wang Q, Zhang J, Lu Q, Liu W, Yin S, Cao W. (2019). Towards efficient photocatalytic degradation of organic pollutants in hierarchical TiO2/SnO p-n heterojunction under visible-light irradiation. Nanotechnology. 30 (43), 434001.

Zhao B, Zhang D, Li C, Yuan Z, Yu F, Zhong S, Jiang G, Yang YG, Le XC, Weinfeld M, Zhu P, Wang H. (2017). ATPase activity tightly regulates RecA nucleofilaments to promote homologous recombination. Cell Discov. 3 (16053).

Zhou G, Shi QS, Huang XM, Xie XB. (2015). The three bacterial lines of defense against antimicrobial agents. Int J Mol Sci. 16 (9), 21711-33.